



**HAL**  
open science

# Towards the long-term, conditional and tractable disruption of Notch3 signaling in zebrafish neural stem and progenitor cells

Mathilde Chouly

► **To cite this version:**

Mathilde Chouly. Towards the long-term, conditional and tractable disruption of Notch3 signaling in zebrafish neural stem and progenitor cells. *Development Biology*. Sorbonne Université, 2024. English. NNT : 2024SORUS346 . tel-04926218

**HAL Id: tel-04926218**

**<https://theses.hal.science/tel-04926218v1>**

Submitted on 3 Feb 2025

**HAL** is a multi-disciplinary open access archive for the deposit and dissemination of scientific research documents, whether they are published or not. The documents may come from teaching and research institutions in France or abroad, or from public or private research centers.

L'archive ouverte pluridisciplinaire **HAL**, est destinée au dépôt et à la diffusion de documents scientifiques de niveau recherche, publiés ou non, émanant des établissements d'enseignement et de recherche français ou étrangers, des laboratoires publics ou privés.

Sorbonne Université

Ecole doctorale 515 Complexité du vivant

*UMR 3738 / Zebrafish Neurogenetics*

**Towards the long-term, conditional and tractable  
disruption of Notch3 signaling in zebrafish neural stem  
and progenitor cells**

Par Mathilde CHOULY

Thèse de doctorat de BIOLOGIE

Dirigée par le Dr. Laure BALLY-CUIF

Présentée et soutenue publiquement le 31 octobre 2024

Devant un jury composé de :

Dr. Estelle HIRSINGER

*Directrice de recherche, Institut de Biologie Paris-Seine, Paris*

Examinatrice

Présidente du jury

Dr. Maximilian FÜRTHAUER

*Directeur de recherche, Institut de Biologie Valrose, Nice*

Rapporteur

Dr. Muriel PERRON

*Directrice de recherche, Institut NeuroPSI, Gif-sur-Yvette*

Rapportrice

Dr. Laure BALLY-CUIF

*Directrice de recherche, Institut Pasteur, Paris*

Directrice de thèse





# Table of contents

<b>Acknowledgments.....</b>	<b>2</b>
<b>Abbreviations.....</b>	<b>5</b>
<b>Summary .....</b>	<b>8</b>
<b>Résumé .....</b>	<b>10</b>
<b>Introduction .....</b>	<b>12</b>
General introduction.....	12
1 Definitions.....	14
1.1 Progenitor versus stem cells.....	14
1.2 Nomenclature along lifetime progression in zebrafish and mouse .....	14
2 The neurogenesis process.....	16
2.1 Progenitor cells over a lifetime .....	16
2.2 NPs and NSCs localization and neurogenic domains .....	19
2.3 Molecular markers.....	21
2.4 NPs and NSCs morphology.....	22
2.5 NPs and NSCs local environment .....	24
2.6 Division process and division modes .....	26
2.7 Early delamination and migration processes involved in neurogenesis.....	28
2.8 Neuronal lineage progression.....	30
2.9 Quiescence of NSCs.....	31
3 Notch signaling pathway .....	34
3.1 Introduction .....	34
3.2 Canonical pathway .....	35
3.2.1 Receptors .....	35
3.2.2 Ligands .....	36
3.2.3 Mechanism of action .....	36
3.2.4 Regulations.....	40
3.2.5 Non-canonical alternatives .....	42
3.3 Functions of the Notch signaling pathway .....	43
3.3.1 General functions .....	43

3.3.2 Early expression and loss-of-function.....	45
3.3.3 Functions during neurogenesis.....	46
3.3.3.1 In mouse .....	47
In the mouse embryo .....	47
In the adult mouse .....	50
3.3.3.2 In zebrafish.....	54
In the zebrafish embryo.....	54
In the adult zebrafish .....	58
Conclusion.....	63
3.4 Why study Notch3 in zebrafish neural progenitors?.....	64
4. Development of a new method to study the functions of Notch3 signaling .....	65
4.1 Objectives of the method developed in my PhD.....	67
4.2 Conditional, long-term, and tractable loss-of-function .....	68
4.3 Targeting nuclear protein functions .....	69
4.4 deGradFP and related methods .....	71
4.5 Adapting Ab-SPOP for conditional, long-term, and tractable nuclear Notch3 knock-down <i>in vivo</i> .....	73
4.6 Alternative method of knock-down: <i>notch3</i> RNAi .....	78
<b>Results .....</b>	<b>79</b>
1. Tagging endogenous Notch3 to selectively expose its signaling component as a target for degradation .....	79
Generation of an endogenous <i>notch3</i> <sup>GFP</sup> fusion by CRISPR knock-in.....	79
Validation of the functionality of the Notch3-GFP fusion <i>in vivo</i> .....	82
The Notch3-GFP protein localizes to the plasma membrane as well as recycling vesicles in NSCs .....	84
Nuclear N3ICD-GFP levels provide quantitative measures of Notch3 signaling <i>in situ</i> . .....	90
Conclusions .....	100
2. Generation of a transgenic nanobody tool selective of nuclear GFP fusion proteins and conditionally activatable in NPs/NSCs .....	101
Validation of anti-GFP nanobodies targeted to the nucleus for the selective degradation of nuclear GFP protein in zebrafish embryos .....	101

VhhGFP4-hSPOP-nls .....	105
Nfbxw11b-VhhGFP4 .....	105
Generation of a transgenic line conditionally expressing a tractable anti-GFP nanobody upon Cre-loxP recombination .....	106
Preliminary validations .....	108
N3ICD degradation by VhhGFP4-hSPOP-nls .....	108
Expression of <i>VhhGFP4-hSPOP-nls</i> upon <i>loxP-stop-loxP</i> recombination .....	111
Generation of the <i>Tg(VhhGFP4-hSPOP-nls-P2A-nlsRFP)</i> line .....	113
Degradation of N3ICD-GFP <i>in vivo</i> using the inducible VhhGFP4-hSPOP-nls nanobody .....	118
Conditional and sporadic loss of Notch3-GFP in embryo creates clones in adult .....	124
Conditional and sporadic expression of the degradation system in adults .....	128
Conditional and sporadic loss of <i>notch3</i> mRNA in adults .....	134
Supplementary Figures .....	141
Validation of anti-RFP/mCherry nanobodies targeted to the nucleus for the selective degradation of nuclear RFP/mCherry protein in zebrafish embryos .....	141
<b>Materials and Methods .....</b>	<b>145</b>
Zebrafish husbandry and strains .....	145
Generation of <i>pXT7_Nfbxw11b-VhhGFP4</i> .....	145
Capped mRNA for embryonic microinjections .....	145
Generation of zebrafish transgenic line <i>bact2:loxP-stop-loxP-VhhGFP4-hSPOP-nls-P2A-nlsRFP</i> .....	146
Generation of <i>pXT7-VhhGFP4-hSPOP-nls-P2A-nlsRFP</i> .....	147
Generation of zebrafish knock-in line <i>notch3<sup>GFP/GFP</sup></i> .....	148
RNAi-mediated gene silencing .....	149
Genotyping .....	150
LY treatment .....	150
4-hydroxytamoxifen treatment .....	150
Induction in embryos .....	150
Induction in adults .....	150
Immunohistochemistry .....	151

RNAscope smFISH against <i>notch3</i> .....	151
Image acquisition, processing and cell counting.....	152
Statistical analysis .....	153
<b>Discussion.....</b>	<b>154</b>
The <i>notch3</i> <sup>GFP</sup> line: a multifunctional tool for studying the Notch3 signaling pathway ....	156
The nanobody tool: a promising method for analyzing the nuclear functions of Notch3 protein and many other proteins.....	160
The <i>notch3</i> shRNA: an alternative method targeting all Notch3 functions in isolated cells or clones.....	164
Conclusion.....	166
<b>Annex.....</b>	<b>168</b>
Review article.....	168
<b>References .....</b>	<b>193</b>

## Acknowledgments

Before presenting my project, I would like to thank in a few words the persons who contributed to its completion. The PhD was a demanding experience through which I learned many scientific skills across bench work, readings, writings, conferences, and scientific discussions, but it was even more educational at the personal level. While spending most of my time in the lab, I got closer to my co-workers who became one of my main motivations to come in the lab.

For her huge help throughout the four years of the project and her availability despite a tight schedule, I would like to thank my thesis supervisor, Laure. Her tough demands pushed me always to surpass my limits and improve myself. She is a model of mental strength and succeeded in creating a friendly group where we work among super-talented and nice people.

For her training, advice, and patience, I would like to thank Sara. She taught me all the molecular biology needed for the project and the tips to become even better. She is a great scientist but above all a wonderful woman.

During my last year of PhD, I got the chance to closely work with Isabelle and Ilona, and I wanted to thank them. Since I arrived in the lab, Isa helped me with ISH and many other techniques. Last year, she did a lot of experiments for my project that were decisive for the coming steps. She is nice and sensitive and I was happy to share the office with her.

Ilona was freshly arrived in the lab but she directly showed her implication in the project. She rapidly learned the techniques, worked cleverly, and even became an expert in electroporations. She is a super nice person. I wish her the best for the future.

The project was challenging but with the fish breeding and health, everything was smooth and easy, and for that, I would like to thank Sébastien, Colas, and Nathan. Seb guided me in the use of the zebrafish model and taught me animal manipulation techniques. Beyond his help, his kindness and his humor made the fish facility and our office even more pleasant places.

For his work at the fish facility and his help, I would like to thank Nathan. He is always positive and I enjoyed working and discussing with him. He also helped me take a step back on the project and feel better.

For their support and their kindness, I would like to thank Melina and Tanya. They always took the time to help and discuss while leading their challenging projects as masters. I am very proud to have shared their journeys for a time. Melina's maturity in her vision of science and her



personal life has been very inspiring for me. She always found good words to give me back the courage to face the project.

Tanya helped me through our many discussions and times at the bench. She has a radiant personality and made the lab a better place to work. She was attentive and sensitive to my feelings and we laughed a lot together.

For his help with picture analyses and microscopy, I would like to thank Nico. He was a good teacher, patiently explaining the concepts step by step. His calmness and kindness make him a super nice person to work with.

For having shared their experience of PhDs in the lab, I would like to thank David, Miriam, and Marielle. They were all impressive in their way of cleverly and strongly managing their project. David nicely helped me with the scRNAseq data and the coding on R. Miri helped me with the shRNA protocol and was always supportive and positive with me. Marielle has a fantastic personality and I was delighted to share the office with her. We spent a lot of time together, and we will again in different circumstances. I wish them the best.

For his way of enjoying the world and approaching science, I would like to thank Georg.

For his help on techniques such as ISH during my first years of PhD, I would like to thank Fred. He is super nice and I missed our morning discussions at the bench after his retirement.

For their help on the administrative and organizational plans, and their kindness, I would like to thank Vesna and Sonia.

I would also like to thank all the other super nice members of the lab: Laure M., Udi, Asna, Anne, Iris, Miguel, and Naomi.

For their trust and the nice times together, I would like to thank the previous labs that gave me the opportunity to discover the bench work and the passion for science. I would like to thank Antoine Guichet, Romain Levayer, and their teams, in particular the wonderful Véronique, Léo, and Florence.

For having shared the time of the PhD with them, I would like to thank Tara and Alina. They are brilliant in their work and exceptional women who improved my PhD time with their friendship.

For making our floor a nicer place, I would like to thank all my colleagues from there, in particular Névé, Loan, Arantxa, Florence, Léo, Romain, Alexis, Ralitza, Tom, and Flora.

For making the department of research a better place, I would like to thank other nice colleagues, and in particular Sarah, Carole, Jérémy, Claire, Laurianne, and Maria.

For having accepted to be part of my PhD committee, for their time and all their advice, I would like to thank Pauline Spéder, Robert Kelsh, and Fiona Francis.

For being part of my PhD jury, for their time, their advice, and the great scientific discussion, I would like to thank Maximilian Fürthauer, Estelle Hirsinger and Muriel Perron.

To finish, my family and my friends have also been super important to me during the PhD.

For always being here for me and her trust, I would like to thank my sister Emma. For their unlimited support and their help, I would like to thank my parents. For his way of making everything beautiful, for his support and his patience, I would like to thank Sébastien. I would also like to thank Adeline, Louis-Marie, and Cécile. For their trust and positivity, I would like to thank my grandparents, my aunts and uncles, and my cousins.

For their friendship and for being great, I would like to thank my friends: Camille, Benoit, Camilla, Marie, Claire, Catherine, Arlane, and Alain. In another life, I would also like to thank Ivan for his support for years.

## Abbreviations

4-OHT	4-Hydroxytamoxifen
ADAM10	A Disintegrin and metalloproteinase domain-containing protein 10
AJ	Apical junction
AKT	Protein kinase B
ANK	Ankyrin
aNSC	Activated neural stem cell
Ascl	Achaete-Scute homolog
ATP	Adenosine triphosphate
BAC	Bacterial artificial chromosome
Bact2	Beta-actin2
BBB	Blood-brain barrier
bHLH	Basic Helix-Loop-Helix
BMP	Bone morphogenetic protein
Bp	Base pair
BrdU	5'-bromo-2'-deoxyuridine
CADASIL	Cerebral Autosomal Dominant Arteriopathy with Subcortical Infarcts and Leukoencephalopathy
CBF1	Centromere Binding Factor 1
Cmlc2	Cardiac myosin light chain 2
CMV	Cytomegalovirus
CNS	Central nervous system
CRISPR	Clustered regularly interspaced short palindromic repeats
CSF	Cerebrospinal fluid
DAPI	4',6-diamidino-2-phenylindole
DAPT	N-[N-(3,5-difluorophenacetyl)-L-alanyl]-S-phenylglycine-butyl ester
DG	Dentate gyrus
Dll, Dl	Delta-like, Delta
dMG	Differentiating Müller glial cell
DMSO	Dimethyl sulfoxide
DNA	Deoxyribonucleic acid
Dpe	Day post-electroporation
Dpf	Day post-fertilization
E	Embryonic day
EGF	Epidermal growth factor
Elavl3, Hu	ELAV-like neuron-specific RNA binding protein
ER	Endoplasmic reticulum
ERT2	Mutant Estrogen Receptor
F	Founder
Fng	Fringe
GA	Golgi apparatus
Gfap	Glial fibrillary acidic protein
GFP	Green fluorescent protein
GS	Glutamine synthetase
H	Hour
HD	Heterodimerization domain
Hes/her/Hey	Hairy and Enhancer of Split-related
Hmgb1	High-mobility group box 1 protein

Hpf	Hour post fertilization
Id	Inhibitor of DNA binding
IHC	Immunohistochemistry
INM	Interkinetic nuclear migration
IP	Intermediate progenitor
Jag	Jagged
KD	Knockdown
KI	Knock-in
KO	Knockout
LAMP1	Lysosomal-associated membrane protein 1
LFP	Lateral floor plate
LNR	Lin12-Notch repeats
LY	LY411575
MAML1	Mastermind-like transcriptional co-activator 1
Mcm	Minichromosome maintenance protein complex
MHB	Midbrain-hindbrain boundary
Mib	Mindbomb E3 ubiquitin protein ligase
MN	Motor neuron
MO	Morpholino
Mpf	Month post-fertilization
mRNA	Messenger RNA
mTORC	Mechanistic target of rapamycin complex
NE	Neuroepithelial cell
NECD	Notch extracellular domain
Neurog	Neurogenin
NEXT	Notch extracellular truncation
NICD	Notch intracellular domain
Nls	Nuclear localization signal
NP	Neural progenitor
NRR	Negative regulatory region
NSC	Neural stem cell
NSPC	Neural stem and progenitor cell
OB	Olfactory bulb
OPC	Oligodendrocyte progenitor cell
PCNA	Proliferating cell nuclear antigen
PDGFR $\beta$	Platelet-derived growth factor receptor beta
PEST	Proline, Glutamic acid, Serine and Threonine rich domain
PI3K	Phosphoinositide 3-kinase
pMN	Motor neuron progenitor cell
POI	Protein of interest
PSA-NCAM	Polysialylated neuronal cell adhesion molecule
PTEN	Phosphatase and tensin homolog
qNSC	Quiescent Neural stem cell
Rab	Ras-related proteins
RAM	RBP-J $\kappa$ -association module
RBP-J $\kappa$	Recombination signal Binding Protein for immunoglobulin kappa J region
RFP	Red fluorescent protein
RG	Radial glial cell
RGL	Radial glia-like cells
RMS	Rostral migratory stream

RNA	Ribonucleic acid
RPC	Retinal progenitor cell
S100 $\beta$	S100 calcium-binding protein beta
Sara	Smad anchor for receptor activation
SGZ	Subgranular zone
shRNA	Short hairpin RNA
smFISH	Single molecule fluorescence <i>in situ</i> hybridization
SOP	Sensory organ precursor cell
Sox2	SRY-Box transcription factor 2
SVZ	Subventricular zone
TAD	Transactivation domain
TJ	Tight junction
UTR	Untranslated region
VZ	Ventricular zone
ZO1	Zonula-occludens 1

## Summary

Throughout the lifespan of most vertebrates, new neurons are continuously generated, playing a crucial role in the development and homeostasis of the nervous system. This neurogenesis is driven by neural stem and progenitor cells (NSPCs), which have the potential to divide, differentiate, or self-renew. In embryos, NSPCs are highly proliferative but gradually become quiescent, a state that is predominant in adult NSPCs. Extensive research demonstrated that Notch signaling is involved in the control of NSPC states and fates, however, the precise mechanisms by which it maintains NSPCs remain only partially understood. In Dr. Laure Bally-Cuif's laboratory, we investigate the molecular, cellular, and population-level principles that balance NSPCs maintenance and neurogenesis, using the zebrafish brain as our model system.

My PhD research focused on the role of the Notch3 signaling pathway in NSPCs. The canonical Notch pathway is activated through interactions between a transmembrane Notch receptor and a ligand, both exposed on neighboring cells. This triggers cleavage of the intracellular domain of the receptor (NICD), which then translocates into the nucleus to activate target genes' transcription. Understanding Notch3 signaling is complicated by its diverse roles across different tissues and life stages, as well as its varying effects both at the plasma membrane and in the nucleus. Previous studies have shown that Notch3 is critical for maintaining NSPC progenitor status during development and promoting NSPC quiescence in adulthood. However, existing methods have not met the combined objectives of enabling conditional, long-term, and tractable Notch3 loss-of-function in NSPCs, nor have they effectively targeted only the nuclear functions of Notch3.

To address this, I adapted the Ab-SPOP technique, which relies on a GFP tag fused to the protein of interest (POI). This tag is recognized by a modified nanobody that promotes *in vivo* ubiquitination and proteasomal degradation of the POI. Using CRISPR-Cas9, I generated an endogenous *notch3-GFP* fusion by inserting *GFP* at the extremity of the NICD coding region and validated the functionality of the Notch3-GFP fusion protein. This GFP tag enabled me to monitor Notch3 signaling dynamics in NSPCs and assess the feasibility of quantifying nuclear NICD-GFP as a proxy of the canonical Notch3 signaling activity.

After preliminary validations of the functionality of the nanobody tool, I created a transgenic line conditionally expressing the modified nanobody and an expression marker in NSPCs under *Cre-loxP* recombination. I then crossed these transgenic fish with the *notch3<sup>GFP</sup>* knock-in (KI) line. I confirmed the efficiency of NICD-GFP degradation in the nuclei of NSPCs in 6 days post-fertilization larvae. I also validated the inducibility of the transgene expression directly in adult fish and the formation of transgene-expressing cell clones in the telencephalon. Moreover, adult fish induced as embryos exhibited large transgene-expressing cell clones, including a few NSPCs and many differentiated cells.

My work prepared the analysis of Notch3 functions and set up a method easily transposable to other proteins. To continue my project, I will quantify NICD-GFP in the nuclei of transgene-expressing adult NSPCs to validate the efficiency of the system in adult cells. Additionally, I have developed and conducted initial validations of *notch3* shRNAs as an alternative method for medium-term and tractable knock-down -although not restricted to nuclear signaling-. Ultimately, I will use these new tools to induce Notch3 loss-of-function in NSPCs, and analyze the resulting phenotypes inside the clones and their neighboring cells.

## Résumé

Chez la plupart des vertébrés, de nouveaux neurones sont continuellement générés au cours de la vie, jouant un rôle essentiel dans le développement et l'homéostasie du système nerveux. Cette neurogénèse provient des cellules souches et progénitrices neurales (CSPNs), qui ont le potentiel de se diviser, et se différencier, ou s'auto-renouveler. Chez l'embryon, les CSPNs sont prolifératives et deviennent progressivement quiescentes, un état dominant des CSPNs adultes. La voie de signalisation Notch est impliquée dans la régulation des CSPNs, mais les mécanismes précis par lesquels il maintient les CSPNs ne sont encore que partiellement compris. Dans le laboratoire du Dr Laure Bally-Cuif, nous étudions les processus moléculaires, cellulaires et populationnels qui contribuent à l'équilibre entre le maintien des CSPNs et la neurogénèse, en utilisant le cerveau du poisson zébré comme système modèle.

Mes recherches doctorales ont porté sur le rôle de la voie Notch3 dans les CSPNs. La voie canonique est activée par l'interaction entre un récepteur transmembranaire Notch et un ligand, les deux exposés sur des cellules voisines, déclenchant le clivage du domaine intracellulaire du récepteur (NICD), qui se déplace ensuite dans le noyau pour activer la transcription de gènes cibles. Etudier Notch3 est complexe en raison de ses multiples rôles dans plusieurs tissus et stades de la vie, ainsi que par ses activités à la fois à la membrane plasmique et dans le noyau. Des études ont montré que Notch3 est essentiel pour maintenir le statut de progéniteur des CSPNs au cours du développement, et pour promouvoir leur quiescence à l'âge adulte. Cependant, ces méthodes ne permettent pas de combiner la perte de fonction conditionnelle de Notch3 à la possibilité d'une perte de fonction à long-terme, qui soit traçable dans les CSPNs, et ciblant efficacement uniquement les fonctions nucléaires de Notch3.

Pour créer cette méthode, j'ai adapté la technique Ab-SPOP, qui utilise une étiquette GFP fusionnée à la protéine d'intérêt (POI), et un nanobody modifié qui reconnaît GFP et promeut *in vivo* l'ubiquitination et la dégradation de la POI par le protéasome. Par CRISPR-Cas9, j'ai créé le gène *notch3-GFP* en insérant *GFP* à l'extrémité de la région codante du NICD endogène, puis j'ai validé la fonctionnalité de la protéine de fusion Notch3-GFP. Cette GFP m'a permis d'approcher la dynamique de la signalisation Notch3 dans les CSPNs, et de valider la faisabilité d'utiliser la quantité de NICD-GFP dans le noyau comme indicateur de l'activité de la signalisation Notch3.



Après validation du nanobody, j'ai créé une lignée transgénique exprimant, de manière conditionnelle le nanobody modifié et un marqueur d'expression dans les CSPNs via *Cre-loxP*. J'ai ensuite croisé ces poissons transgéniques avec la lignée KI *notch3<sup>GFP</sup>*. J'ai confirmé l'efficacité de la dégradation de NICD-GFP dans les noyaux de CSPNs sur des larves de 6 jours. J'ai validé l'expression du transgène, après induction chez le poisson adulte, et observé la formation de clones de cellules exprimant le transgène dans le télencéphale. De plus, les poissons adultes induits en tant qu'embryons présentaient de grands clones, comprenant quelques CSPNs et de nombreuses cellules différenciées.

Mes travaux ont préparé l'analyse des fonctions de Notch3 et mis en place une méthode transposable à d'autres protéines. Dans la suite de mon projet, je quantifierai NICD-GFP dans les noyaux des CSPNs adultes exprimant le transgène afin de valider l'efficacité du système dans les cellules adultes. De plus, j'ai développé et effectué les premières validations de shRNAs ciblant *notch3* comme méthode alternative (bien qu'efficace sur des échelles de temps moindres et ne ciblant pas spécifiquement les fonctions nucléaires de Notch3). Finalement, j'utiliserai ces outils pour étudier la perte de fonction de Notch3 dans les CSPNs, en analysant la composition des clones et leurs cellules voisines.

# Introduction

## General introduction

Neurogenesis is a multistep and multifactorial process by which new functional neurons are generated from neural stem and progenitor cells (NSPCs) in the nervous system (Götz et al., 2016; Bond et al., 2015). It involves several stages: commitment of NSPCs to a neuronal lineage, cell cycle exit, differentiation into specific neuron types, migration to appropriate brain regions, and functional integration into neural circuits (Lim and Alvarez-Buylla, 2014; Urbán and Guillemot, 2014). Neurogenesis also involves some degree of amplification or self-renewal of NSPCs to maintain the progenitor pool, at least temporarily.

In NSPCs in the brain, neurogenesis is regulated by a complex interplay of intrinsic genetic programs (e.g., sub-cellular organization, cell morphology, transcription factors...) and extrinsic environmental factors (e.g., secreted signals, cell-cell interactions), which change significantly from the embryonic to the adult brain, and can include systemic states such as physical exercise, enriched environment, diet, stress or aging (Toda and Gage, 2018; Chen et al., 2016; Pérez-Domínguez et al., 2018, Kempermann et al., 2015). It evolves from being widespread and dynamic in embryonic neurogenic domains, to being more restricted in adult neurogenic niches, and it plays distinct roles at these different life stages (Lim and Alvarez-Buylla, 2016; Navarro Negredo et al., 2020). In embryos, it is involved in brain growth, regional specification, and neuronal circuit formation. During development, it supports brain maturation, and the refinement of brain functions, including learning and memory formation (Götz et al., 2016; Bond et al., 2015). In the adult mouse, neurogenesis is necessary for hippocampal function, mood regulation and brain plasticity, balancing neural circuit homeostasis with neural stem cell protection (Ming and Song, 2011; Toda et al., 2019).

In addition to these fundamental physiological functions, neurogenesis can go astray, often with dramatic consequences. For example, it is believed that the derailment of NSPCs can lead to the development of brain tumors, and abnormal neurogenesis has also been implicated in various neurodegenerative and psychiatric diseases, such as Alzheimer's disease and Major Depressive Disorder (MDD) (Loras et al., 2023; Fontán-Lozano et al., 2020; Yelle et al., 2019; Azzarelli et al., 2018; Winner et al., 2011; Berger et al., 2020). However, in humans, the

existence of adult neurogenesis participating in brain homeostasis remains controversial (Zhou et al., 2022b; Kempermann et al., 2018).

Most *in vivo* studies of neurogenesis have been conducted in rodents, notably the mouse, which offers powerful genetic tools for lineage tracing and functional assays, and standardized behavioral assays to probe neurogenesis output at the organismal level (Pereira et al., 2019; Yamakawa et al., 2020; Hoffman, 2018; Lyon et al., 2021). Until 15 years ago or so, the zebrafish with its transparent embryos and rapid development, was mainly used to study developmental neurogenesis. However, the discovery of its prominent adult neurogenesis, and the development of interventional and imaging methods to transiently perturb and film NSPCs in the zebrafish adult dorsal telencephalon (pallium), more recently pushed it to become an important complementary model to mouse (Kizil et al., 2012; Schmidt et al., 2013). The zebrafish is the model I have been using, and which I will also introduce below, with details on its advantages but also technical limitations as I started my PhD.

The outstanding importance of neurogenesis for organismal functionality and health makes it fundamental to understand its control mechanisms in time and space. In the Bally-Cuif lab, a specific focus is placed on Notch signaling, a pleiotropic pathway controlling cell fate decisions in particular in the nervous system: in the brain, Notch signaling contributes to maintaining NSPC populations, balancing proliferation and quiescence, and regulating differentiation. The lab more specifically identified one Notch receptor, Notch3, as a regulator of neural stem cell quiescence from juvenile stages onwards in the zebrafish telencephalon. A lot however remains to be studied to understand Notch3 function “in context”, i.e., its effect in individual vs populations of NSPCs, its specific impact at different stages of life and in different brain territories, and the long-term consequences of its invalidation, *in vivo*. This is the context of my PhD work.

Within this frame, I will briefly cover the following points in my introduction: I start with general definitions (1) and then touch upon three major subjects: neural progenitors (NPs) and neural stem cells (NSCs) (2), the Notch signaling pathway (3), and methodologies used to probe gene function, notably in the specific case of Notch3 signaling in adult NSPCs (4).

# 1 Definitions

## *1.1 Progenitor versus stem cells*

Neurogenesis is extensively studied, and depending on the type of progenitor cell, their cellular hallmarks, the developmental stage, or the species, the nomenclature varies. Here we will adopt a simple rule, which mostly reflects the cell neurogenic potential, the lifetime of the cell and the developmental stage. In sum, within NSPCs, **NPs** will define cells with a limited (typically a few weeks in a vertebrate model species such as zebrafish or mouse) or unknown neuron-generation potential, and **NSCs** will define cells with an extensive long-term potential (typically a few months or more). Both NPs and NSCs can generate neurons and glial cells via the production of more committed and proliferating progenitors that will exhaust at short term. When committed to generate neurons, the latter progenitors will be defined as intermediate neuronal progenitors (**IPs**). NPs typically refer to embryonic cells and NSCs to post-embryonic and adult cells.

## *1.2 Nomenclature along lifetime progression in zebrafish and mouse*

The embryonic periods of brain development in zebrafish and mouse have different durations, but the two species have comparable lifespans in the wild (2-3 years). In mouse, the embryonic period covers the gestation time, around 20 days, whereas in zebrafish, which have an external development in the chorion, the embryonic period covers the time before hatching, i.e., 48 hours (Figure 1A) (Kaufman, 1992; Kimmel et al., 1995). While, in animals, the adult age is considered the age at which the individual can reproduce, the age at which the brain is considered adult does not necessarily coincide with sexual maturity. The human brain is generally considered to reach adulthood around the age of 25 (Sowell et al., 2004). This is when the prefrontal cortex, responsible for executive functions like decision-making and impulse control, is fully developed. The mouse brain is considered to reach adulthood around 2-3 months of age, when it reaches a stable structure and function with continued but slower-paced neurogenesis (Semple et al., 2013).

In zebrafish, the situation is complicated by the fact that sexual maturation, as well as overall body and brain growth, strongly depend on external stimuli such as temperature, food and physical space (Singleman and Holtzman, 2014). Under standard laboratory conditions, the zebrafish is considered to reach sexual adulthood around 3 months of age, and this also

coincides with a plateauing in brain growth and slowed-down neurogenesis (Figure 1A) (Labusch et al., 2020; Singleman and Holtzman, 2014; Parichy et al., 2009). At this stage, the brain is believed to be fully functional, including in the telencephalon, where protracted neurogenesis in the hippocampal area starts at around 2-3 weeks of age (Dirian et al., 2014; Valente et al., 2012). In mouse, between embryonic and adult stages, individuals are named juveniles (Figure 1A). In zebrafish, an intermediate “larval” stage is also identified, between 3 and 21 days post-fertilization approximately (Figure 1A) (Stednitz and Washbourne, 2020; McMenamain and Parichy, 2013).

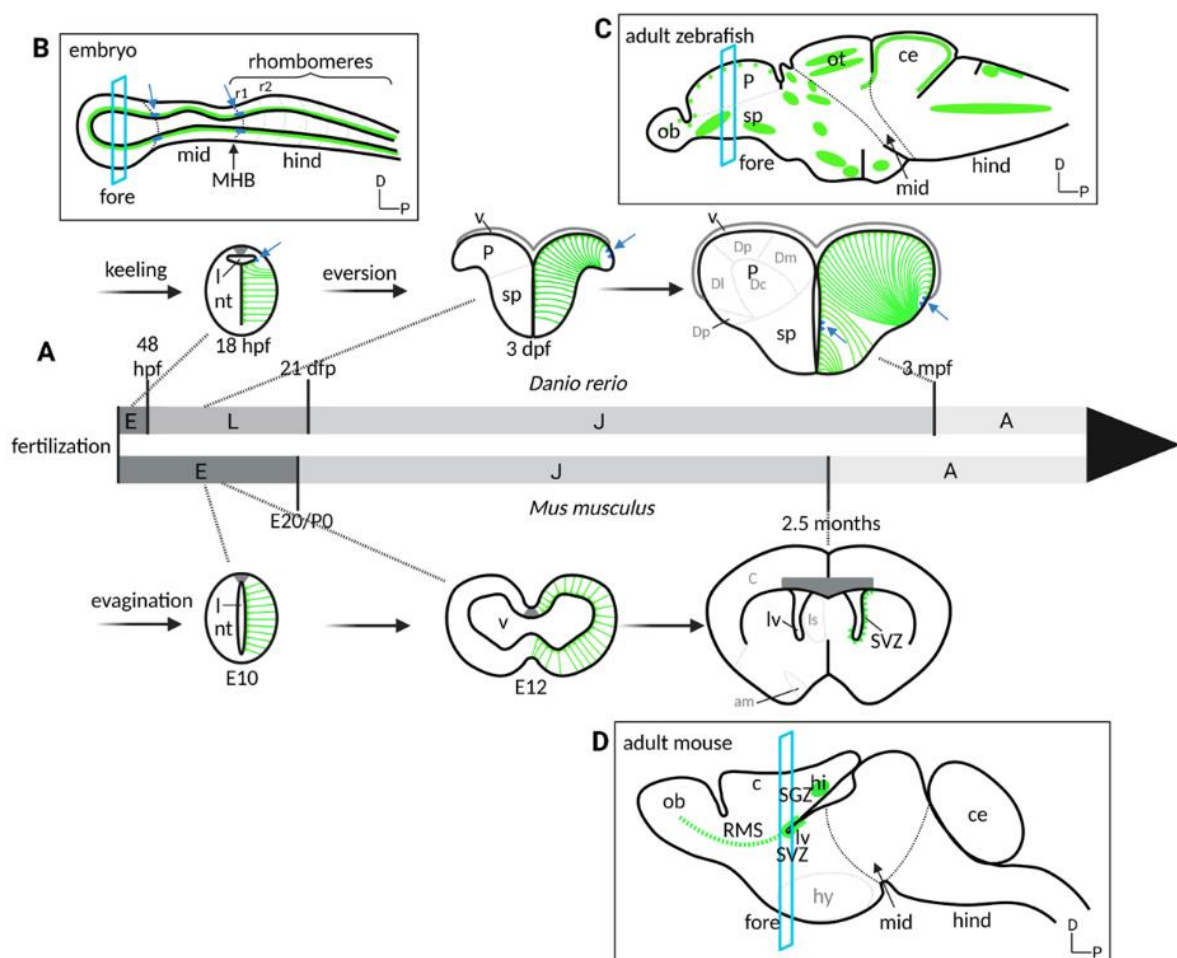


**Figure 1: Neurogenic domains and niches in zebrafish (*Danio rerio*) and mouse (*Mus musculus*) brains at different ages, and comparison of forebrain anatomies (see references in text)**

(A) Chronology of the different life steps in zebrafish and mouse, and coronal sections of forebrain neurogenic domains and niches. In mouse, the neural tube is created by the evagination of the neural plate. In zebrafish, the neural plate forms a neural keel generating a neural rod, and finally forms a lumen to create the neural tube. In zebrafish, at the level of the future pallium, the neural tube is everted: the tube is turned outward, exposing dorsally the cells lining its ventricular surface. By this mechanism, the dorsal *tela choroidea*, represented as a dark grey line, is stretched to cover the ventricle. NEs are represented in dark blue (also indicated by arrows) and RGs in green. am, amygdala, c, cortex, Dc, dorso-central pallium, Dd, dorso-dorsal pallium, Dl, dorso-lateral pallium, Dm, dorso-medial pallium, Dp, dorso-posterior pallium, l, lumen, ls, lateral septum, lv, lateral ventricle, nt, neural tube, P, pallium, sb, subpallium, SVZ, subventricular zone, v, ventricle.

(B) Sagittal section of the anterior neural tube in early embryos, and neurogenic domains. The anterior neural tube is regionalized into three primary brain vesicles: the forebrain, the midbrain, and the hindbrain. Black dotted lines separate these regions. The hindbrain region is subdivided into rhombomeres, each with its own identity, and separated by rhombomeres boundaries (grey dotted lines). The neurogenic domain covers the ventricular surface of the neural tube and contains NEs represented in blue (also indicated by arrows) and RGs represented in green. The blue square represents a coronal section presented in A (left pictures). fore, forebrain, hind, hindbrain, mid, midbrain, MHB, midbrain-hindbrain boundary, r1/2, rhombomere 1/2.

(C) Sagittal section of the zebrafish adult brain, and neurogenic niches. The adult zebrafish brain contains many neurogenic niches, which are represented in green here. Black dotted lines separate these regions. In the pallium, which is the equivalent of the mammalian dorsal telencephalon, neurogenesis is spread along the dorsal surface (indicated by the green dots). A grey dotted line separates the pallium from the subpallium. The blue square represents a coronal section presented in A (upper right picture). ce, cerebellum, fore, forebrain, hind, hindbrain, mid, midbrain, ob, olfactory bulb, ot, optic tectum, p, pallium, sp, subpallium.

(D) Sagittal section of the mouse adult brain, and neurogenic niches. The adult mouse brain contains two main neurogenic niches, which are represented in green here: the subgranular zone of the dentate gyrus of the hippocampus, and the subventricular zone of the lateral ventricles. From the latter, newly generated cells migrate toward the olfactory bulb via the rostral migratory stream. The blue square represents a coronal section presented in A (lower right picture). ce, cerebellum, c, cortex, fore, forebrain, hind, hindbrain, mid, midbrain, hi, hippocampus, hy, hypothalamus, lv, lateral ventricle, ob, olfactory bulb, RMS, rostral migratory stream, SGZ, subgranular zone, SVZ, subventricular zone.

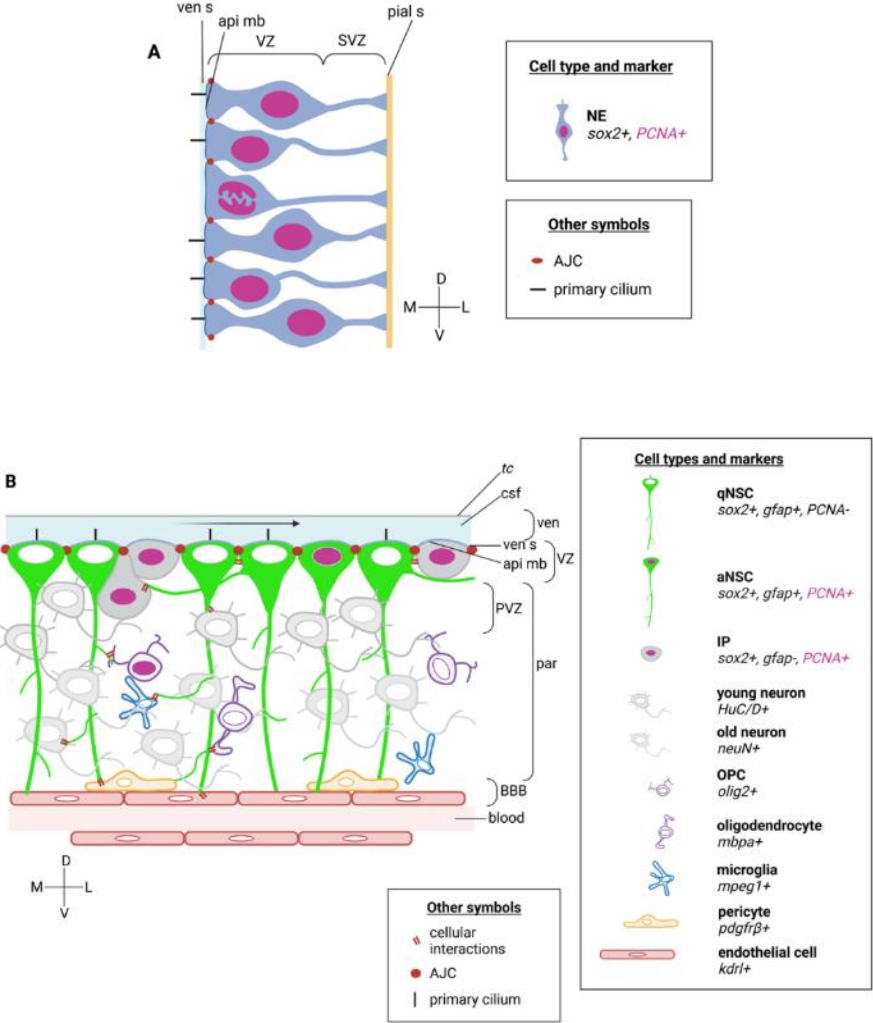
## 2 The neurogenesis process

### *2.1 Progenitor cells over a lifetime*

At early developmental stages (before embryonic day 10 -E10- in mouse, and before 10 hours post-fertilization -hpf- in zebrafish), NPs are neuroepithelial cells (**NEs**), readily specified from the neuroectoderm (Figure 2A) (Pinto and Götz, 2007; Neely and Lyons, 2021). After a phase of self-amplification, they elongate, express astroglial markers together with progenitor markers, and become radial glial cells (**RGs**) (Figure 1A-D, 2B,C). Embryonic NEs and RGs are very similar between species, although, compared to mouse, zebrafish NEs polarize relatively late and the transition from NEs to RGs is blurred. The transition from NEs to RGs takes place around E10-E12 in mouse, and during the first 10-18 hours post fertilization in zebrafish (focusing in that case on the acquisition of a polarized and elongated morphology), and is accompanied by the reduction of the cells potency (Figure 1A) (Götz and Huttner, 2005; Pinto and Götz, 2007; Neely and Lyons, 2021). Embryonic RGs are actively dividing to generate IPs and neurons in the neural tube.

In mouse, most neurogenic activity by NEs and RGs is terminated at birth (NPs are then transformed into other glial cells such as astrocytes, or in ependymal cells (Akdemir et al., 2020; Spassky et al., 2005; Kramer-Zucker et al., 2005), except for some limited forebrain territories, the future adult neurogenesis niches (Figure 1D). In zebrafish, numerous embryonic neurogenic niches persist into adulthood (Figure 1C). At least in zebrafish, some NEs with long-lasting

neurogenic capacity are also maintained at the boundaries between neural tube subdivisions at mid- to late embryogenesis, and persist in the adult brain where they stay highly proliferative to generate new NSCs and NEs (Figure 1A,B) (Ganz et al., 2010; Kaslin et al., 2017).



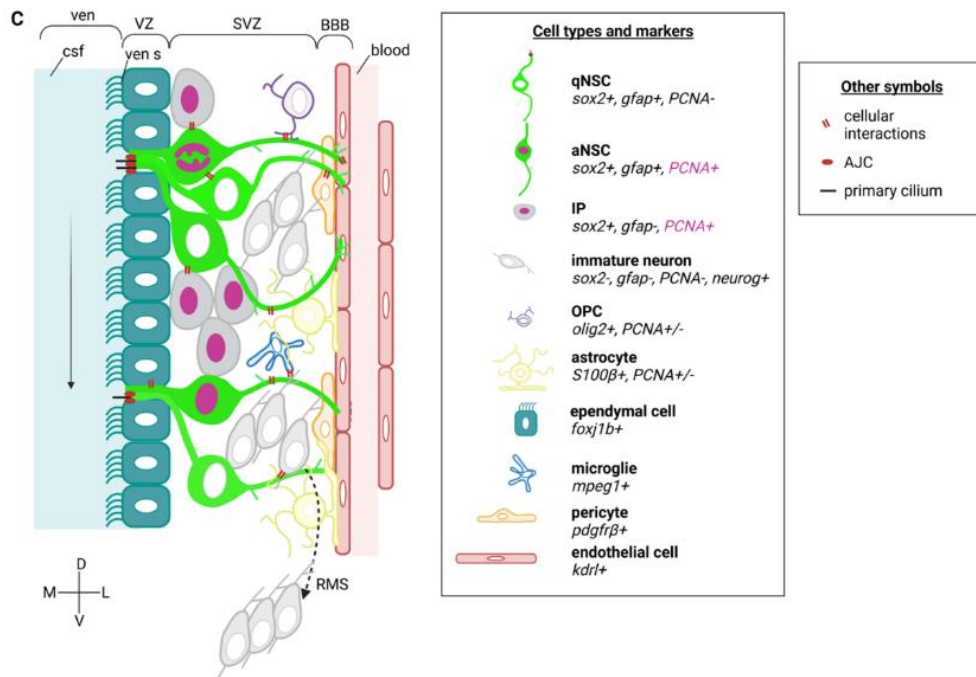


**Figure 2: Neurogenic niches in the early embryo, the adult zebrafish pallium, and the adult mouse SVZ (adapted from Taverna and Huttner, 2010; see other references in text)**

(A) NEs in the early embryonic neural tube. Nuclei from proliferating cells are represented in pink. NE, neuroepithelial cell, pial s, pial surface, SVZ, subventricular zone, ven s, ventricular surface, VZ, ventricular zone. (B) Neurogenic niche of the adult zebrafish pallium. Two short red lines represent some examples of direct cellular interactions. Nuclei from proliferating cells are represented in pink. AJC, apical junction complex, aNSC, activated neural stem cell, api mb, apical membrane, BBB, blood-brain barrier, csf, cerebrospinal fluid, IP, intermediate progenitor, OPC, oligodendrocyte progenitor cell, qNSC, quiescent neural stem cell, tc, *tela choroidea*, PVZ, periventricular zone, par, parenchyma, ven, ventricle, ven s, ventricular surface, VZ, ventricular zone. (C) Neurogenic niche of the adult mouse SVZ. Two short red lines represent some examples of direct cellular interactions. Nuclei from proliferating cells are represented in pink. AJC, apical junction complex, aNSC, activated neural stem cell, BBB, blood-brain barrier, csf, cerebrospinal fluid, IP, intermediate progenitor, OPC, oligodendrocyte progenitor cell, qNSC, quiescent neural stem cell, RMS, rostral migratory stream, SVZ, subventricular zone, ven, ventricle, ven s, ventricular surface, VZ, ventricular zone.

Overall, embryonic and juvenile NPs are more proliferative, plastic and neurogenic compared to juvenile and adult NSCs that are more quiescent, and with a more limited capacity for neurogenesis and plasticity (Labusch et al., 2020). These adult characteristics are acquired from around E13.5 to E15.5 in the mouse subventricular zone (SVZ) with an acceleration of proliferation decline at birth, and from 5 and 10 days post-fertilization (dpf) in the zebrafish pallium (Figure 3A) (Furutachi et al., 2015; Alunni et al., 2013; Than-Trong et al., 2018).

A further transition can be observed from adult NSCs to aging NSCs. It is linked with reduced neurogenesis potential and proliferation, and correlates with altered extracellular matrix integrity, and increased senescence, inflammation, and apoptosis. In mouse, depending on the genetic background, the environment, and the health status, this transition begins around approximately 12-18 months, whereas in zebrafish, this transition is less pronounced and may



occur later (Encinas and Sierra, 2012; Lupo et al., 2019). It has been described in 3-year-old animals (Edelmann et al., 2013; Van Houcke et al., 2021).

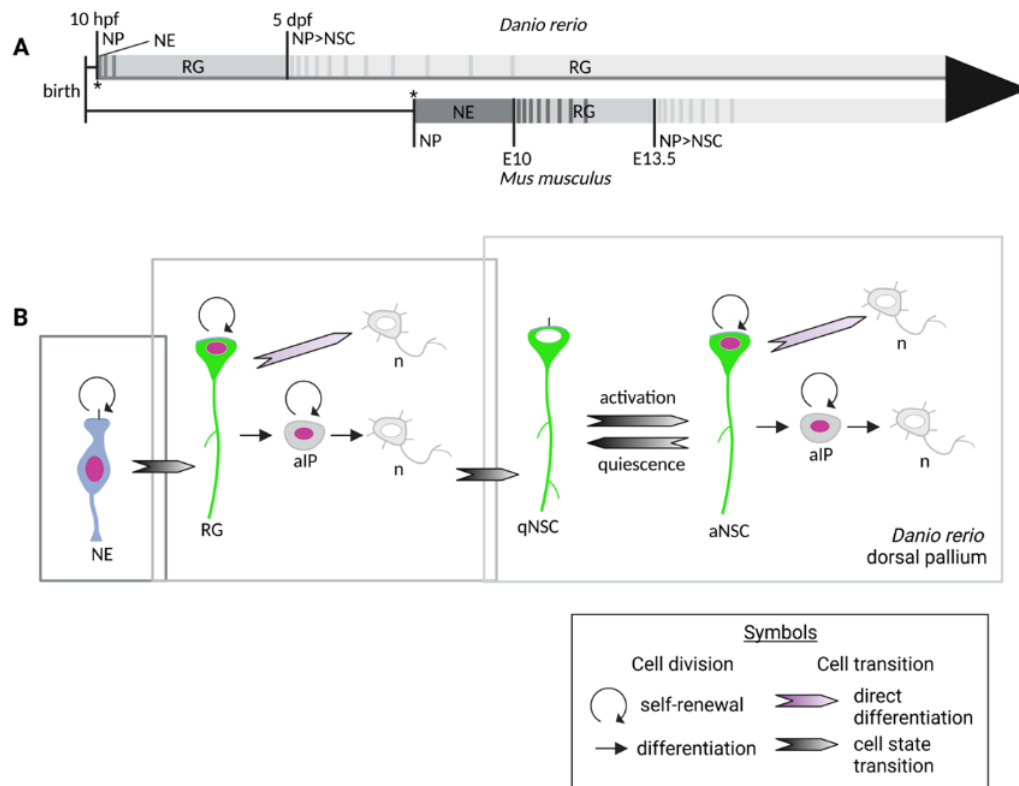


**Figure 3: Chronology of neural stem and progenitor cells in zebrafish (*Danio rerio*) and mouse (*Mus musculus*), and illustration of their division modes using the example of the zebrafish dorsal pallium (see references in text)**

(A) Different neural stem and progenitor cell (NSPCs) types follow one another during the first two weeks of life of zebrafish and mouse. At least in zebrafish, some neuroepithelial cells (NEs) are maintained until adulthood. The neurulation step is indicated with a star. dpf, day post-fertilization, E, embryonic day, hpf, hours post-fertilization, NE, neuroepithelial cell, NP, neural progenitor, NSC, neural stem cell.

(B) NSPC divisions and state transitions in the zebrafish dorsal pallium. NEs divide exclusively in a symmetric amplifying manner. When NEs become radial glia cells (RGs), they can follow the three division modes: symmetric amplifying, symmetric neurogenic, and asymmetric. In the zebrafish dorsal pallium, NSCs have lost their ability to generate OPCs. Division-independent differentiation from RGs to neurons also exists. Nuclei from proliferating cells are represented in pink. aNSC, activated neural stem cell, IP, intermediate progenitor, n, neuron, NE, neuroepithelial cell, NP, neural progenitor, qNSC, quiescent neural stem cell.

## 2.2 NPs and NSCs localization and neurogenic domains

Embryonic NEs and RGs distribute broadly along the neural tube ventricle, in a pattern comparable between vertebrate embryos in different species (Figure 1B). A progressive restriction of the neurogenic regions occurs at juvenile stages, and neurogenic niches in adults display a species-specific distribution, much broader in zebrafish than in mammals (Figure 1C,D).

In mouse, two major niches, restricted to the forebrain and especially active in the young adult are the SVZ of the forebrain lateral ventricle, and the subgranular zone (SGZ) of the dentate gyrus (DG) of the hippocampus (Figure 1D) (Diotel et al., 2020; Obernier and Alvarez-Buylla, 2019; Altman, 1969; Altman and Das, 1965; Altman, 1963; Miale and Sidman, 1961; Uzman, 1960). In contrast, 16 neurogenic niches, distributed in all brain subdivisions, exist in the adult zebrafish as well as in the retina, and are active until a comparably late age (Figure 1C) (Diotel et al., 2020; Labusch et al., 2020; Byrd and Brunjes, 1998; Marcus et al., 1999; Byrd and Brunjes, 2001; Zupanc, 2001; Pellegrini et al., 2007; Grandel et al., 2006; Adolf et al., 2006; Kaslin et al., 2009; Ito et al., 2010). In the SVZ, immature neurons generated by NSCs travel long distances along the rostral migratory stream (RMS) and integrate into existing neural circuits in the olfactory bulb (OB) (Figure 1D) (Ming and Song, 2011). These new neurons participate in olfactory functions and their activity is modulated by environmental factors. In the SGZ, new neurons are continuously generated, contributing to hippocampal functions (learning, memory, mood regulation) (Ming and Song, 2011).

In adult zebrafish, neurogenesis is observed across the entire ventricular surface of the telencephalon, both dorsally (pallium) and ventrally (subpallium) (Figure 1C) (Grandel et al., 2006; Adolf et al., 2006; Diotel et al., 2020; Labusch et al., 2020). The pallium contains regions homologous to the mammalian amygdala (Dm), hippocampus (Dl), cortex (Dc) and olfactory cortex (Dp) (Figure 1A) (Ganz et al., 2014; Anneser et al., 2024; Mueller et al., 2011). This broad neurogenic domain therefore encompasses territories homologous to SVZ and SGZ of mammals. In the ventral domain of the subpallium, a region homologous to the mammalian lateral septum, immature neurons generated by NSCs can migrate tangentially in an RMS-like stripe to reach the OB, where they differentiate into GABAergic and other neuron subtypes to participate in olfactory functions (Mueller et al., 2011; Ncube et al., 2022; Kishimoto et al., 2011; Grandel et al., 2006; Zupanc et al., 2005). Some other immature neurons settle in the subpallium, which contains neurons co-expressing GABA and Acetylcholine and is implicated in social orienting behavior, similarly to the mammalian lateral septum (Grandel et al., 2006; Anneser et al., 2024; Ncube et al., 2022; Stednitz et al., 2018).

Due to a morphogenetic process of eversion taking place during pallial development in the zebrafish embryo, the pallial neurogenic niche becomes exposed dorsally, with a mediolateral inversion in the relative position of homologous pallial subdivisions compared to mammals

(Figure 1A,C,D) (Folgueira et al., 2012). In the adult pallium, immature neurons do not migrate but rather accumulate under their mother NSCs, following an outside-in organization (Furlan et al., 2017). In the pallium, superficial neurons (e.i. young neurons) are small and stellate with widely branching dendrites receiving ascending sensory input, whereas deep neurons in the Dc domain are large and efferent, receiving input from the more superficial neurons and projections to the optic tectum (Furlan et al., 2017). The adult pallium contains a lot of glutamatergic neurons and some GABAergic neurons, and is involved in odor stimulation response (Dp), emotional response (Dl and Dm), and motivational response (Dm), similarly to the mammalian olfactory cortex, hippocampus and amygdala (Anneser et al., 2024; Jacobson et al., 2018; von Trotha et al., 2014).

The everted morphology of the zebrafish pallium has many advantages. *In vivo*, the ventricle surrounding pallial NSCs is easily reachable dorsally for drug or plasmid injections, and the NSCs can be directly imaged in mutant fish with transparent skin (e.g., *casper* mutants (White et al., 2008)). Moreover, after brain extraction, whole-brain stainings and imaging is sufficient to analyze NSCs without the need for brain sections.

Some niches, such as the zebrafish telencephalon and the mouse SGZ, display continuous neurogenic activity during the transition from embryo to juvenile and to adult, and therefore a continuous transition from NPs to NSCs (Figure 3A,B) (Diotel et al., 2020; Urbán and Guillemot, 2014; Obernier and Alvarez-Buylla, 2019). Other niches, such as the mouse SVZ, derive from NPs that are set aside and neurogenically silent from mid-embryonic stages onwards (Fuentelba et al., 2015; Furutachi et al., 2015).

### ***2.3 Molecular markers***

*In situ*, cells in neurogenic domains or niches can be identified by their location and morphology, as well as by specific markers indicating their identity or state (proliferating or quiescent). Interestingly, due to the evolutionary gene conservation among vertebrates, similar cell-type markers can be used for the study neurogenesis in mouse and zebrafish (Howe et al., 2013; Labusch et al., 2020). In the following, I will non-exhaustively indicate the more frequently used markers.

NEs exhibit characteristics typical of epithelial cells and express genes encoding transcription factors that indicate both their neural and progenitor states, such as *SRY-Box transcription factor 2 (sox2)* (Figure 2A), and members of the *Hairy/Enhancer-of-split (Hes/her)* family, particularly *her9/Hes4*. NEs also express neural progenitor cytoskeleton components like *Nestin*. During the transition of NEs to RGs, the expression of genes encoding astroglial markers, such as the structural and membrane proteins *Glial fibrillary acidic protein (gfap)* (Figure 2B,C) and *Vimentin (vim)*, the cytosolic Ca<sup>2+</sup>-binding protein *S100 calcium-binding protein beta (S100β)*, and proteins involved in energetic processes of glycogen synthesis and fatty acid oxidation, such as *Glutamine synthetase (GS)*, and *Fatty acid binding protein 7 brain a (fabp7a)*, also named *blbp*, begins. NPs and NSCs also express transcription factors involved in stemness and/or quiescence, such as *Hes5* in mouse and *her4* in zebrafish. Adult NSCs and astrocytes share the same astroglial molecular markers, such as GS and Fapb7a (Morizet et al., 2024).

Newly formed IPs rapidly lose astroglial markers. Downstream of IPs, cells can be identified by transcription factor-encoding genes such as *Neurogenin (Neurog)* (Figure 2C), and consist of immature neurons that specifically express the Deoxyribonucleic acid (DNA)-binding protein *Distal-less homeobox (DLX)*, in mouse) and *ELAV-like neuron-specific RNA binding protein (Elavl3)*, also named *Hu*, in zebrafish) genes, particularly *HuC/D*, and mature neurons, which among other markers, express the *RNA binding fox-1 homolog 3a (rbfox3a)*, also named *neuN* gene (Figure 2B).

#### **2.4 NPs and NSCs morphology**

Embryonic NEs and RGs are polarized cells that contact the ventricle on one side (apical surface) and the pia (outer surface of the developing brain) on the other side (basal endfoot) (Figure 2A-C) (Kriegstein and Alvarez-Buylla, 2009).

In adults, the majority of NSCs across species are radial astroglia, frequently referred to as RG-like cells (RGL) (Götz and Huttner, 2005). They share with embryonic NEs and RGs a radial shape and therefore an apicobasal polarity. In mouse, non-radial astroglial NSCs coexist with radial NSCs in the neurogenic niches, in slightly lower proportions (Doetsch et al., 1999). As at earlier stages, adult RGL NSCs of the SVZ are in contact with both the ventricular surface and the pial surface, whereas in the SGZ, RGL NSCs processes extend through the granule cell

layer but their apical surface does not contact the brain ventricle (Kriegstein and Alvarez-Buylla, 2009; Fuentealba et al., 2012). Likewise, in the adult zebrafish brain, some neurogenic niches are in contact with the brain ventricles, such as the pallium and the tectal proliferation zone, while others are not, such as in the cerebellum (Labusch et al., 2020; Kaslin and Brand, 2022).

In the embryonic neural tube, the mouse SVZ, and the zebrafish pallium, the NP/NSC soma is oriented toward the ventricular surface and exposes its primary cilium inside the ventricle (Figure 2A-C) (Sirerol-Piquer et al, 2019; Labusch et al., 2020; Louvi and Grove, 2011). In the mouse SVZ, this cilium is an important contact of the NSC with the ventricle, as the ventricular zone (VZ) is overlaid by ependymal cells (Sirerol-Piquer et al, 2019). The transcription factors involved in cilium assembly, such as *Forkhead box J1b* (*foxj1b*) are common ependymal cell markers. The primary cilium, a microtubule-based organelle that is derived from the mother centriole of the centrosome at the level of the basal body, is present in interphasic and quiescent cells, senses the ventricular environment, and is essential for the proper functioning of signaling pathways that regulate neurogenesis (Sokpor et al., 2022; Pala et al., 2017). During mitosis, primary cilia are resorbed or partially internalized (Sokpor et al., 2022). Additionally, embryonic NPs and zebrafish adult pallial NSCs directly contact the ventricular surface via a significant apical membrane portion covered with signaling receptors to allow the transduction of cerebrospinal fluid (CSF) signaling molecules, influencing cell differentiation, migration, etc. (Figure 2B) (Sokpor et al., 2022).

Neighboring NEs or RGs are maintained in close contact at the level of the apical junction complexes through tight junctions (TJs, also called zonula occludens) and apical junctions (AJs, also called zonula adherens) (Figure 2A-C) (Sokpor et al., 2022). TJs seal neighboring cells together to prevent leakage of molecules between them while AJs link the actin cytoskeleton of neighboring cells via the transmembrane glycoprotein Cadherin 2 (Cdh2, also named N-cadherin) (Hartsock and Nelson, 2008). The latter is often used as an AJ marker whereas Zonula-occludens 1 (ZO1) is a TJ marker. The maintenance of apical junction complexes is necessary to maintain the proper ventricular localization, proliferation, and fate choice of the NSPCs and their daughter cells (Sokpor et al., 2022).

NSPCs basal processes contact blood vessels in the brain parenchyma or the basal surface via extending/retracting dynamic branches, and develop short lateral processes, enhancing the

sensing surface of the cell (Figure 2B,C) (Yokota et al., 2010; O'Brown et al., 2018). The blood-brain barrier (BBB) site is the capillary endothelial cells connected by TJs and in close contact with brain pericytes (Figure 2B,C). Endothelial cells and pericytes can be identified by marker genes such as *Kinase insert domain receptor-like (kdrl)* and *Platelet-derived growth factor receptor beta polypeptide (pdgfr $\beta$ )*, respectively. In mouse, the RGL end feet enwrap these cells whereas in zebrafish, the NSC processes only touch the endothelial cells and NSC roles in the BBB have not been well characterized (Figure 2B,C) (O'Brown et al., 2018).

Together, the radial morphology of the NSPCs allows multiple cell-cell contacts and interactions with the local environment.

### ***2.5 NPs and NSCs local environment***

The microenvironment surrounding NSPCs varies over time and in the different neurogenic regions. The first interface between NSPCs and their environment is the extracellular matrix (ECM), regulating cell behavior by influencing cell adhesion, migration, signaling (such as the Notch pathway), differentiation, and maintenance of the neurogenic environment, and the cerebrospinal fluid, containing many circulating molecules (Long and Huttner, 2019; Rasmussen et al., 2022). During development, the CSF contains elements supporting brain development, such as growth factors and nutrients (Figure 2B,C) (Bueno et al., 2020). Besides its protective, nutritive, and recycling roles, the CSF can also transport molecular information over long distances (Lehtinen et al., 2011; Bueno et al., 2020). While the CSF flow is essentially driven by pulsatile movements of blood in the neural tube, the generation of multiciliated ependymal cells participates in the flow by ciliary movement in later stages (Spassky et al., 2005; Kramer-Zucker et al., 2005). In adult zebrafish forebrain, the ependymal cells are regionalized in the *tela choroidea*, the forebrain choroid plexus, and the midline of both the pallium and the subpallium (D'Gama et al., 2021). Physical interaction between the *tela choroidea* epithelium, which is underlined by blood vessels and contributes to CSF production, and the pallial NSCs, remains to be proven. From early developmental stages, NSPCs also exchange with the blood, at the level of the BBB. At the BBB, endothelial cells secrete factors like Vascular endothelial growth factor (VEGF), which influence NSC behavior and neurogenesis (Shen et al., 2004).

Over time, NSCs develop more stable interactions with the cells around them, they contact more cells that are also more mature. In the adult zebrafish pallium, NSCs also develop lateral

processes that reach NSCs and IPs beyond their immediate neighbors (Figure 2B) (Bally-Cuif lab, unpublished). NSCs generate immature neurons that can migrate out of the neurogenic niche or stay, and signal back to the NSCs (Figure 2B,C) (Nóbrega-Pereira and Marín, 2009; Sun et al., 2010; Schmidt et al., 2013, Zhang et al., 2021a).

The NSPCs microenvironment also includes neighboring cells and can dynamically change during development or after injury, or be more constant in adults, depending on cell migration, cell diversity, and cell number. After early neurogenesis, cellular diversity increases in the NSPCs local environment with the generation of other glial cells, such as oligodendrocytes and astrocytes (Figure 2B,C), and the colonization by microglia, which are resident immune cells of the central nervous system (CNS) that originate from the yolk sac (YS) in mouse and the anterior-lateral-plate-mesoderm (ALPM) and in the intermediate cell mass (ICM) in zebrafish (Kuhn et al., 2019; Schebesta and Serluca, 2009; Akdemir et al., 2020; Casano and Peri, 2015).

Microglia in the brain parenchyma can be spotted using immunity-related markers like Macrophage expressed 1, tandem duplicate 1 (Mpeg1). Mature “branched” microglia, watch over for brain immunity but are also necessary for neural circuit refinement by synaptic pruning (elimination of the excess synapses) and apoptosis, and the release of chemokines, cytokines, and growth factors that influence neurogenesis and differentiation of NPs (Araki et al., 2021). Adult microglia, generated from embryonic microglia cells, continue the tissue surveillance but also promote or inhibit neurogenesis depending on the context (Pérez-Rodríguez et al., 2021). Oligodendrocytes come from activated parenchymal Oligodendrocyte progenitor cells (OPCs) that migrate to their final destination and mature (Kuhn et al., 2019). Oligodendrocytes notably contribute to the myelination of the CNS neurons by enwrapping their axons. The oligodendrocyte lineage expresses specific transcription factors such as Oligodendrocyte lineage transcription factor 2 (Olig2), while mature oligodendrocytes express markers related to their myelination function, such as Myelin basic protein a (Mbpa).

Astrocytes have a branched morphology that allows many contacts to contribute to the neuronal activity (tripartite synapse), the structuration of the CNS, the maintenance of the BBB, and the immunity (release cytokines and chemokines, modulate microglia activity...) (Khakh and Deneen, 2019). Unlike mammals, zebrafish do not have astrocytes but their NSCs exhibit spontaneous calcium transients and respond to damage in the CNS and therefore assume astrocyte functions (Jurisch-Yaksi et al., 2020).

## ***2.6 Division process and division modes***

Embryonic NPs and RGs exhibit interkinetic nuclear migration (INM), where the nucleus migrates between apical (G2 and M phases) and basal positions (G1 and S phases) during the cell cycle and allows the cells to divide while maintaining a dense packing (Taverna and Huttner, 2010; Miyata et al., 2014). In particular, this was documented in the mouse embryonic cortex and retina, in the zebrafish embryo hindbrain and retina, and in the adult regenerative retina (Miyata et al., 2014; Fousse et al., 2019; Kawasoe et al., 2020; Baye and Link, 2007; Leung et al., 2011; Lahne and Hyde, 2016; You et al., 2019; Lahne and Hyde, 2023). In the developing mouse brain, NEs nuclei migrate between the apical and basal extremities of the cell, while in RGs, nuclei migrate between the apical extremity and the boundary between the ventricular or subventricular zone (Figure 2A) (Götz and Huttner, 2005; Taverna and Huttner, 2010). At adult stage in the zebrafish telencephalon, INM was observed in subpallial NSCs, but not in the pallium (Grandel et al., 2006). Moreover, while the basal process is inherited by one of the two daughter cells in mouse, this mechanism has not been studied in zebrafish (Miyata et al., 2001).

Different division outputs exist. They distinguish NSC/NSC and NP/NP symmetric amplifying, NSC/IP and NP/IP asymmetric, and IP/IP symmetric differentiative divisions (Kageyama et al., 2020). During early development, NEs divide in an NP/NP manner to amplify the pool of progenitors, whereas later on most NPs divide asymmetrically (Figure 3B) (Kageyama et al., 2020). Indeed, in E17-E19 mouse, NP/IP divisions represent 79%, while NP/NP divisions only account for 10% (Noctor et al., 2004). In addition, NPs divide in an IP/IP manner during an early stage of the zebrafish hindbrain development to generate neurons used to build the first larval neuronal scaffold (Hevia et al., 2022, Belmonte-Mateos et al., 2023). The three division modes are also observed at adult stage, both in mouse and zebrafish. Similarly to NPs, the majority of NSCs in the adult SGZ, VZ-SVZ, and zebrafish pallium divide asymmetrically (Bonaguidi et al., 2011; Encinas et al., 2011; Calzolari et al., 2015; Bottes et al., 2021; Than-Trong et al., 2020). Intravital imaging of mouse SGZ revealed that NSC/NSC divisions represent 18%, NSC/IP represent 78%, IP/IP represent 4% (Bottes et al., 2021). However, these percentages were changed over consecutive divisions. The situation is different in mouse post-embryonic VZ-SVZ, where asymmetric divisions of NSCs are rare. Time-lapse imaging and lineage tracing methods have shown that about 75% of the NSCs divisions are symmetric differentiative (IP/IP), and 25% are symmetric amplifying (NSC/NSC) (Basak et al., 2018;



Obernier et al., 2018). These studies suggest that the maintenance of adult NSCs and the production of neurons might be regulated at the population level through population asymmetry rather than invariant asymmetric divisions.

Finally, in the adult zebrafish pallium, Than-Trong et al. estimated that among the total number of division events, NSC/NSC accounted for 29%, NSC/IP for 42%, and IP/IP for 9%, while direct neuronal differentiation accounted for 20% (Figure 4) (Than-Trong et al., 2020). In the mouse SGZ, symmetric amplifying divisions never followed asymmetric divisions (Encinas et al., 2011; Bottes et al., 2021). In contrast, in zebrafish NSCs, modeling predicts that the choice of the mode of division is stochastic (Dray et al., 2021).

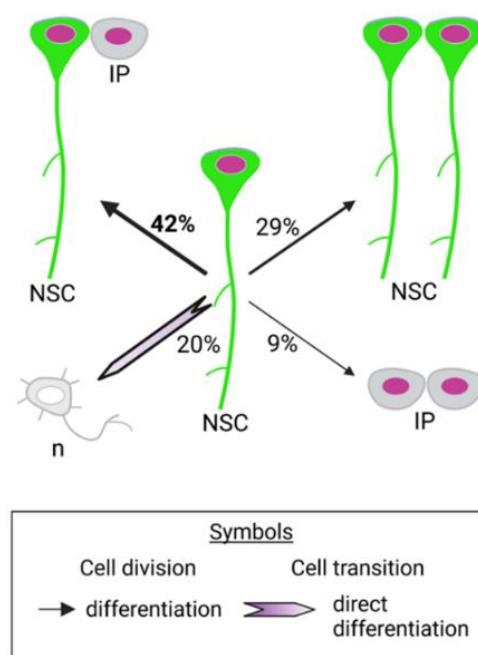


**Figure 4: NSC fate choices in the adult zebrafish pallium (from Than-Trong et al., 2020)**

Results were obtained by intravital imaging on *Tg(gfap:dTomato)* fish in the *casper* background. *dTomato* was expressed in the NSCs and was used as a cell tracker. Between 300 and 400 cells were tracked over eight time points (23 days) in the pallial Dm region. Nuclei from proliferating cells are represented in pink. n, neuron, NSC, neural stem cell, IP, intermediate progenitor.

The molecular mechanisms regulating the modes of division are still poorly characterized. In embryos, the symmetric or asymmetric NSPCs modes of division may be influenced by the orientation of the mitotic spindle, and subsequent asymmetric partitioning of the apical membrane surface (Penisson et al., 2019). The impact of the mitotic spindle angle has not been formally demonstrated in vertebrates. In this case, the fate of the daughter cell can be determined by the mother cell, which asymmetrically partitions fate determinants. During differentiative divisions, the basal body and the ciliary membrane, where signaling receptors

are concentrated and isolated from the rest of the plasma membrane, are preferentially inherited by daughter cells whose NSPCs identity is to be maintained (Sokpor et al., 2022). Other cellular components are asymmetrically inherited by the future NSPC daughter cell and participate in fate determination, such as the polarity protein Par3 or Notch pathway-related proteins (Bultje et al., 2009; Dong et al., 2012; Coumailleau et al., 2009; Fürthauer et al., 2009; Loubéry et al., 2014; Kressmann et al., 2015). Moreover, the surrounding cells and niches have been suggested to influence neuronal cell fates (Obernier and Alvarez-Buylla, 2019).

In the adult, *in vitro* experiments on NSCs from the mouse SVZ showed that during asymmetric divisions, Notch1 activity is inherited by the daughter cell that is fated to stay a NSC, while Notch ligand Delta-like 1 (Dll1) is inherited by the IP (Kawaguchi et al., 2013; Andreu-Agulló et al., 2009). In adult zebrafish, the mechanisms controlling NSC division modes remain to be addressed. However, recent work from our lab has shown that during symmetric NSC/NSC divisions, the Notch ligand DeltaA (Dla) is asymmetrically inherited by one of the two daughter cells, and the cell having Dla is fated to neurogenesis (Mancini et al., 2023).

During development and in adults, NSPCs have also the ability to divide asymmetrically to generate non-neurogenic cells, which are glial cells, namely OPCs and astrocyte progenitors, that further divide to generate oligodendrocytes and astrocytes. This gliogenesis begins during embryonic stages with the generation of OPCs at E9.5 in mouse and at 22 hpf in zebrafish (Kuhn et al., 2019; Schebesta and Serluca, 2009). In mouse, the generation of the first astrocytes arrives later, at E18 (Akdemir et al., 2020). During late embryonic stages (from E14 in mouse and 24 hpf in zebrafish), NEs also generate ependymal cells (Spassky et al., 2005; Kramer-Zucker et al., 2005). In the zebrafish pallium, NSCs have lost their ability to generate oligodendrocyte progenitors (which migrate from other neurogenic niches to colonize the pallium during embryogenesis then are produced from dispersed parenchymal progenitors in adults) (Figure 3B) (Park et al., 2002; Shin et al., 2003; Kirby et al., 2006; Park et al., 2007; Buckley et al., 2010; März et al., 2010b; Masson and Nait-Oumesmar, 2023).

### ***2.7 Early delamination and migration processes involved in neurogenesis***

NSPCs differentiation to give rise to IPs or neurons is generally followed by cell delamination from the ventricular surface after mitosis (Sokpor et al., 2022). The initiation of delamination,

triggered by the expression of proneural genes, essentially depends on the loss of cell adhesion and polarity-related factors (Das and Storey, 2014; Sokpor et al., 2022).

In the differentiating daughter cell, the apical junction complexes are progressively dismantled, loosening cell-cell junctions, driving modifications of the cell cytoskeleton, and causing loss of the apical membrane by actin-myosin-dependent apical constriction and pinching off of extracellular membrane fragments (ectosomes) (Dubreuil et al., 2007; Sokpor et al., 2022). The cell moves away from the ventricle surface and loses its apicobasal polarity with the disappearance of the apical membrane on one side and the retraction of the basal process on the other. The newly formed neuron possibly stays attached to the ventricle surface by a thin cell process until abscission, which ends with an abscised particle that remains at the ventricle and the withdrawal of the apical neuron's process, as described in chick (Kasioulis and Storey, 2018).

After their detachment from the ventricular surface, IPs and/or future neurons become localized in the underlying layer and can maintain contact with their NP/NSC of origin. In the mouse embryonic cortex, the newly formed neurons migrate along RGs processes to reach the furthest neuronal layer (Nóbrega-Pereira and Marín, 2009). In the mouse SVZ, IPs intercalate just under the NPs/NSCs layer, form cell clusters through spontaneous homophilic interactions, and differentiate to give rise to immature neurons (Figure 2C). Thanks to cytoskeleton reorganization, diffusible factors and migratory scaffold formed by astrocytic processes and blood vessels, immature neurons migrate in chains along the RMS to the OB where they differentiate into olfactory interneurons (Kaneko et al., 2017).

In the zebrafish pallium, both in embryo and adult, despite the presence of RGs processes reaching the basal surface, newly formed neurons do not migrate but intercalate in the parenchyma under their NPs/NSCs of origin (except for olfactory bulb-fated neurons) (Figure 2B) (Schmidt et al., 2013). Therefore, the different layers of neurons correspond to different ages, with the youngest neurons being the closest to the NPs/NSCs layer (Furlan et al., 2017). In the zebrafish pallium, closely related cells stay in contact with their sibling or daughter cells. These features make the pallium a good model for clonal and cell fate analysis.

## 2.8 Neuronal lineage progression

The neurogenic lineage defines the successive differentiation steps from RG NPs or NSCs to IPs, immature neurons, and finally mature neurons (Figure 5). In embryos and adults, the neuronal engagement of RG NPs is signaled by the expression of neural Sox proteins, such as Sox4, and Sox11 within Sox2-positive (Sox2<sup>pos</sup>) domains (Stevanovic et al., 2021; Kavayanifar et al., 2018). NPs also express Notch receptors, and the mechanisms regulating Notch target genes create permissive conditions for the generation of IPs. The main neurogenic drivers are basic Helix-Loop-Helix (bHLH) transcription factors from Neurog, Atonal (Ato), Achaete-Scute (Ascl) and NeuroD (specifically Neurod4) families (Baker et al., 2018). For example, in the forebrain, the main transcription factors are Neurog1 (ventrally) and Ascl1 (dorsally).

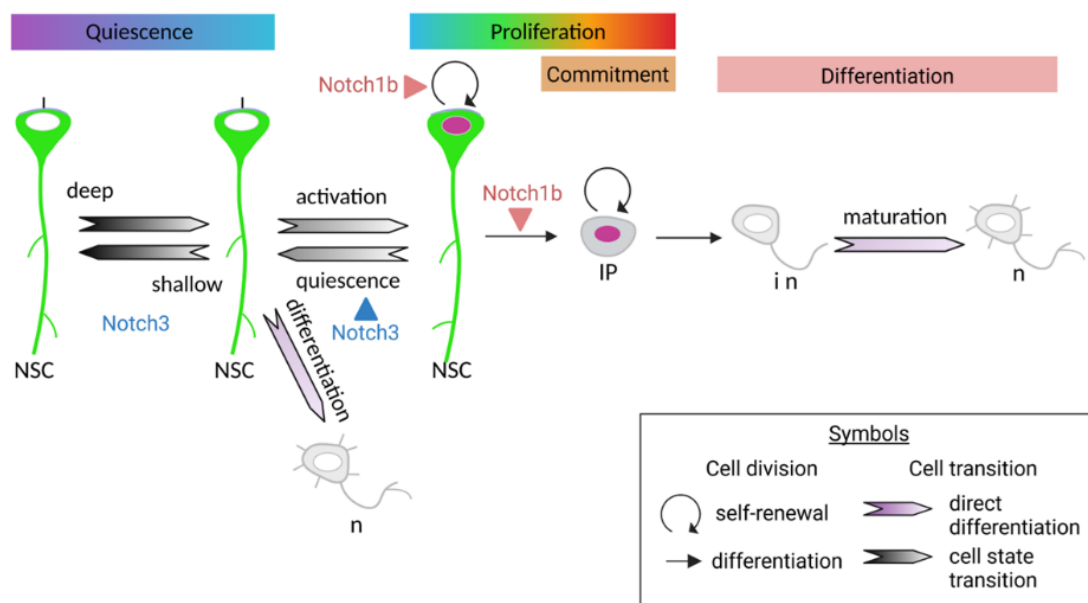


**Figure 5: Schematic representation of the neurogenic lineage in the adult zebrafish pallium (see references in text)**

The successive phases of quiescence, proliferation, commitment and differentiation are represented from the left to the right. The implications of Notch3 for the maintenance of NSCs quiescence, and Notch1b for NSCs proliferation and differentiation are indicated. Nuclei from proliferating cells are represented in pink. n, neuron, NSC, neural stem cell, i n, immature neuron, IP, intermediate progenitor.

IPs are more restricted in their fate than RG NPs, and are programmed to multiply themselves in a limited number of time. In embryos, the number of IP divisions is limited to three (Pontious et al., 2008). The amplification potential of IPs varies between adult mouse SVZ, where IPs divide three to four times, and SGZ, where IPs only divide once or twice (Ponti et al., 2013; Seri et al., 2004; Encinas et al., 2011; Lugert et al., 2012; Labusch et al., 2020). In adult zebrafish pallium, the amplification by IPs also consists of only one or two division events

(Rothenaigner et al., 2011; Furlan et al., 2017). The differentiation of IPs to immature neurons involves transcription factors such as *Ascl1*, *Neurog*, and the T-box protein *Tbr2/Eomes*, a specific marker of IPs (Shimojo et al., 2024).

IPs terminally divide to generate immature neurons expressing a cascade of conserved differentiation factors (such as Neuronal differentiation 1 (*Neurod1*), 2 or 6) and effectors of neuronal functionality or identity (cytoskeletal elements, axonal differentiation, synaptic components, neurotransmitters, etc.) (Bertrand et al., 2002; Guillemot et al., 2017; Wilkinson et al., 2013; Dennis et al., 2017). For example, immature neurons start expressing doublecortin, which is essential for neuronal migration. Importantly, the previous factors are also the prime activators of the expression of Notch ligand genes, thereby triggering Notch signaling in neighboring cells (Vasconcelos et al., 2014).

The final step of neurogenesis involves changes that promote maturation, synaptogenesis, and functional integration into neural circuits. In this phase, proteins like *NeuroD* and *Prox1* are crucial for promoting the survival and terminal differentiation of neurons (Gao et al., 2009; Stachniak et al., 2021). For instance, *NeuroD1* regulates dendritic growth and synaptic connectivity, while *Prox1* is involved in final subtype specification in some neuronal lineages. In embryos, RG NPs generate a wide range of neuronal subtypes, including excitatory and inhibitory neurons. In adult mouse SVZ, immature neurons migrating to the OB give rise to two types of interneurons, GABAergic granule cells, and dopaminergic periglomerular interneurons (Alvarez-Buylla and Garcia-Verdugo, 2002), while in adult mouse SGZ, immature neurons migrate short distances inside the hippocampus and give rise to one type of neuron, granule neurons. In the adult zebrafish pallium, newly generated neurons do not migrate far away from the VZ (Adolf et al. 2006; Grandel et al. 2006; Kroehne et al. 2011; Rothenaigner et al. 2011). The diversity of their subtypes is just beginning to be unraveled. Different markers (*ascl1*, *eomesa*, *emx1*, and *emx3*) are expressed in a scattered pattern in the VZ and might be involved in the differentiation of neuronal pallial subpopulations (Ganz et al., 2014). More recently, single-cell data provided resources for future investigations into the neuronal diversity of adult zebrafish forebrain (Morizet et al., 2024; Pandey et al., 2023; Mitic et al., 2024).

## ***2.9 Quiescence of NSCs***

During embryonic mouse and larval zebrafish stages, NPs progressively enter a reversible state of cell cycle arrest, between the M and G1 phase of the cell cycle, named Gap (G) 0 or

quiescence. A quiescence state during the G2 phase in NEs and NPs also exist in medaka and *drosophila*, but whether adult NSCs from mice or zebrafish can enter G2 quiescence remains unresolved (Dambroise et al., 2017; Otsuki and Brand, 2018).

Quiescent NSCs (qNSCs) are negatively revealed by their lack of proliferation markers, such as Proliferating cell nuclear antigen (PCNA) (Figure 6) and Minichromosome maintenance complex components (Mcm), such as Mcm2.

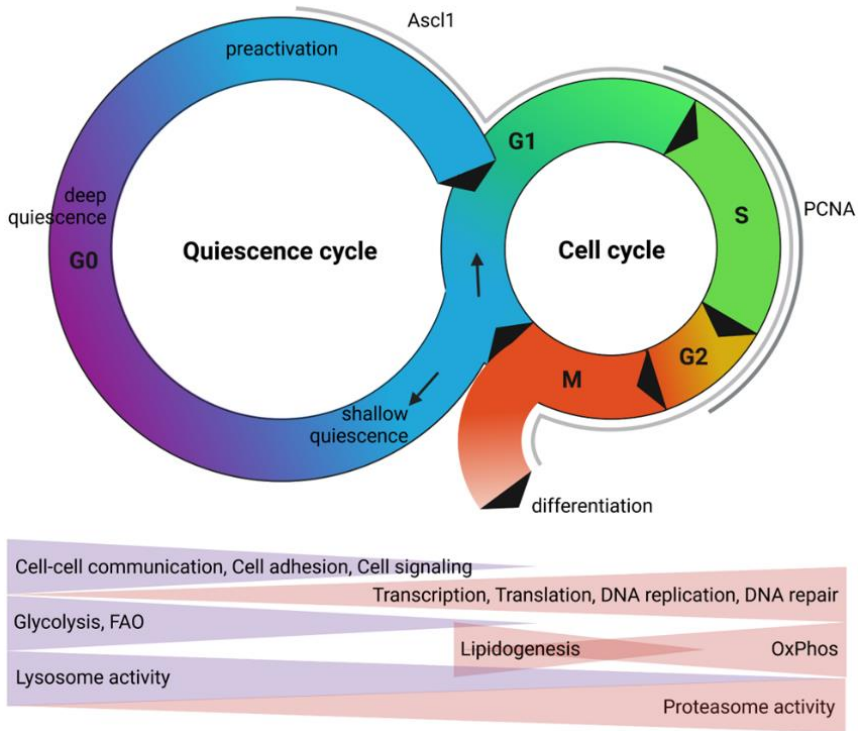


**Figure 6: Schematic representation of the quiescence cycle and the cell cycle with associated cell metabolism switches (from Labusch et al., 2020)**

Quiescence and cell cycles. The expression of the pre-activation factor Ascl1 and the marker of proliferation PCNA are indicated along the cycles. G0, gap 0, G1, gap 1, G2 gap 2, M, mitosis, S, replication. Main cell metabolism switches between quiescence and cell cycling.

Quiescence is a prominent state of adult NSCs in both zebrafish and mouse. In the adult zebrafish brain, at any given time, 95% of the NSCs are quiescent, and their recruitment frequency is heterogenous, from weeks to months (Chapouton et al., 2010; März et al., 2010a; Alunni et al., 2013; Than-Trong et al., 2018; Dray et al., 2021; Than-Trong et al., 2020; Mancini et al., 2023). Tracking of division events in the pallium of adult zebrafish showed that during NSC/NSC divisions from a Notch ligand *deltaA<sup>neg</sup>* mother cell, one of the two daughter cells is systematically *deltaA<sup>pos</sup>*, and even if this cell returns to quiescence with its *deltaA<sup>neg</sup>* sister, it remains quiescent for less time, dividing several times before definitely differentiating by a IP/IP division (Mancini et al., 2023). The doubling time for *deltaA<sup>neg</sup>* NSCs is estimated to be

120 days, and that for *deltaA<sup>pos</sup>* NSCs 30 days (Than-Trong et al., 2020; Mancini et al., 2023). In the mouse adult SVZ, at any given time, around 80% of NSCs are quiescent, and each NSCs is activated approximatively every 20 days (Basak et al., 2018). In the SGZ, 60% of NSCs are quiescent, and each NSCs is activated every 11 days (Bottes et al., 2021).

Quiescence is believed to be necessary to preserve genome integrity of the NSC and optimize their long-term maintenance (Cheung and Rando, 2013; Tümpel and Rudolph, 2019). Quiescent cells favor energetic metabolisms that do not produce damaging reactive oxygen species (ROS), such as glycolysis and fatty acid oxidation (FAO) (Shin et al., 2015; Llorens-Bobadilla et al., 2015). When cells activate, i.e., emerge from their quiescent state to divide, they progressively switch for lipogenesis and finally, neurons exclusively use the oxidative phosphorylation pathway (OxPhos), which comparatively produces more energy as Adenosine triphosphate (ATP) (Figure 6). Other molecular players of NSCs quiescence have been analyzed by Ribonucleic acid sequencing (RNAseq) and are in agreement with a protective strategy of the qNSCs: pathways involved in transcription, translation, DNA replication and DNA repair, and cell cycle progression, are downregulated, while cell-cell communication, cell adhesion, cell signaling and lipid metabolism are upregulated (Figure 6) (Labusch et al., 2020). Another aspect of quiescent NSCs metabolism is their protein recycling strategy. In the adult mouse SVZ, while the lysosomal activity is more important in qNSCs and contributes to maintaining their quiescence, the proteasomal activity is more important in activated NSCs (aNSCs) where it contributes to the activation potential of the NSCs (Figure 6) (Leeman et al., 2018).

In addition to the differences between qNSCs and aNSCs, the quiescence state is heterogeneous in different aspects. As highlighted above for zebrafish, quiescence varies in duration between NSCs. Other analyses based on transcriptomic data from mouse SGZ (Harris et al., 2021; Shin et al., 2015), mouse SVZ (Basak et al., 2018; Dulken et al., 2017; Llorens-Bobadilla et al., 2015; Marcy et al., 2023; Mizrak et al., 2019), and zebrafish pallium (Cosacak et al., 2019; Lange et al., 2020; Morizet et al., 2024), determined the existence of different quiescent sub-states in adult NSCs. These results validate previous analyses conducted in zebrafish: by pharmacological blockade of the quiescence-promoting Notch signaling pathway for 2 days, around 50% of qNSCs entered the cell cycle and it took an additional day for 95% of the cells to be proliferative, while the remaining 5% did not respond to the blockage and stayed quiescent (Alunni et al., 2013), pointing to asynchronous responses. These results likely reflect different

quiescence depths, depending on the ease with which the qNSCs can be activated (Figure 6). We can note that shallow quiescent cells are labeled with the marker of pre-activation *Ascl1*, which is necessary for NSCs proliferation, as well as, more broadly, with the Notch ligand *DeltaA*. Interestingly, after Notch signaling blockage, more NSCs express *ascl1a* and *deltaA* in the adult zebrafish pallium (Morizet et al., 2024).

Multiple molecular pathways are directly implemented in promoting quiescence, such as Notch and growth factors related pathways (Bone morphogenetic proteins (BMPs), Neurotrophin-3 (NT-3), or *Pdgfr $\beta$*  (Kobayashi et al., 2021; Delgado et al., 2021)). For example, Inhibitor of DNA binding (Id) protein, such as *Id1* in zebrafish and *Id4* in mouse, are targets of BMP signaling and were shown to promote NSCs quiescence and limit regenerative neurogenesis (Roschger and Cabrele, 2017; Rodriguez Viales et al., 2015; Gao et al., 2015; Zhang et al., 2020; Zhang et al., 2021; Blomfield et al., 2019; Zhang et al., 2019). Interestingly, mouse *Id4* is also a target of the Notch signaling (Li et al., 2012). The role of Notch signaling in quiescence will be further detailed in the next chapter.

### 3 Notch signaling pathway

#### 3.1 Introduction

The Notch signaling pathway belongs to the juxtacrine type of intercellular signaling, which usually involves direct cell-to-cell physical contact between two adjacent cells (Li et al., 2023; Zhou et al., 2022a). The transduction event is unidirectional at the molecular level, with a ligand on one cell activating a Notch receptor on a neighboring cell (a process referred to as transactivation).

The binding of a ligand to a Notch receptor triggers a series of proteolytic cleavages of the receptor that results in the release of its intracellular domain (NICD). The latter translocates to the nucleus, where, by associating with the transcription factor Recombination signal Binding Protein for immunoglobulin kappa J region (RBP-J $\kappa$ , also known as Centromere Binding Factor 1 (CBF1), ortholog of *Drosophila* Suppressor-of-Hairless) and the co-activator Mastermind-like transcriptional co-activator 1 (MAML1), it promotes the transcription of target genes (Li et al., 2023; Zhou et al., 2022a). The transduction of Notch signaling is direct from the



membrane to the nucleus and does not involve intermediate signal amplification, resulting in a response proportional to receptor-ligand interactions (Li et al., 2023; Zhou et al., 2022a).

The Notch signaling pathway has been discovered in *Drosophila melanogaster* and is widely conserved in metazoans (Pinot and Le Borgne, 2024; Chen et al., 2023). It is implicated in fate regulation of many cells including NSPCs and its outcomes are context-dependent (Zhou et al., 2022a; Guo et al., 2023). At the tissue scale, it participates in pattern and boundary formation during development. At the cellular scale, the signaling outcomes range from proliferation or quiescence to progenitor maintenance to apoptosis. An aberrant Notch pathway leads to several human diseases, such as Cerebral Autosomal Dominant Arteriopathy with Subcortical Infarcts and Leukoencephalopathy (CADASIL), Alagille syndrome, Adams-Oliver syndrome, organ-associated diseases (e.g. heart, muscles), tumorigenesis and cancer progression (e.g. leukemia), psychotic disease (e.g. Schizophrenia), and age-related disease (e.g. Alzheimer disease) (Sachan et al., 2024; Megaly et al., 2024).

### **3.2 Canonical pathway**

#### **3.2.1 Receptors**

The Notch receptors are type I transmembrane proteins exposing their N-terminal domain in the extracellular space. *Drosophila* possesses only one Notch receptor, whereas four receptors are found in both mammals (Notch1, Notch2, Notch3, Notch4) and zebrafish (Notch1a, Notch1b, Notch2, Notch3) (Sprinzak and Blacklow, 2021; Ramesh and Chu, 2023).

The extracellular domain of all Notch proteins contains between 29 and 36 Epidermal growth factor (EGF)-like repeats, which permit interactions with the ligands in a Ca<sup>2+</sup>- and glycosylation-dependent manner (Figure 7) (Handford et al. 2018). These are followed by a negative regulatory region (NRR) which comprises three Lin12-Notch repeats (LNR) together with the heterodimerization domain (HD) (Figure 7). By masking the S2 cleavage site in the absence of ligand, the NRR plays a critical role in preventing unspecific receptor activation. On the cytoplasmic side, the Notch receptor comprises an RBP-J $\kappa$ -association module (RAM), followed by a long unstructured linker containing nuclear localization sequences and a series of seven Ankyrin (ANK) repeats that, in the nucleus, also contribute to the binding of both RBP-J $\kappa$  and MAML1. The C-terminus of the receptor contains a loosely defined and evolutionarily divergent transactivation domain (TAD), which may contribute to protein-protein interactions, and terminates with a conserved motif that is enriched in proline, glutamic

acid, serine and threonine (PEST) (Figure 7). This motif is implicated in the ubiquitin-dependent degradation of NICD (Bray and Gomez-Lamarca, 2018).

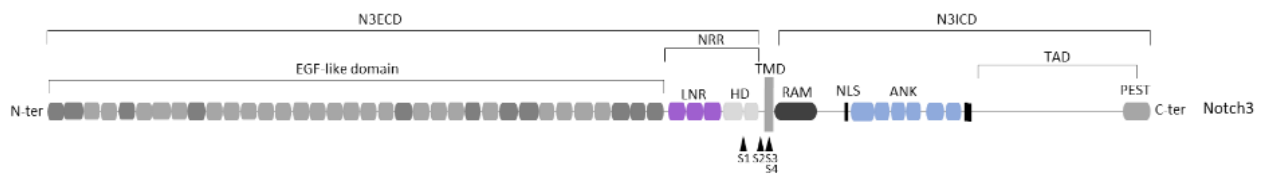


**Figure 7: Schematic illustration of the zebrafish Notch3 protein**

In zebrafish, Notch3 protein contains 35 epidermal growth factor (EGF)-like repeats. The calcium-binding EGF-like repeats are color-coded in lighter grey. The positions of the proteolytic cleavage sites are indicated (S1-4).

Protein domains obtained from InterPro (<https://www.ebi.ac.uk/interpro/>) and SMART ([http://smart.embl.de/smart/set\\_mode.cgi?NORMAL=1](http://smart.embl.de/smart/set_mode.cgi?NORMAL=1)). ANK, ankyrin repeat, HD, heterodimerization domain, LNR, Lin12-Notch repeat, NLS, nuclear localization signals, NRR, negative regulatory region, N3ECD, Notch3 extracellular domain, N3ICD, Notch3 intracellular domain, PEST, proline glutamine serine and threonine rich region, RAM, RBP-J $\kappa$ -association module, TAD, transactivation domain, TMD, transmembrane domain.

The highly conserved structure of the receptor is illustrated in Figure 7 with the example of the zebrafish Notch3 protein and the extracellular (NECD), transmembrane (TMD) and NICD domains. The four cleavage sites are also indicated (S1-4).

### 3.2.2 Ligands

Notch ligands are also type I transmembrane proteins exposing their N-terminal domain, containing EGF-like repeats and specific ligand domains, into the extracellular space. *Drosophila* possesses two ligands (Serrate and Delta), whereas five ligands are found in mammals (Delta-like1, Delta-like3, Delta-like4, Jagged1, Jagged2) and eight in zebrafish (DeltaA, DeltaB, DeltaC, DeltaD, Jagged1a, Jagged1b, Jagged2a, Jagged2b) (Sprinzak and Blacklow, 2021; Ramesh and Chu, 2023; The Zebrafish Information Network (ZFIN)). Ligands are classified into two broad categories based on the presence (Jagged/Serrate) or absence (Delta/Delta-like) of a cysteine-rich domain. From what is known, ligands are not specific to one type of Notch receptor; rather, their interaction is limited by their expression patterns and the glycosylations of their EGF-repeats (Kuintzle et al., 2024; Henrique and Shweisguth, 2019).

### 3.2.3 Mechanism of action

After their translation in the endoplasmic reticulum (ER), Notch receptors are transported to the Golgi apparatus (GA) for O-linked glycosylation of EGF-repeats, and for the S1 cleavage by a furin-like protease (Figure 8) (Zhou et al., 2022a). Mature heterodimers, held together by

noncovalent interactions, are transported to the cell membrane where they can bind a neighboring Notch ligand.

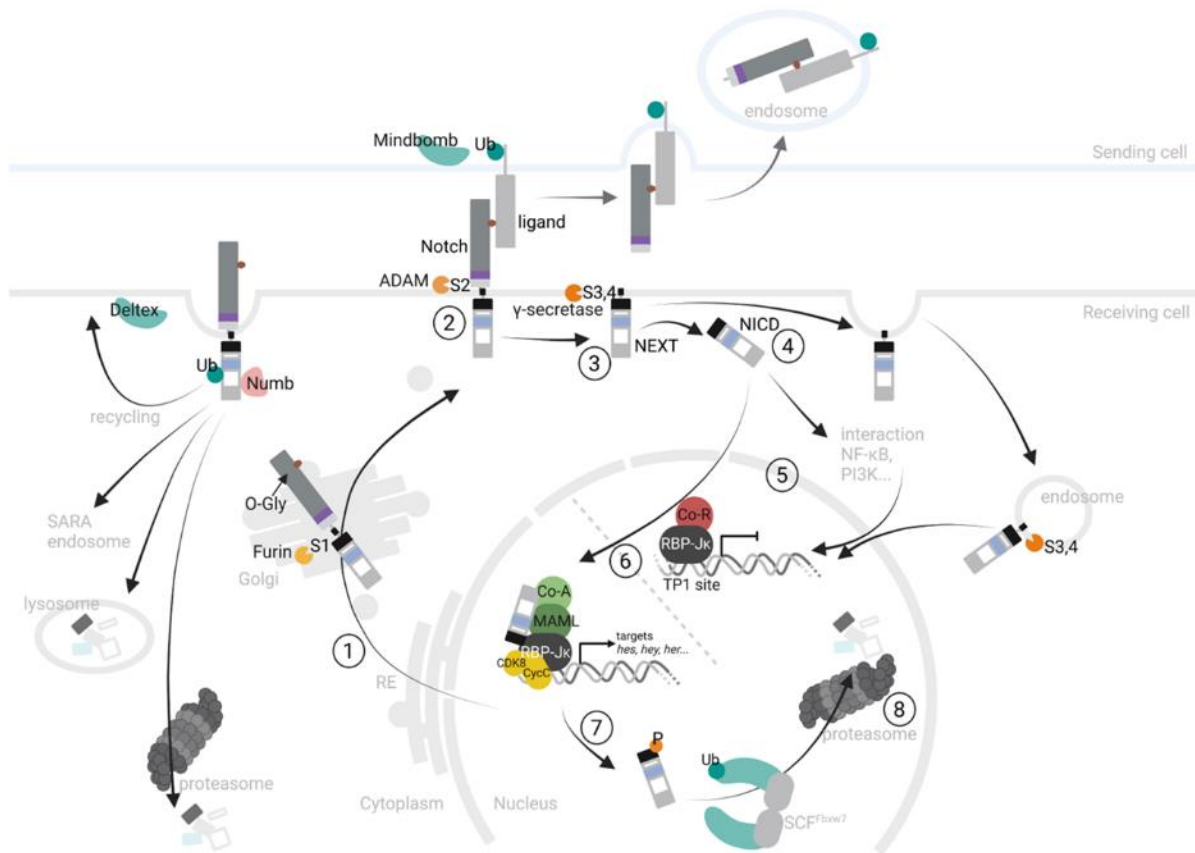


**Figure 8: The Notch signaling pathway (adapted from Kopan and Ilagan, 2009; see other references in text)**

On the left of the picture, endocytosis trafficking regulating Notch activation is represented. Notch receptor endocytosis depends on the ubiquitination of its intracellular domain by the ubiquitin ligase Deltex. This endocytosis, which is favored by Numb, can lead to the recycling of the receptor at the membrane, the lysosomal or proteasomal degradation of the receptor, or the ligand-dependent intracellular activation of the receptor in Sara endosomes.

(1) The newly translated Notch receptor protein transits through the GA where it is glycosylated on specific EGF repeats and cleaved by Furin protease at the S1 site. The receptor is then targeted to the cell surface.

(2) The Notch receptor is activated by binding to a ligand presented by a neighboring cell. This interaction triggers the endocytosis of the ligand in the neighboring cell after the ubiquitination of the ligand intracellular domain by the ubiquitin ligase Mib. The S2 site becomes accessible for cleaving, and ADAM metalloproteases cleave the receptor. The extracellular part of the receptor is processed by the neighboring cell. In contrast, the rest of the receptor is still anchored at the membrane and forms the Notch extracellular truncation (NEXT) domain.

(3) The  $\gamma$ -secretase complex cleaves the transmembrane domain of NEXT in the S3 and S4 sites and releases the Notch intracellular domain (NICD) and the remaining transmembrane domain. The  $\gamma$ -secretase cleavages can occur at the cell membrane or in endosomal compartments.

(4,5) NICD is released in the cytoplasm where it can interact with other proteins and signaling pathways before being translocated into the nucleus.

(6) In the nucleus, NICD associates with the DNA-binding transcription factor RBP-J $\kappa$ , which recognizes TP1 sites on DNA, and the co-activator MAML. These interactions release transcriptional co-repressors (Co-R) while co-activators (Co-A) are recruited and activate the transcription of Notch target genes, such as *hes*, *hey* or *her*.

(7) MAML recruits Cyclin C (CycC) and Cyclin-dependent kinase 8 (CDK8), which phosphorylates NICD. Phosphorylated NICD is recognized and ubiquitinated by the SCF<sup>Fbxw7</sup> ubiquitin ligase complex.

(8) NICD is degraded by the proteasome. For more details, see text.

The receptor-ligand interaction followed by ligand endocytosis is thought to generate a mechanical force that promotes a conformational change within the receptor and results in the exposure of the S2 cleavage site (Figure 8). A Disintegrin and Metalloproteinase domain-containing protein 10 (ADAM10), located at the cell surface, proceeds to the S2 cleavage of the receptor and releases the cleaved Notch extracellular domain that is internalized by the signal-sending cell along with the ligand (Figure 8). The remaining membrane-embedded Notch extracellular truncation fragment (NEXT) either stays at the plasma membrane (common model) or is endocytosed before undergoing S3 and S4 cleavages by the gamma ( $\gamma$ )-secretase enzymatic complex (consisting of four essential subunits: Presenilins 1 and 2, Nicastrin, Anterior pharynx defective 1, and Presenilin enhancer 2) at the transmembrane domain (Figure 8) (Zhou et al., 2022a; Zhang et al., 2014). Notch activation was also discovered to take place in endosomes in *Drosophila*, and this process appears conserved in the spinal cord of the zebrafish embryo (Richard et al., 2024; Kressmann et al., 2015; Coumailleau et al., 2009; Fürthauer and González-Gaitán, 2009). There, the neural progenitors dividing asymmetrically, segregate Smad anchor for receptor activation (Sara) endosomes, containing Delta ligands and Notch receptors, in one of the two daughter cells. In this cell, the Notch signaling is activated in a ligand-dependent manner in Sara endosomes and orient the cell towards a progenitor identity. After S3 and S4 cleavages, the remaining transmembrane fragment is recycled and NICD is released into the cytoplasm of the signal-receiving cell (Figure 8) (Zhou et al., 2022a).

After its release, NICD can directly translocate to the nucleus and acts as a transcription factor for its target genes, or before that, crosstalk through protein-protein interactions with other signaling pathways, including Nuclear factor-kappa B (NF- $\kappa$ B), Mechanistic target of rapamycin complex (mTORC), Phosphatase and tensin homolog on chromosome 10 (PTEN)/ Phosphoinositide 3-kinases (PI3K)/ Protein kinase B (AKT), Wnt/ $\beta$ -catenin, Transforming growth factor type beta (TGF- $\beta$ ), or BMP, at the cytoplasmic and/or nuclear level to regulate the transcription of target genes (Zhou et al., 2022a; Borggreffe et al., 2016). As an example of inter-pathway interactions, membrane Notch receptors, and nuclear NICD can inhibit Wnt/ $\beta$ -catenin signaling, and the nuclear NICD- $\beta$ -catenin interaction is stabilized by RBP-J $\kappa$  (Acar et al. 2021).

For its canonical transcription factor function, NICD forms the tripartite activation complex by binding to the DNA-binding transcription factor RBP-J $\kappa$  and the co-activator MAML (Figure

8) (Zhou et al., 2022a). These interactions dislodge the RBP-J $\kappa$ -associated co-repressors. The DNA-binding sites (TP1 elements) can be found as monomers or dimers arranged in a head-to-head orientation, and therefore, the NICD can be engaged in dimers that generate a synergistic activation of Notch responsive promoters (Gazdik et al., 2024). The tripartite complex associates with co-activators, RNA polymerase II, and DNA sequences (promoter and enhancers) at the level of transcription “hubs” in a non-stoichiometric manner, which enables a small number of transcription factor molecules to drive productive transcription of Notch target genes. These include genes encoding transcriptional repressors of the bHLH Hairy/Enhancer-of-split (H/E(Spl)) with WRPW motif (Hes/Her) (in mouse/zebrafish) family, or with YRPW motif (Hey) family (Kopan and Ilagan, 2009; Demmerle et al., 2023). These optimizations could explain why NICD nuclear levels are frequently below the level of detection *in vivo* (Trylinski et al., 2017). The HLH domain of Hes/Her/Hey proteins promotes the formation of homo- or heterodimeric protein complexes, while the basic domain binds to DNA targets (Hu and Zou, 2022). The C-terminal domain of Hes/Her/Hey proteins recruits co-repressors, such as histone deacetylases, which alter the chromosomal structure and silence transcription. Depending on the tissue and the developmental stage, the *Hes/her/Hey* genes directly targeted by Notch signaling can vary, and Hes/Her/Hey proteins have different target genes associated with specific functions. For example, the direct target of Notch involved in mouse neurogenesis are *Hes1*, *Hes5*, *Hey1*, *Hey2*, *HeyL* (Hu and Zou, 2022; Harada et al., 2021; Sakamoto et al., 2003; Satow et al., 2001). We can note that NICD can share the same target genes that its interacting pathways, such as *Hes1*, which acts as a hub for the molecular crosstalk among signaling pathways (Hu and Zou, 2022; Borggreffe et al., 2016). In zebrafish, the *her* family is expanded compared to mammals, but until now, only the *Hes5* orthologs *her4* and *her15*, the *Hes6* ortholog *her6*, and *hey1* have been identified as direct targets of Notch involved in neurogenesis (Sigloch et al., 2023; Than-Trong et al., 2018; Kageyama et al., 2007). Still during neurogenesis, these proteins can target pro-neural genes such as *Ascl1* (also called *Mash1*), *Dll1*, and *Neurog2*.

Some other direct Notch target genes are *Notch* itself, the Notch receptor ubiquitin ligase *Deltex* (see part *Regulations*), as well as the cell cycle regulating *Cyclin D1*, and the universal transcription amplifier *C-myc* (Borggreffe and Oswald, 2009).

In parallel to its transcriptional function, the complexed MAML also recruits Cyclin C and Cyclin-dependent kinase 8 that phosphorylate the PEST domain of NICD (Figure 8).

Phosphorylated NICD is the target for ubiquitination by the nuclear ubiquitin ligase SCF<sup>Fbxw7</sup> and subsequent degradation in the proteasome (Qi et al., 2024). Experiments using bioluminescence and pulse-chase indicated that the half-life of NICD is around 180 minutes (Ilagan et al., 2011; Fryer et al., 2004).

### ***3.2.4 Regulations***

A stock of Notch receptors is kept in the ER-GA system and can be released to the cell membrane after the activation or the depletion of Notch receptors at the membrane (Bian et al., 2023).

Notch receptors are exposed at the membrane as isolated heterodimers. Their EGF-like repeats domain can interact with similar domains in ligands from neighboring cells (trans-activation), as well as with ligands from the same cell, inhibiting Notch activation by preventing the exposure of the S2 site (cis-inhibition). The balance between trans-activation and cis-inhibition defines cells with the highest number of receptors as receiving cells and cells harboring more ligands than receptors as sending cells (Bray, 2016). Forced clustering of Delta ligands at the cell membrane of the sending cells, leading to clustering of Notch receptors in the receiving cell, has also been proven to inhibit the Notch signaling pathway (Viswanathan et al., 2019). Before exocytosis of the mature Notch receptor, some O-linked glycosylations of the EGF-like repeat (Figure 8) are elongated by the glycosyltransferase Fringes (Fngs), differing in cells by number, variants, and activity, and modifying the cis- and trans- ligand-receptor strength of interaction (Granados et al., 2024).

The number and the localization of Notch receptors at the cell membrane are finely tuned by their endocytosis, activated by the ubiquitination of the intracellular domain of the receptor by the E3 ubiquitin ligase Deltex, binding to Notch ANK repeats, and leading to Notch degradation via the lysosome, or to Notch recycling via exocytosis (Figure 8). Endocytosis plays similar roles for the Notch ligands, with the difference that their intracellular domain is ubiquitinated by the E3 ubiquitin ligase Mindbomb (Mib), and that endocytosis also participates in the maturation of the ligand (Figure 8). Numb antagonizes Notch signaling by inducing endocytosis and proteasomal degradation of the receptor (Figure 8) (Ortega-Campos and García-Heredia, 2023; McGill et al., 2009; McGill and McGlade, 2003). However, Numb and Notch might also have similar functions in maintaining NPs (Luo et al., 2020; Petersen et al., 2002). The shape

and polarity of cells also modulate Notch activity (Xu et al., 2023; Perez-Mockus and Schweisguth, 2017).

The Notch response is influenced by post-translational modifications of NICD, that regulate its protein-protein interactions, its half-life and therefore the NICD-dependent transcriptional output. For instance, acetylation of Notch3 NICD increases its ubiquitination and therefore decreases its stability, and regulates its proteasomal-dependent turnover (Borggrefe et al., 2016). In the cytoplasm, NICD can also be targeted to the autophagy degradation pathway (Zada et al., 2022).

In the nucleus, NICD/RBP-J $\kappa$  interactions do not depend on the DNA-binding activity of RBP-J $\kappa$ , and RBP-J $\kappa$  binding to DNA appears to be dynamic and enhanced by its interaction with NICD (Ilagan et al., 2011; Castel et al., 2013; Kovall et al., 2017; Skalska et al., 2015; Wang et al., 2014a).

Her/Hes proteins downregulate their expression and the expression of other Notch targets by directly binding to promoter sequences (negative feedback) (Sueda and Kageyama, 2020). When *her/Hes* promoters are repressed, both *her/Hes* messenger RNAs (mRNAs) and corresponding proteins disappear rapidly because they are extremely unstable, which cancels the negative feedback and autonomously initiates the next round of expression. For example, in mouse embryos, *Hes1* expression oscillations create a salt-and-pepper pattern of *Hes1* expression among the NPs of the VZ (Sueda and Kageyama, 2020). These oscillatory expression patterns reflect the oscillatory behavior of cell fate-determining genes, such as the pro-neural genes *Ascl1* and *Dll1*. These oscillations are necessary for sustaining the proliferative state of NSPCs and are lost upon differentiation (Kageyama et al., 2023; Sueda and Kageyama, 2020; Kageyama et al., 2019; Kageyama et al., 2018; Shimojo and Kageyama, 2016; Kageyama et al., 2007). The periodicities of the oscillations are respectively 2-3 hours (h) in cultured NPs from the telencephalic region of mouse embryos, 1-2 h in NPs from zebrafish embryo hindbrain, and 1-3 h in NPs from zebrafish embryo telencephalon (Marinopoulou et al., 2021; Imayoshi et al., 2013; Doostdar et al. 2024; Soto et al., 2020). In aNSCs of adult mouse SVZ, *Hes1* oscillations are maintained in a periodicity of 2-3 h, complementary to *Ascl1* oscillations, while in qNSCs, the periodicity is higher (5-6 h), as well as the levels of *Hes1* oscillations, suppressing *Ascl1* expression (Sueda et al., 2019). One factor maintaining higher levels of *Hes1* in qNSCs is the BMP pathway, which induces the expression

of *Id1*, inhibiting *Hes1* negative feedback, therefore upregulating *Hes1* expression and inhibiting neurogenesis (Sueda and Kageyama, 2020). The oscillations of *Ascl1* are necessary for NSPCs proliferation, while in IPs, where Notch is inactive, the sustained *Ascl1* level is necessary for differentiation (Sueda et al., 2019). In adult zebrafish, however, the periodicity of *her/ascl1* expression is still to be proven.

### 3.2.5 Non-canonical alternatives

Evidence of non-canonical Notch activity came from  $\alpha$ -secretase, ligands, or RBP-J $\kappa$ /CBF1 loss-of-function experiments where some functions of Notch were maintained (Andersen et al., 2012; Sanalkumar et al., 2010). Across species, non-canonical Notch functions have mostly been identified in stem/progenitor cells or embryonic cells, capable of expansion and/or differentiation (Andersen et al., 2012). Activations of Notch targets via Notch-independent RBP-J $\kappa$  activity and *hes1* transcription also exist but will not be discussed (Harbuzariu et al., 2018; Sanalkumar et al., 2010).

In a ligand-independent manner, Notch receptors can be endocytosed, and rather than being degraded or recycled, their S2, S3, and S4 sites can be cleaved at the membrane of the late endosomes by hydrolases, to which ADAM10 belongs, and  $\alpha$ -secretase complex, and subsequently release NICD in the cytoplasm (Figure 9) (Hounjet and Vooijs, 2021; Harbuzariu et al., 2018). Non-conventional Notch ligands, such as the secreted Y-box binding protein 1 (YB-1) protein, can trigger Notch signaling by interacting with the Notch3 extracellular domain (Figure 9) (Lindquist and Mertens, 2018; D'Souza et al., 2010). In a ligand-dependent manner, Notch3 can promote the apoptosis of tumor endothelial cells, independently of cleavage and transcription regulation (Zhou et al., 2022a). Full-length Notch receptors were also found in the mitochondria's outer membrane where they regulate mitochondrial and mTORC activities (Figure 9) (Lee et al., 2013). In the nucleus, non-canonical activations of target genes transcription by NICD, independently of RBP-J $\kappa$ , are also possible (Figure 9) (Harbuzariu et al., 2018; Johnson and Macdonald, 2011).



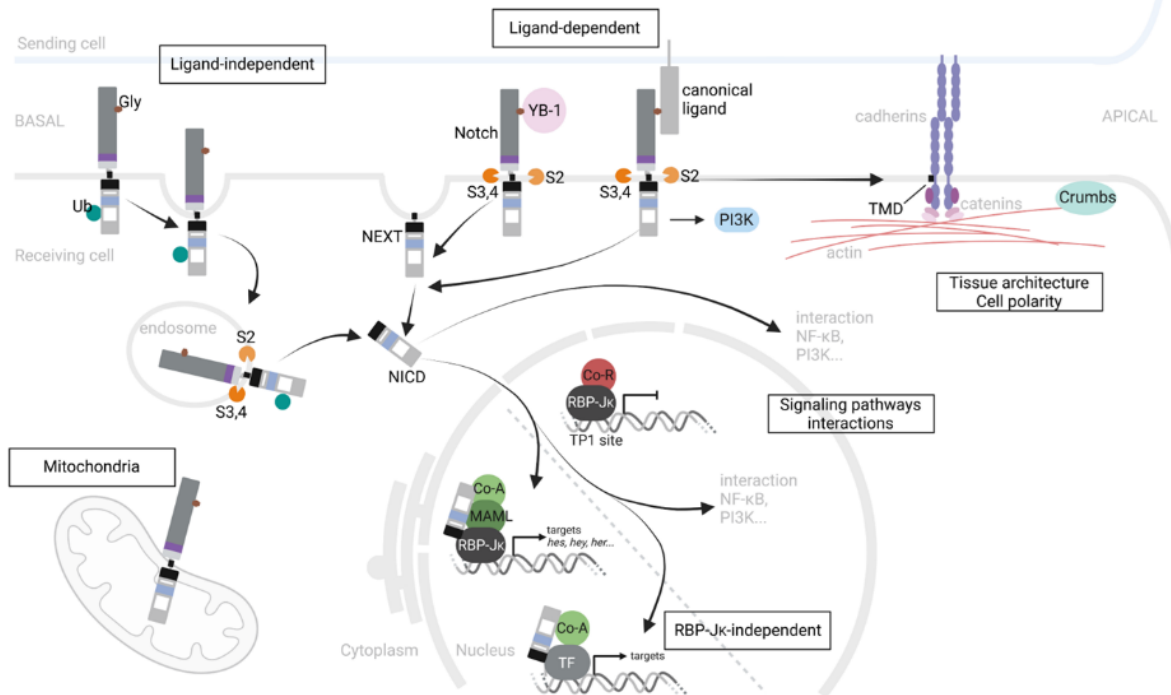


**Figure 9: Some examples of non-canonical Notch**

See text for description and references.

At the plasma membrane, Notch receptors can also participate in the activation of the PTEN/PI3K/AKT pathway (Figure 9) (Zhou et al., 2022a). Still at the membrane, Notch is involved in tissue architecture and cell polarity in a transcription-independent manner (Figure 9). For example, in stressed blood vessels, Notch transmembrane domain, revealed after the ligand-dependent activation of Notch, forms a mechanosensory complex by recruiting other proteins, including cadherins, driving adherens junction and cortical actin assemblies, and establishing barrier function (Polacheck et al., 2017). Similarly, in the ductal epithelium, where Notch is localized at lateral cell-cell contacts, Notch transmembrane domain recruits a protein complex, stabilizing epithelial adherens junctions and cortical actin organization (White et al., 2023). In the retina, adherens junctions and cell-polarity Crumbs complexes contribute to Notch activation (Falo-Sanjuan and Bray, 2021; Ohata et al., 2011).

### ***3.3 Functions of the Notch signaling pathway***

#### ***3.3.1 General functions***

As a highly conserved pathway, Notch signaling plays crucial roles in various biological processes, including organ development, tissue homeostasis, and repair (Zhou et al., 2022a). As

main examples, Notch signaling acts for the maintenance of stem cells and their differentiation in many tissues, and the development and maintenance of healthy immune and cardiovascular systems. Depending on the context, Notch signaling can drive opposite outcomes such as cell proliferation or quiescence, growth or differentiation, apoptosis or survival, attachment or migration, and more. In so doing, it is involved in the homeostasis, morphogenesis and patterning of tissues (Shi et al., 2024; Zhou et al., 2022a; Siebel and Lendahl, 2017). In its role as a guardian of tissue homeostasis and organ function, Notch signaling is upregulated in response to tissue injury or stress to restore homeostasis by stimulating the proliferation and de-differentiation of neighboring cells (Zhou et al., 2022a). It is evident that Notch signaling is crucial for the remarkable regenerative abilities observed in the zebrafish model (examples in the nervous system: Campbell et al., 2022; Diotel et al., 2020; Noorimotlagh et al., 2017). The Notch signaling capacity to maintain stem cells, stimulate cell proliferation, and de-differentiate cells also contribute to the implication of Notch in various cancers (Zhou et al., 2022a; Pagliaro et al., 2020; Teoh and Das, 2018).

Depending on the Notch receptor and the context, the Notch signalization modes and the signaling effectors may be different. This complexifies the understanding of the pathway and the identification of specific mechanisms responsible for phenotypes observed in Notch-deficient organisms.

Human syndromes further illustrate this complexity. For example, CADASIL is the most common hereditary cause of stroke and vascular dementia in adults, linked to abnormalities in arterioles and loss of vascular smooth muscle (Yuan et al., 2024). CADASIL is mediated by mutations in the *NOTCH3* gene, which is normally expressed in pericytes and vascular smooth muscles but is abnormally folded in patients. However, it still remains unclear whether *NOTCH3* signaling per se is affected by CADASIL mutations. Additionally, other mutations in human *NOTCH* genes are implicated in cancer, revealing the context-dependent functions of Notch signaling in tumorigenesis. For example, in the case of glioma, which are the most frequent and aggressive brain tumors in adults, depending on their subtype, Notch signaling may act as an oncogene, maintaining cell proliferation and promoting tumor vascularization, or as a tumor suppressor, inhibiting cell proliferation (Parmigiani et al., 2020).

### 3.3.2 Early expression and loss-of-function

The expression patterns of Notch receptors and ligands are tightly regulated and tissue-specific, reflecting their roles in various developmental and adult processes. The precise timing and spatial distribution of expression ensure the proper coordination of cell fate decisions and tissue morphogenesis.

In mouse embryos, *Notch1* is broadly expressed since early developmental stages in many tissues, including the neuroepithelium, somites, and developing vasculature, *Notch2* is prominently expressed in the developing kidney, liver, heart, and vasculature, while *Notch3* and *Notch4* expression are slightly delayed and concern vascular smooth muscle cells and certain neural tissues (*Notch3*) and the endothelium of developing blood vessels (*Notch3*, *Notch4*) (Batista et al., 2020; Mouse Genome Informatics database (MGI)). In parallel, Jagged ligands are expressed before Delta-like ligands, and in the developing central nervous system, only *Jagged 1* (*Jag1*), which has the broader expression, and *Dll1* are present (Batista et al., 2020; MGI).

Dysregulation of the Notch pathway leads to severe developmental abnormalities, embryonic lethality, and various pathological conditions. For instance, *Notch1*- and *Notch2*-deficient mice die prematurely (around E9.5) respectively due to defects in somitogenesis and development of various organs. In contrast, *Notch3*- and *Notch4*-deficient mice are viable and fertile, with only minor defects observed in small arteries in *Notch3*-deficient mice (Swiatek et al., 1994; Conlon et al., 1995; Hamada et al., 1999; Krebs et al., 2003, Krebs et al., 2000). When the deletion of one Notch receptor is viable, its activity is frequently redundant with another Notch receptor expressed in the same cells and therefore the loss of activity is compensated.

In zebrafish embryos, *notch2* is expressed from 5-6 hpf onwards, while the expression of the other receptors begins around 9-10 hpf. The first ligand expressed is *jagged2* (*jag2*) (from the 1-cell stage onwards), and it is followed by the expression of *delta C* (*dlc*), *delta D* (*dld*), *jagged 1a* (*jag1a*), and *jagged 1b* (*jag1b*) at around 4-5 hpf. The last ligands to be expressed are *dla* and *delta B* (*dlb*) at around 9 hpf (The Zebrafish Information Network (ZFIN)). All Notch receptors and ligands are expressed in the central nervous system of the developing embryo. The expression of *notch1a* is also found in somites and the developing heart; *notch1b* is found in somites and pharyngeal arches; *notch2* is found in the developing vasculature and pharyngeal arches; and *notch3* is also expressed in vascular tissues.

Like in mouse, dysregulations of Notch signaling in zebrafish embryos impact the development and survival of the fish. For example, *notch1a*-deficient larvae die around 9-10 dpf from defects in somitogenesis secondarily preventing the development of the swim bladder (*notch1a* is also referred to as *deadly seven (des)*, Gray et al., 2001; van Eeden et al., 1998). *notch1b*- and *notch2*-deficient embryos are viable despite highly dysmorphic aortic valves and defects in the vascular system, respectively (Faucherre et al., 2020; Ando et al., 2019). *notch3*-deficient larvae die around 10-15 dpf from vascular abnormalities leading to a reduction of the number of pericytes, disruption of the BBB, and brain hemorrhages (Wang et al., 2014).

### ***3.3.3 Functions during neurogenesis***

Notch signaling is, in particular, a prominent regulator of neurogenesis. This function was initially described in *Drosophila*, where *notch* signaling orchestrates a salt-and-peppery neurogenesis program in proneural clusters through a lateral inhibition mechanism (Bahrampour and Thor, 2020; Bray, 1998). One well-studied example of lateral inhibition is the selection of the sensory organ precursor (SOP) cell for the future sensory bristle among clusters of competent proneural cells in the *Drosophila* epithelium. All the cells in the group initially express ligands and receptors and can signal to one another. However, subtle differences between cells, such as more Delta ligands in one cell that activate more Notch receptors in the surrounding cells, are fixed by Notch feedback loops, where the expression of Notch is inhibited in the sending cell and stimulated in the receiving cells. The cell “source” of ligands is the only one escaping Notch-mediated neural fate inhibition and dividing to give rise to the bristle, while the Notch active cell remains non-proliferative (Bray, 1998).

The *Drosophila* model was also interesting to study the implication of the Notch pathway in neuronal lineage decisions. For example, in the SOP lineage, at each division step, only one daughter cell inherits Notch activity because of a Numb-dependent inhibition of Notch in other daughter cell. This Notch asymmetry determines an oriented Notch signaling between the two daughter cells, acquiring two different fates (e.g. Notch is active in the precursor pIIb and not in pIIa, and in the glia cell and not in precursor pIIIb), while in the absence of Notch, only neurons are formed (Deasy, 2009; Bray, 1998). Notch signaling was also studied for its role in the formation of tissue boundaries during *Drosophila* retina morphogenesis. There, Notch signaling make a dorsal-ventral boundary between the two dorsal and ventral cell fields. Notch is particularly active at the boundary, considered an organizing center by coordinated growth

and patterning of the eye. This occurs because of a dorsoventral asymmetry of activating and inhibiting factors, such as Fng, and contributes to the activation of Notch specifically at the midline of the eye (Singh et al., 2012).

The works reported below identified and characterized Notch signaling functions during mouse and zebrafish neurogenesis. The described experiments and conclusions were preceded by verification of *Notch* expression in the considered neurogenic region, and, most of the time, by a widespread inhibition of the Notch pathway, either with a tissue non-specific Notch inhibitor (e.g.  $\gamma$ -secretase inhibitor) or with a conditional and tissue-specific deletion of Notch pathway actors (e.g. RBP-J $\kappa$ ). After these preliminary results, the contribution of each Notch receptor to the observed phenotypes was interrogated *in vivo* under homeostatic conditions.

### ***3.3.3.1 In mouse***

#### ***In the mouse embryo***

In the mouse embryo, expression of Notch receptors and downstream components of the pathway starts in the neural tube around E8-9, and continues into the VZ and the SVZ during neural development. Embryo NSPCs express Notch receptors *Notch1*, *Notch2*, and/or *Notch3*, and the canonical Notch signaling is active based on the expression of the canonical Notch target *Hes5*. IPs also express Notch receptors, but not *Hes5*, possibly reflecting the activity of a non-canonical Notch pathway.

*Notch4* is almost exclusively expressed in vascular endothelial cells, and the viability of the mutant suggests that *Notch4* has a minor role in embryonic neurogenesis (James et al., 2014). Its functions in mouse neurogenesis are less likely to be significant.

#### ***Maintenance of NSPCs***

One important role of Notch during neurogenesis is the mechanism of NSPC maintenance. In the neural tube of *RBP-Jk*-deletion mouse mutants, the expression of the effector gene *Hes5* is downregulated, while the expression of the proneural genes *Ascl1* and *Dll1* are increased (De la Pompa et al., 1997). These results are accompanied by increased and ectopic expression of early differentiating neuron markers, such as *NeuroD*. Interestingly, these results are comparable to those in *Notch1*-deletion mouse mutants. This may well represent premature neuronal differentiation and a loss of NSPCs in the nervous system, which cannot be assessed in the two mutants due to their early lethality.

To circumvent this lethality, several studies have addressed the effect of conditional deletion of *Notch1* in specific brain structures. Conditional *Cre-loxP* tamoxifen-dependent *RBP-Jk*-deletion in the developing mouse telencephalon highlighted a burst of neuron generation at the expense of RGs. In parallel, the VZ is absent (Imayoshi et al., 2010). For the analysis of Notch1 functions, in one case, *Cre-loxP*-mediated recombination was used to delete *Notch1* in the NEs at the midbrain-hindbrain boundary (MHB). Similarly to the *Notch1* mutant, this deletion induces early expression of early differentiating neuron markers in the cerebellum, and increases the expression of two ligands: *Dll1* in NEs and *Dll3* in neurons (Lütolf et al., 2002). In combination with other *Cre-loxP*-mediated recombination to delete *Notch1* (Yang et al., 2004; Yoon et al., 2004), these results indicate that *Notch1* maintains NSPCs, promotes the glial fate and prevents precocious neurogenesis in mouse embryos.

Similarly, gain-of-function experiments by the expression of the constitutively active *NIICD* in NSPCs of the embryonic telencephalon blocked neurogenesis and promoted glial fate, indicating an important role for Notch in cell fate decision-making (Gaiano et al., 2000). Interestingly, the overexpression of *N3ICD* in telencephalic NSPCs gives the same phenotype (Dang et al., 2006). In the developing spinal cord, *notch1*, *notch2*, and *notch3* are expressed along the dorsoventral axis in the ventricular zone, and their expression is higher in the ventral spinal cord (Yang et al., 2006). Conditional deletion of *notch1* in spinal cord NSPCs increases the ventral spinal cord neuronal population since E11.5, leading to the disappearance of the ventral half of the central canal. In parallel, all the progenitor populations along the dorsoventral axis are reduced, accompanied by an increased generation of V2 interneurons at the expense of motor neurons, and neurons impaired migration (Yang et al., 2006). These results show that Notch1 maintains spinal cord NSPCs and participates in binary fate decisions in the pV2 population.

Notch2 functions during neurogenesis were less studied *in vivo*. In the roof plate of the diencephalon and mesencephalon of *Notch2*-deletion mutants, the repression of expression of proneural genes, such as *Ascl1*, is lost, while the expression of the effector genes *Hes1* and *Hes5* remain unchanged (Kadokawa and Marunouchi, 2002). This result either suggests the use of another effector or the activity of a non-canonical Notch2 pathway. Interestingly, *Hes5* and *Notch2* expression were complementary. These data show that Notch2 may have redundant functions with Notch1 in the maintenance of NSPCs and in preventing neurogenesis.

*Notch1*, *Notch2*, and *Notch3* are also expressed in the embryonic retina. *Notch3* deletion in the developing retina leads to neuron number increase and neural progenitor number decrease (retinal progenitor cells, RPCs) without affecting the IPs (Riesenberg et al., 2009). After six weeks, *Notch3*-deleted mice show a decrease in the number of neurons (Dvorianchikova et al., 2015). However, the effects of *Notch3* knockout (KO) are mild: a *Notch1* compensation could explain this outcome (Riesenberg et al., 2009; Dvorianchikova et al., 2015). Dvorianchikova et al. suggest that Notch1 activity is major in the retina for the maintenance of RPCs and the regulation of the onset of neurogenesis (Dvorianchikova et al., 2015).

#### *NSPCs viability*

Notch is also implicated in NSPCs viability in the mouse embryo. In one case, *NIICD* overexpression induces the apoptosis of NSPCs in a p53-dependent manner, while in the *Presenilin-1*-deletion mutant, a marked reduction in NSPCs cell death is observed (Yang et al., 2004). In another case, Cre-*loxP*-mediated deletion of *Notch1* in mouse embryos increases cell death in the forebrain NSPCs and differentiating neurons (Mason et al., 2006). In *Notch1*- and *Notch3*-deleted double mutants, the increase in cell death is even more important than in the *Notch1* mutant. This result shows that *Notch3* can partially compensate for the survival-promoting effects of *Notch1*. These data indicate that Notch is involved in the regulation of NSPCs apoptosis. Oishi et al. showed that Notch promotes survival in a *Hes*-independent manner (Oishi et al., 2004). The opposite results of the two cases may reflect experimental context-dependent Notch activity (Mason et al., 2006).

#### *Oligodendrocyte generation*

More recently, Notch signaling has been linked with the mechanism of oligodendrocyte generation (oligodendrogenesis) from NSPCs in mouse embryos. Notch pathway inhibition by the  $\gamma$ -secretase inhibitor N-[N-(3,5-difluorophenacetyl)-L-alanyl]-S-phenylglycine-butyl ester (DAPT) reduces the number of OPCs independently of cell death events (Tran et al., 2023). Electroporation of a dominant negative form of *RBP-Jk* also reduces the number of OPCs while neuronal production increases. Interestingly, *Notch* overexpression in NSPCs also inhibits oligodendrogenesis, suggesting that Notch levels must be precisely balanced to generate the oligodendrocyte lineage. *Hes1* and *Hes5* are responsible for the negative regulation of OPCs production by Notch signaling by repressing *Ascl1* expression. Together, these results indicate

that Notch signaling is important during the transition from neurogenesis to oligodendrogenesis.

#### Roles of Notch ligands

*Dll1*, *Dll3*, and *Jag* are expressed in NEs, RGs and/or differentiating cells in the neural tube (Engler et al., 2018b). *Jag1*-deleted mutants are embryonic lethal and mice die shortly after E10.5. To circumvent this lethality, conditional Cre-*loxP*-mediated recombination was conducted in the MHB of mouse embryos (Weller et al., 2006). This experiment showed defects in hippocampal NSPCs migration, which are accumulated in a portion of the cerebellum, and consequently, differentiate ectopically. However, this result does not support a role for *Jag1* in maintaining hippocampal NSPCs as it would be expected that reduced Notch signaling by ablation of its ligand should result in precocious differentiation (Lütolf et al., 2002).

#### Roles of Notch effectors

The classical Notch effectors in embryonic neurogenesis are *Hes1* and *Hes5*. *Hes1* and *Hes5*-deleted double mutant embryos show severe defects in neural development: disorganization of the neural tube, premature neuronal differentiation, and loss of RGs (Hatakeyama et al., 2001). The abnormal phenotype is even stronger than in *Hes1* mutants, which die perinatally. In *Hes1* mutants, the elevated *Hes5* expression was detected, suggesting the existence of compensatory mechanisms between these Notch targets (Yoon and Gaiano, 2005). Moreover, *Hes1* is capable of almost completely compensating for the lack of *Hes5* function in *Hes5*-deleted mutants. In the developing spinal cord, *Hes1* and *Hes5* are Notch1 immediate targets for the maintenance of NSPCs and binary cell fate decisions (Yang et al., 2006). More recently, *Hey1* function in maintaining a population of NSPCs in a subdomain of the SVZ has been shown (Harada et al., 2021). Contrary to *Hes* effector expressions which are probably oscillatory in adult NSCs, the expression of *Hey1* is non-oscillatory.

#### In the adult mouse

In the adult mouse brain, all four Notch receptors are expressed in various cell types, including NSCs (*Notch1*, *Notch2*, and *Notch3*), astrocytes (*Notch1* and *Notch2*), neurons (*Notch1* and *Notch2*), endothelial cells (*Notch1* and *Notch4*), and vascular smooth muscle cells and pericytes (*Notch3*) (Lampada and Taylor, 2023). As in mouse embryos, IPs and cells downstream in the



neuronal lineage can express Notch receptors and ligands but only the NSCs express the *Hes/Hey* classical effectors.

#### Maintenance of NSCs

In the adult mouse SVZ and SGZ, Notch plays a pivotal role in the maintenance of NSCs. Conditional Cre-*loxP* tamoxifen-dependent recombination to delete *RBP-Jk* in NSCs of the adult telencephalon and hippocampus resulted in an initial transient increase in neurogenesis that is followed by a total depletion of the NSC pool and loss of neurogenesis in the long-term (Ehm et al., 2010; Imayoshi et al., 2010; Lugert et al., 2010). These results were comparable to those obtained in conditionally *Notch1*-deleted mutants. In the SVZ and the SGZ of *Notch1*-deleted mice, the number of NSCs was decreased, as well as the number of IPs, immature neurons, and mature neurons (Ables et al., 2010). These results show that Notch1 is necessary for sustained adult neurogenesis in the adult mouse brain. In the adult mouse forebrain, astrocytes express *Notch1* and *Notch2*, as well as the effector *Hes5*, while endothelial cells express high levels of *Dll4*, *Jag1*, and *Jag2* ligands (Cahoy et al., 2008). After spinal cord injury, reactive astrocytes down-regulate Notch signaling for the activation of the neurogenic program and their astrocyte-neuron transition (Bringuier et al., 2023; Farmer and Murai, 2017). In uninjured *RBP-Jk*-deleted mutant mice, astrocytes also become neurogenic, whereas the overexpression of *NIICD* in astrocytes prevents neurogenesis after injury (Magnusson et al., 2014). These results demonstrate that persistent Notch signaling maintains the quiescence of astrocytes and prevent neurogenesis (Farmer and Murai, 2017).

#### Maintenance of aNSCs

Notch1 promotes the maintenance of aNSCs in the adult brain. Conditional Cre-*loxP* tamoxifen-dependent *Notch1*-deletion in NSCs led to selective loss of the aNSCs pool while qNSCs remained unchanged (Engler et al., 2018a; Basak et al., 2012). In the adult rodent spinal cord, *notch3* is expressed in IPs and immature neurons in the grey matter, in a pattern complementary to *Gfap*, while *Notch1* and *Notch2* are broadly expressed throughout the spinal cord white and grey matters in non-neuronal cells (Rusanescu and Mao, 2017). *Notch2* is described in a subset of *Gfap*<sup>pos</sup> cells and is excluded from the upper dorsal horn. Interestingly, in the grey matter, *Notch1* and *Notch3* expression are mutually exclusive, found in pairs of adjacent cells, and *Dll1*, *Dll4*, and *Jag1* have expressions complementary to *Notch3*, while *Jag2* is expressed in the same cells as *Notch3*. These patterns suggest non-classical lateral inhibition

mechanisms segregating individual Notch receptors and individual ligands, and a role of Notch3 in promoting neuronal differentiation, in contrast to Notch1 function. *In vitro* experiments showed Notch3 implication in neuronal differentiation, and *Notch3*-deleted mutant mice have impaired neuronal maturation (Rusanescu and Mao, 2017). *In vitro*, Notch1 was shown to promote the proliferation of spinal cord-derived NSPCs (Wang et al., 2018). These results indicate that Notch1 regulates NSPCs proliferation, while Notch3 is involved in neuronal differentiation in the adult rodent spinal cord. Notch1 is also implicated in the case of adult spinal cord injury, where it is upregulated during the acute phase of injury (Patel et al., 2021).

#### Maintenance of qNSCs

*Notch1*, *Notch2*, and *Notch3* are co-expressed in SVZ and SGZ qNSCs. Conditional *Notch2*-deletion in NSCs induces the activation and proliferation of qNSCs and leads to precocious differentiation and increased neurogenesis in the SVZ (Engler et al., 2018a). The NSCs pool is progressively exhausted, and the neurogenic potential disappears. Interestingly, the *Notch1*- and *Notch2*-deleted double mutant phenocopies the *RBP-jk* mutant, highlighting that Notch1 and Notch2 regulate NSC maintenance with the canonical pathway, at least until RBP-Jk-mediated transcription (Engler et al., 2018a). Similarly, conditional *Notch2* deletion in *Hes5*<sup>pos</sup> SGZ NSCs induces a rapid loss of qNSCs and decreases IPs, effects that culminate 100 days after *Notch2* inactivation. These phenotypes were accompanied by the downregulation of qNSC-associated genes, such as Notch signaling genes, including *Notch2*, and the upregulation of genes associated with NSC activation (Zhang et al., 2019). Overexpression of *N2ICD* in SGZ NSCs maintains qNSCs, blocks their entry into cell cycle, and decreases the number of IPs and neurons (Zhang et al., 2019). These results support the role of Notch2 in the regulation of NSCs quiescence.

Numerous other niches in addition to the SVZ and SGZ are under investigation for neurogenic potential, and neurogenic qNSCs have already been identified in the dorsal septal wall of the lateral ventricle (Lampada and Taylor, 2023; Leal-Galicia et al., 2021). In these cells, *Notch2* deletion increases cell proliferation and the production of IPs and neurons, but these neurons do not migrate to the OB (Lampada et al., 2022). These results show that Notch2 functions are conserved in the different adult neurogenic niches for NSCs quiescence regulation, and prevention of NSCs activation and neurogenesis.

Notch3 has at least a partially redundant function with Notch2 in qNSCs. *Notch3* is expressed by qNSCs located at the lateral and ventral walls of the VZ-SVZ (Kawai et al., 2017). In *Notch3*-deleted mouse, fewer NSCs are present in the SVZ (Kitamoto et al., 2005; Kawai et al., 2017). The numbers of qNSCs, IPs, and immature neurons are negatively impacted, whereas the number of aNSCs remains unchanged. It was suggested that qNSCs in *Notch3* KO mice increase their activation but fail to complete lineage progression (Kawai et al., 2017). Moreover, short hairpin RNA (shRNA)-mediated knock-down (KD) of *Notch3* in the lateral ventricle of adult mice increases NSCs proliferation (Kawai et al., 2017). Overexpression of *Notch3* by CADASIL-causing point mutations reduces NSC activation and proliferation without affecting levels of neurogenesis in the adult DG (Ehret et al., 2015). Interestingly, while, as expected, the overexpression of *N3ICD* suppresses NSCs proliferation, the same phenotype is observed when *NIICD* is overexpressed (Basak et al., 2012; Kawai et al., 2017). This result indicates that high expression levels of both activated Notch1 and Notch3 are capable of suppressing the proliferation of NSPCs.

#### Roles of Notch ligands

*Dll1* and *Jag1* are expressed in the SVZ and the SGZ of adult mouse. *Dll1* deletion from the SVZ NSCs decreases the number of qNSCs while increasing the number of aNSCs and IPs (Kawaguchi et al., 2013). Moreover, *Dll1* is expressed in cells negative for NICD and near qNSCs. In the SVZ, *Jag1* and *Notch1* expressions are mutually exclusive. *In vitro* in adult mouse SVZ-derived neurospheres, *Jag1* deletion blocks NSCs self-renewal without affecting their differentiation, while the reverse is true when *Jag1* is overexpressed (Nyfeler et al., 2005). These results suggest that Notch function on quiescence regulation may be Dll1- or Jag1-dependent via lateral inhibition.

#### Roles of Notch effectors

Notch effector functions and specificities are still under investigation. As in the embryo, *Hes1* and *Hes5* are the most studied in the adult brain. In the SVZ and the SGZ, *Hes1* expression is higher in qNSCs than in aNSCs, while *Hes5* expression level is equivalent in both (Lampada and Taylor, 2023). *Hes1* has been identified as the main Notch effector regulating quiescence versus activation in adult mouse NSCs (Sueda and Kageyama, 2020; Sueda et al., 2019).

### 3.3.3.2 *In zebrafish*

#### *In the zebrafish embryo*

In the zebrafish embryo, single-cell transcriptomic data have highlighted the expression of *notch* genes as early as 5 hpf (Liu et al., 2022). At 24 hpf, Gfap<sup>pos</sup> cells express *notch1a* and *notch3* at higher levels than *notch1b*, while *notch2* expression is weak. IPs progressively lose the expression of *gfap* and *notch* genes while accumulating expression of the newborn neuron marker *huC* (Liu et al., 2022).

#### *Maintenance of NSPCs and regulation of neurogenesis*

Notch signaling is implicated in the maintenance of NSPCs and the regulation of neurogenesis in the developing zebrafish nervous system. Treating 2 dpf zebrafish embryos for 9 hours with the inhibitor of  $\gamma$ -secretase LY411575 (LY) caused an almost complete loss of *her4*-expressing RG in the telencephalon, presumably through premature differentiation into neurons (Figure 10A-C) (Dirian et al., 2014). Loss-of-function mutations in *mib* decrease the expression of RG markers such as Gfap (Jiang et al., 1996). In parallel, the number of newborn neurons is increased throughout the CNS, and this phenotype is particularly striking in the Mauthner cells, a type of primary hindbrain sensory interneurons (Schier et al., 1996; Jiang et al., 1996). These results show that the activities of the  $\gamma$ -secretase and Mib contribute to the maintenance of NSPCs in zebrafish embryos and the regulation of the onset of neurogenesis. However,  $\gamma$ -secretase cleaves the transmembrane domain of more than 90 type I membrane proteins, and Mib might have Notch-independent roles (Lv et al., 2024; Dho et al., 2019), therefore the Notch implication in the observed phenotype must be analyzed further.

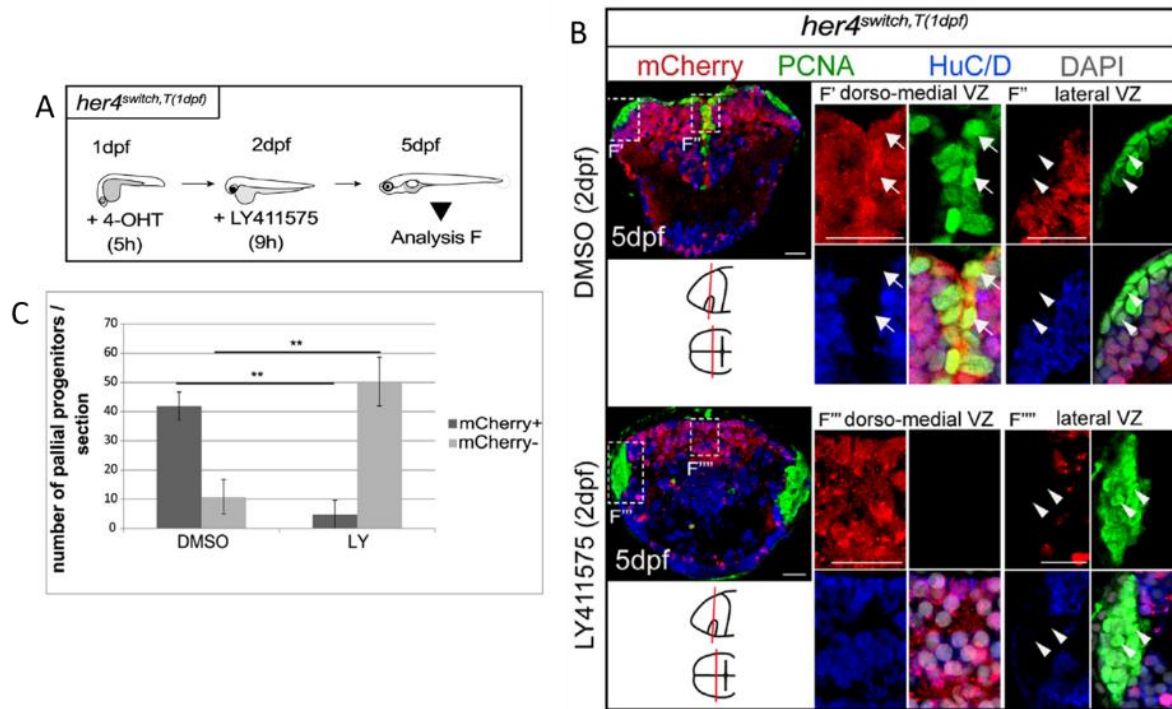


**Figure 10: Notch inhibition reduces the number of dorsomedial pallial progenitors (from Dirian et al., 2014)**

(A) Experimental design to assess Notch sensitivity of pallial progenitors at 2 dpf. *Tg(her4:ERT2CreERT2; ubi:switch)* were treated with 4-OHT to induce *mCherry* expression in progenitors at 1 dpf.

(B) Medial cross-sections of the telencephalon of 5 dpf larvae treated with DMSO or LY. Magnification of the dorsomedial VZ (F' and F''') and lateral VZ (F'' and F'''). *mCherry* marked ventricular progenitors and their progeny, PCNA proliferative cells, HuC/D neurons, and DAPI the nuclei. Arrows and arrowheads highlight, respectively, the dorsomedial progenitors ( $mCherry^{pos}/PCNA^{pos}$  cells) and the lateral progenitors ( $mCherry^{neg}/PCNA^{pos}$  cells).

(C) Compared number of pallial dorsomedial progenitors (dark gray) and of lateral progenitors (light gray) in control (DMSO) and treated (LY) conditions. Values are presented as mean  $\pm$  95% confidence interval (ANOVA, \*\*  $p < 0.05$ ).

In the hindbrain, *notch1a* is expressed throughout the rhombomeres and their boundaries. In *notch1a*-deleted mutants, only a small increase in neurogenesis is observed in the CNS, while the number of Mauthner cells is also positively impacted (Gray et al., 2001). Interestingly, the increased number of Mauthner cells is compensated for by a reduced number of synapses formed on target cells in the spinal cord, maintaining overall normal neuronal signals (Liu et al., 2003). The phenotype of the increased number of Mauthner cells is rescued by overexpressing *NIICD*, which indicates that Notch1a contributes to the regulation of neurogenesis, at least in the hindbrain. In the developing spinal cord, *notch1b* and *notch3* are expressed in NSPCs, while *notch1a* is expressed in both NSPCs and IPs (Appel et al., 2001). When treating embryos with DAPT, or in *mib*-deleted mutants, the NSPCs of the spinal cord are lost and all the progeny generated are neurons (Kim et al., 2008a; Park and Appel, 2003). These results show that Notch maintains spinal cord progenitors and prevents their

differentiation. Interestingly, in NSPCs, Notch signaling was shown to potentialize Hedgehog signaling (Jacobs and Huang, 2019; Huang et al., 2012).

Still using the *mib*-deleted mutants, Sharma et al. showed that the inhibition of neurogenesis by canonical Notch signaling is essential for the initial formation and apicobasal polarization of NSPCs in the dorsomedial domains and not the ventral domains of the anterior spinal cord (Sharma et al., 2019).

#### Maintenance of tissue boundaries

In the hindbrain, Notch signaling has also been shown to maintain the morphogenetic rhombomere boundaries. *notch1a* is co-expressed with *notch1b* and *notch3* at the centers of rhombomeres, whereas at rhombomeres boundaries *notch1a* is only co-expressed with *notch3* (Qiu et al., 2009). *mib* deletion induces disruption of the rhombomere boundaries by inhibiting Notch signaling, using *her4* or *her6* as activation readouts (Qiu et al., 2009; Zhang et al., 2007). At 24 hpf, *notch1a*-deleted mutants as well as *notch1b* and *notch3* morphant embryos do not show a rhombomere boundary phenotype (Qiu et al., 2009). In the *notch1a* mutant injected with *notch3* morpholino (MO), cells aggregate and organize in rosette-like structures in the posterior hindbrain, while boundary cells differentiate into neurons therefore reducing the total number of boundary cells. These results indicate that Notch1a and Notch3 have redundant functions in controlling hindbrain patterning and neurogenesis. *notch3* deletion leads to the loss of the progenitors at rhombomeres centers, impacting overall neurogenesis, and to the differentiation of the majority of rhombomere boundary progenitor cells (Alunni et al., 2013; Belmonte-Mateos et al., 2023; Hevia et al., 2022). This result reveals that Notch3 is necessary for the maintenance of the progenitor state at rhombomere centers and boundaries, which therefore are maintained during embryonic development. Interestingly, at boundaries, *deltaD* is expressed underneath NPs, which supports the possibility of a lateral inhibition mechanism along the dorsoventral axis, maintaining progenitor cell stemness before their final neurogenic differentiation (Hevia et al., 2022).

#### Binary cell fate choice

Notch signaling maintains neural progenitors by lateral inhibition, but also mediates binary cell fate choices in NSPCs. In the developing zebrafish retina, *notch1b* and *notch3* are expressed by differentiating Müller glial cells (dMGs), and *jag2b* is expressed by photoreceptors (Jin et al., 2022). *jag2b* deletion prevents the maturation of the dMGs and generates another type of cells

instead, the bipolar cells. Conversely, overexpression of *notch3* or *notch1b* in dMGs increases the number of mature MGs. These results indicate that Notch1b/Notch3 and Jag2b participate in the regulation of binary cell fate choice by promoting glial fate in the zebrafish developing retina.

Other studies have shown that *notch3* deletion also decreases the NPs pools and the number of OPCs in the medial region of the hindbrain, and increases the number of neurons (Zaucker et al., 2013). This result suggests that Notch3 maintains the progenitors in the hindbrain but also contributes to the binary cell fate choice by stimulating the generation of OPCs and limiting the generation of neurons. Interestingly, heterozygote mutants express higher levels of progenitor markers and display elevated cell death compared to wild-type and homozygous mutants (Zaucker et al., 2013). This result suggests that the differentiation of some progenitors might be delayed by the partial reduction of Notch3 signaling and that some delayed progenitors could undergo apoptosis. Further analyses will have to consider the potential dose-dependent effect between heterozygote and homozygote mutants.

The developing spinal cord features distinct neurogenic regions along the dorsoventral axis (Frith et al., 2024). In the more ventral regions, the progenitors are classified as p3, motor neuron progenitors (pMNs), and p2. The MO-mediated deletion of *notch3* reveals its role in binary cell fate decision and maintenance of pV2 progenitors together with Notch1a and Notch1b (Okigawa et al., 2014). Notch1 was implicated in binary cell fate decision in pMNs progenitors by specifying sibling cells for different neuronal fates and contributing to lateral inhibition mechanisms maintaining the neighboring pMNs progenitor state (Shin et al., 2007). In the P3 domain of the developing spinal cord, Notch regulates binary cell fate choice between neurons and perineurial glia, and in the pMN domain, Notch limits the generation of motor neurons and promotes the formation of OPCs by respecting a specific timeline (Kim et al., 2008b; Kim et al., 2008b; Park and Appel, 2003). The importance of the timeline for the fate decision is also true in the lateral floor plate (LFP) where the total quantity of Notch signaling received by a cell, which depends on the duration of signaling, guides the cell fate toward Kolmer-Agduhr (KA) interneurons, V3 interneurons, and LFP progenitors fate in a sequential manner (Jacobs et al., 2022). In the p2 domain, where NSPCs divide asymmetrically to give rise to V2a and V2b neuron pairs, Delta-Notch interactions between sister cells are crucial for the asymmetry (Kimura et al., 2008).

### Roles of Notch ligands

Regarding Notch ligands, single-cell transcriptomic data highlights their medium expression in NSPCs and their increased expression in IPs (Liu et al., 2022). In the developing hindbrain of 24 hpf embryos, *dla* and *dld* are expressed in stripes adjacent to the rhombomere boundaries, while *dlc* is weakly expressed (Cheng et al., 2004; ZFIN). In the developing spinal cord, *dla* and *dld* are broadly expressed in all the cells, whereas *dlb* expression is specific to the newborn neurons (Appel et al., 2001). In single *dlc*- or *dld*-deleted zebrafish mutants, neurogenesis is increased in the hindbrain at similar levels than in the double mutants (Jülich et al., 2005; Holley et al., 2000). This result indicates that Dlc and Dld do not have overlapping functions during hindbrain neurogenesis, but allow lateral inhibition in distinct cells (Jülich et al., 2005). In the ventral spinal cord, Jag, and in particular Jag2b is involved in the maintenance of NSPCs by Notch signaling, while Dla has the same function but throughout the dorsoventral domains (Jacobs et al., 2022; Yeo and Chitnis, 2007; Appel et al., 2001).

### Roles of Notch effectors

One possible effector of Notch signaling in zebrafish embryos is Her6, whose expression has been described since 8 hpf embryos in the hindbrain and the forebrain midline (Pasini et al., 2001). *her6* is expressed in an oscillatory manner (around 2 hours periodicity) in proliferating NPs of the embryonic telencephalon. However, the fact that PEST-domain-mediated protein destabilization in early embryos only mildly affects neurogenesis was suggested to be due to compensation by a cell-cell coupling mechanism (Doostdar et al., 2024).

### In the adult zebrafish

In adult zebrafish, the functions of Notch signaling are mostly studied in the telencephalon, the retina, and the spinal cord. In adult zebrafish pallium, *notch1a*, *notch1b*, *notch2*, and *notch3* are expressed along the telencephalic ventricular zone (Chapouton et al., 2010). *In situ* hybridizations showed that the expression *notch1a* appeared too weak to be reliably assigned to a specific cell type, and *notch2* expression was not detectable (Alunni et al., 2013). *notch3* expression is enriched in qNSCs, and co-expressed with *notch1b* in aNSCs (Chapouton et al., 2010).



### Maintenance of NSCs (in larvae)

The Moens lab generated the *notch3*<sup>fh332</sup> null allele, which harbors a nonsense mutation that introduces a premature *stop* codon in the 8<sup>th</sup> Notch3 EGF repeat (Alunni et al., 2013; <https://research.fredhutch.org/moens/en.html>). As homozygous *notch3*<sup>fh332</sup> mutants die at 10-15 dpf, analyses of the effect of a complete genetic blockage of Notch3 signaling were conducted in the larval pallium. At 7 dpf, 75% of all NSCs are proliferating. In homozygous *notch3*<sup>fh332</sup> mutants, on the contrary, 100% of NSCs are activated (Alunni et al., 2013). As in the adult, this forced NSCs activation is biased toward symmetric gliogenic divisions. At 10 dpf, the proportion of neurons is significantly increased in homozygous *notch3*<sup>fh332</sup> mutants, with a concomitant decrease in the proportion of IPs, while in wild-type siblings these values are not significantly changed (Than-Trong et al., 2018). Together, these findings indicate that, in addition to promoting NSCs quiescence and limiting amplifying NSCs divisions, Notch3 is necessary to maintain the NSCs progenitor state.

### Maintenance of qNSCs

In the adult zebrafish pallium, Notch signaling maintains NSCs quiescence via lateral inhibition. Treating zebrafish for 2 days with DAPT increases the number of PCNA<sup>pos</sup> cells, which represent aNSCs, while the percentage of qNSCs is divided by two (85.8 to 42.5%) (Chapouton et al., 2010). Similarly, electroporation or lipofection of constructs inhibiting Notch signaling (e.g. expression of D11-dominant negative) also increases the percentage of proliferating cells. Adult heterozygous *notch3*<sup>fh332</sup> mutants (viable and fertile) were treated with suboptimal doses of LY, showing that lower LY treatment was sufficient to induce proliferation in a subpopulation of NSCs (Figure 11) (Alunni et al., 2013). In addition, MO-mediated *notch3* deletion increased the proportion of proliferating NSCs (Figure 12A-C) (Alunni et al., 2013). These results indicate that Notch signaling, and particularly Notch3, contributes to the maintenance of NSCs quiescence.

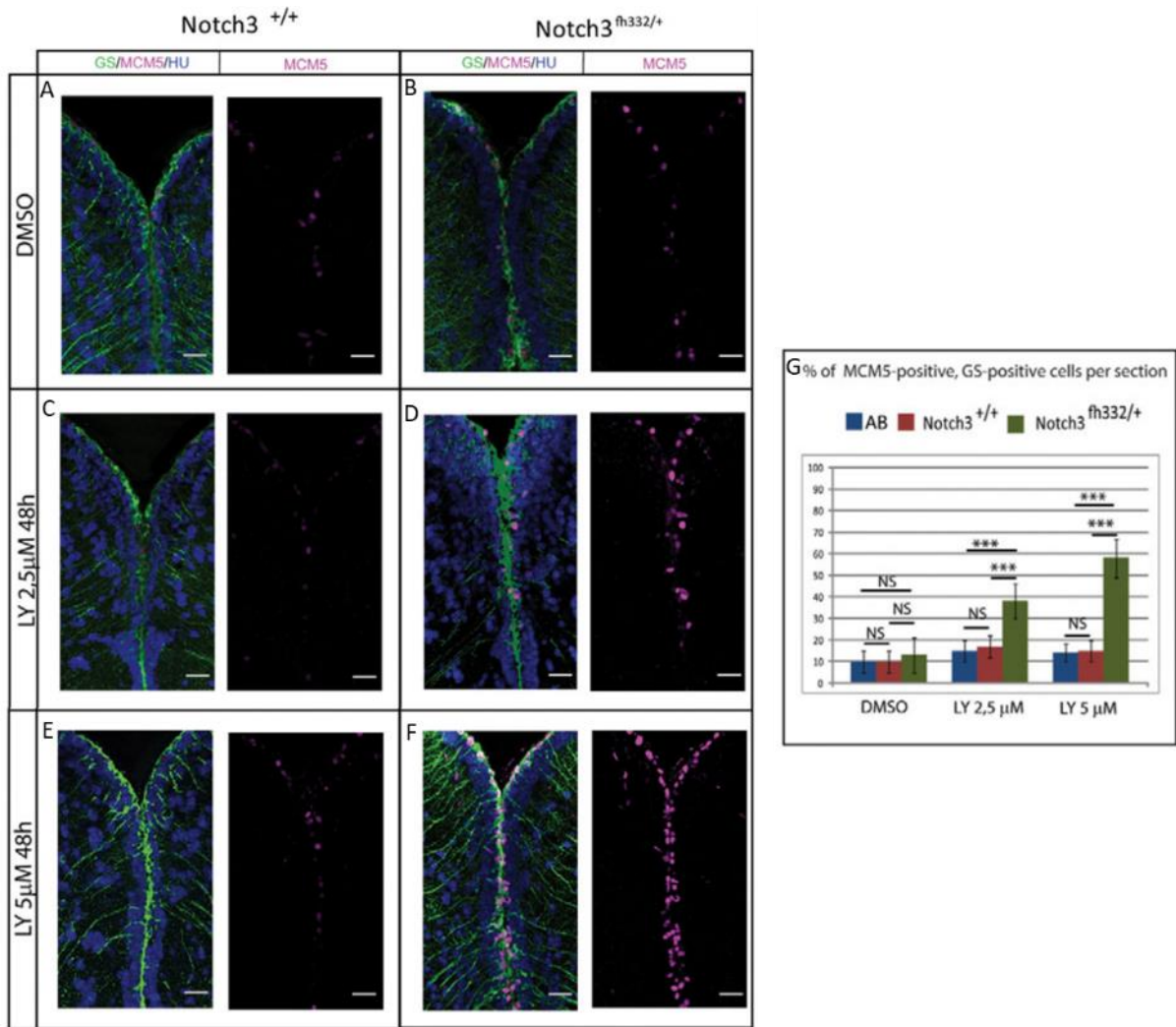


**Figure 11: Notch3 inhibition accounts for the effect of Notch blockade on RG activation (from Alunni et al., 2013)**

(A-F) Triple immunohistochemistry for the radial glia marker glutamine synthetase (GS, green), the proliferation marker MCM5 (magenta) and the neuron marker HuC/D (blue) on telencephalic cross-sections from adult *notch3*<sup>+/+</sup> siblings and *notch3*<sup>fh332/+</sup> heterozygotes under control conditions (top row) or upon LY treatment (middle and bottom rows). Scale bar: 20 μm. Confocal projection images from four optical planes, each 1 μm thick.

(G) Proportion of RGs in proliferation in the different genotypes and treatment conditions, as well as in the standard AB wild-type line.  $p < 0.0001$  (n = 3 brains for AB, *notch3*<sup>+/+</sup> and *notch3*<sup>fh332/+</sup>, respectively).

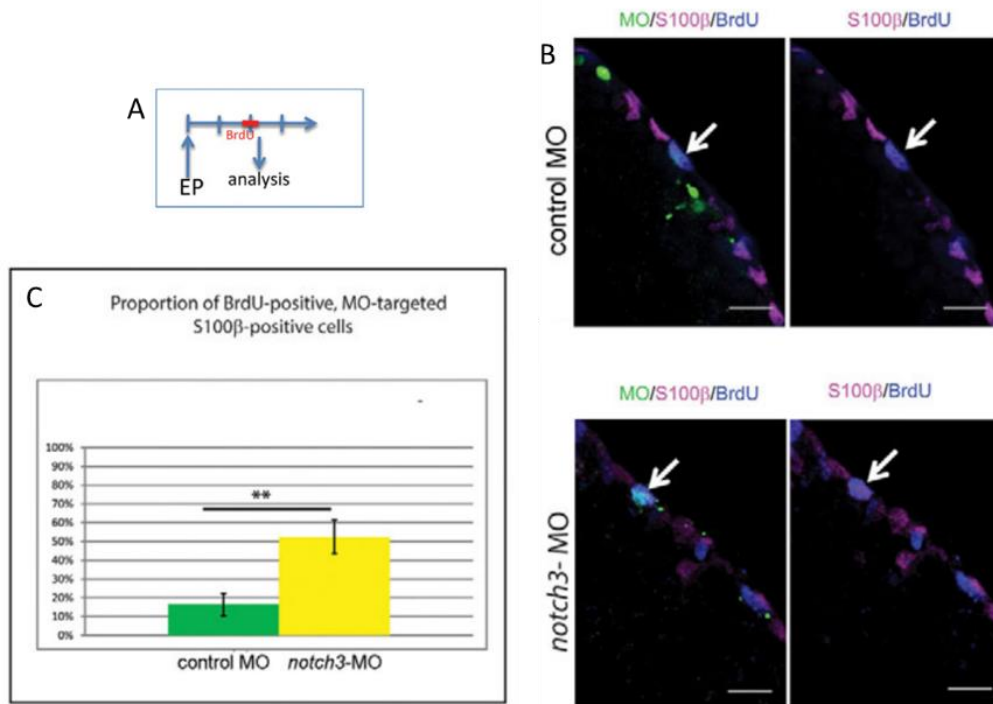


**Figure 12: Notch3 inhibition in isolated pallial neural stem cells induces their proliferation (from Alunni et al., 2013)**

(A,B) Adult brains were electroporated (EP) with a fluorescein-tagged splicing MO against *notch3* (*notch3*-MO) or a control MO, and the proliferation status of the electroporated cells was analyzed two days after using BrdU and immunostaining. S100β marked radial glia (RG). Arrows indicate fluorescein-labeled RG BrdU<sup>pos</sup> cells. Scale bar: 20 μm. Confocal projection images from four optical planes, each 1 μm thick.

(C) Proportion of BrdU<sup>pos</sup> cells within the radial glia MO-targeted population.  $p < 0.001$  (n= 3 brains for each condition).

In the adult zebrafish retina, which displays active proliferative and neurogenic activities throughout life, *notch3* is expressed in Müller glia cells, while *deltaB* expression is enriched in neurons, and Notch3 is required to maintain the Müller glia in a quiescent state, via its interaction with Dlb (Campbell et al., 2022; Hernández-Núñez et al., 2021). In the adult zebrafish retina, the other Notch receptors are necessary for proliferation during regeneration (Campbell et al., 2021). Similarly, in the adult zebrafish spinal cord, which shows very little, if any, proliferation and neurogenesis, Notch signaling is involved in the regulation of cell proliferation during regeneration (Hernández-Núñez et al., 2021; Reimer et al., 2008). In lesioned spinal cords, the expressions of *notch1a*, *notch1b*, and *notch2* are increased in the VZ (Cardozo et al., 2017; Dias et al., 2012). As indicated by the upregulation of *notch1b* and *her4.1* in pMNs, Notch signaling is activated in these cells. In the lesion condition, overexpression of *NIICD* prevents pMNs proliferation around the lesion site, whereas DAPT treatment increases their proliferation (Dias et al., 2012). Interestingly, the increased number of motor neurons (MN) does not improve the fish recovery. These results show that Notch signaling maintains

pMNs in a non-proliferating state, and Notch is precisely regulated to control the onset of neurogenesis in the lesioned spinal cord.

In the adult zebrafish pallium, Notch regulates the onset of neurogenesis. In the DAPT condition, the expressions of *ascl1a*, as well as the IP marker Polysialylated neuronal cell adhesion molecule (*PSA-NCAM*) and the newly formed neurons marker *hu* are increased (Chapouton et al., 2010). Interestingly, even if *PSA-NCAM* is also detected in S100 $\beta$ <sup>pos</sup> cells, suggesting that the transition from aNSC to IP is accelerated, forced aNSCs follow the same schedule as normal progenitors for neural differentiation.

#### Maintenance of aNSCs

In the adult zebrafish pallium, Notch maintains aNSCs. Electroporation of a MO mediating *notch1b* blockade does not affect the proportion of proliferating NSCs 2 days after electroporation but strongly decreases this proportion by 5 days (Alunni et al., 2013). This decrease is mostly due to the acquisition of premature neuronal fate by aNSCs. This result shows that Notch1b has a striking different role than Notch3, and prevents the differentiation of aNSCs.

#### Cell fate choice

In the adult zebrafish pallium, Notch contributes to the cell fate choice of daughter cells. Indeed, the aNSCs negative for the expression of *dla*, divide to generate one *dla*-negative (*dla*<sup>neg</sup>) NSC seemingly identical to its mother, and one *dla*<sup>pos</sup> NSC, that will further divide at higher frequency and finally generate IPs (Mancini et al., 2023). The mechanisms underlying this molecular asymmetry are still unknown. However, Notch signaling may be activated at a higher level in the *dla*<sup>neg</sup> cells by lateral inhibition to maintain the NSCs pool over time.

#### Roles of Notch ligands

Classically, lateral inhibition preferably relies on Delta ligands and Her, while lateral induction involves the Jagged ligand and an Hey1 effector (Yoshihara and Takahashi, 2023). While *dla*, *dlb*, *dld*, *dll4*, *jag1a*, *jag1b*, and *jag2* are also expressed in the telencephalic VZ, almost all dividing cells express *dla* (Chapouton et al., 2010). Interestingly, in control pallia of the DAPT experiment, PCNA<sup>pos</sup> dividing cells are spaced from each other by several cell diameters, and most of the newly dividing cells were not in contact with former 5'-bromo-2'-deoxyuridine (BrdU)<sup>pos</sup> dividing cells (Chapouton et al., 2010). In contrast, in DAPT-treated pallia, many

newly dividing cells are located close to the former dividing cells. Conversely, overexpression of *NIICD* is sufficient for the NSCs to enter quiescence. These results demonstrate that Notch signaling is activated by dividing neighbors to maintain quiescence. In the lesioned spinal cord of adult zebrafish, the expression of *jag1b* is increased in the VZ, while the expression of *dlc* is increased in newly generated MN (Dias et al., 2012). This result suggests that Notch1b is activated in pMNs by its neuronal progeny and that the interaction Notch1b-DeltaC prevents pMNs proliferation.

#### Roles of Notch effectors

On the side of the effectors, in the adult zebrafish telencephalon, *hey1*, *her4*, and *her6* are expressed at the midline and dorsally, while the expression of *her8*, *her9*, and *her15* are limited to the midline (Than-Trong et al., 2018; Chapouton et al., 2011). As in the hypothalamus and the posterior midbrain, these genes are expressed by qNSCs but are generally excluded from aNSCs in the telencephalon (Chapouton et al., 2011). In the pallium, it has been shown that Notch3 drives the NSC quiescence with the effector Her4, and the NSC stemness with the effector Hey1 (Than-Trong et al., 2018). In the adult zebrafish retina, *her4* and *hey1* are expressed in Müller glia cells and *her6* in Müller glia cells and retinal IPs, and Notch3 effector for the maintenance of quiescence is Her4, possibly with the help of Hey1, whereas Her6 promotes retinal IPs proliferation and inhibits neurogenesis (Campbell et al., 2022). In the lesioned spinal cord of adult zebrafish, the Notch1b effector for maintaining pMNs quiescence may be Her4.1 (Dias et al., 2012).

#### Conclusion

In general, in the studied neurogenic regions of mouse embryos (neural tube, MHB and cerebellum, all forebrain, telencephalon, hippocampus, roof plates of the diencephalon and the mesencephalon, spinal cord, and retina) and zebrafish embryos (telencephalon, hindbrain, spinal cord, and retina), Notch signaling has redundant functions for maintaining NSPCs, and precisely balancing self-renewal and differentiation, therefore gating gliogenesis and neurogenesis and participating in binary cell fate decisions. Notch activity also contributes to the correct morphogenesis of neural tissues. However, some functions have only been seen in one of the two models. In mouse embryos, Notch signaling participates in the regulation of NSPCs apoptosis, whereas in zebrafish embryos, Notch contributes to maintaining tissue boundaries.

In the studied neurogenic niches of adult mice (SVZ, SGZ, and spinal cord) and adult zebrafish (telencephalon, retina, and regenerative spinal cord), Notch signaling still has redundant functions for the maintenance of the stemness of NSCs and therefore their sustained neurogenic potential, the binary cell fate decisions, the proliferative capacities of aNSCs, and the quiescence of qNSCs. In both models, Notch activity also regulates the neurogenic regeneration process. Moreover, in adult mouse, Notch maintains astrocytes quiescent and inhibits their astrocyte-to-neuron differentiation, while it also participates in neuronal differentiation of IPs in the spinal cord.

In embryos, Notch1 and Notch2 in mice, and Notch1a, Notch1b, and Notch3 in zebrafish, play at least partially redundant roles in maintaining NSPC progenitor states. In adult mice and zebrafish, Notch1 and Notch1b prevent aNSC differentiation. In adult mice, Notch2 keeps NSCs in a quiescent state, sharing a partially redundant function with Notch3, while in larval zebrafish, Notch3 maintains the progenitor state of NSCs, and in adult zebrafish, Notch3 ensures that NSCs remain quiescent.

### ***3.4 Why study Notch3 in zebrafish neural progenitors?***

Notch3 signaling sustains neural progenitors throughout life and maintains quiescence in adult NSCs, but its precise mechanisms of action and the long-term effects of its invalidation remain only partially understood. To gain insight into these aspects, we need to delineate the specific characteristics of the Notch3 pathway compared to other Notch pathways in the NSC context, including its ligands, targets, and regulatory mechanisms. Additionally, we must distinguish the functions of Notch3 in the nucleus, such as the role of N3ICD as a transcription factor, and the functions of Notch3 at the membrane, as a signaling pathway modulator or guardian of epithelial integrity. Moreover, it is crucial to examine the consequences of Notch3 loss-of-function using mosaic contexts, to be able to address its effects in both directly invalidated cells and the surrounding tissue.

Traditional KD methods commonly used in our lab to test gene function in adult pallial NSCs, present significant limitations hindering the detailed analysis of these aspects.

#### 4. Development of a new method to study the functions of Notch3 signaling

I will focus here on loss-of-function methods, which are often more informative than gain-of-functions to reveal gene function. Indeed, while gain-of-functions provide information about what a gene can do (i.e., on sufficiency), overexpression conditions can mimic the activity of related genes, can lead to non-physiological responses due to dose effects, and do not necessarily reveal what a gene is needed for under physiological conditions (i.e., necessity).

Loss-of-function methods, including both KD and KO approaches, are extensively employed in functional genomics to investigate the roles of specific genes *in vivo* (Zimmer et al., 2019). These methods involve either reducing or eliminating gene expression or activity. KD involves reducing the amount of functional protein through perturbation at the DNA, RNA, or protein level, while KO results in a genetic alteration that entirely abolishes gene function. Gene functions are then examined through changes in phenotype, transcriptome, and other molecular markers. To study Notch3 signaling functions in zebrafish NSPCs, researchers have used both MO-mediated gene KD and genomic *notch3* KO mutants (Sidik and Talbot, 2015; Jin et al., 2022; Zaucker et al., 2013; Pogoda et al., 2006; Alunni et al., 2013; Belmonte-Mateos et al., 2023; Hevia et al., 2022; Than-Trong et al., 2018). It is worth remembering that pharmacological methods, e.g., the use of  $\gamma$ -secretase inhibitors, which have been used in zebrafish, including by our lab, are not specific to Notch3 (Feng et al., 2024).

When used in the study of NSCs in zebrafish, classic MOs, coupled to a fluorophore or mixed with DNA to be charged, are typically injected into embryos at the one-cell stage or injected into the ventricle and electroporated into the adult brain (Figure 12A-C) (Alunni et al., 2013). Vivo-MOs are injected into the ventricle of the adult brain where they passively penetrate the membranes of contacting cells thanks to their delivery moiety, consisting of positively charged arginine-rich polypeptides that aggregate at the membrane, promote membrane pore formation and stabilization, and eventually cross (Vazdar et al., 2018). Two types of MO applications in zebrafish are splice blocking and translational blocking (Bill et al., 2009). MO are antisense oligonucleotides designed to bind to an intron/exon boundary of a target gene pre-mRNA, blocking splicing through complementary base-pairing, or binding the 5' Untranslated region (UTR) or the sequence containing ATG to prevent ribosomal activity. Both types of MOs are used against zebrafish *notch3* and almost exclusively in embryos (Kim et al., 2014; Okigawa et

al., 2014; Alunni et al., 2013; Mizoguchi et al., 2011; Qiu et al., 2009; Hsiao et al., 2007; Liu et al., 2007; Ma and Jiang, 2007). In the laboratory, we use a splice MO that binds between exon 1 and intron 1 and generates a small non-functional polypeptide lacking all the functional domains of the Notch3 protein (Alunni et al., 2013). As previously described, this MO revealed that Notch3 plays a crucial role in maintaining the quiescent state in adult NSCs (Alunni et al., 2013). However, both classic and vivo-MOs remain functional for only a few days, depending on MO dose, delivery method, metabolism and dilution, and target mRNA turnover, and most MO KD are incomplete and result in the formation of small amounts of protein, while increasing the injection dose is strongly discouraged (Moulton, 2017; Zimmer et al., 2019; Bill et al., 2009). Further, MOs are prone to off-target effects, binding to non-target transcripts or causing toxicity, which often results in significant non-specific phenotypes in zebrafish, primarily due to the activation of p53-mediated apoptosis (Robu et al., 2007). The mechanisms of MO-induced p53 activation, immune responses, splice defects, and non-target binding are not well understood, making it difficult to minimize off-target effects (Zimmer et al., 2019).

Loss-of-function studies were similarly conducted using Notch3 mutants and resulted in similar phenotypes as those observed with the *notch3*-MOs. As described before, analysis of *notch3* mutants revealed the important role of Notch3 in maintaining the progenitor state in NPs (Alunni et al., 2013; Belmonte-Mateos et al., 2023; Hevia et al., 2022). The *notch3<sup>fh332</sup>* allele has a nonsense mutation that introduces a premature *stop* codon at amino acid 669 within the EGF repeats region, and results in a non-functional truncated protein lacking most of the extracellular and all of the transmembrane and intracellular domains of Notch3, and at the origin of a complete loss-of-function in homozygous mutants (Alunni et al., 2013). The homozygous *notch3<sup>fh332</sup>* mutants die prematurely at the juvenile stage, which prevents their use in adult studies (Alunni et al., 2013). Two other *notch3* mutants inducing complete loss-of-function have been described: *notch3<sup>ion36h</sup>* which generates a premature *stop* codon at amino acid 1303 within the EGF repeats region, and *notch3<sup>zm</sup>* which has a sequence of 158 pb inserted in its 5'-UTR region (Jin et al., 2022; Zaucker et al., 2013; Pogoda et al., 2006). The hypomorph *notch3<sup>st51</sup>* mutant, which mostly forms transcripts with a premature *stop* in the EGF repeat region, also forms a minority of transcripts deleted from 15 pb conserving their reading frame and having a residual gene activity (Zaucker et al., 2013). Interestingly, while the *notch3* heterozygotes mutants do not display any overt morphological abnormalities, in the hindbrain of 2-3 dpf *notch3<sup>st51</sup>* and *notch3<sup>zm</sup>* heterozygotes, the number of RGs progenitors is increased,



and apoptosis is exacerbated when compared to WT and homozygotes (Zaucker et al., 2013). However, the adult *notch3*<sup>fh332</sup> heterozygote pallium appears normal (Alunni et al., 2013). *notch3* loss-of-function mutants can have effects starting from early embryonic stages, and for a pleiotropic gene like *notch3*, it affects not only neural progenitors but also other cell types, such as brain pericytes (Bahrami and Childs, 2018; Wang et al., 2014). The *notch3*<sup>fh332</sup> larvae exhibit a reduced pericyte population, and compromised BBB and brain vascular integrity, resulting in brain hemorrhage. This makes it challenging to distinguish the direct effects of *notch3* KO on NSCs from those in other cell types that contribute to the NSC niche and thereby may affect neural progenitor behavior. In heterozygous *notch3* mutants, the mild embryonic defects may have consequences on adult NSCs and complexify the analysis of the loss-of-function effects in adults. Further, mutations inducing a premature *stop* codon have been reported to be able to evoke transcriptional adaptation-derived genetic compensation leading to complications and confusion in the study of gene functions (Rossi et al., 2015; El-Brolosy et al., 2019; Ma et al., 2019). Both MOs and mutants targeting *notch3* have technical limitations, yet these can be addressed through the use of alternative methods to further dissect Notch3 function.

#### ***4.1 Objectives of the method developed in my PhD***

My PhD research aims to circumvent the limitations of existing methods, particularly for long-term loss-of-function studies, by developing a new approach to achieve conditional *in vivo* loss-of-function of *notch3* in zebrafish neural progenitors. I also wished the loss-of-function to be tractable *in vivo*, i.e., monitored using molecular markers to identify the *notch3*-depleted cells. Finally, given the complexity of canonical and non-canonical Notch3 signaling (membrane activity, potential cytoplasmic roles, etc.), I also wanted loss-of-function effects to be confined to the nucleus, where the activated effector N3ICD acts as a transcription factor, to accurately interpret phenotypes resulting from canonical Notch3 activity.

In summary, the method must meet the following objectives:

- (i) Enable conditional (with cell type and time specificity), long-term, and tractable *notch3* loss-of-function specifically in neural progenitors
- (ii) Target only the nuclear functions of *notch3*

#### ***4.2 Conditional, long-term, and tractable loss-of-function***

Conditional expression systems offer precise control over the timing, duration, extent, chase period, and targeted cell types for the induction of gene expression. The Cre-*loxP* system, widely used in mice for conditional genetics, involves two transgenes: one transgene expressing Cre, a site-specific recombinase from bacteriophage P1, and one transgene bearing two *loxP* sites, recognized by Cre (Carney and Mosimann, 2018). Each *loxP* site comprises two 13 base pairs (bp) palindromic repeats flanking an asymmetric core spacer (Tian and Zhou, 2021). Cre recombinase mediates either excision (if the *loxP* sites are oriented in the same direction) or inversion (if oriented oppositely) of the sequence between the sites (Carney and Mosimann, 2018). The latter sequence can be an endogenous coding exon ("floxed" allele) or a transgenic cassette with *stop* and/or coding sequences ("switch" allele), allowing for the switching of multiple fluorophores, such as in the *ubi:loxP-GFP-loxP\_mCherry* (*ubi:Switch*) and the *ubi:zebrabow* lines (Mosimann et al., 2011; Pan et al., 2013). Coupling this with a Cre driven by a cell-specific promoter enables tissue-specific gene KO or regulation of transgene expression.

The timing of Cre activity is controlled using Cre fused to a mutant estrogen ligand-binding domain that binds tamoxifen (CreERT2) (Felker et al., 2016). This fusion protein keeps Cre in the cytoplasm until chemically induced for nuclear import. ERT2 is insensitive to natural estrogen but highly affine to synthetic estrogen mimics like tamoxifen metabolites (4-hydroxytamoxifen (4-OHT) and N-desmethyl-4-hydroxytamoxifen (Endoxifen)). The choice of drug, its concentration, and treatment duration influence the extent of tissue recombination, facilitating either mosaic induction for clonal analysis or complete induction in all cells expressing Cre.

In mice, many floxed alleles are available for conditional gene deletion, whereas this approach has been less common in zebrafish due to challenges in generating endogenous floxed alleles (Li et al., 2019). Zebrafish homologous recombination (HR)-mediated KI is less efficient than in mice, but recent advances in KI strategies are promising. One-step non-homologous end joining (NHEJ)-mediated insertion now provides an alternative to low-efficiency HR insertion and multiple KI steps (Shin et al., 2023; Li et al., 2019). This method enables the insertion of a dual-function allele for both tagging the protein of interest (POI) and conditional gene KO.

In zebrafish, numerous *loxP-stop-loxP* transgenic lines have been created. These lines prevent downstream transgene expression until Cre recombination, allowing for temporal control of expression (Carney and Mosimann, 2018). To maximize post-recombination transgene expression, ubiquitous promoters like *beta-actin2* (*bact2*) or *ubiquitin b* (*ubi*) are used. These promoters are broadly and robustly expressed during development, and, except for the erythrocyte-specific silencing of the *bact2* promoter, their activity remains strong in later stages (Lalonde et al., 2022). Cre-mediated recombination is irreversible, ensuring permanent transgene expression in recombined cells and their progeny.

Fluorescent cassettes downstream of *loxP* sites can track recombination in transgenic cells (Carney and Mosimann, 2018). For example, when a fluorescent cassette is downstream of *loxP*-flanked *stop* codons, recombined cells fluorescence can serve as an expression reporter for lineage tracing. Conversely, when the fluorescent cassette is between two *loxP* sites, recombination results in a loss of fluorescence.

### ***4.3 Targeting nuclear protein functions***

Loss-of-function techniques targeting DNA (gene editing) or RNA (interfering RNA) are not specific to particular cell compartments, whereas methods that directly target a POI can be compartment-specific, such as targeting a POI inside the nucleus. Direct protein targeting is also faster than targeting DNA or RNA because it does not depend on the presence and the half-life of RNAs and proteins. *In vivo*, proteins can be depleted by sequestering (Rothbauer et al., 2008), neutralizing (Joshi et al., 2023), cleaving (Harder et al., 2008), or degrading (Joshi et al., 2023; Caussin et al., 2011). Further, degrading the POI is likely to minimize non-specific phenotypes resulting from protein aggregation, hypomorphism, or conserved protein functions when compared to the sequestering, neutralizing, and cleaving methods.

Within cells, proteolysis is primarily conducted by the lysosomes and the proteasomes. Lysosomes are cellular compartments restricted to the cytoplasm, where they eliminate long-lived proteins, insoluble protein aggregates, entire organelles, macromolecular compounds, and intracellular parasites via endocytosis, phagocytosis, or autophagy pathways (Zhao et al., 2022). Proteasomes are protein complexes present in various cell compartments, including the nucleus (but excluding the nucleolus), where they eliminate poly-ubiquitinated short-lived proteins and soluble misfolded proteins (Zhao et al., 2022).

The ubiquitin-proteasome pathway relies on the ATP-dependent covalent attachment of multiple ubiquitin molecules to lysine residues of the target protein through a cascade of enzymes (E1, E2, and E3) (Nandi et al., 2006). E3 enzymes, known as ubiquitin ligases, are crucial for substrate specificity and thus exhibit significant diversity. SKP1-CUL1-F-box protein ligase complexes (SCFs) are a type of E3 enzyme. The F-box protein within these complexes is responsible for substrate specificity through its interaction motifs and for interacting with SKP1 through its F-box domain.

The 26S proteasome, the primary proteasome for protein degradation in both the cytosol and nucleus of eukaryotic cells, recognizes poly-ubiquitinated proteins via its 19S regulatory particle (Bard et al., 2018). The protein is then de-ubiquitinated and translocated through one of the proteasome's axial pores into the 20S core, which contains the proteolytic active sites. This process is ATP-dependent. Protein degradation within the proteasome generates short peptides, which diffuse out of the proteolytic chamber and are subsequently hydrolyzed to amino acids by soluble peptidases (Tanaka, 2009).

Various techniques leverage the ubiquitin-proteasome pathway to deplete endogenous proteins and achieve protein KD. One such technique involves antibody-based proteolysis targeting chimeras (PROTACs), which consists of a ligand binding to the POI and an E3 ubiquitin ligase, connected by a linker (Joshi et al., 2023). This tool binds to the POI, inducing its ubiquitination and subsequent degradation. Some PROTACs have been modified by replacing the POI ligand with consensus DNA or RNA sequences, enabling efficient targeting of RNA-binding proteins and transcription factors (Li et al., 2021; Liu et al., 2021; Samarasinghe et al., 2021).

Other techniques use POI-specific antibodies to direct the protein for proteasomal degradation, such as the auxin-inducible degron (AID), zinc finger 1 (ZIF-1), and degrade Green Fluorescent Protein (deGradFP) systems, which utilize nanobodies (Yamaguchi et al., 2019; Caussin et al., 2011). Nanobodies (Vhh) are derived from camelid antibodies and have the advantage of being small in size, making it easier to access the nucleus or other cellular compartments that can be difficult to reach (Harmand et al., 2021). Additionally, nanobodies consist of only one Fv portion, simplifying their genomic integration for transgenesis. However, in zebrafish, both AID and ZIF-1 have shown inefficiency, with AID also exhibiting leakage and toxicity at high doses (Yamaguchi et al., 2019).

#### 4.4 deGradFP and related methods

The deGradFP system operates with two main components: a destabilizer, or degron, fused to the POI, and an effector that targets the POI for degradation (Figure 13A) (Caussinus et al., 2011). The degron is the Green Fluorescent protein (GFP) or one of its derivatives, and the effector comprises the F-box domain of the drosophila F-box protein Slimb (NSlmb), fused to the nanobody VhhGFP4, which specifically binds GFP. NSlmb interacts with SKP1 of the SCF ubiquitin ligase complex, and VhhGFP4 binds to the GFP tag. This arrangement brings the tagged protein close to the E3 ligase, facilitating its ubiquitination and subsequent degradation.

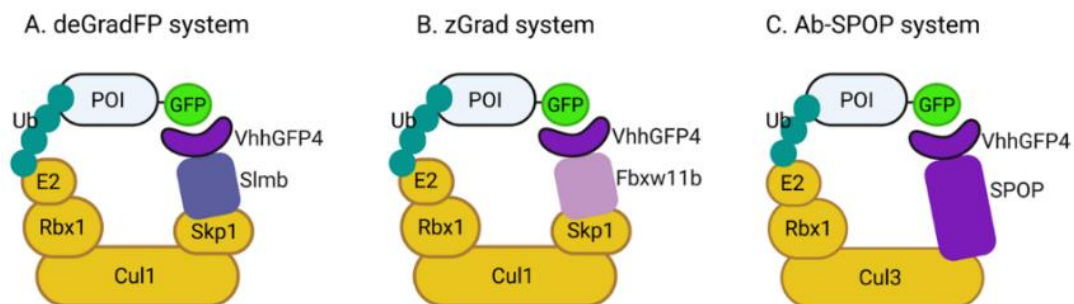


**Figure 13: Three degron-based protein degradation systems: deGradFP, zGrad and Ab-SPOP (from Yamaguchi et al., 2019)**  
See text for description.

By making use of the proteasomal pathway, the deGradFP system exploits a conserved, “universal” protein degradation pathway. Its efficiency has been demonstrated in transfected mammalian cells and *in vivo* in drosophila for nuclear, cytoplasmic, and transmembrane proteins (Caussinus et al., 2011). Efficiency was assessed by monitoring GFP degradation in fusion proteins, conducting Western Blotting, confirming the phenocopy of the corresponding loss-of-function mutations, and partially rescuing these phenotypes using the proteasome inhibitor MG132 (Caussinus et al., 2011).

Although deGradFP is less effective for degrading proteins within large complexes and free GFP, it has several advantages (Caussinus et al., 2011). It uses a single nanobody to target GFP-tagged proteins, eliminating the need to develop a specific nanobody for each target. deGradFP is relatively easy to implement due to the availability of libraries of endogenous GFP-tagged proteins in zebrafish and requires only one transgene. The GFP tag allows for monitoring the presence and localization of the POI through live imaging. Additionally, the effect of deGradFP is observable *in vivo* less than three hours after expression induction (Caussinus et al., 2011).

To increase its efficiency for use in zebrafish, deGradFP was adapted by replacing the drosophila NSlmb portion of the effector with the F-box portion of the zebrafish ortholog Fbxw11b (F-box and WD-40 domain protein 11b), creating a method named zGrad, for zebrafish deGradFP (Figure 13B) (Yamaguchi et al., 2019). To test its efficacy, *zGrad* mRNA was injected into one-cell-stage embryos or expressed under the control of a heat-shock promoter or a tissue-specific promoter to degrade GFP-tagged proteins in specific tissues. This showed that zGrad is effective on nuclear, cytoplasmic, and transmembrane proteins but not on secreted proteins, with effects visible within 2-3 hours of expression induction (Yamaguchi et al., 2019).

Additionally, zGrad phenocopies loss-of-function mutations in developing embryos, showing phenotype severities inversely proportional to the remaining quantity of the POI (Yamaguchi et al., 2019). The degradation efficiency varied depending on the POI and its localization and was affected by the production levels of the tagged POI (not monitored). For instance, the GFP signal fused with the plasma membrane protein Cxcr4b (chemokine (C-X-C motif) receptor 4b) in the posterior lateral line primordium was reduced by 86% in the presence of zGrad, slowing down primordium migration (Yamaguchi et al., 2019).

The initial deGradFP system has also been adapted to specifically target nuclear proteins by replacing NSlmb with a portion of the human F-box SPOP (speckle type BTB/POZ protein) which includes an F-box sequence and a nuclear localization signal (nls) (Figure 13C) (Shin et al., 2015). This adapted technique, named Ab-SPOP, has been successfully used in transfected mammalian cells and *in vivo* in zebrafish. Notably, Ab-SPOP is more efficient than deGradFP for nuclear protein degradation and depletes GFP-tagged proteins more rapidly than specific RNAi (Shin et al., 2015).

*In vitro*, both Ab-SPOP and Ab-SPOP $\Delta$ nls (lacking the *nls* signal) were effective for nuclear protein degradation (Shin et al., 2015). The mutated SPOP $\Delta$ nls formed a heterodimer with endogenous SPOP, allowing it to enter the nucleus and remain functional for at least two days (Shin et al., 2015). Microinjections of *Ab-SPOP* mRNA into zebrafish embryos rapidly depleted nuclear GFP fusion proteins *in vivo*, creating KD phenotypes without causing developmental toxicity (Shin et al., 2015). For example, Citrine fused to Hmga2 (high mobility group AT-hook 2), a nuclear protein involved in nucleosome and chromatin structure modulation, was efficiently depleted, and around 90% of the injected embryos exhibited various defects during early embryogenesis (Shin et al., 2015).

#### ***4.5 Adapting Ab-SPOP for conditional, long-term, and tractable nuclear Notch3 knock-down in vivo***

In a recent study on planar cell polarity (PCP) signaling components, Jussila et al. conditionally expressed the zGrad system in newborn zebrafish embryos (Jussila et al., 2022). This system was placed downstream of a *loxP-mCherry-stop-loxP* sequence and activated using an improved Cre (iCre) specific to floorplate cells of the neural tube, driven by the *foxj1a* promoter. They targeted the degradation of a plasma membrane-localized PCP component, VANGL planar cell polarity protein 2 (Vangl2), and examined the mispositioning of the basal bodies of the floorplate cells (Jussila et al., 2022). The *bact2:loxP-mCherry-stop-loxP\_zGrad* transgene was previously integrated into the genome using the tol2/transposase method, while Clustered regularly interspaced short palindromic repeats (CRISPR)-Cas9 was employed to KI the *super folder GFP* gene (*sfGFP*) at the endogenous *vangl2* locus. The system functioned effectively, resulting in a mosaic depletion of sfGFP-Vangl2 fusion protein among floorplate cells. This allowed the researchers to highlight the cell non-autonomous functions of Vangl2. The depleted embryos exhibited varying severities of axial body curvature, with some surviving to adulthood despite having obvious spinal curvature.

Building on this article and previous studies, my goal was to adapt the method to drive the conditional expression of the Ab-SPOP system, which targets nuclear proteins, in NSPCs, while also tagging endogenous Notch3 with GFP (Figure 14). To achieve this, I needed to generate zebrafish containing the KI at the *notch3* locus and two specific transgenes. The GFP tag will be inserted in the intracellular domain of the Notch3 protein, marking the N3ICD, the only part of Notch3 translocated to the nucleus during pathway activation. This setup will also allow us to characterize Notch3 localization and the dynamics of Notch3 signaling by creating a tagged endogenous Notch3 protein.

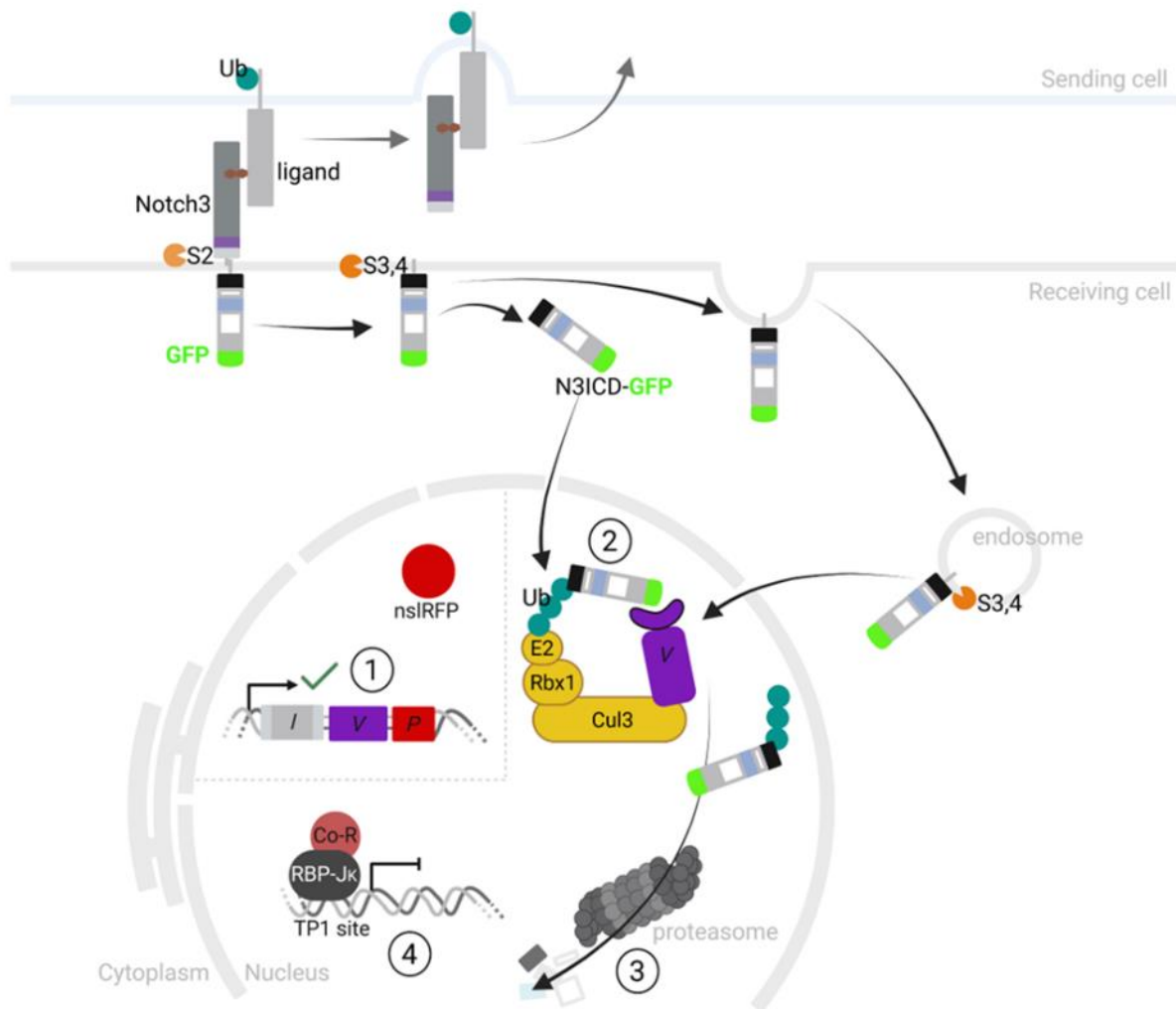


**Figure 14: Adapting Ab-SPOP for conditional, long-term, and tractable nuclear Notch3 knock-down *in vivo***  
 (1) *Ab-SPOP*, also known as *VhhGFP4-SPOP* (V) is expressed after the recombination of the *loxP-stop-loxP* (1) cassette by Cre recombinase specifically in *her4*-expressing neural stem and progenitor cells (NSPCs). The Cre recombinase is fused to ERT2 sites and enters the nucleus in the presence of 4-OHT. Together with *Ab-SPOP*, a marker of expression is transcribed: *P2A-nlsRFP* (P).  
 (2) Once translated, *Ab-SPOP* enters the nucleus, recognizes the GFP-tag on N3ICD and binds the endogenous ubiquitin ligase complex (Cul3, Rbx1, E2). N3ICD-GFP is then ubiquitinated (3) and degraded by the proteasome.  
 (4) The transcription of Notch3 target genes is knocked down.

The driver transgene, already existing, comprises the *ERT2CreERT2* sequence (which includes two *ERT2* sites to minimize background Cre activity and enhance inducibility) under the control of the NSPC-specific *her4* promoter (Yeo et al., 2007). The second transgene, which I needed to generate, drives the conditional expression of the *Ab-SPOP* system, along with a fluorescent reporter, controlled by the *bact2* promoter and a *loxP-stop-loxP* sequence.

The degradation system will enable us to knock down Notch3 nuclear functions at various developmental stages (timing of treatment), control the number of recombined NSPCs (treatment conditions), track recombined NSPCs (via the fluorescence reporter), and monitor



Notch3-GFP degradation (using the GFP tag). Most notably, this approach provides the first opportunity to study the long-term effects of canonical Notch3 KD in NSPCs.

## Hypotheses

Three main questions particularly motivated the project:

1. Among Notch signaling functions in NSPCs, what functions are characteristic of Notch3?
2. What are the functions of Notch3 that are dependent (vs. independent) of nuclear NICD activity in NSPCs?
3. What are the impacts of Notch3 loss-of-function in isolated NSPCs or cell clones?

Question 1 had already been approached *in vivo* in embryos and young larvae using mutants and MOs (Sidik and Talbot, 2015; Jin et al., 2022; Zaucker et al., 2013; Pogoda et al., 2006; Alunni et al., 2013; Belmonte-Mateos et al., 2023; Hevia et al., 2022; Than-Trong et al., 2018). However, due to the lethality of the mutants and the short-term activity of MOs, the long-term effect of the loss-of-function in older larvae, juveniles, and adult NSPCs has never been addressed. Notch3 is necessary for setting up quiescence and maintaining the NSPCs in the pallium of young larvae, while it maintains quiescence in adults (Alunni et al., 2013). Moreover, the numbers of RGs and newborn neurons increase until 3 weeks of LY cyclic treatment and tend to normalize after 5 weeks (Figure 15A-E) (Alunni et al., 2013). However, after 5 weeks of LY treatment, the total number of RGs begins to decrease while the percentage of RGs among the proliferative cells is stable (Alunni et al., 2013; supplementary material). If we agree with the hypothesis that Notch3 is the main LY target, this result could indicate that after 5 weeks of Notch3 depletion, NSPCs are not only permanently proliferative but also begin to lose their progenitor state and differentiate into IPs. However, by targeting only Notch3 signaling, we open the possibility of possible compensation by the other Notch receptors for protecting the NSPCs pool. I hypothesized that long-term Notch3 loss-of-function in adults will be at the origin of NSPCs activation, and after a few weeks of KD, of the progressive NSPCs pool depletion.

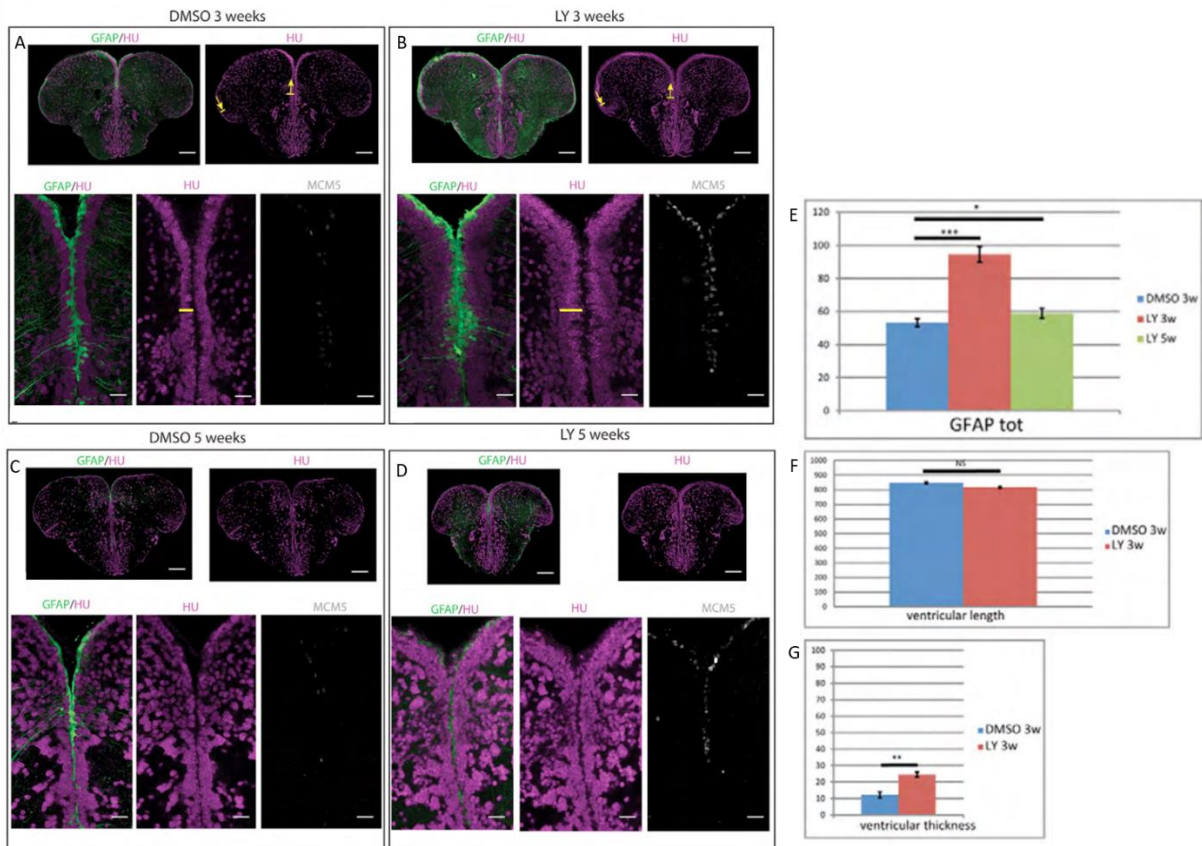


**Figure 15: LY treatments of 3 and 5 weeks highlight a regulation of RG amplification but the maintenance of a NSC zone (from Alunni et al., 2013)**

(A-D) Cross-sections of the adult pallial ventricular zone in *Tg(gfap:GFP)* brains processed in triple immunocytochemistry for the detection of GFP (RG, green), HuC/D (neuron, magenta) and MCM5 (proliferation, gray). Adult fish were continuously treated with LY (or DMSO for controls) for 3 weeks (A,B) or 5 weeks (C,D). The LY solution was exchanged every week, with no loss of efficiency (not shown). Low magnification panels (A and B top panels) were used to measure the pallial ventricular surface (between arrows, see F). The horizontal yellow bar in A and B indicates the width of the subventricular neuronal domain. Scale bar: 10  $\mu$ m. Confocal projection images from four optical planes.

(E) Quantification of the total number of RGs per section following control (blue), 3-week (red) or 5-week (green) treatments.

(F,G) Quantification of the pallial ventricular length (F) and width of the subventricular neuronal population (G) following control (blue) and 3-week (red) treatments. \*  $p < 0.05$ ; \*\*  $p < 0.001$ ; \*\*\*  $p < 0.0001$  ( $n = 3$  brains for each condition).

Our adapted Ab-SPOP method knocks down the nuclear functions of *notch3* only in *her4<sup>pos</sup>* cells and their progeny. Therefore, we hypothesized that even in the case of an early induction of the KD system in all the *her4<sup>pos</sup>* cells, the larvae must survive the mutant deadline of 10-15 dpf, and long-term loss-of-function experiments could be conducted.

Question 2 will be addressed for the first time in zebrafish with the Ab-SPOP method. Indeed, while mutants and MOs deplete all Notch3 functions, Ab-SPOP targets only Notch3 nuclear functions, including canonical signaling functions (Shin et al., 2015). The zebrafish pallium consists of an epithelial layer composed of NSPCs and IPs maintained together by AJCs, and

separating the CSF from the brain parenchyma (Sokpor et al., 2022). Moreover, NSPCs metabolism is regulated by many signaling pathways, and therefore, actors of different signaling pathways can be present at their membrane and in their cytoplasm (Zhou et al., 2022a; Acar et al. 2021; Borggreffe et al., 2016). Notch has been implicated in the regulation of cell junctional complexes and crosstalk with other signaling pathways, but the Ab-SPOP method will not approach these possible functions in NSPCs (White et al., 2023; Zhou et al., 2022a; Acar et al. 2021; Polacheck et al., 2017; Borggreffe et al., 2016). However, analyses of *her4.1* expression in adult zebrafish brains revealed that *her4.1* is a direct target of Notch3 in NSCs, and that the functions of Notch3 in NSCs are essentially the result of the activation of the canonical pathway (Alunni et al., 2013). I, therefore, hypothesized that Ab-SPOP-mediated Notch3 KD will generate a phenotype close to the MO-mediated loss-of-function.

For question 3, MOs showed that short-term *notch3* loss-of-function in isolated adult pallial NSCs induces their activation (Alunni et al., 2013). However, the long-term effects of nuclear Notch3 depletion in isolated NSCs have never been studied. I hypothesized that after the induction of Ab-SPOP, isolated NSCs would activate and form clones of NSCs and more differentiated cells. Alunni et al. showed that Notch loss-of-function biased the fate of the daughter cells toward a gliogenic fate (Alunni et al., 2013). However, the ventricular surface was not increased after 3 weeks of LY treatment, instead, RGs formed multiple layers and the population of newborn neurons was increased (Figure 15F-G). Therefore, if we postulate that Notch3-depleted NSCs will proliferate and that the ventricular surface will not be increased after a long-term loss-of-function of Notch3, I considered four possible situations:

If the total number of ventricular NSCs stays constant:

i. Notch3-depleted NSCs proliferate and the young NSCs are integrated into the NSCs epithelium, forming clones with a measurable ventricular surface, also displaying increased neurogenesis. To keep the number of ventricular cells constant, we can hypothesize that native NSCs elsewhere in the pallium would compensate by reducing their proliferation or increasing their differentiation. In this scenario, in the longer term, the depleted NSCs should be in majority in the pallium.

ii. Notch3-depleted NSCs proliferate but their ventricular expansion is limited by the neighboring cells and the young NSCs accumulate below the NSCs epithelium with their progeny.

If the total number of ventricular NSCs increases:

iii. Notch3-depleted NSCs proliferate and the increased number of ventricular NSCs could be compensated for by a reduction of their apical surfaces.

iv. Notch3-depleted NSCs proliferate and finally break the homeostasis of the NSCs epithelium, deforming the tissue in a “mini tumor” pattern.

#### ***4.6 Alternative method of knock-down: notch3 RNAi***

The development of the main method of KD by adapting Ab-SPOP to *notch3* is challenging and therefore, I also constructed a tool using RNAi targeting *notch3*.

RNAi-mediated gene KD relies on the processing of injected double-stranded RNAs (dsRNAs) or shRNAs by cells to ultimately produce small interfering RNAs (siRNAs). These siRNAs are incorporated into the RNA-induced silencing complex (RISC), where the antisense siRNA strand guides RISC to the target mRNA for degradation or translational repression. siRNA are prone to off-target effects, but unlike MOs, many siRNA off-target mechanisms have been characterized (Jackson and Linsley, 2004; Seok et al., 2018). Using shRNAs instead of dsRNAs generates fewer off-target effects, as shRNA processing utilizes the endogenous miRNA pathway and is less likely to trigger immune responses (Rao et al., 2009).

shRNA-mediated gene KD has been successfully used in the adult zebrafish brain, employing a method that allows long-term KD and concomitant tracing of the electroporated cells (Labusch et al., 2024; Giacomotto et al., 2015). Notably, the KD effects were still visible 14 days post-electroporation (dpe). Electroporation of a similar construct containing *notch3*-specific shRNA could potentially meet objectives (i) and (ii). However, functional shRNAs targeting *notch3* in zebrafish have not yet been published.

# Results

## 1. Tagging endogenous Notch3 to selectively expose its signaling component as a target for degradation

### *Generation of an endogenous notch3<sup>GFP</sup> fusion by CRISPR knock-in*

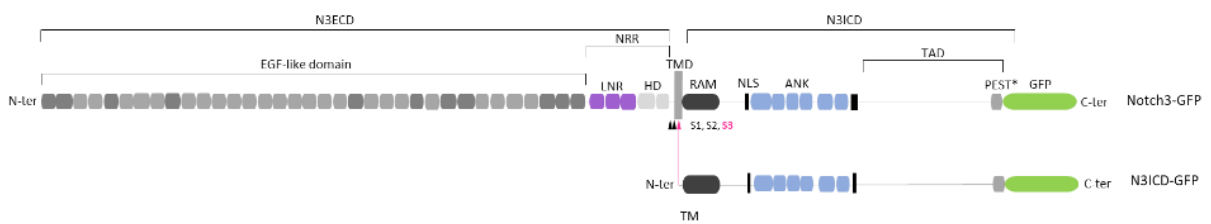
To visualize the dynamic regulation of endogenous Notch3 signaling in zebrafish NSCs, I used CRISPR-Cas9 genome editing to insert a GFP-encoding cassette into the *notch3* locus. Notch3 C-terminus is conserved among the three zebrafish isoforms (ZFIN). To preserve and track Notch3 signaling activity, I aimed to create a Notch3-GFP fusion protein at the C-terminus of the Notch3 protein, immediately distal to N3ICD (Figure 16A). Upon Notch3 pathway activation, N3ICD, which is the effector part of the receptor, is translocated into the cell nucleus where it acts as a transcription factor.

The insertion site was defined as close as possible to the *notch3 stop* codon to conserve the intracellular portion of the protein containing the ANK repeats, important for protein-protein interactions, the following low complexity region, whose function is still unknown, but excluding the extremity, containing a PEST domain which is found in Notch and Notch-related proteins (the protein sequence is available in Ensembl, <http://www.ensembl.org/index.html>) (Figure 16B). Besides the inherent possibility that N3ICD stability is increased by the fusion with GFP, this fusion also removed the PEST domain, which is supposed to contain degrons that regulate the stability of N3ICD (Kopan and Ilagan, 2009).

I chose the homologous recombination KI method, previously validated in the lab at the same locus. The *notch3*-specific dual-guide RNA, as well as the two homology arms, already existed and had been successfully used for the creation of another fish line (Ortica et al., in prep.) encoding a tagged-Notch3 protein (Figure 16C). I first validated the dual-guide RNA efficiency by injecting it into one-cell stage AB embryos and performing a T7E1 assay at 48 hpf (Figure 16D,E). Then, to generate the KI allele, AB embryos were injected at the one-cell stage with the dual-guide RNA, the Cas9 protein, and the donor vector containing the two homology arms, which frame a linker (Hisano et al., 2015) followed by the *GFP* sequence (Figure 16D,F). The linker is composed of glycines and serines that create a linear protein portion to minimize the impact of the tag on the conformation of GFP and Notch3 proteins, and on the function of

Notch3. The mean percentage of early mortality associated with injections was 49.6% at 48 hpf. I raised injected fish to adulthood and genotyped 3 adult fish to obtain one founder (named F0, for founder F at generation 0), who had the correct insertion (Figure 16F), was fertile, and was able to transmit the KI to its offspring. The F1 and F2 generations were used in the next experiments. The KI allele will be referred to as *notch3*<sup>GFP</sup> (*notch3*<sup>GFP/+</sup>: heterozygotes; *notch3*<sup>GFP/GFP</sup>: homozygotes).

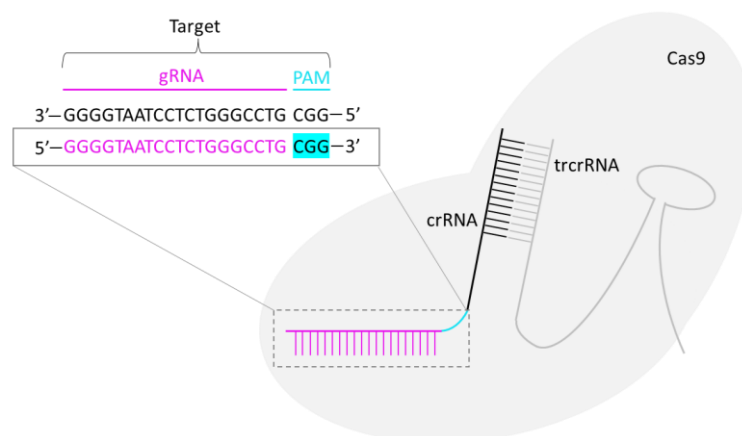
**A**

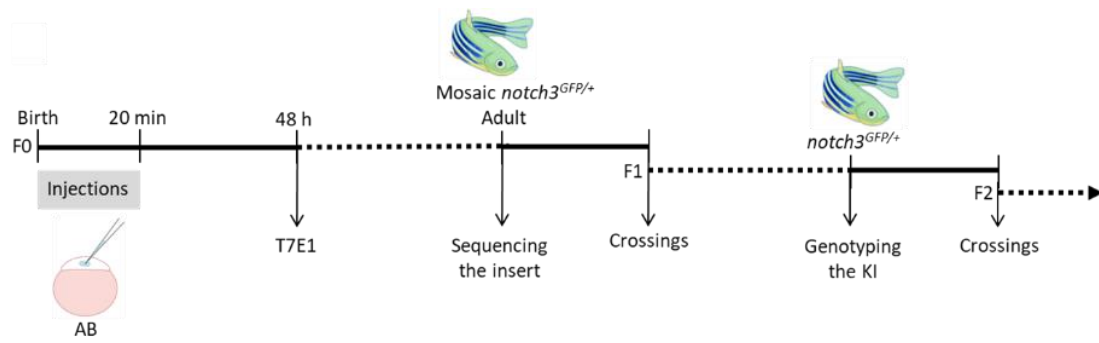
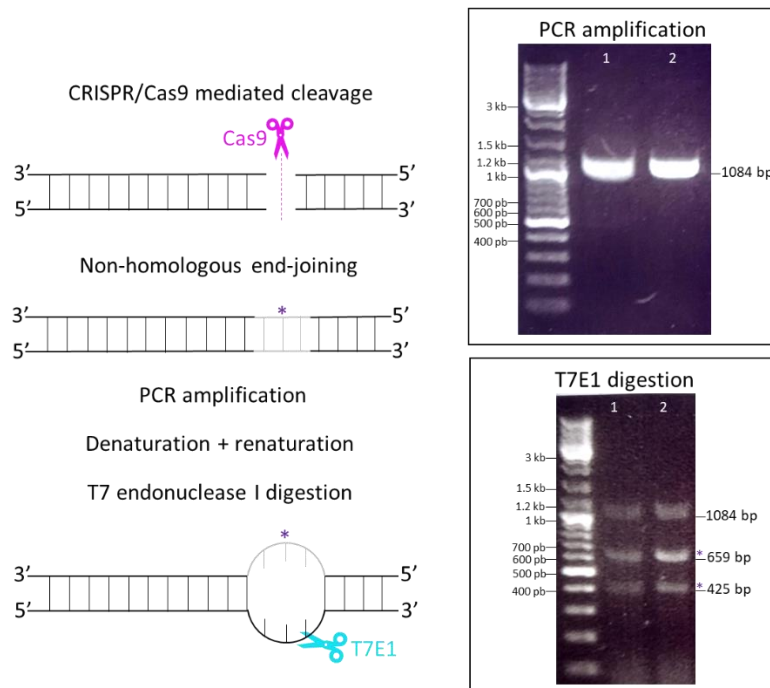


**B**



**C**



**D****E**

F

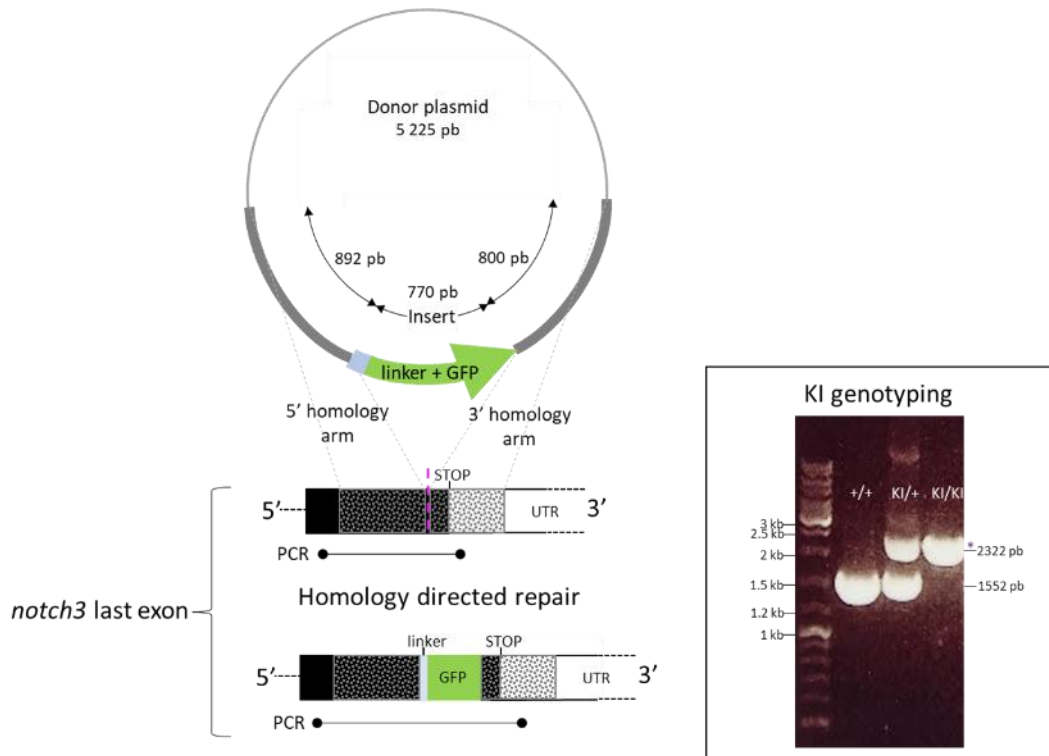


**Figure 16: Generation of an endogenous *notch3*-GFP fusion by CRISPR-Cas9 knock-in**

(A) Schematic illustration of the Notch3-GFP protein before the S1, S2 and S3 cleavages and after the S3 cleavage. GFP is fused to the Notch3 protein in C-terminal extremity of the intracellular N3ICD. ANK, ankylin repeats, C-ter, C-terminal, EGF, epithelial growth factor, LNR, cysteine-rich LNR repeats, NLS, nuclear localization sequence, NOD/NODP, Notch domain present in many Notch proteins, N-ter, N-terminal, N3ECD, Notch3 extracellular domain, N3ICD, Notch3 intracellular domain, PEST\*, N-terminal part of the domain rich in proline, glutamine, serine and threonine residues, RAM, RBP- $\text{J}\kappa$ -associated module, TM, transmembrane domain.  
 (B) *notch3* gene locus and target crRNA location. Double-strand break (DSB) occurs 260 bases upstream from the stop codon. Exons are represented by squares and introns by lines.  
 (C) Schematic illustration of the CRISPR-Cas9 ribonucleoprotein complex and sequence of the crRNA.  
 (D) Experimental design to create the CRISPR-Cas9 KI line.  
 (E) T7 endonuclease 1 assay (T7E1) to evaluate the cleavage efficiency of the crRNA.  
 (F) Donor plasmid and KI of the insert into the 3' end of the *notch3* gene by homology-directed repair after the CRISPR-Cas9 mediated DSB. Genotyping gel for a *notch3*<sup>+/+</sup> fish (+/+), a *notch3*<sup>GFP/+</sup> fish (KI/+) and a *notch3*<sup>GFP/GFP</sup> fish (KI/KI).

### ***Validation of the functionality of the Notch3-GFP fusion in vivo***

Embryos carrying the KI allele showed a GFP signal in the entire body at 28 hpf, with an intensity depending on the homozygous or heterozygous status of the *notch3*<sup>GFP</sup> allele (Figure 17A). The expression of *notch3* in the nervous and vascular systems in zebrafish embryos (ZFIN) explains this broad GFP signal.

To determine whether the Notch3-GFP fusion protein was functional, I compared morphological and quantitative cellular phenotypes of *notch3*<sup>GFP/GFP</sup> embryos and larvae with those described in homozygous *notch3*<sup>fh332/fh332</sup> loss-of-function mutants (Alunni et al., 2013).

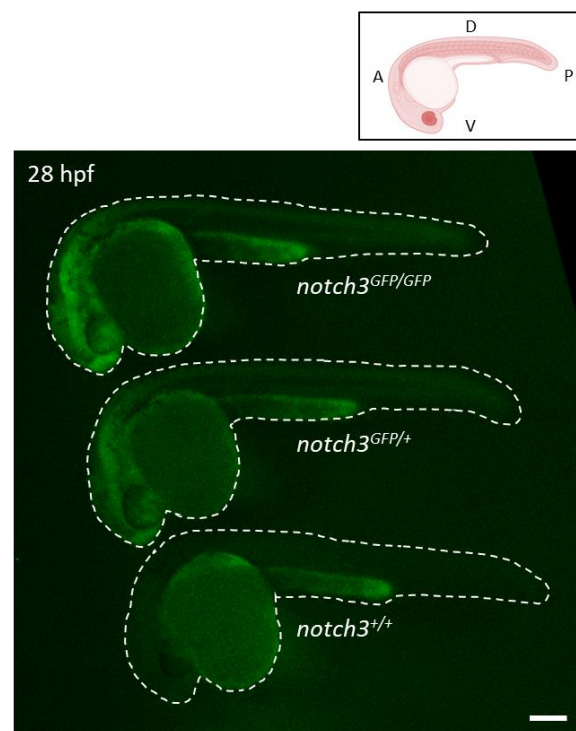


Morphologically, these mutants develop normally until 3 dpf (Wang et al., 2014), but then slow down in growth and the majority dies by 10-15 dpf under normal husbandry conditions. The length and the morphology of homozygote and heterozygote *notch3<sup>GFP</sup>* larvae appeared normal, comparable to wild-type larvae at 10 dpf (Figure 17B). In addition, adult homozygotes and heterozygotes *notch3<sup>GFP</sup>* fish were viable, fertile, and appeared morphologically normal (data not shown).

At the cellular level, the percentage of proliferating Sox2<sup>pos</sup> cells in *notch3<sup>GFP/GFP</sup>* adult pallia were comparable to the published percentage in the adult zebrafish pallium (Chapouton et al., 2010), respectively 8.3% and 8.2% (see Figure 19B).

Together, these data indicate that the Notch3-GFP fusion protein is functional, at least sufficiently to cope with normal development and NPs/NSCs proliferation rate.

**A**



B

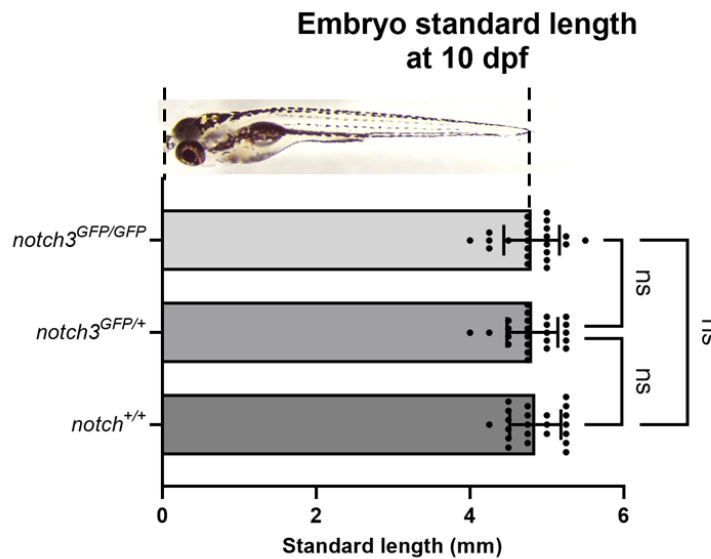


**Figure 17: Notch3-GFP is functional and localized in the central nervous and the vascular system in zebrafish embryos**

(A) 28 hpf embryos expressing *notch3<sup>GFP/GFP</sup>*, *notch3<sup>GFP/+</sup>* or *notch3<sup>+/+</sup>*. The scale bar represents 200  $\mu$ m.

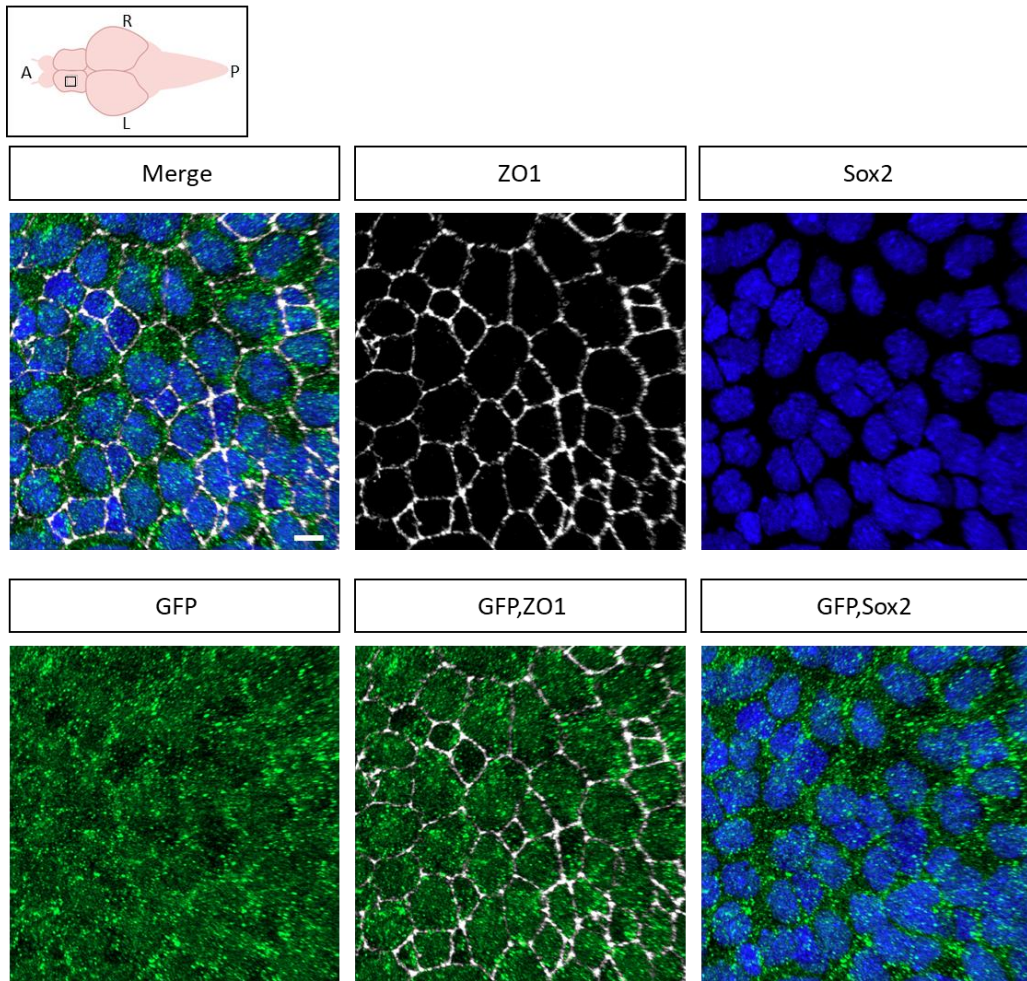
(B) Quantification of 10 dpf standard embryo lengths. Bar at median and bracket for interquartile range. Two-way ANOVA, Tukey's multiple comparison test, ns, not significant  $p= 0.9917$  (*notch3<sup>GFP/GFP</sup>* vs. *notch3<sup>GFP/+</sup>*),  $p= 0.8699$  (*notch3<sup>GFP/GFP</sup>* vs. *notch3<sup>+/+</sup>*),  $p= 0.9226$  (*notch3<sup>GFP/+</sup>* vs. *notch3<sup>+/+</sup>*). Number of larvae: *notch3<sup>GFP/GFP</sup>*  $n= 23$ , *notch3<sup>GFP/+</sup>*  $n= 24$ , *notch3<sup>+/+</sup>*  $n= 22$ .

### ***The Notch3-GFP protein localizes to the plasma membrane as well as recycling vesicles in NSCs***

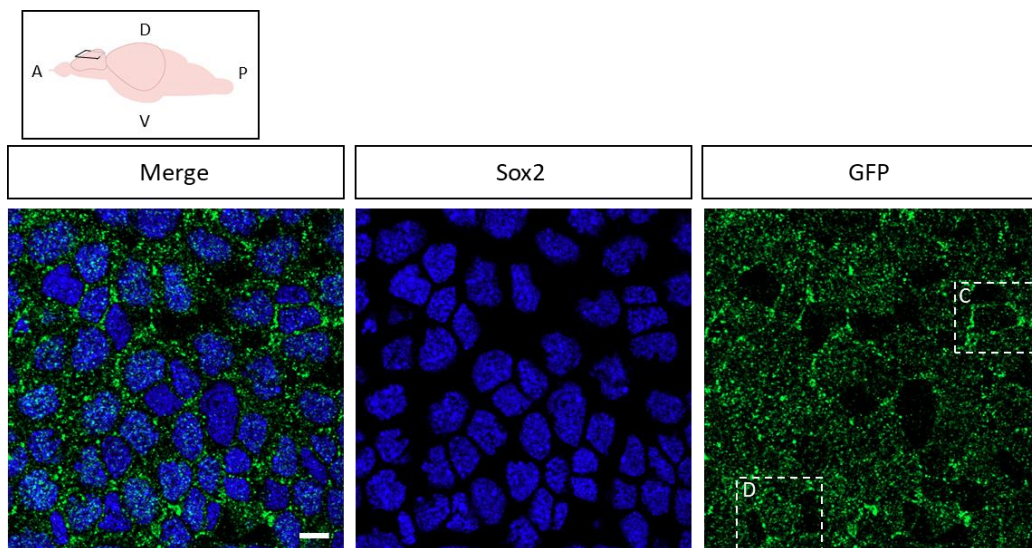
As a first important application, the *notch3<sup>GFP</sup>* KI line offers the possibility to characterize the cellular distribution of the Notch3 protein, in the absence of antibodies recognizing zebrafish Notch3 in tissues. To characterize Notch3-GFP protein localization, I imaged immunostained adult pallia, homozygotes for the KI, and analyzed the GFP signal.

At the level of the entire adult pallium, the Notch3-GFP signal was condensed in the more dorsal cell layer, corresponding to the NSC layer. The signal was also visible but weaker in the parenchyma and very bright in blood vessels. These results were expected as *notch3* expression is enriched in NSCs and pericytes, and Notch3 protein is particularly accumulated at the cell membranes. Adult pallial NSCs have their soma dorsally located in contact with the ventricle, and their long processes cross the telencephalon parenchyma. Thus, we interpret the weak but detectable parenchymal signal as Notch3-GFP located at the basolateral membranes of NSCs.

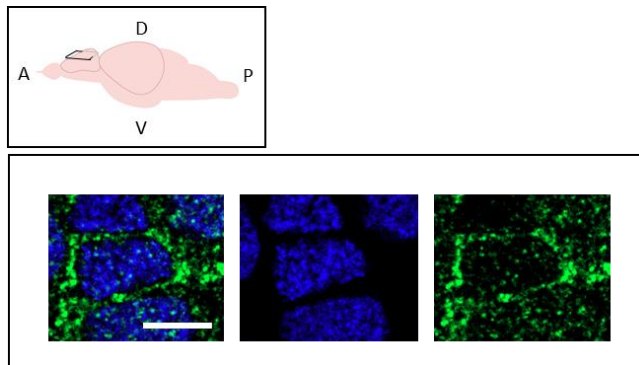
**A**



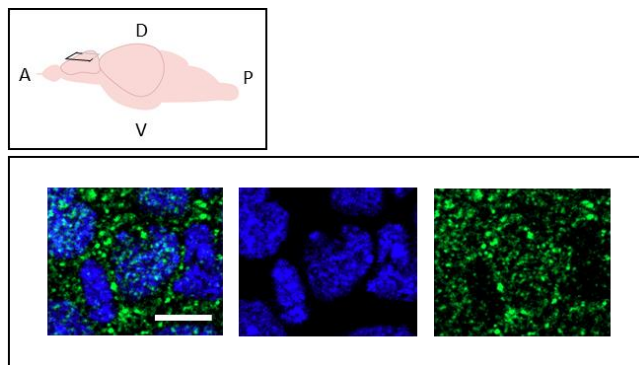
**B**



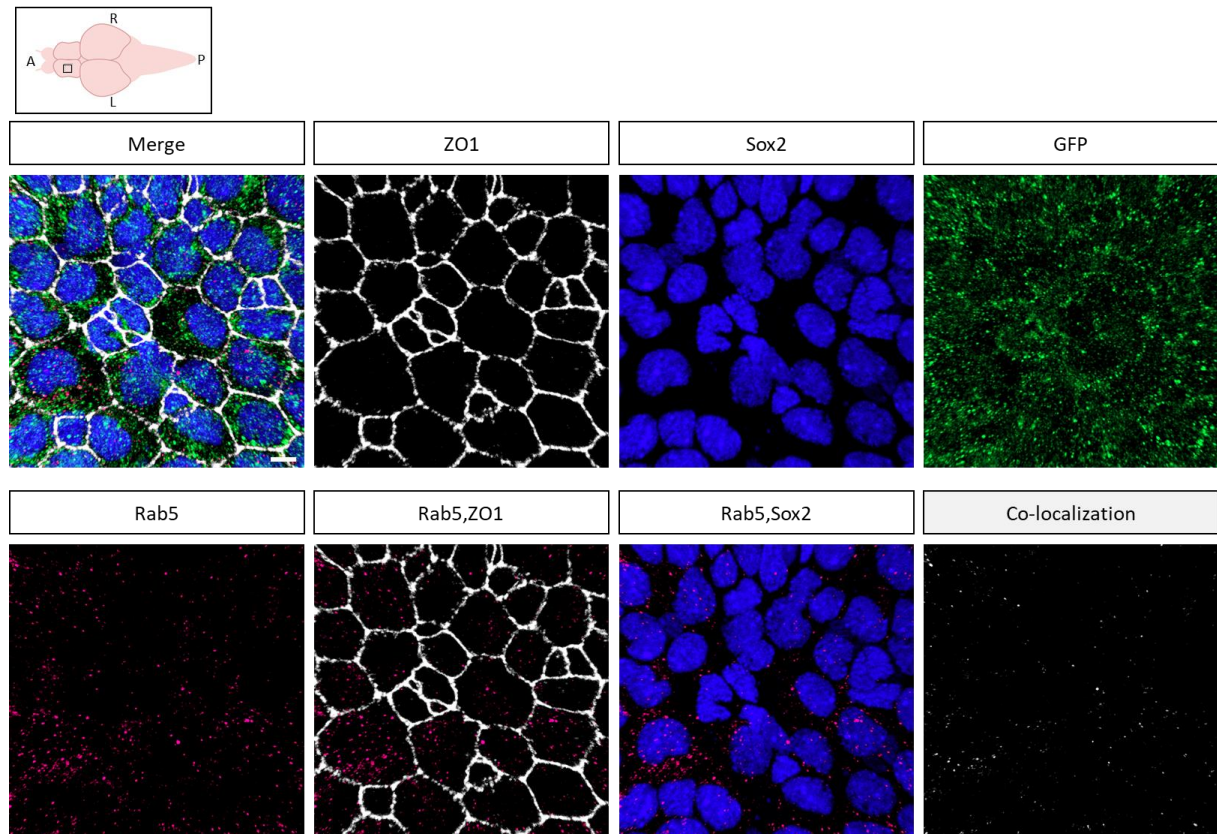
C

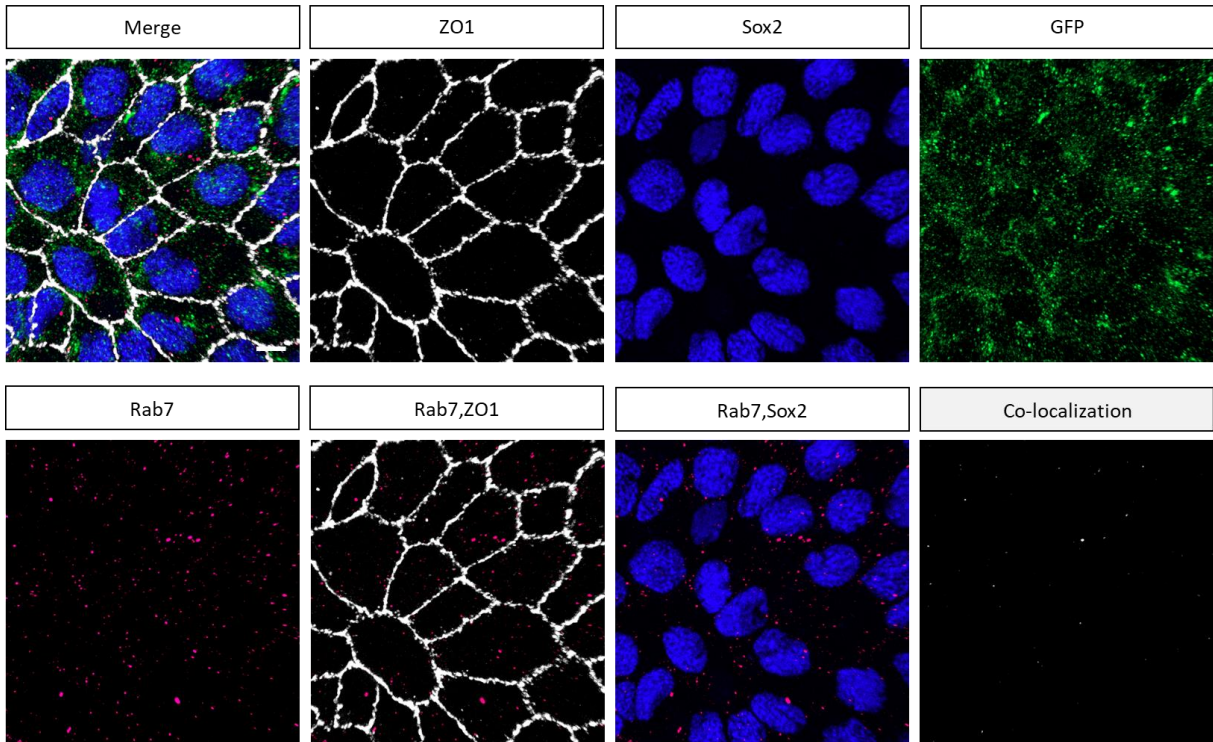
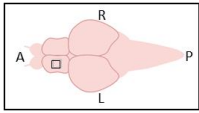
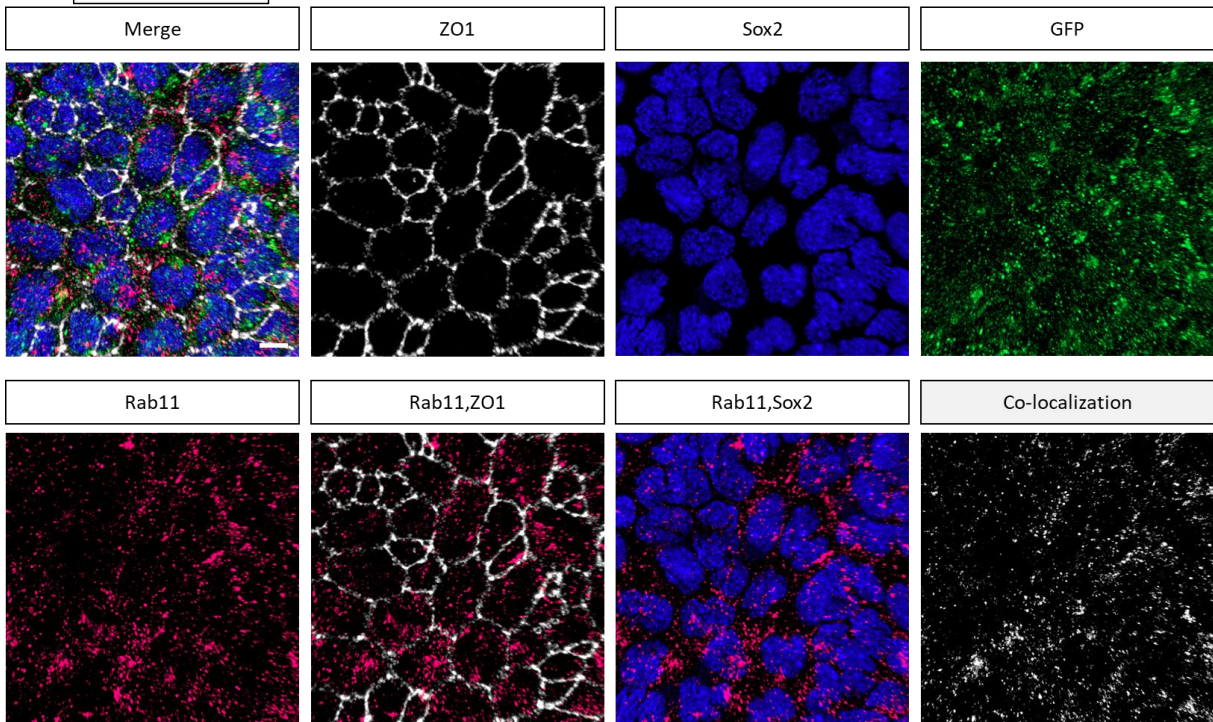
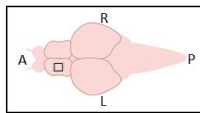


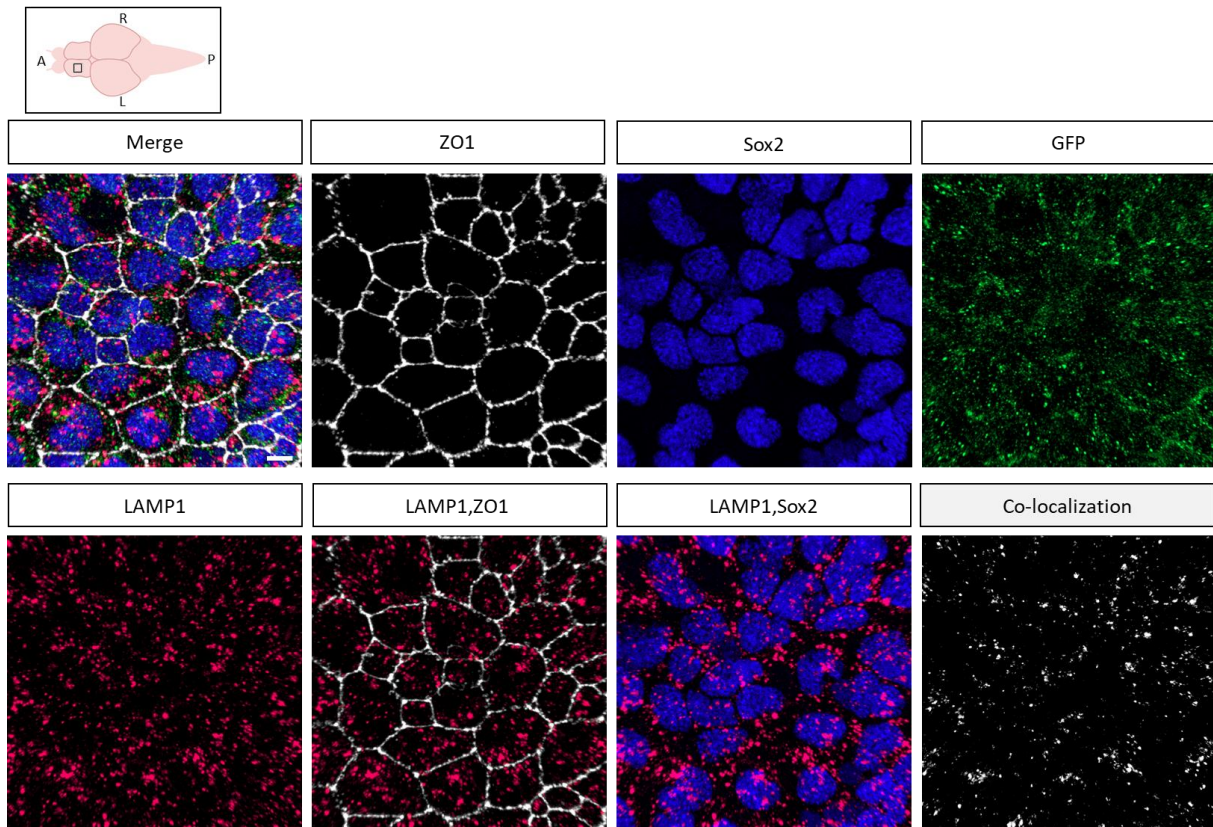
D



E



**F****G**

**H**

**Figure 18: The Notch3-GFP protein localizes to the plasma membrane as well as recycling vesicles in adult Sox2<sup>pos</sup> cells**

(A) Immunostaining of an adult pallium of *notch3<sup>GFP/GFP</sup>* fish. The picture is a Z projection over 12  $\mu\text{m}$ . ZO1 highlights the apical membranes, Sox2 the nucleus of the neural stem and progenitor cells, and GFP the Notch3 signaling. The scale bar represents 5  $\mu\text{m}$ .

(B) Horizontal optical section of the *notch3<sup>GFP/GFP</sup>* pallium: at 3  $\mu\text{m}$  below the ZO1 level. The dotted squares are the regions used in Figures 18C and D. The scale bar represents 5  $\mu\text{m}$ .

(C,D) Zoomed pictures. The scale bar represents 5  $\mu\text{m}$ .

(E-H) Immunostaining of adult pallia of *notch3<sup>GFP/GFP</sup>* fish using endosome markers (Rab5, Rab7 and Rab11) and lysosome marker (LAMP1). The GFP channel was adapted to the co-localization analysis: the minimum intensity of the channel was set up to 7000 to remove the pixels with a weak intensity and keep the vesicles. Pictures are Z projections over 12  $\mu\text{m}$ . The scale bar represents 5  $\mu\text{m}$ .

Focusing on the NSC cell bodies, the Notch3-GFP signal could be observed in several compartments: it was strong and condensed in dots at the membrane and in cytoplasmic punctae (Figure 18A,B), and was a weak and more homogenous signal in the nucleus (Figure 18A,B). These localizations are consistent, respectively, with the roles of Notch3 as a transmembrane receptor, with the dynamic regulation of its membrane presentation (relying on the intracellular production and maturation of new receptors, and recycling of old receptors) and with its role as a transcription factor. The difference in signal intensities depending on the cell compartments could reflect the dynamics of Notch3 signaling: a lot of receptors are integrated into the membrane, and their number is regulated by endocytose; the signaling fragment N3ICD, in

contrast, is highly regulated and quickly degraded or exported outside the nucleus after transcription of target genes. To reinforce these observations in adult NSCs, I compared the GFP signal in the *notch3<sup>GFP</sup>* line with the AzamiGreen signal in the previously characterized *notch3<sup>AzamiGreen-P2AnlsRFP</sup>* line (Ortica et al., in prep.), generated using the same gRNA by CRISPR-Cas9. I observed that the two signal patterns were globally similar (data not shown). To characterize the nature of the GFP<sup>pos</sup> bright cytoplasmic punctae that I hypothesized to be endosomes and lysosomes, I studied the presence of the Ras-related proteins Rab5 for early endosomes, Rab7 for late endosomes, Rab11 for recycling endosomes, and the transmembrane glycoprotein Lysosomal-associated membrane protein 1 (LAMP1) for lysosomes, and their co-localization with GFP (Figure 18E-H).

The immunostaining on *notch3<sup>GFP/GFP</sup>* adults revealed the presence of Rab5 and Rab7 as small dots in the cytoplasm of the cells (Figure 18E,F). The number of these dots, corresponding to endosomes, was variable between cells. Rab5 signal was expected close to the plasma membrane, where early endosomes are localized and Rab7 signal deeper in the cells. However, these pictures did not allow us to observe that. The co-localization channel showed co-localizations between Rab5 and GFP but almost none between Rab7 and GFP. The immunostaining revealed a higher concentration of Rab11 endosomes visible as dots and larger punctae, probably corresponding to several neighboring endosomes (Figure 18G). The co-localization analysis showed that GFP colocalizes with many recycling endosomes (Figure 18G).

To assess whether some Notch3-containing vesicles were also lysosomes, I studied the LAMP1 signal. The LAMP1 signal formed big dots of different sizes and bundled together in certain cytoplasmic areas (Figure 18H). The signal distribution was broad, which is in agreement with the already published LAMP1 protein pattern in adult quiescent NSCs (Kobayashi et al., 2019). The co-localization analysis showed that GFP colocalizes with many lysosomes (Figure 18H). Sara Ortica (together with Louis Degroux) tested the same markers in the *notch3<sup>AzamiGreen-P2AnlsRFP</sup>* line and obtained similar co-localization patterns. Moreover, by live imaging in *notch3<sup>AzamiGreen-P2AnlsRFP</sup>* embryos, Sara highlighted the dynamic movements of AzamiGreen<sup>pos</sup> punctae in the cytoplasm of brain cells (Ortica et al., in prep.).

To conclude, bright GFP<sup>pos</sup> cytoplasmic punctae were essentially recycling endosomes and lysosomes. However, we cannot exclude that some punctae could be Notch3-GFP receptors maturing in the ER or stocked in the GA, or free cytoplasmic N3ICD, slowed down in the cytoplasm by interaction with other proteins.

***Nuclear N3ICD-GFP levels provide quantitative measures of Notch3 signaling in situ***

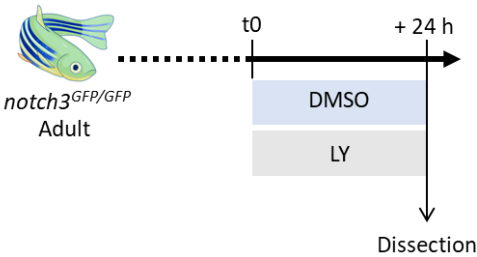
I next focused on the nuclear GFP signal, interpreted to correspond to the cleaved N3ICD-GFP fragment after nuclear translocation. To validate this interpretation and gain insight into the dynamics of Notch3 signaling, I treated *notch3*<sup>GFP/GFP</sup> adult fish and 3 dpf larvae with the inhibitor of  $\alpha$ -secretase LY and analyzed nuclear GFP intensity in pallial NSCs. Without  $\alpha$ -secretase, the N3ICD part of the receptor cannot be cleaved, thus GFP should remain membrane-bound. NSCs were identified by their ventricular apical surface (surrounded by staining for ZO1) and the expression of Sox2, a transcription factor specific to NSCs and neural progenitors, which was also used to segment the nuclei after immunohistochemistry (IHC).

The adult fish were treated with LY for 24h and their brains were directly dissected (Figure 19A). By applying this short treatment to adult NSCs, which are in vast majority in quiescence, it was possible to bring them closer to activation yet without reaching the proliferative state. Indeed, the percentages of PCNA<sup>pos</sup> cells among the Sox2<sup>pos</sup> cells (which include both NSCs and NPs), were comparable between Dimethyl sulfoxide (DMSO) and LY conditions, respectively 8.3% and 9.5% (Figure 19B). In IHC, while ZO1 and Sox2 profiles were comparable between DMSO and LY, GFP intensity was higher in the LY condition (Figure 19C). This observation was striking in cross and horizontal tissue sections (Figure 19D-F): in the LY condition, GFP accumulates at the NSC membranes (not quantified), in contrast GFP intensity seems reduced in the Sox2<sup>pos</sup> cell nuclei. To focus on nuclear N3ICD-GFP, I applied a segmentation pipeline based on Imaris Surface segmentation (Figure 19G). I found that the nucleus of the adult Sox2<sup>pos</sup> cells treated with LY accumulates significantly less GFP than the nucleus in the DMSO condition (Figure 19H). Together, these findings are in agreement with nuclear GFP being a qualitative and quantitative tracer of N3ICD-GFP, cleaved by  $\alpha$ -secretase and translocating into the nucleus as a mediator of Notch3 signaling. Finally, another interesting observation is the difference in GFP intensity among Sox2<sup>pos</sup> cells between PCNA<sup>pos</sup> and PCNA<sup>neg</sup> cells, which is even more striking in the DMSO condition: proliferating cells



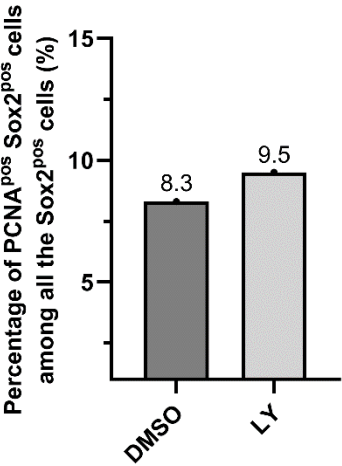
accumulate less N3ICD in their nucleus (Figure 19I). This is in agreement with previous work functionally associating Notch3 signaling with NSC quiescence, while blocking Notch3 expression in adult NSCs is sufficient to promote NSC proliferation.

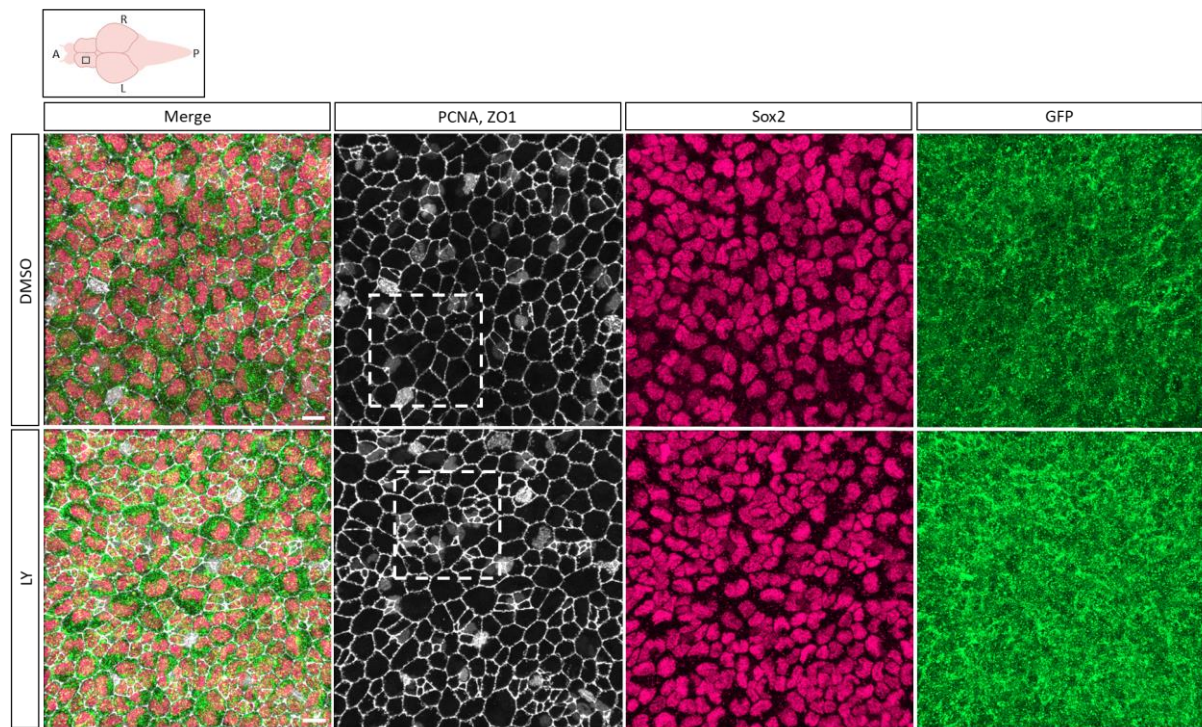
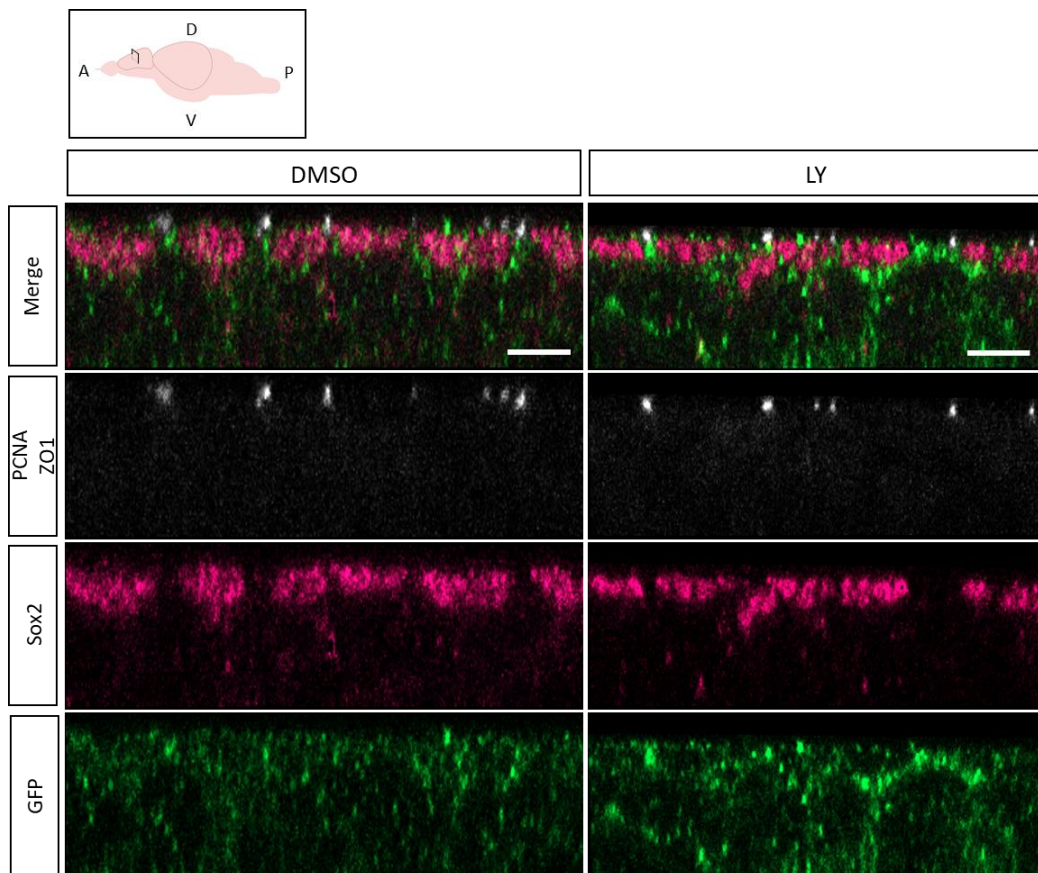
A

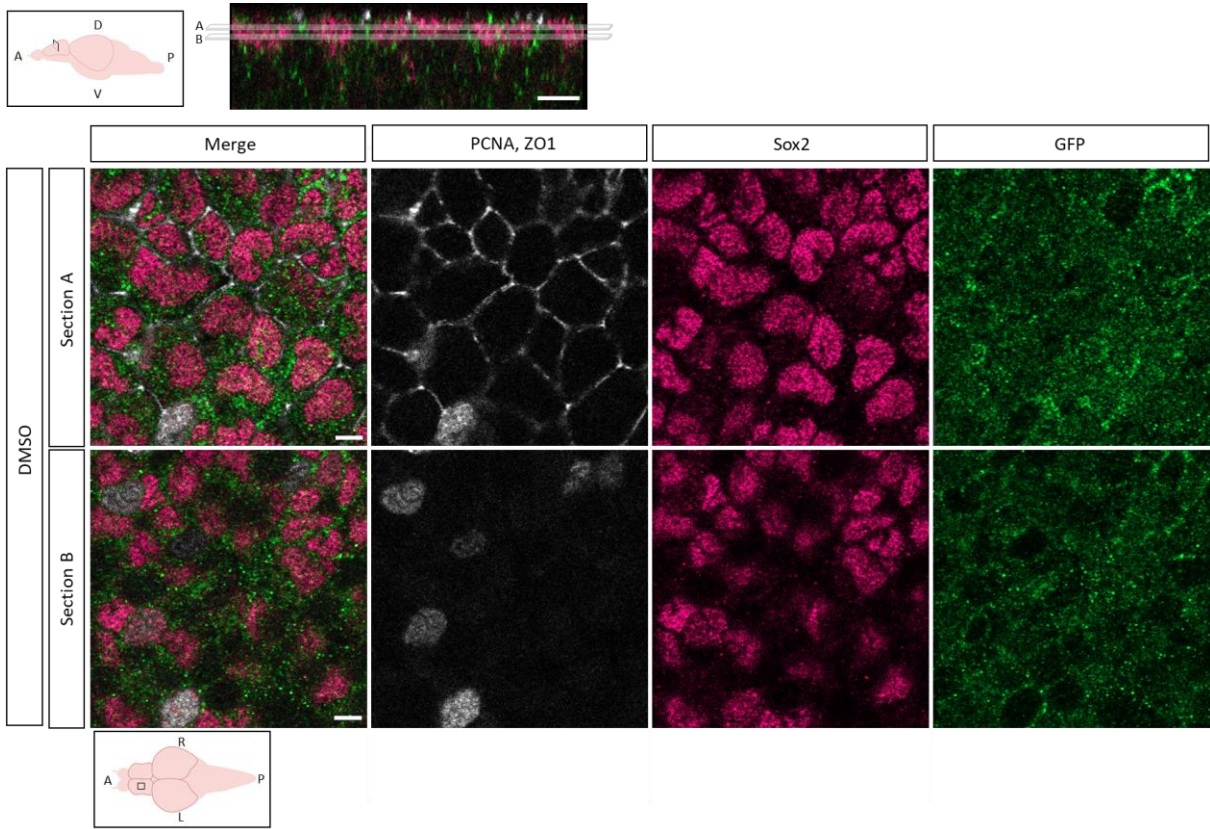
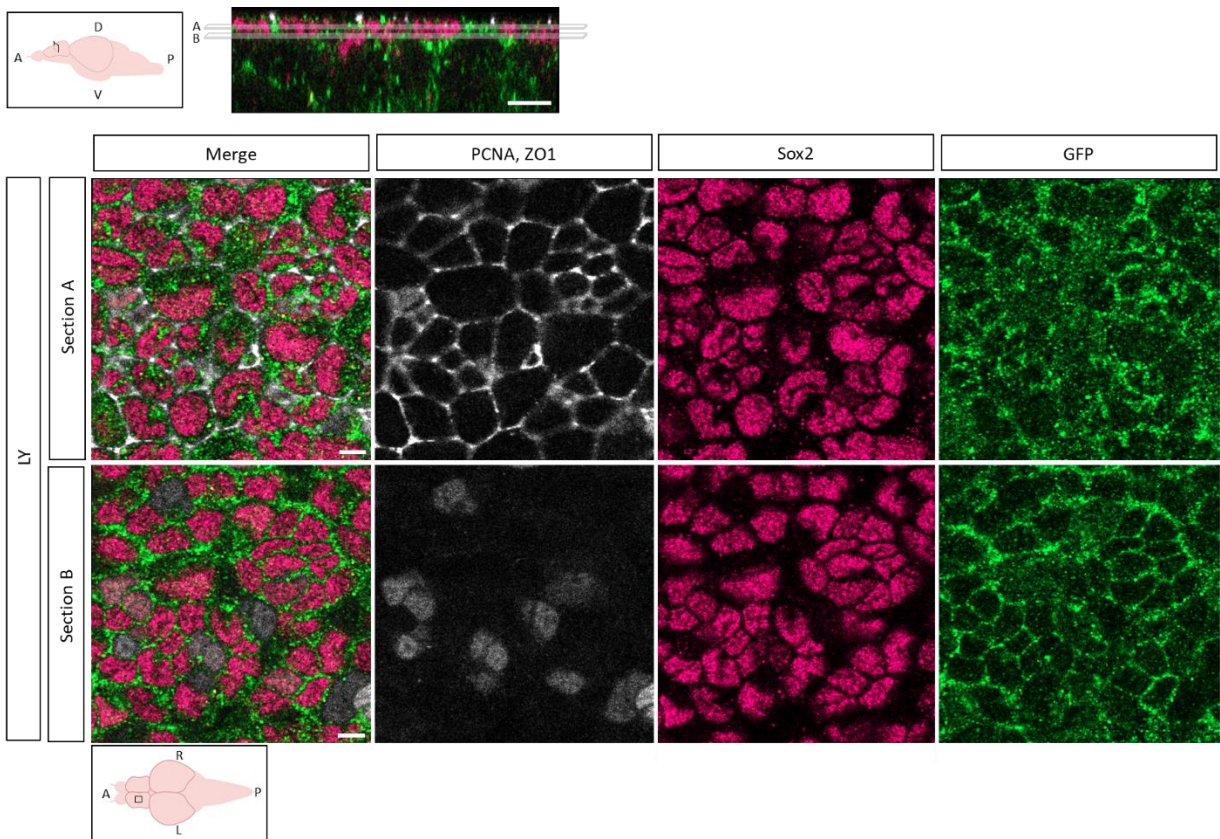


B

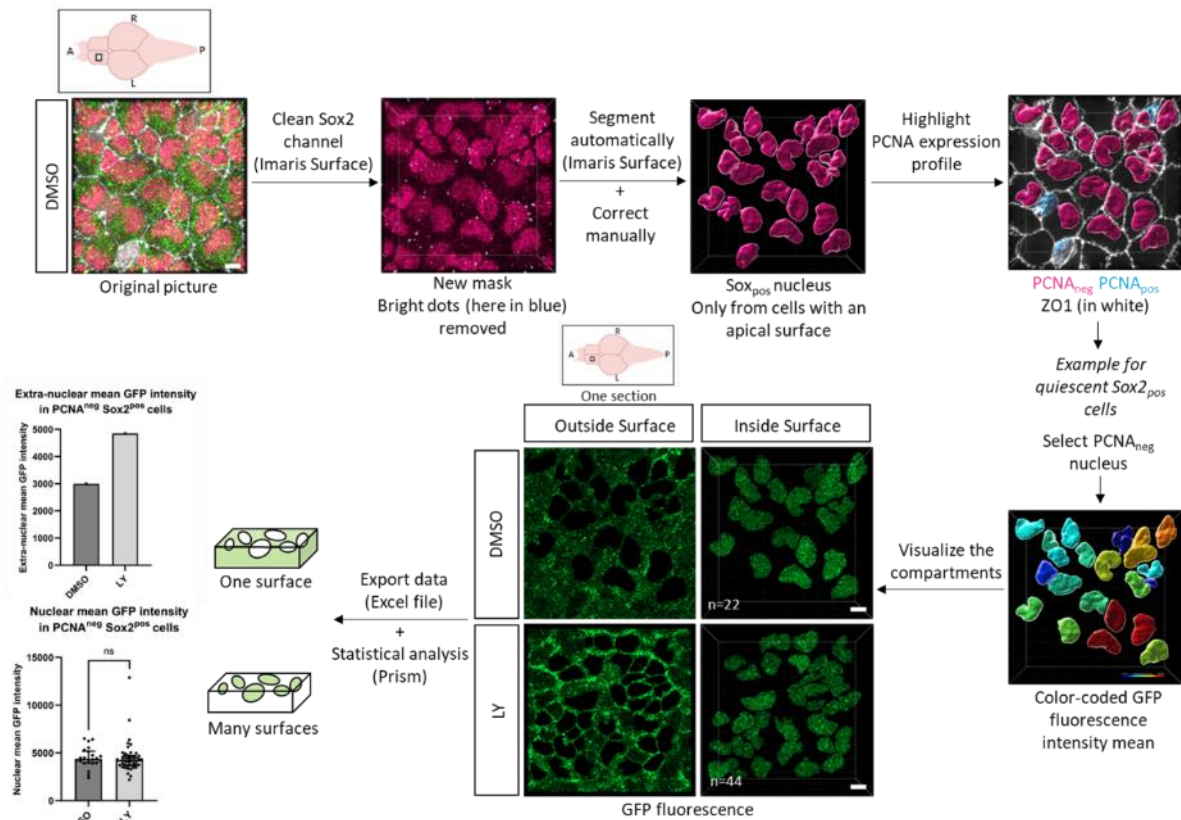
Percentage of proliferating Sox2<sup>pos</sup> cells



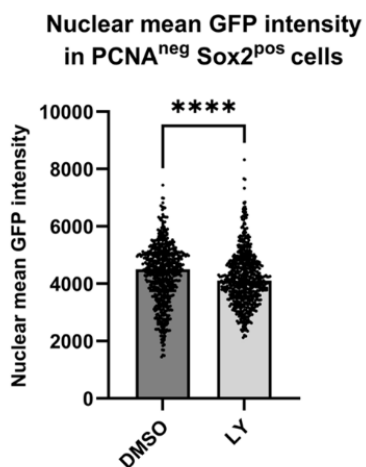
**C****D**

**E****F**

G



H



I

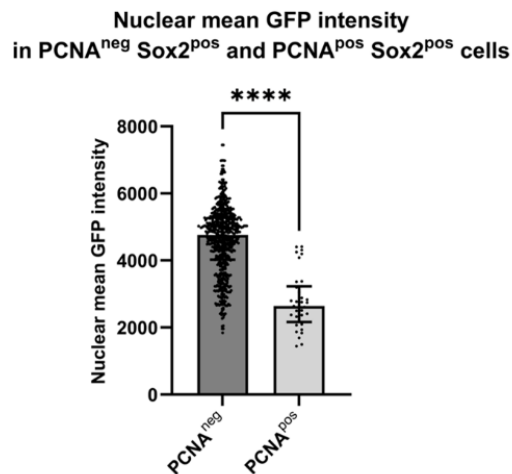


**Figure 19: Nuclear N3ICD-GFP levels provide quantitative measures of Notch3 signaling *in situ***

(A) Experimental design to treat adult *notch3*<sup>GFP/GFP</sup> fish with DMSO or LY.

(B) Percentage of proliferating Sox2<sup>pos</sup> cells in DMSO vs. LY. Total number of cells in DMSO Sox2<sup>pos</sup> n=660, in LY Sox2<sup>pos</sup> n= 678.

(C) Immunostaining after the DMSO and LY treatments in the adult pallium of *notch3*<sup>GFP/GFP</sup> fish. Both pictures are Z projections over 15.6 μm. PCNA highlights the nucleus of the proliferative cells, ZO1 the apical membranes,

Sox2 the nucleus of the neural stem and progenitor cells, and GFP the Notch3 signaling. The dotted squares are the regions used in Figures 4C, D and E. The scale bar represents 10  $\mu\text{m}$ .

(D) Optical cross sections in the pallium (15.6  $\mu\text{m}$  tissue deep). The scale bar represents 5  $\mu\text{m}$ .

(E,F) Horizontal optical sections at two different tissue depths: at the ZO1 level and just below. The scale bars represent 5  $\mu\text{m}$ .

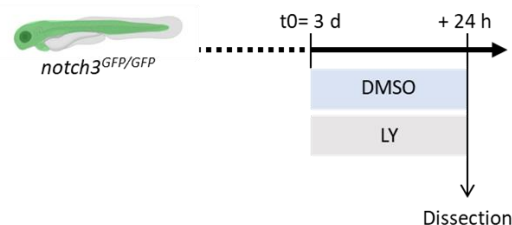
(G) Pipeline for nuclei segmentation and quantification of nuclear GFP using Imaris and Prism. The original picture is a Z projection over 15.6  $\mu\text{m}$ . The scale bar represents 5  $\mu\text{m}$ . Mann Whitney test, ns, not significant  $p=0.3906$ . DMSO  $n=22$ , LY  $n=44$ .

(H) Nuclear mean GFP intensity in non-proliferating Sox2<sup>pos</sup> cells in DMSO vs. LY. Each dot is one nucleus among 3 pooled brains in DMSO and LY. Bar at median and bracket for interquartile range. Mann Whitney test, \*\*\*  $p<0.0001$ . Number of Sox2<sup>pos</sup>PCNA<sup>neg</sup> cells from DMSO  $n=625$ , from LY  $n=619$ .

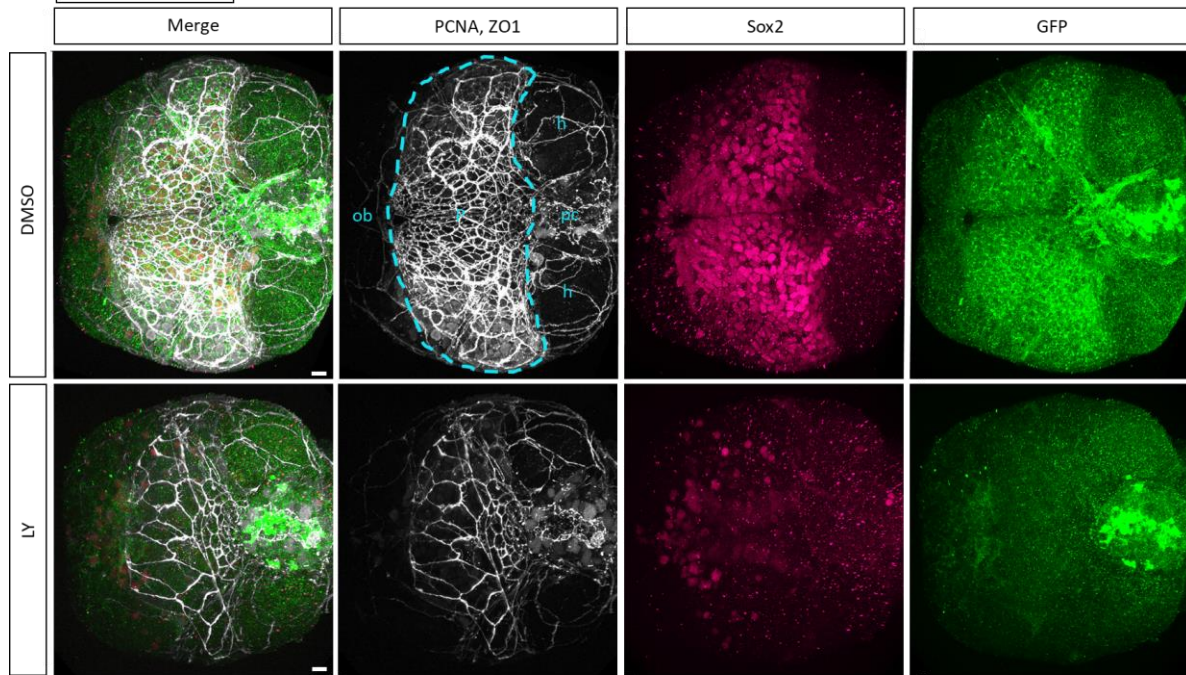
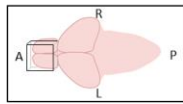
(I) Nuclear mean GFP intensity in proliferating and non-proliferating Sox2<sup>pos</sup> cells in DMSO. Each dot is one nucleus among 3 pooled brains. Bar at median and bracket for interquartile range. Mann Whitney test, \*\*\*\*  $p<0.0001$ . Number of cells: PCNA<sup>neg</sup>  $n=625$ , PCNA<sup>pos</sup> cells  $n=35$ .

I also worked to validate the quantitative measure of Notch3 signaling in NPs at larval stages. 3 dpf larvae were treated with LY for 24h and directly dissected (Figure 20A). This treatment was not validated yet in our hands in embryos. Because of the rapid growth of the zebrafish embryos and the absence of detectable quiescence among pallial NPs at this age (Than-Trong et al., 2018), a 24-hour time frame is more dynamic, including more cell divisions, migrations, and regulations in embryos than in adults. In addition, LY will block all Notch signaling, including Notch1, which is necessary for early development. I thus expected a more striking phenotype.

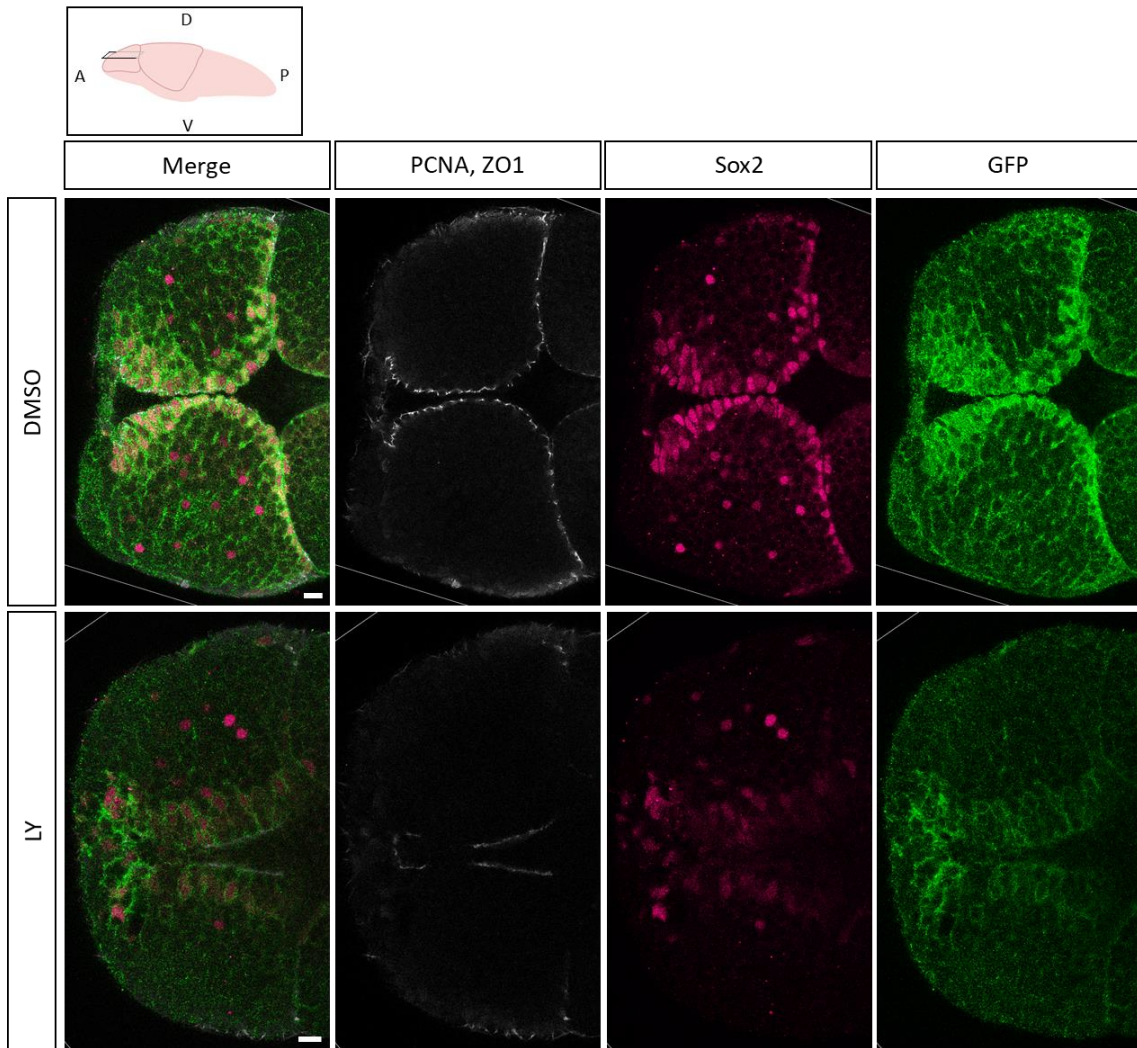
**A**

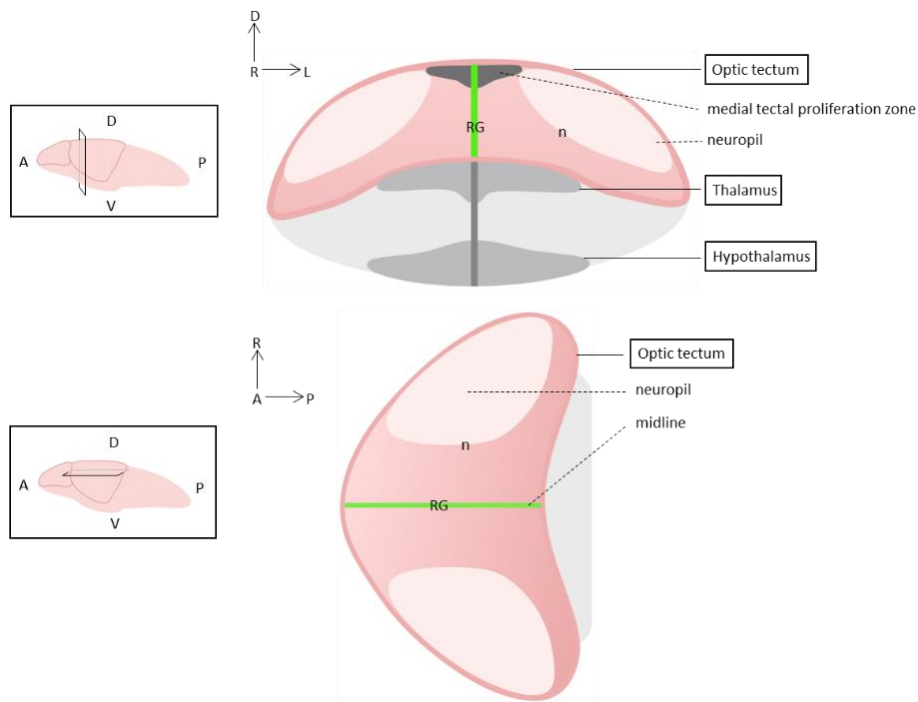
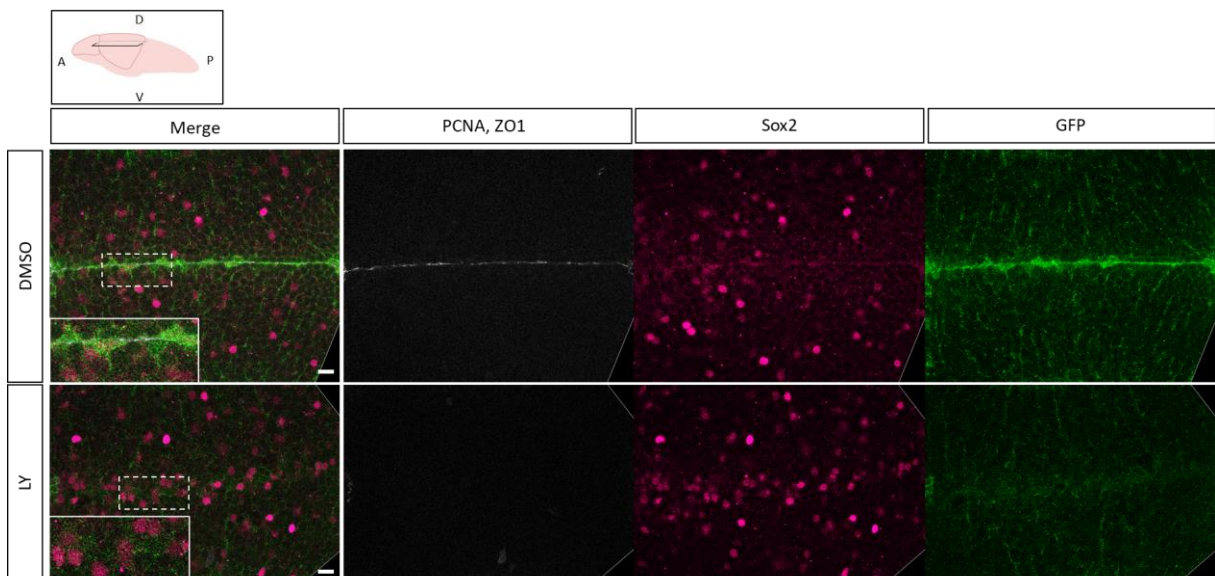


**B**



C



**D****E**

**Figure 20: Notch3-GFP levels highlight the loss of neuronal progenitors in larvae after LY treatment**

(A) Experimental design to treat 3 dpf *notch3<sup>GFP/GFP</sup>* embryos with DMSO or LY.

(B) Immunostaining after the DMSO and LY treatments in 4 dpf forebrains of *notch3<sup>GFP/GFP</sup>* larvae. The picture is a Z projection over 60  $\mu\text{m}$  in DMSO and 90  $\mu\text{m}$  in LY (different tissue curvature). PCNA highlights the nucleus of the proliferative cells, ZO1 the apical membranes, Sox2 the nucleus of the neural stem and progenitor cells, and GFP the Notch3 signaling. The different visible brain regions are indicated in the panel DMSO/ PCNA, ZO1: h, habenula, ob, olfactory, P, pallium (inside the blue dotted line), pc, pineal complex bulb. The scale bar represents 10  $\mu\text{m}$ .

(C) Horizontal optical sections of the forebrain at 30.1  $\mu\text{m}$  and 50.9  $\mu\text{m}$  from the ventricular surface in DMSO and LY respectively (different tissue curvature). The scale bar represents 10  $\mu\text{m}$ .



(D) Schematic illustration of optical cross and horizontal sections of the zebrafish larvae midbrain. The optic tectum is represented in pink while the underneath tissues are grey. N, neurons, RG, radial glia.

(E) Horizontal optical sections of 4 dpf midbrains after DMSO or LY treatment at 38.1  $\mu\text{m}$  from the midbrain dorsal surface. The pictures are centered on the midline and delimited laterally by the neuropil frontiers and longitudinally by the limits of the midline. The scale bar represents 10  $\mu\text{m}$ .

In the DMSO-treated condition, most of the Sox2<sup>pos</sup> cells, corresponding to NPs, were spread all over the dorsal ventricular surface of the pallium and were heterogeneous in their Sox2 signal intensity (Figure 20B). Some isolated Sox2<sup>pos</sup> cells were also visible deeper in the telencephalon parenchyma and probably correspond to neurons. This cell organization is comparable to the adult zebrafish telencephalon. Because the *tela choroidea* covering the pallial surface is difficult to dissect out at this stage, the cellular junctions (ZO1<sup>pos</sup>) of the *tela choroidea* cells are superposed to the NPs cellular junctions and render the identification of NPs apical surfaces difficult (Figure 20B). The Notch3-GFP signal was strong at NPs membranes including in their basolateral processes but also inside their nuclei (Figure 20C). Interestingly, NPs with a strong Sox2 signal also had a stronger nuclear GFP signal (Figure 20C).

At the level of the entire pallium, the GFP signal was weaker in LY-treated larvae compared to the DMSO-treated larvae (Figure 20B). Focusing on the Sox2<sup>pos</sup> cells, I observed that their number was strongly reduced in the LY condition (Figure 20B; not quantified). Some sparse Sox2<sup>pos</sup> cells were maintained in the dorsal ventricular surface or inside the parenchyma of the pallium, but the majority of the remaining Sox2<sup>pos</sup> cells were located at the midline (Figure 20B,C). In these cells, Sox2 expression was weaker and the nuclei were localized away from the apical surface, i.e., deeper in the parenchyma. These nuclei had also lost their round shape for a stretched shape (Figure 20C). These observations are characteristic of a progressive differentiation of neural progenitors into neurons. Contrary to control brains, I was only able to identify NP apical surfaces at the midline in the ventral most domains, while no ZO1 signal was visible in the dorsal pallium (data not shown). Focusing on GFP in the sparse and midline-located Sox2<sup>pos</sup> cells, I found that the Notch3-GFP signal was weak and only detected at cell membranes, i.e., it was undetectable in nuclei (Figure 20C; not quantified). Although the strong phenotype renders a precise analysis difficult, these results confirm that the nuclear GFP signal in *notch3<sup>GFP</sup>* larvae is abolished in the presence of a  $\gamma$ -secretase inhibitor, thus that it reads N3ICD-GFP.

To extend these observations to another brain territory where radial glia are present although no longer actively neurogenic, I analyzed the midbrain of 4 dpf larvae treated with LY for 24h at 3 dpf, focusing on RGs located at the midline between the medial tectal proliferation zone and the thalamus (Figure 20D). RGs contained in this bracket are normally not proliferative at 4 dpf (Mueller and Wulliman, 2002). In both hemispheres, the ventricular surface is covered by RGs, juxtaposed to numerous layers of neurons. More laterally, the neuropil is composed of a dense network of cell processes, notably the basolateral processes of RG, axons, and dendrites (Figure 20D). In the DMSO condition, the cells with a strong Sox2 signal were spread among the neuronal layers, while the first three layers of nuclei close to the ventricle displayed a weak Sox2 signal (Figure 20E). Among the latter, RG nuclei appeared flattened, aligned to the ventricular surface, while round-shaped nuclei located more laterally were likely committed progenitors or freshly-born neurons. I observed that RGs had a strong N3ICD-GFP signal in their nucleus and Notch3-GFP signal at their membrane (Figure 20E).

After LY treatment, similarly to what I saw in the pallium, the Notch3-GFP signal was overall weaker. Cells with a strong Sox2<sup>pos</sup> signal were not excluded from the more ventricular cell layers as in the control, and the Notch3-GFP signal was maintained only weakly at the membranes of some apical cells. No GFP signal was detectable in nuclei (Figure 20E). These results confirm the conclusions drawn in the larval pallium.

### ***Conclusions***

- The Notch3-GFP fusion generated by CRISPR-Cas9 KI at the endogenous *notch3* locus is functional, in particular in NPs and NSCs;
- Tracking the GFP signal in *notch3*<sup>GFP</sup> embryos, larvae and adults permits to reveal the dynamics of Notch3 signaling (membrane targeting, recycling through the endocytic-lysosomal pathway, nuclear targeting of N3ICD upon  $\alpha$ -secretase cleavage);
- The nuclear N3ICD-GFP signal permits to quantify variations in signaling intensities and to measure Notch3 signaling *in situ*. Its high levels in quiescent NSCs in the adult pallium, and its weaker detection or absence in activated NSCs, are in agreement with the previously demonstrated role of Notch3 as a promoter of NSC quiescence;
- The *notch3*<sup>GFP</sup> line can be used to target canonical Notch3 signaling by triggering the degradation of N3ICD-GFP.

## 2. Generation of a transgenic nanobody tool selective of nuclear GFP fusion proteins and conditionally activatable in NPs/NSCs

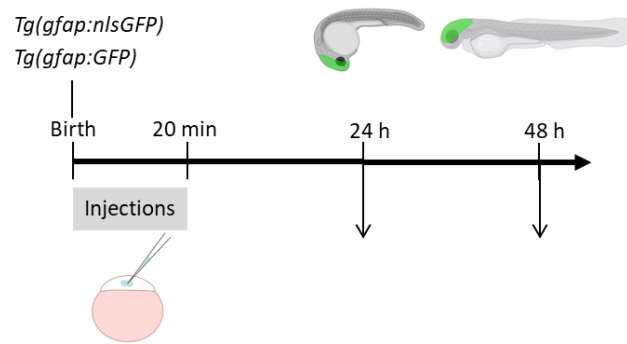
### *Validation of anti-GFP nanobodies targeted to the nucleus for the selective degradation of nuclear GFP protein in zebrafish embryos*

To conditionally KD Notch3-GFP fusion protein specifically in the nucleus of NPs/NSCs, I aimed to adapt an *in vivo* GFP-nanobody degradation system targeted to nuclear proteins (Shin et al., 2015).

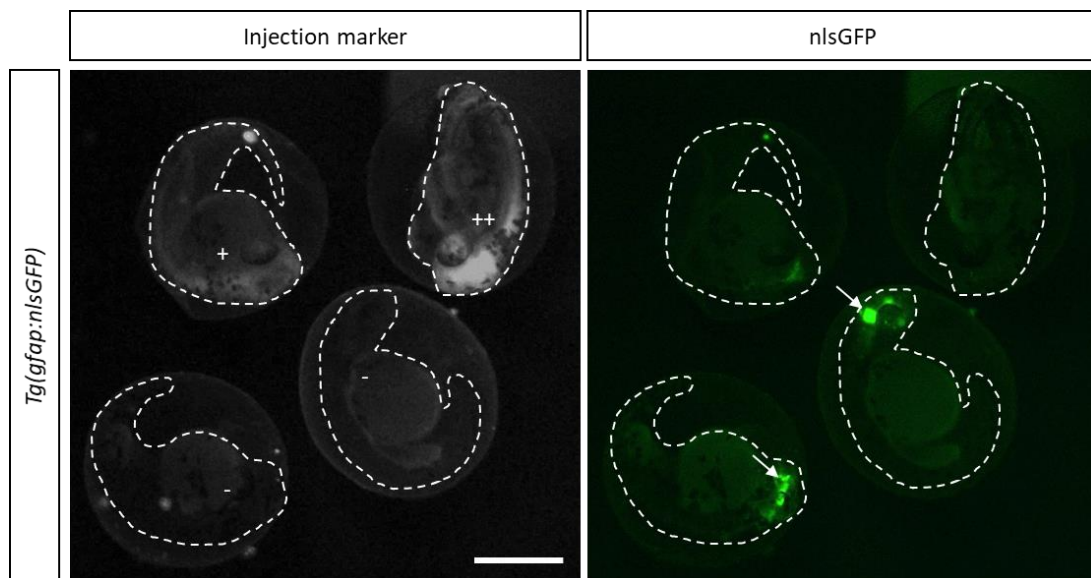
Preliminary validations of the most efficient and selective nanobody tool in the central nervous system were necessary. Thus, I tested the capacity of the VhhGFP4 nanobody to degrade GFP proteins specifically in the nucleus vs in all the cell, when the nanobody is fused with a fragment of hSPOP-nls vs Nfbxw11b protein, respectively.

*VhhGFP4-hSPOP-nls/Ab-SPOP* and *Nfbxw11b-VhhGFP4* capped mRNAs were injected at the one-cell stage in transgenic embryos expressing nuclear or cytoplasmic GFP or other fluorophores, and the embryos were screened for fluorescence at 24 or 48 hpf (Figure 21A,D). To validate the importance of each element in *VhhGFP4-hSPOP-nls*, injected embryos were also compared to embryos injected with *VhhGFP4-hSPOPdelnls*, where *hSPOP* is devoided of *nls* sequence (6 amino acids are deleted from the C-terminal end), or with *VhhGFP4mut-hSPOPdelnls*, where additionally to the lack of *nls* in *hSPOP*, *VhhGFP4* has a deletion mutation of one of the three complementarity-determining regions defining the antibody-binding-specificity. *VhhGFP4mut-hSPOPdelnls* was considered the negative control in this experiment. The efficiency of the three capped-mRNA on cytoplasmic or nuclear GFP degradation was tested in *Tg(gfap:GFP)* or in *Tg(gfap:nlsGFP)* embryos, expressing GFP in the cytoplasm or the nucleus of NPs/NSCs respectively (Figure 21A-C). Injected embryos were generated from an outcross between heterozygous transgenic fish and wildtype fish; thus, we expected 50% of GFP<sup>pos</sup> and 50% of GFP<sup>neg</sup> embryos.

**A**

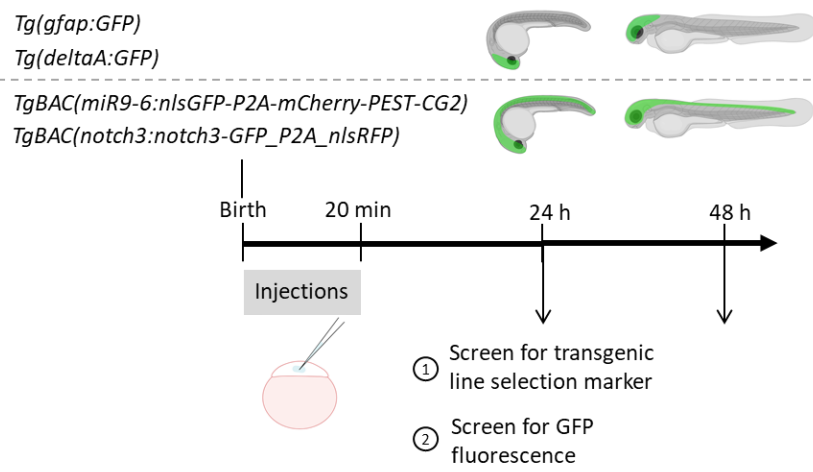
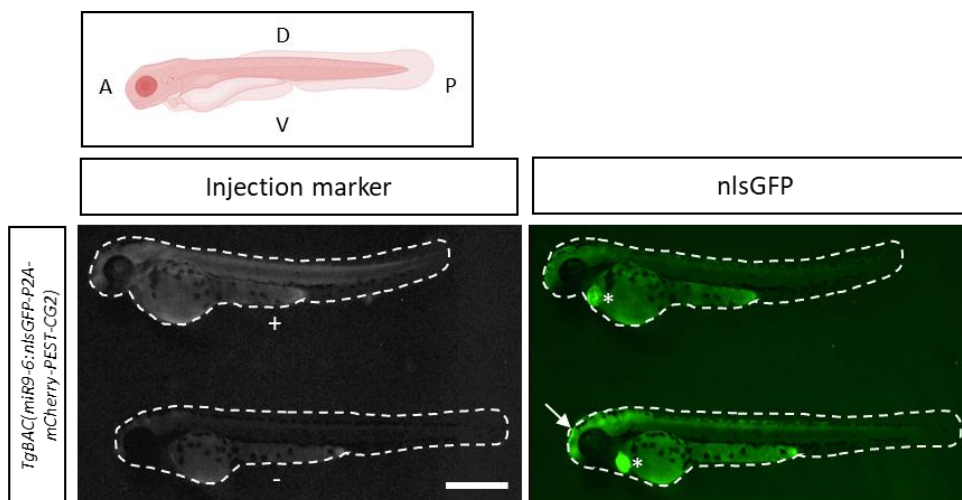


**B**

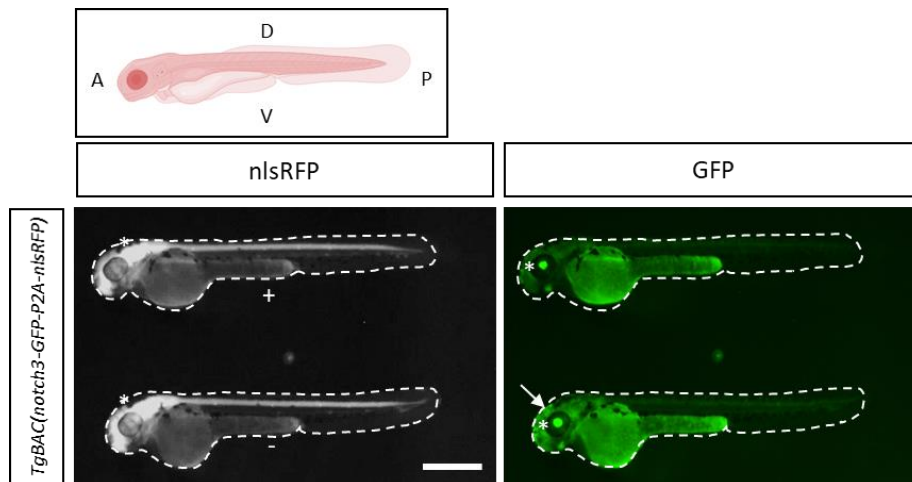


**C**

Test degradation	Transgenic line	Transgenics selection	Age for screen (hpf)	Control not injected, no green	Total injected	Injected, green	Injected, no/less green
<b>VhhGFP4-hSPOP-nls</b>							
nlsGFP	<i>Tg(gfap:nlsGFP)</i>	No	24	50%	90	0	90 (100%)
GFP	<i>Tg(gfap:GFP)</i>	No	24	50%	41	21	20 (50%)
<b>VhhGFP4-hSPOPdelnls</b>							
nlsGFP	<i>Tg(gfap:nlsGFP)</i>	No	24	50%	120	0	120 (100%)
<b>VhhGFP4mut-hSPOPdelnls</b>							
nlsGFP	<i>Tg(gfap:nlsGFP)</i>	No	24	50%	100	50	50 (50%)
GFP	<i>Tg(gfap:GFP)</i>	No	24	50%	90	47	43 (48%)

**D****E**

F



G

Test degradation	Transgenic line	Transgenics selection	Age for screen (hpf)	Control not injected, no green	Total injected	Injected, green	Injected, no/less green
<b>Nfbxw11b-VhhGFP4</b>							
nlsGFP	<i>TgBAC(miR9-6:nlsGFP-P2A-mCherry-PEST-CG2)</i>	GFP in the heart	24	62%	176	0	176 (100%)
GFP	<i>Tg(gfap:GFP)</i>	No	24	58%	193	62	131 (68%)
			48			87	106 (55%)
GFP	<i>Tg(deltaA:GFP)</i>	No	24	50%	150	69	81 (54%)
Notch3-GFP	<i>TgBAC(notch3:notch3-GFP-P2A-nlsRFP)</i>	BFP in the eyes, RFP in the central nervous system	24	50%	155	8	147 (95%)
			48			83	72 (46%)

**Figure 21: VhhGFP4-hSPOP-nls, VhhGFP4-hSPOPdelnls and Nfbxw11b-VhhGFP4 mediate degradation of nuclear GFP in embryos**

(A) Experimental design to test the different variants of the nanobody VhhGFP4-hSPOP-nls. *5'-cap\_VhhGFP4-hSPOP-nls*, *5'-cap\_VhhGFP4mut-hSPOPdelnls*, *5'-cap\_VhhGFP4-hSPOPdelnls* mRNA are injected with *5'-cap\_kusabira-orange* mRNA (injection marker), independently, in embryos coming from crossings between AB and *Tg(gfap:nlsGFP)* or *Tg(gfap:GFP)* fish, to respectively test nuclear and cytoplasmic GFP degradation.

(B) 48 hpf embryos coming from crossing between AB and *Tg(gfap:nlsGFP)* and injected (+, ++) or not injected (-, control) with *5'-cap\_VhhGFP4-hSPOP-nls*. The embryos are still in the chorion. The arrows point the GFP fluorescence in the central nervous system of the control embryos. The scale bar represents 500  $\mu$ m.

(C) Results of the fluorescent screens at 24 hpf. The *Tg(gfap:nlsGFP)* and *Tg(gfap:GFP)* embryos do not have transgenic line selection marker but 50% of transgenic embryos with GFP fluorescence in the brain is expected in the control condition and less than 50% if the nanobody-mediated degradation is working.

(D) Experimental design to test the nanobody Nfbxw11b-VhhGFP4. *5'-cap\_Nfbxw11b-VhhGFP4* mRNA is injected with *5'-cap\_kusabira-orange* mRNA (injection marker) in embryos coming from crossings between AB and *TgBAC(miR9-6:nlsGFP-P2A-mCherry-PEST-CG2)* to test nuclear GFP degradation, and AB and *Tg(gfap:GFP)* or *Tg(deltaA:GFP)* to test cytoplasmic GFP degradation. Embryos coming from crossings between AB and *TgBAC(notch3:notch3-GFP-P2A-nlsRFP)* are injected to test the degradation of GFP-tagged Notch3.

(E) *TgBAC(miR9-6:nlsGFP-P2A-mCherry-PEST-CG2)* 48 hpf embryos injected (+) or not injected (-, control) with *5'-cap\_Nfbxw11b-VhhGFP4*. The arrow points the GFP fluorescence in the central nervous system of the control embryo. The stars highlight the transgenic line selection marker: GFP fluorescence in the heart. The expression of *mCherry* in the central nervous system, visible in the control, is weak. The yolk sac is autofluorescent in green. The scale bar represents 500  $\mu$ m.

(F) *TgBAC(notch3:notch3-GFP-P2A-nlsRFP)* 48 hpf embryos injected (+) or not injected (-, control) with *5'-cap\_Nfbxw11b-VhhGFP4*. The arrow points the GFP fluorescence in the central nervous system of the control embryo. The stars highlight the transgenic line selection markers: blue fluorescent protein (BFP) fluorescence (also visible in green) in the eyes, and the RFP fluorescence in the central nervous system. The injection marker is hidden by the expression of *RFP* in the central nervous system. The scale bar represents 500  $\mu$ m.

(G) Results of the fluorescent screens at 24 and 48 hpf. The *TgBAC(miR9-6:nlsGFP-P2A-mCherry-PEST-CG2)* and *TgBAC(notch3:notch3-GFP-P2A-nlsRFP)* embryos are selected at 24 hpf on their transgenic line selection

marker. *Tg(gfap:GFP)* and *Tg(deltaA:GFP)* embryos do not have transgenic line selection marker but 50% of transgenic embryos with GFP fluorescence in the brain is expected in the control condition and less than 50% if the nanobody-mediated degradation is working.

### ***VhhGFP4-hSPOP-nls***

The test for cytoplasmic GFP degradation on *Tg(gfap:GFP)* at 24 hpf showed that 50% or 48% of the embryos injected with *VhhGFP4-hSPOP-nls* or *VhhGFP4mut-hSPOPdelnls*, respectively, were GFP<sup>neg</sup> (Figure 21C). This confirmed the absence of cytoplasmic activity of *VhhGFP4-hSPOP-nls*. The test for nuclear GFP degradation on *Tg(gfap:nlsGFP)* at 24 hpf showed that 100% of the embryos injected with *VhhGFP4-hSPOP-nls* or *VhhGFP4-hSPOPdelnls* were GFP<sup>neg</sup> (Figure 21B,C). These results validate the efficiency of *VhhGFP4-hSPOP-nls* to degrade nuclear GFP. Surprisingly, the deletion of the nls signal in *VhhGFP4-hSPOPdelnls* did not prevent the depletion of nuclear GFP. This is however in agreement with the results reported in the original publication (Shin et al., 2015), where the authors propose that *hSPOPdelnls* creates a heterodimer with endogenous SPOP to generate an active E3 ligase complex that targets nuclear proteins. As expected, the negative control *VhhGFP4mut-hSPOPdelnls* did not induce nuclear GFP degradation.

To test the stability of the *VhhGFP4-hSPOP-nls* nanobody, I also monitored GFP fluorescence at 48 hpf (data not shown). Some *Tg(gfap:nlsGFP)* embryos, injected with capped mRNA encoding *VhhGFP4-hSPOP-nls* and GFP<sup>neg</sup> at 24 hpf, started to re-express GFP at 48 hpf.

These results together validated the efficiency and specificity of *VhhGFP4-hSPOP-nls* and *VhhGFP4-hSPOPdelnls* for the selective degradation of nuclear GFP.

### ***Nfbxw11b-VhhGFP4***

To validate the activity of *Nfbxw11b-VhhGFP4* on cytoplasmic GFP, I injected its encoding capped mRNA into embryos issued from a cross between *Tg(gfap:GFP)* or *Tg(deltaA:GFP)* (*deltaA* is expressed in the central nervous system since 10 hpf) heterozygous fish with wildtype fish (Figure 21D,G). Among the injected embryos, I respectively obtained 68% and 54% of GFP<sup>neg</sup> embryos at 24 hpf, compared to 58% and 50% in non-injected crosses (Figure 21G). To test for *Nfbxw11b-VhhGFP4* stability, as above, I compared the proportion of GFP<sup>neg</sup> embryos at 24 hpf and 48 hpf in the *Tg(gfap:GFP)* context. It decreased from 68% at 24 hpf to 55% at 48 hpf (Figure 21G). Together, these results showed that the cytoplasmic activity of *Nfbxw11b-VhhGFP4* was weak, and I was not able to validate its efficiency on cytoplasmic GFP degradation.

The tests for nuclear activity of Nfbxw11b-VhhGFP4 were conducted in *TgBAC(miR9:6:nlsGFP-P2A-mCherry-PEST-CG2)* embryos, where GFP is expressed in the nucleus of NPs, under control of the *miR9:6* (*microRNA9:6*) promoter, the activity of which responds to both progenitor maintenance and commitment cues (Coolen et al., 2012). This line was used only for reasons of fish availability and mCherry expression was not considered in the analysis. Among injected embryos from a cross between heterozygous *TgBAC(miR9:6:nlsGFP-P2A-mCherry-PEST-CG2)* and wildtype fish, 100% were GFP<sup>neg</sup> at 24 hpf, compared to 62% in non-injected embryos (Figure 21E,G). This confirms the efficiency of Nfbxw11b-VhhGFP4 for nuclear GFP degradation.

To test the degradation efficiency of Nfbxw11b-VhhGFP4 on transmembrane or nuclear GFP-tagged protein, and not only GFP alone, I conducted injections into *TgBAC(notch3:notch3-GFP-P2A-nlsRFP)* embryos (Ortica et al., in prep.) (Figure 21E,G). This fish line was created by Bacteria artificial chromosome (BAC) transgenesis and had integrated a third *notch3* allele by *tol2*/transposase. The GFP-tagged *notch3* (*N3ICD-GFP*) is expressed under the control of the *notch3* regulatory elements in NPs and NSCs. NlsRFP (RFP: Red Fluorescent Protein) expression was not considered in this analysis. The data showed that 95% of transgenic BAC embryos were GFP<sup>neg</sup> or GFP<sup>weak</sup> compared to their non-injected transgenic counterparts at 24 hpf, but re-expressed Notch3-GFP at 48 hpf (Figure 21G). Thus, Nfbxw11b-VhhGFP4 only degrades some Notch3-GFP fusion protein. Considering the results above, it is possible that only the nuclear N3ICD-GFP is properly degraded.

Altogether, these results confirmed that Nfbxw11b-VhhGFP4 is efficient on nuclear GFP, but showed that it was poorly efficient on cytoplasmic GFP. Its effect on GFP fusion proteins is partial and it remains to be determined directly whether this is linked with subcellular localization.

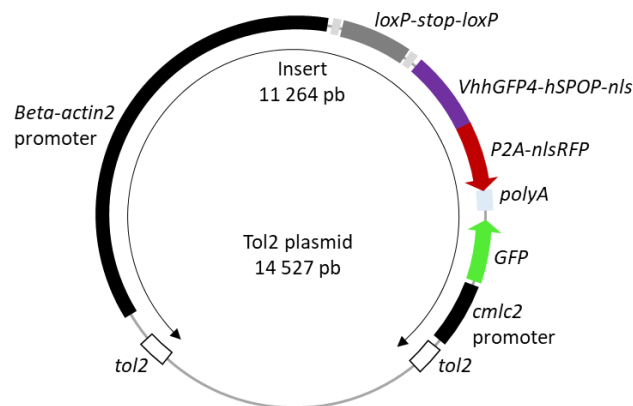
### ***Generation of a transgenic line conditionally expressing a tractable anti-GFP nanobody upon Cre-loxP recombination***

Next, my goal was to generate an effector line expressing *VhhGFP4-hSPOP-nls* in an inducible and tractable manner, at any stage and in a flexible number of cells. For this, I adapted the *in vivo* GFP-nanobody targeting degradation system (Shin et al., 2015), first by creating a *tol2*

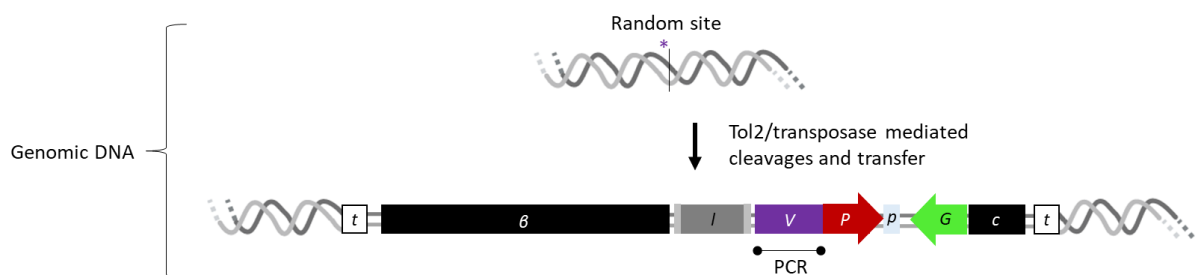


vector containing the *VhhGFP4-hSPOP-nls* sequence, conditionally expressed in frame with *P2A-nlsRFP-polyA* (containing the marker of expression RFP) under the control of the ubiquitous *bact2* promoter and a *loxP-stop-loxP* sequence (Kirchgeorg et al., 2018) (see Figure 22A). For fish selection purposes, the vector also contains a *GFP* sequence expressed specifically in the heart under the control of the *cmlc2* (cardiac myosin light chain 2) promoter (see Figure 22A). The *bact2* promoter, which is specific to one of the two *b-act* isoforms ubiquitously expressed at all stages, is ubiquitous and was already used for the transcription of transgenes in zebrafish lines. In our hands, it was efficient from embryos to adults in driving the expression of a *fluorescent transgene* (Galant et al., 2016). The two *loxP* sites share the same orientation for the deletion of the *stop* cassette in presence of the Cre recombinase.

**A**



**B**



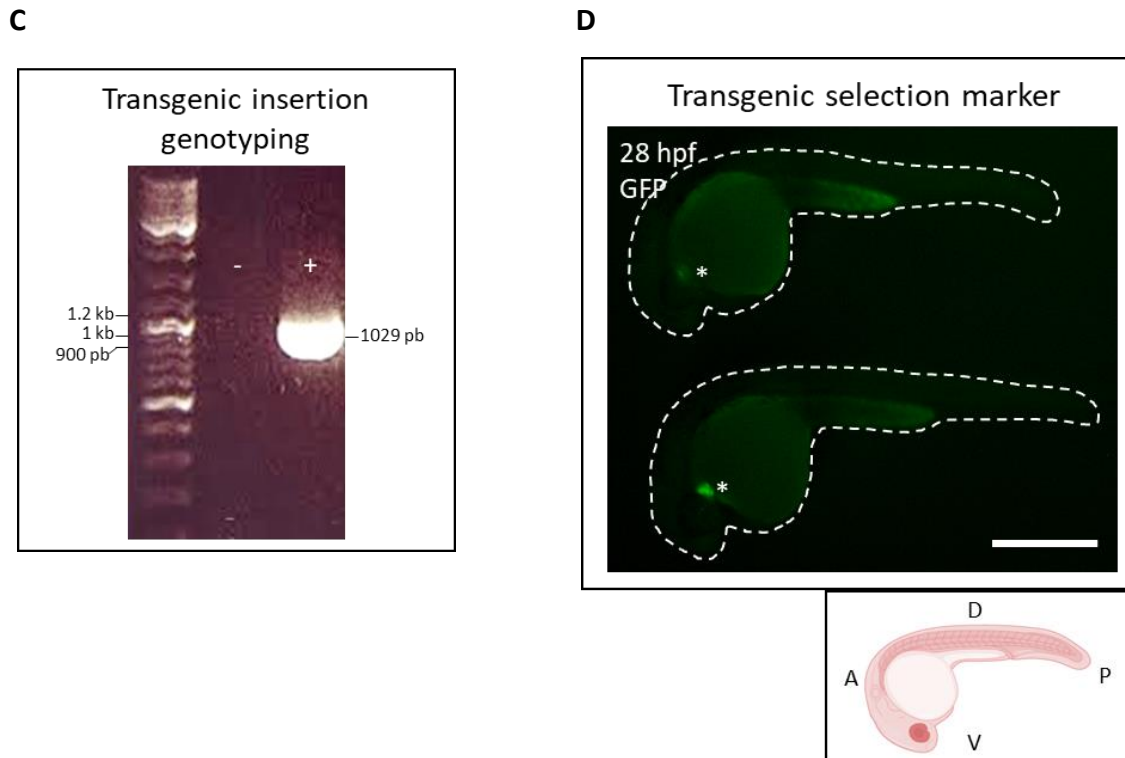


**Figure 22: Generation of transgenic *bact2:loxP-stop-loxP-VhhGFP4-hSPOP-nls-P2A-nlsRFP* fish, validation of the transgene integration and fluorescent screen**

(A,B) Schematic illustration of the Tol2 plasmid and the *tol2* transposase mediated random integration of the transgene sequence into the genome.

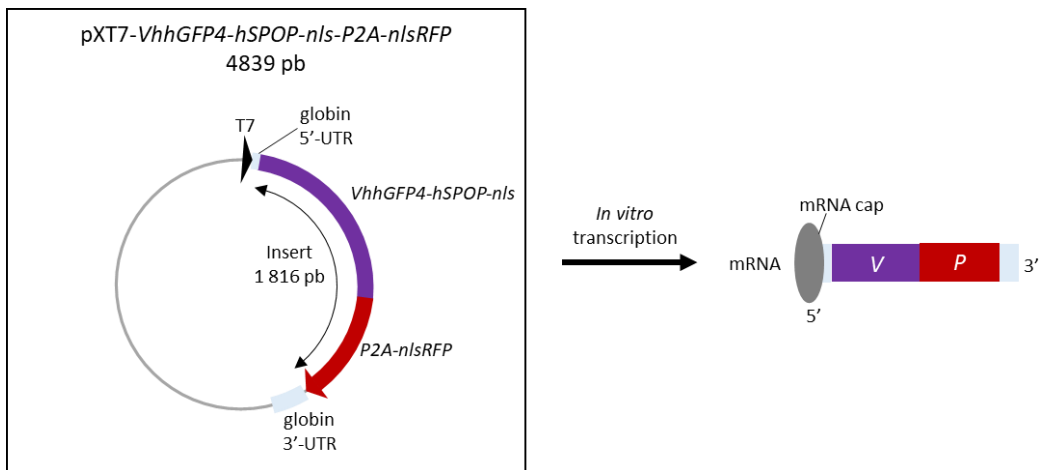
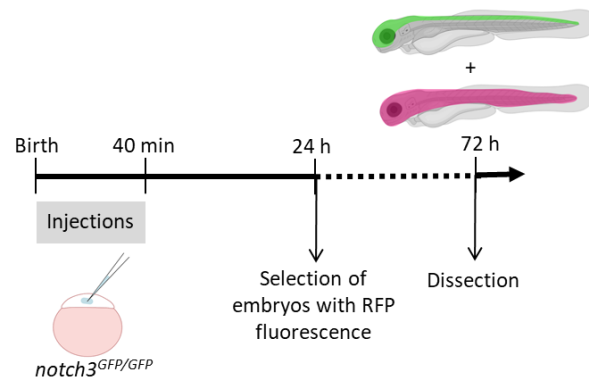
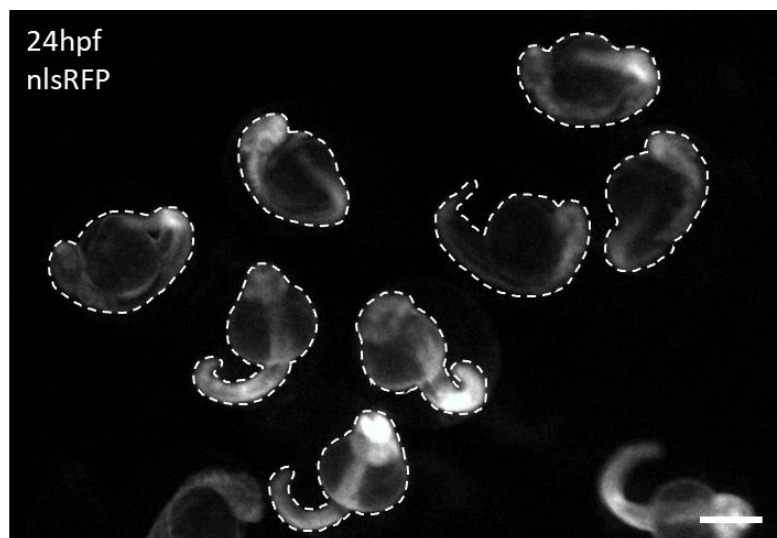
(C) Genotyping gel for a control (-) or a transgenic fish (+).

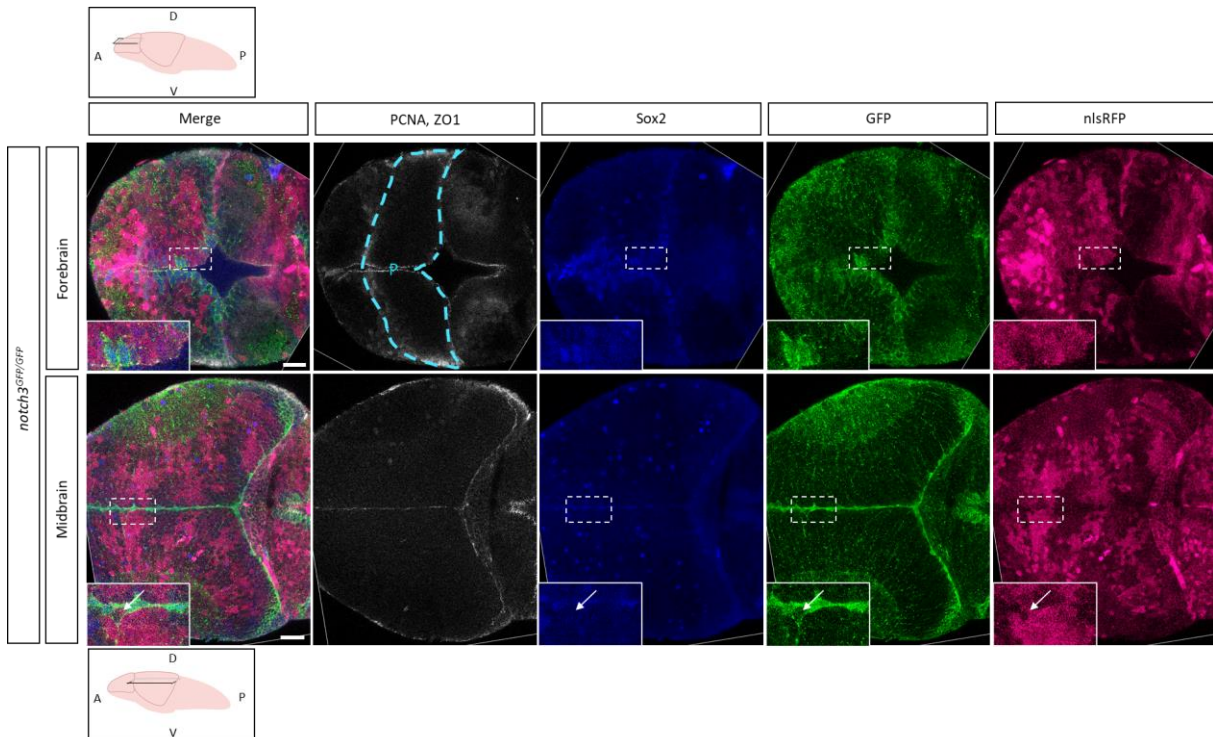
(D) 28 hpf transgenic embryos. The stars highlight the transgenic line selection marker: GFP fluorescence in the heart. The scale bar represents 500  $\mu\text{m}$ .

### *Preliminary validations*

#### *N3ICD degradation by VhhGFP4-hSPOP-nls*

To validate the VhhGFP4-hSPOP-nls efficiency on Notch3-GFP in the *notch3<sup>GFP</sup>* line, I injected the *VhhGFP4-hSPOP-nls-P2A-nlsRFP* capped mRNA into homozygous late one-cell stage embryos (Figure 23A-C). Based on the degradation assays conducted above, I analyzed the resulting larvae at 3 dpf, when pallial NPs are easily tractable in whole-mount and sectioned forebrains, and assuming that a sufficient amount of VhhGFP4-hSPOP-nls protein would still remain. At this age, the pallial ventricular surface is covered with proliferating PCNA<sup>pos</sup> NPs, and the Sox2 signal is visible in the majority of the dorsal most and midline NPs, where *notch3* is expressed (data not shown). In the pallium, the nlsRFP signal tracking of injected cells was heterogenous in intensity and distribution, and weaker than in other brain subdivisions around (in particular the olfactory bulb, the habenula, and the pineal complex) (Figure 23D). Strikingly, in pallial cells, most of the RFP signal was not only limited to the cell nuclei and formed large positive areas containing many cells (including both Sox2<sup>pos</sup> and Sox2<sup>neg</sup> cells) (Figure 23D).

**A****B****C**

**D**

**Figure 23: VhhGFP4-hSPOP-nls mediates degradation of N3ICD-GFP in neural progenitor nuclei after injection of 5'-cap\_VhhGFP4-hSPOP-nls-P2A-nlsRFP into *notch3<sup>GFP/GFP</sup>* embryos**

(A) Schematic illustration of the plasmid of origin and *VhhGFP4-hSPOP-nls-P2A-nlsRFP* capped mRNA.

(B) Experimental design to test the nanobody VhhGFP4-hSPOP-nls. 5'-cap\_VhhGFP4-hSPOP-nls-P2A-nlsRFP is injected in *notch3<sup>GFP/GFP</sup>* embryos to test nuclear N3ICD-GFP degradation.

(C) RFP fluorescence in 24 hpf *notch3<sup>GFP/GFP</sup>* injected embryos. The embryos are still in the chorion. The scale bar represents 500  $\mu$ m.

(D) Immunostaining on injected *notch3<sup>GFP/GFP</sup>* larvae at 3 dpf. Pictures are horizontal optical sections of the forebrain (top panel) and the midbrain (bottom panel) respectively at 30.4  $\mu$ m and 31.3  $\mu$ m from the forebrain ventricular surface and the midbrain dorsal surface. The pallium (P, inside the blue dotted line) is indicated in the panel Forebrain/ PCNA, ZO1. The scale bars represent 20  $\mu$ m in the forebrain and 30  $\mu$ m in the midbrain.

I focused my attention on the NPs located at the pallial midline. I could see that the RFP<sup>pos</sup> NPs had less Sox2 signal, and the nuclear N3ICD-GFP signal was lost (Figure 23D). The membrane N3ICD-GFP signal was also lost in midline RFP<sup>pos</sup> NPs. This loss of nuclear and membrane GFP is similar to what I obtained on 3 dpf LY-treated larvae (see Figure 20B). The possibility of precocious NPs differentiation could be analyzed by neuronal markers.

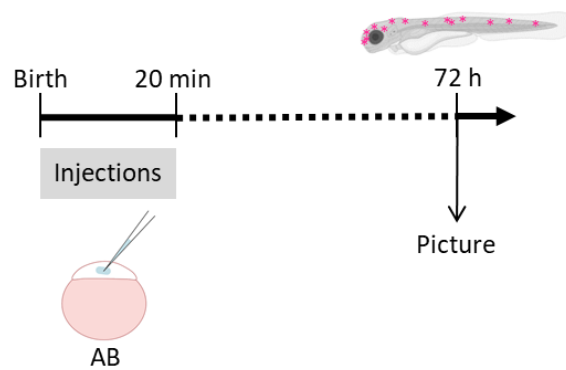
I also imaged the midbrain of injected larvae, where the nlsRFP signal was also heterogenous and mostly spread among the neuron layers (see the cell organization in the midbrain in Figure 20D). Some NPs however were still RFP<sup>pos</sup>. In these cells, the N3ICD-GFP signal in nuclei was also lower than in neighboring RFP<sup>neg</sup> cells (Figure 23D).

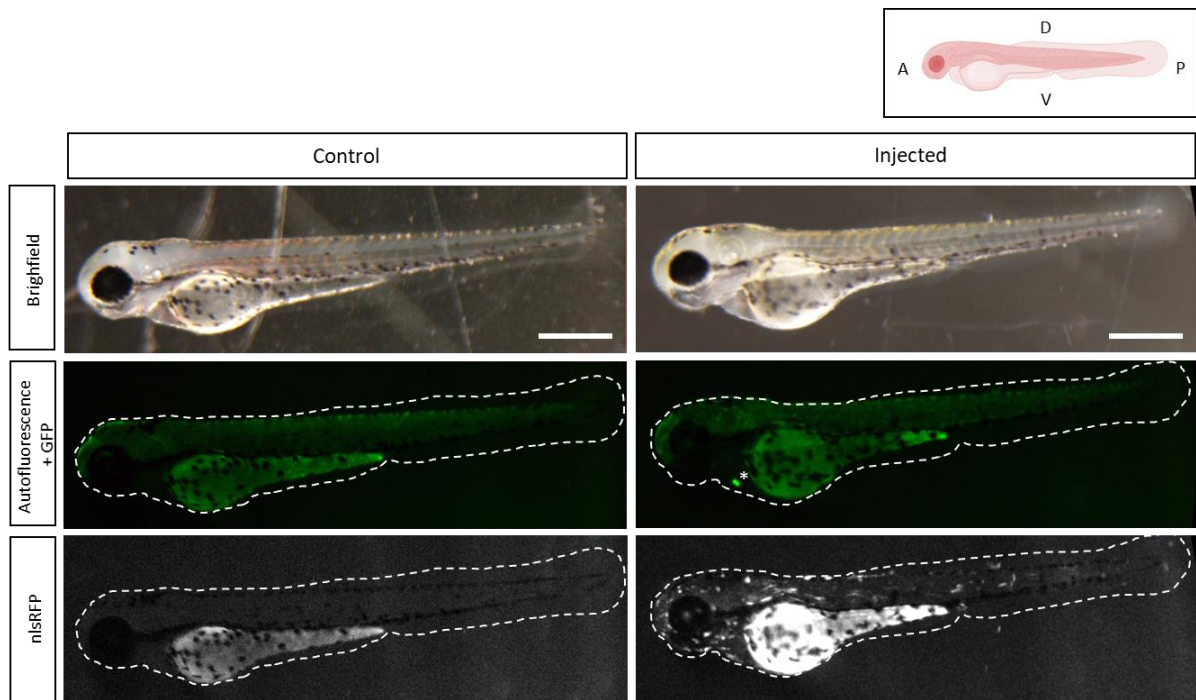
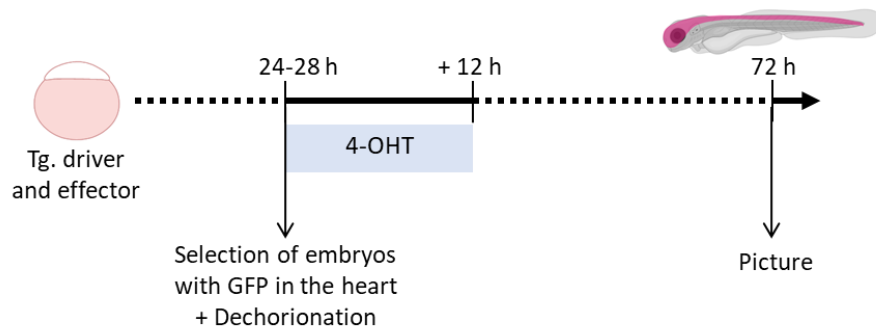
These results confirm the efficient degradation of N3ICD-GFP by VhhGFP4-hSPOP-nls.

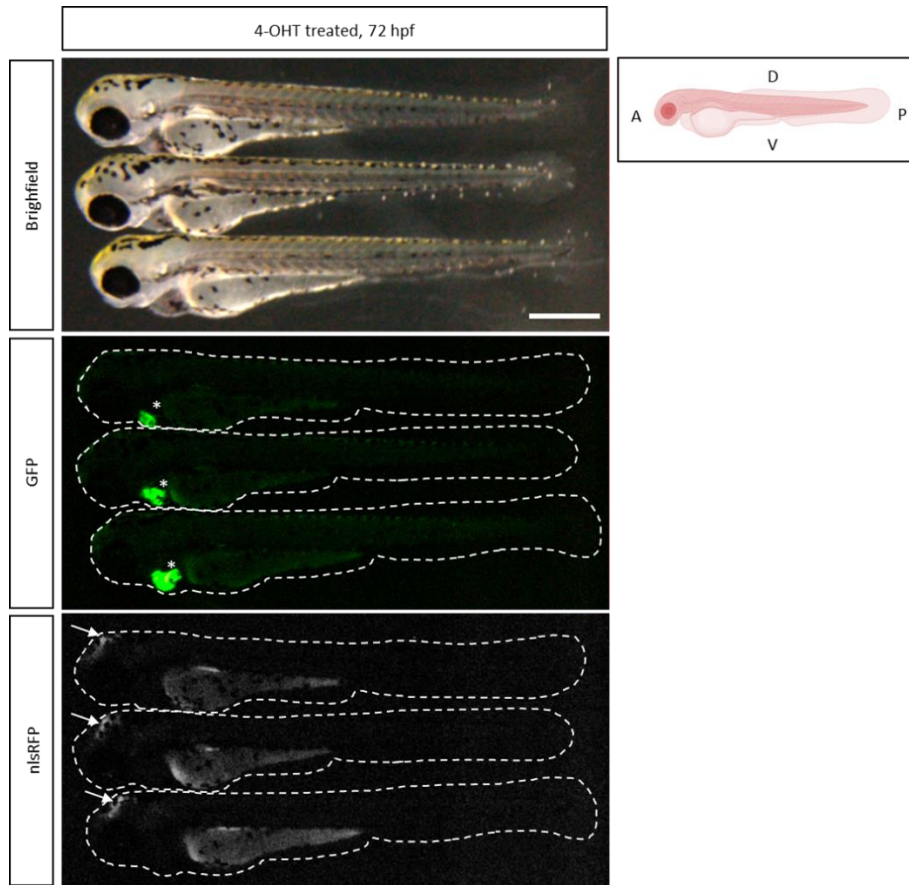
***Expression of VhhGFP4-hSPOP-nls upon loxP-stop-loxP recombination***

To verify the possibility of recombining the *loxP-stop-loxP* sequence *in vivo* to express VhhGFP4-hSPOP-nls, I injected the *VhhGFP4-hSPOP-nls-P2A-nlsRFP* plasmid (containing *tol2* sites) (see Figure 22A) together with the capped mRNAs encoding the *tol2* Transposase and the Cre recombinase into one-cell stage AB embryos, and screened the embryos at 48 hpf for nlsRFP fluorescence (Figure 24A). Many nlsRFP<sup>pos</sup> cells were visible all along the head and the body of injected embryos, likely corresponding to clones of cells where the *stop* cassette was recombined (Figure 24B). These results validate the possibility of recombining the *loxP* sites for the deletion of the *stop* cassette and the expression of the transgene containing the expression marker nlsRFP.

**A**



**B****C**

**D**

**Figure 24: Validations of the expression of *VhhGFP4-hSPOP-nls-P2A-nlsRFP* upon *loxP-stop-loxP* recombination**

(A) Experimental design to test the *loxP-stop-loxP* recombination upon Cre recombinase capped mRNA injection. The Tol2 plasmid, the *tol2* transposase capped mRNA, and the Cre recombinase capped mRNA are injected into AB embryos. The larvae are screened at 72 hpf for RFP fluorescence in their body.

(B) 72 hpf not injected (control) or injected AB larvae. The star highlights the GFP fluorescence in the heart. The yolk sac is autofluorescent in green and red. The scale bar represents 500  $\mu$ m.

(C) Experimental design to test the *loxP-stop-loxP* recombination upon 4-OHT treatment. *Tg(bact2:loxP-stop-loxP-VhhGFP4-hSPOP-nls-P2A-nlsRFP)* effector fish and *Tg(her4:ERT2CreERT2)* driver fish are crossed, their embryos are selected and treated with 4-OHT, and the RFP fluorescence is attested at 72 hpf. As *Tg(her4:ERT2CreERT2)* embryos do not have a transgenic line selection marker, 50% of larvae with RFP fluorescence in their central nervous system is expected.

(D) Treated 72 hpf transgenic larvae. The stars highlight the GFP fluorescence in the heart. The arrows point the RFP fluorescence in the anterior part of the central nervous system. The yolk sac is autofluorescent in green and red. The scale bar represents 500  $\mu$ m.

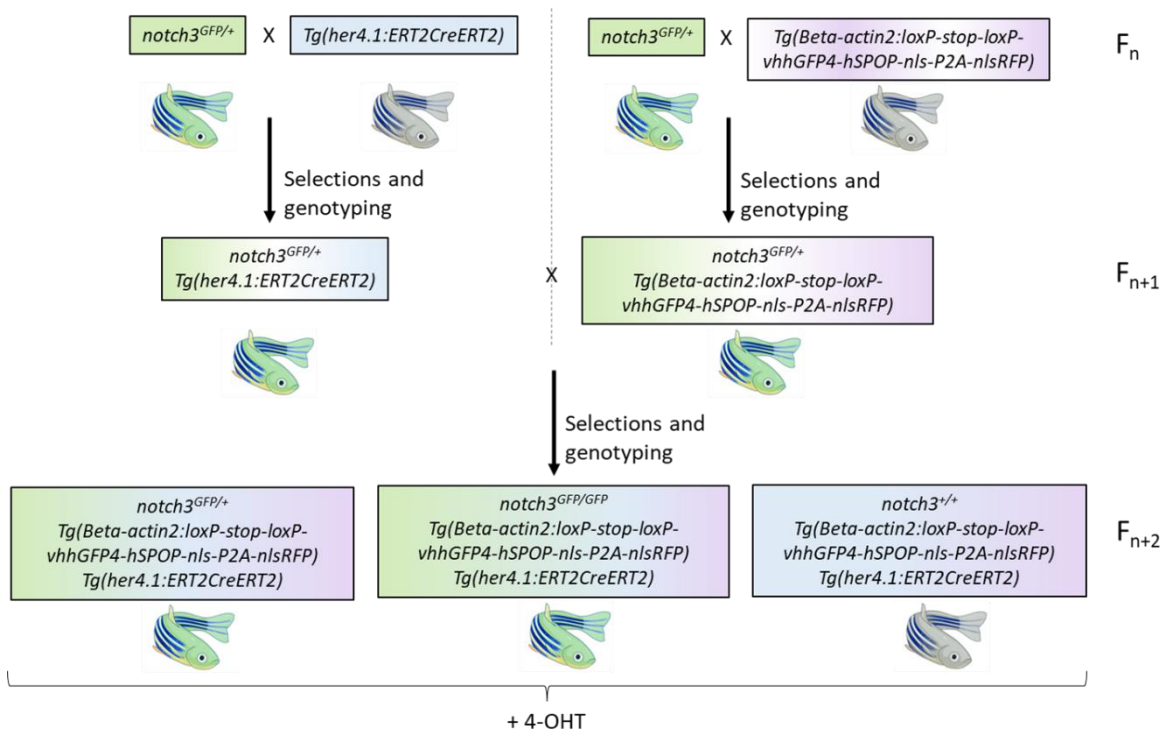
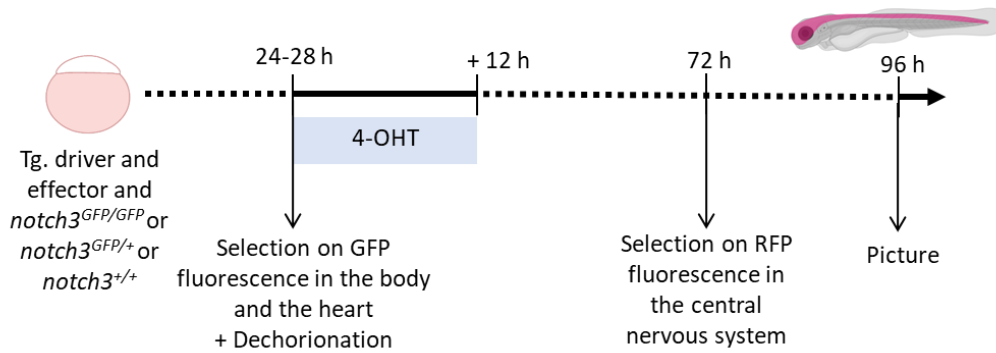
### ***Generation of the *Tg(VhhGFP4-hSPOP-nls-P2A-nlsRFP)* line***

To generate the nanobody effector line, I injected the *VhhGFP4-hSPOP-nls-P2A-nlsRFP* construct together with the transposase mRNA into one-cell stage AB embryos and screened embryos at 24-28 hpf for their expression of GFP in the heart (Figure 22A-D). By using the *tol2/transposase* transgenesis, I expected the long 11 264 bp insert to integrate randomly into the genome, and only once. The mean percentage of early mortality associated with injections was around 74% at 48 hpf. A mosaic cardiac GFP signal was visible in 40% of the surviving

embryos (representing 11% of the total injected embryos), which were considered potential F0 founder fish and raised until adulthood. These fish had normal morphology and development rate. The adult mosaic F0 transgenic fish were crossed with AB fish and the germline transmission of the transgene was tested by screening for the nuclear GFP signal in the heart in the offspring at 24 hpf. 23.5% of the F0 fish (n=98) were able to transmit the *cmhc2:nlsGFP* transgene. The percentages of positive embryos were very variable depending on the selected F0 parent, and varied between less than 1% to 77.6%.

To select between F0 fish for future analyses, I tested the inducibility of *VhhGFP4-hSPOP-nls-P2A-nlsRFP* expression in the central nervous system by crossing some of the selected F0 fish with driver *Tg(her4.1:ERT2CreERT2)* heterozygotes (Figure 24C). The latter transgenic animals carry the *Cre recombinase* sequence fused to two *ERT2* sites, allowing a temporal control of the Cre translocation inside the nucleus for its recombination activity in presence of 4-OHT. The *her4.1* promoter, here at the origin of the spatial control of *ERT2CreERT2* expression, is a target gene of the Notch pathway (Yeo et al., 2007) involved in glial cell specification and activated in NPs/NSCs. The 24 hpf offspring were incubated in 10 mM 4-OHT overnight and screened at 72 hpf for the expression of nlsRFP (Figure 24C,D). nlsRFP appeared weakly expressed in the anterior nervous system in embryos issued from 4 out of the 9 crosses tested (Figure 24D). As 50% of the embryos carry the *her4.1:ERT2CreERT2* transgene, I expected nlsRFP expression in 50% of the embryos with a nlsGFP<sup>POS</sup> heart. I observed variable percentages of embryos with nlsRFP fluorescence, but it was always inferior to 50%. Based on the clutches showing the best correlation, these results allowed the selection of 4 different F0 founders for *bact2:loxP-stop-loxP-VhhGFP4-hSPOP-nls-P2A-nlsRFP*, named D, EN, EK, and EH (for now, the latter founder had not been used), that were able to transmit the transgene to their offspring and in which I verified the 4-OHT-dependent induction of nanobody effector expression.



**A****B**

C

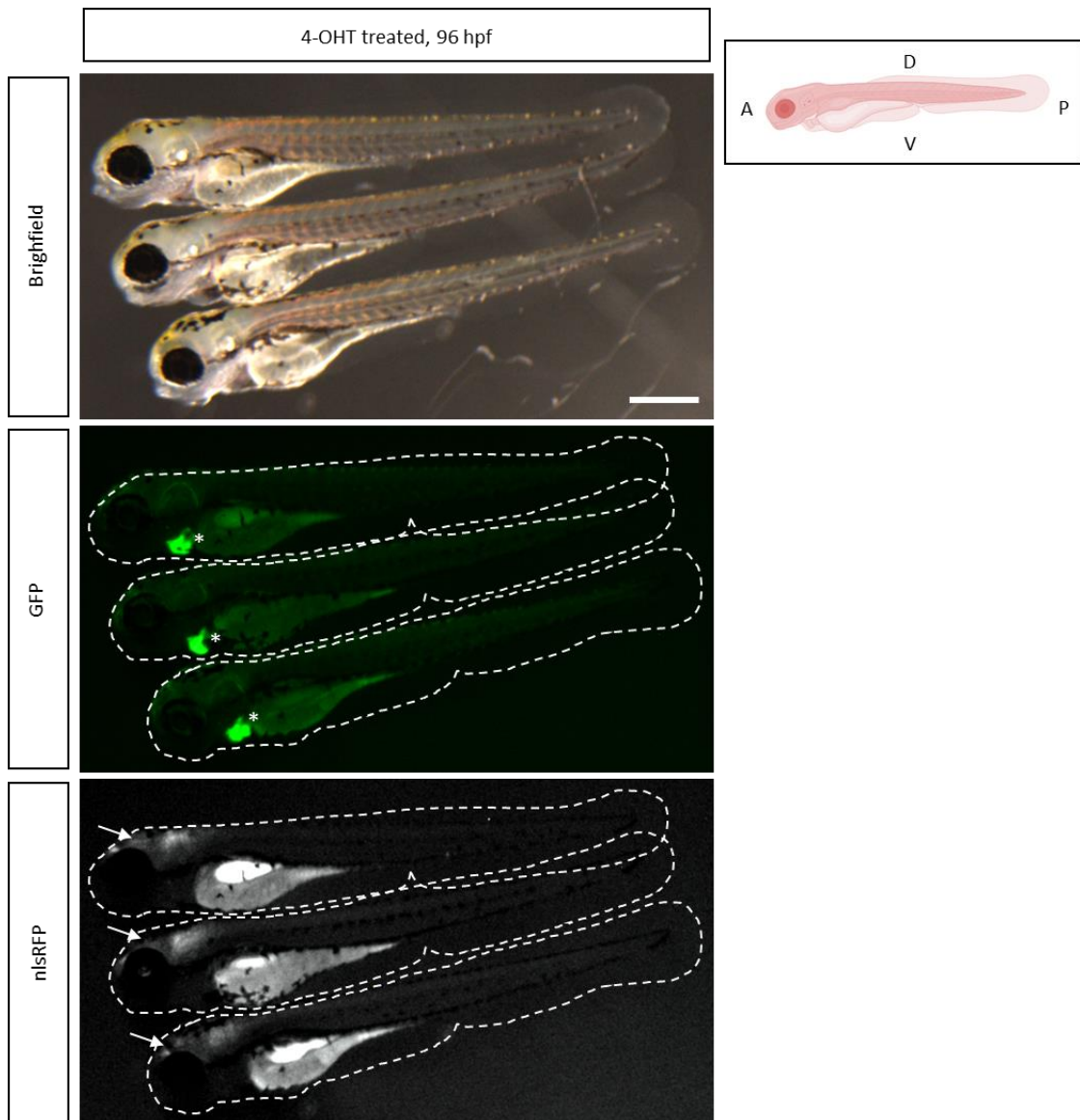


**Figure 25: Crossings for the generation of  $notch3^{GFP/GFP}$  double transgenic fish and validation of the expression of  $VhhGFP4-hSPOP-nls-P2A-nlsRFP$  upon  $loxP-stop-loxP$  recombination in embryos**

(A) Parallel generation of  $notch3^{GFP/+}$  fish carrying either  $her4:ERT2CreERT2$  or  $bact2:loxP-stop-loxP-VhhGFP4-hSPOP-nls-P2A-nlsRFP$  transgenes (Fn+1) and crossing to obtain  $notch3^{GFP/GFP} Tg(bact2:loxP-stop-loxP-VhhGFP4-hSPOP-nls-P2A-nlsRFP; her4:ERT2CreERT2)$  fish (Fn+2). Fish carrying  $notch3^{GFP/GFP}/notch3^{GFP/+}$  and/or  $Tg(bact2:loxP-stop-loxP-VhhGFP4-hSPOP-nls-P2A-nlsRFP)$  are selected at 24-28 hpf. All the fish are genotyped for the KI and the transgenes before analysis.  $notch3^{GFP/+} Tg(bact2:loxP-stop-loxP-VhhGFP4-hSPOP-nls-P2A-nlsRFP; her4:ERT2CreERT2)$  fish are used for comparison (half-capacity of N3ICD degradation).  $notch3^{+/+} Tg(bact2:loxP-stop-loxP-VhhGFP4-hSPOP-nls-P2A-nlsRFP; her4:ERT2CreERT2)$  fish are used as control.

(B) Experimental design to test the  $loxP-stop-loxP$  recombination upon 4-OHT treatment in Fn+2 fish.

(C) 96 hpf 4-OHT treated larvae ( $notch3^{GFP/GFP}$  or  $notch3^{GFP/+}$ ). The stars highlight the GFP fluorescence in the heart. The arrows point the RFP fluorescence in the anterior part of the central nervous system. The scale bar represents 500  $\mu m$ .

To create the fish line containing (i) the effector transgene  $bact2:loxP-stop-loxP-VhhGFP4-hSPOP-nls-P2A-nlsRFP$ , (ii) the driver transgene  $her4.1:ERT2CreERT2$ , and (iii) the KI into

*notch3* to generate the GFP degenon *notch3<sup>GFP</sup>*, I first crossed the KI line independently with the effector and driver transgenic lines (F1 generations) (Figure 25A). I validated the presence of the transgenes and the KI by genotyping. These crossings created F1 parents that were crossed to each other to obtain F2 fish carrying the two transgenes and the KI (Figure 25A). I selectively grew F2 fish carrying *cmlc2:nlsGFP* (indicating the presence of the transgene *bact2:loxP-stop-loxP-VhhGFP4-hSPOP-nls-P2A-nlsRFP*) and expressing Notch3-GFP (recognizable by their green body), selected at 24 hpf, to increase the percentage of fish of interest (these embryos represent 37.5% of the total of embryos in a clutch, incl. 25% of heterozygotes and 12.5% of homozygotes for *notch3<sup>GFP</sup>*). I also grew an equal number of embryos that contained the two transgenes but did not carry the KI (representing 6.25% of the total of embryos in a clutch).

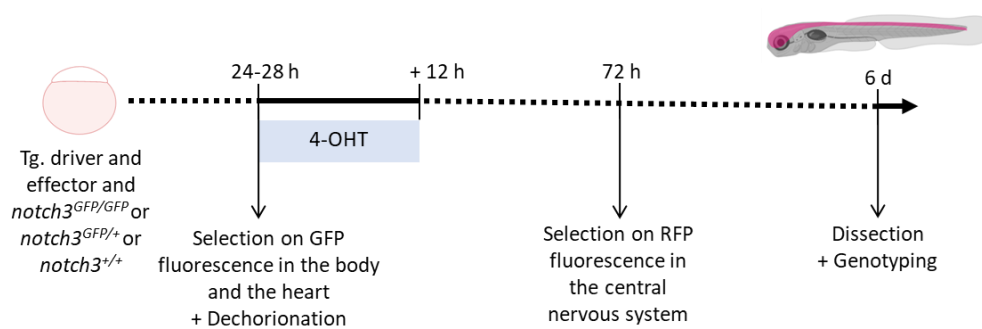
F2 clutches from the three different *bact2:loxP-stop-loxP-VhhGFP4-hSPOP-nls-P2A-nlsRFP* transgenic founders D, EN and EK contained different percentages of embryos carrying *cmlc2:nlsGFP*. This percentage was always superior to 50% for 15 F1 tested from founder D, 1 F1 tested from founder EK, and was 50% for 1 F1 tested from founder EN. These results suggest multiple insertions of the *bact2:loxP-stop-loxP-VhhGFP4-hSPOP-nls-P2A-nlsRFP* transgene in F1 fish from founders D and EK, while the tested F1 fish from founder EN likely carries a single insertion.

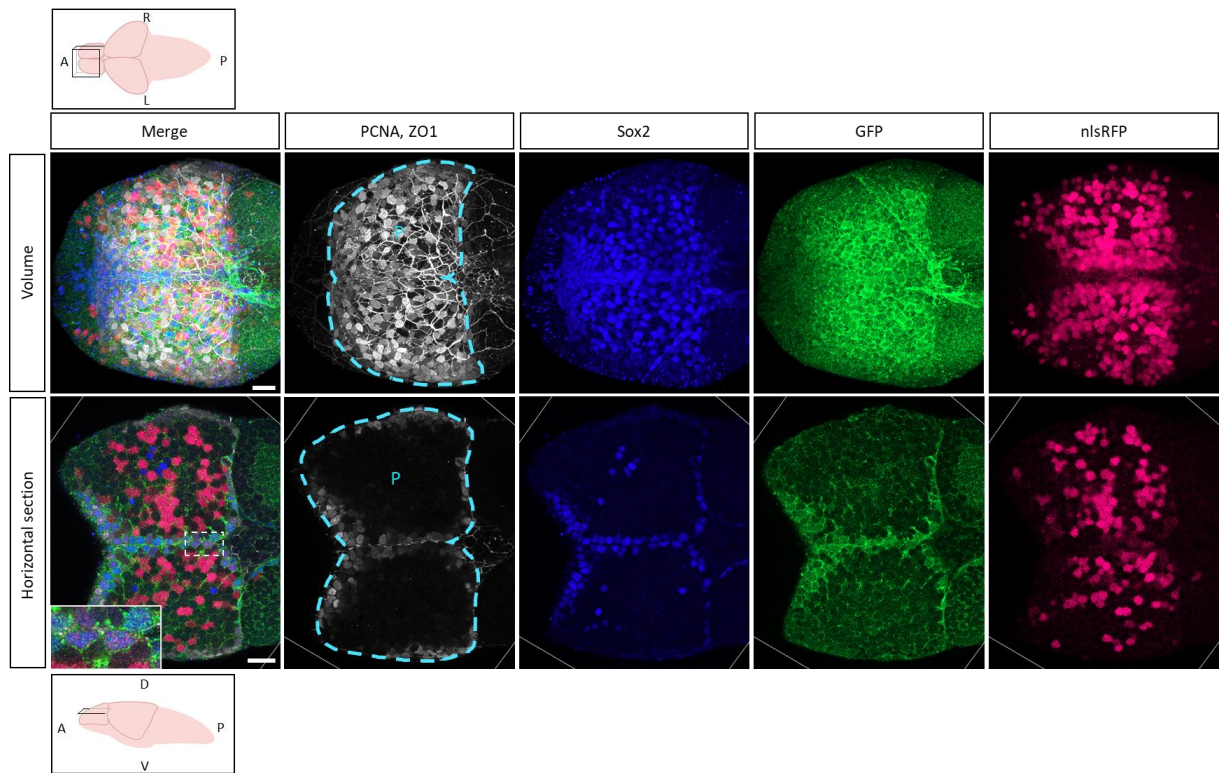
Finally, I compared the inducibility of expression of the nanobody effector in F2 embryos, selected at 24 hpf on *cmlc2:nlsGFP* and *notch3<sup>GFP</sup>* (green heart and green body), and coming from D, EN, or EK F1 fish (Figure 25B). The 24 hpf embryos were treated with 10 mM 4-OHT overnight and screened at 72 hpf for nlsRFP fluorescence. I could validate weak nlsRFP expression in the brain, comparable to the signal obtained in the inducibility test (see Figure 24D), and at 96 hpf, the signal was more intense and spread (Figure 25C). As expected in absence of *her4.1:ERT2CreERT2* selection marker, among the treated F2 larvae with a green heart, 50% had red signal. These results validated the inducibility of the expression of the nanobody effector in 24 hpf embryos carrying the effector transgene, the driver transgene and the KI.

**Degradation of N3ICD-GFP in vivo using the inducible VhhGFP4-hSPOP-nls nanobody**

To validate the degradation of nuclear N3ICD-GFP *in vivo* in the inducible transgenic system, I chose to work on 6 dpf F2 larvae from founder EN (Figure 26A). I selected embryos carrying the transgenes and/or the KI at 24 hpf, treated the 24 hpf embryos with 10 mM 4-OHT overnight, selected larvae showing nlsRFP fluorescence in the head at 72 hpf, and dissected the larval brains at 6 dpf while using the larval bodies for genotyping in parallel (Figure 26A). To test for leakiness of the system, i.e., possible background recombination at the *loxP* sites, I also screened larvae of the same genotype in the absence of 4-OHT treatment. The latter larvae never showed nlsRFP expression, even when revealed using IHC for more sensitivity (n=10, data not shown).

**A**



**B**

C

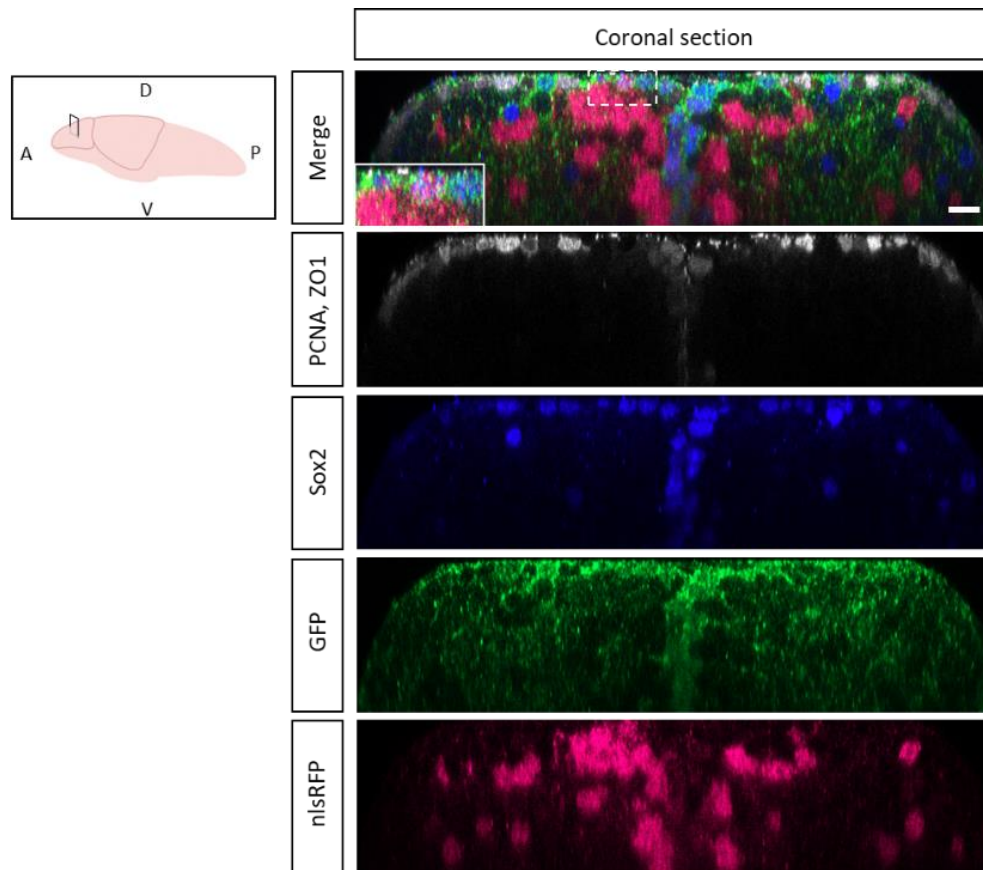


**Figure 26: *VhhGFP4-hSPOP-nls-P2A-nlsRFP* is expressed in pallial neural progenitors in 6 dpf larvae**

(A) Experimental design to validate the expression of *VhhGFP4-hSPOP-nls-P2A-nlsRFP* in the pallium of 6 dpf larvae after the 4-OHT treatment.

(B) Immunostaining on a 6 dpf *notch3<sup>GFP/GFP</sup> Tg(bact2:loxP-stop-loxP-VhhGFP4-hSPOP-nls-P2A-nlsRFP; her4:ERT2CreERT2)* forebrain expressing *VhhGFP4-hSPOP-nls-P2A-nlsRFP*. Pictures are a Z projection over 55  $\mu\text{m}$  (top panel) and a horizontal optical section at 13.3  $\mu\text{m}$  from the ventricular surface of the forebrain (bottom panel). The pallium (P, inside the blue dotted line) is indicated in the PCNA, ZO1 panels. The scale bars represent 20  $\mu\text{m}$ .

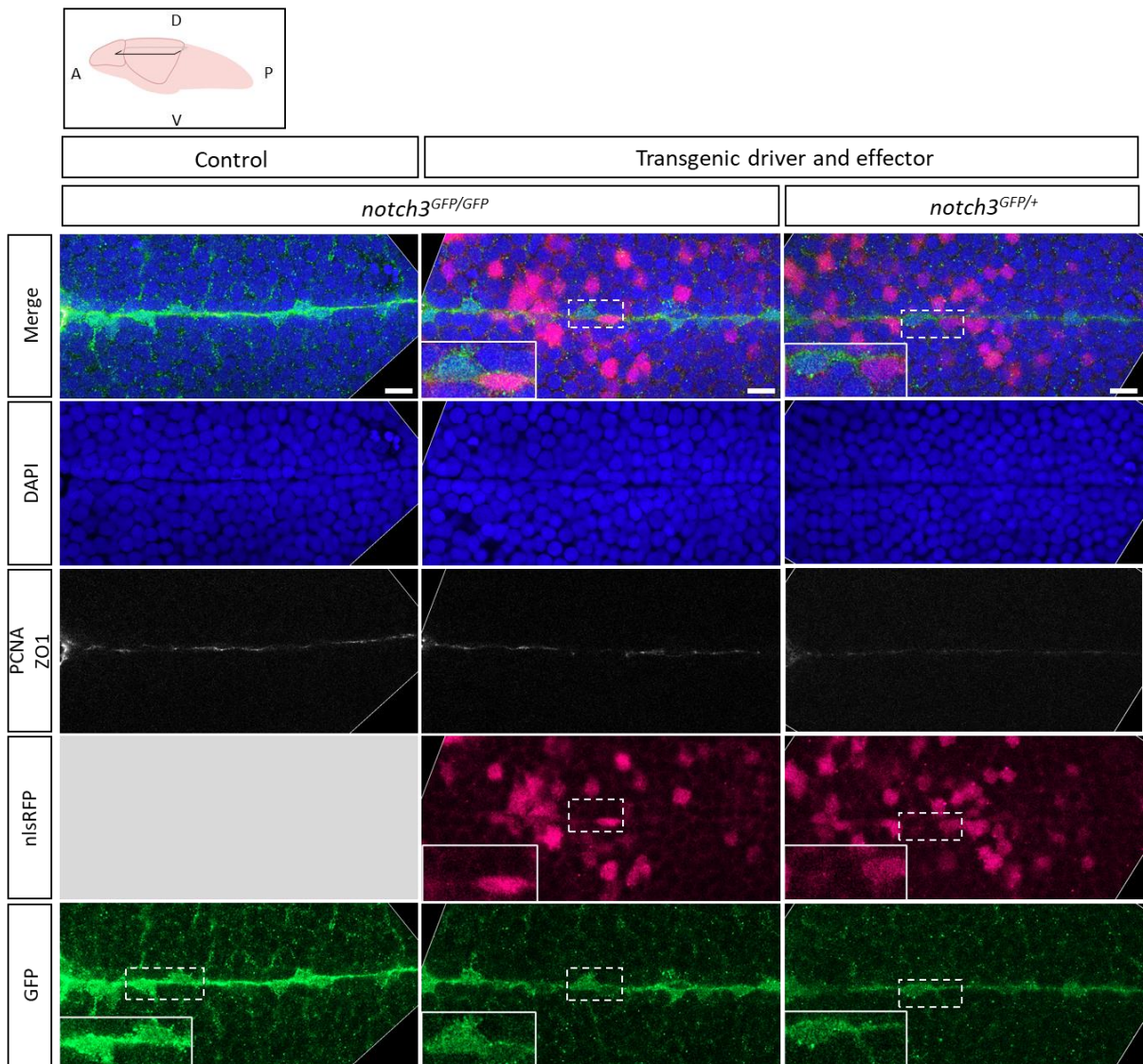
(C) Coronal section in the pallium (45  $\mu\text{m}$  tissue deep). The scale bars represent 10  $\mu\text{m}$ .

I used whole-mount IHC for Notch3-GFP, Sox2 and nlsRFP (nanobody induction tracer) on dissected larval brains at 6 dpf to quantify N3ICD-GFP in NPs of the pallium. At 6 dpf, Sox2<sup>pos</sup> cells represented the majority of pallial ventricular cells, which were mostly proliferating (Figure 26B). The method for segmenting and analyzing pallial NPs in larvae is currently under improvement.

The rare non-proliferative ventricular surface cells were all Sox2<sup>pos</sup> (Figure 26B). These cells were likely NPs that already entered quiescence, as suggested in Than-Trong et al., 2018. Together, the pallial ventricular surface appeared composed of intermingled activated and quiescent NPs, and neurons (mostly Sox2<sup>neg</sup>). As expected, the Notch3-GFP signal was visible

at the membrane and N3ICD-GFP in the nucleus of the majority of cells at the ventricular surface (Figure 26B,C). The induced nlsRFP signal was strong in the nucleus of many cells including at all depths in the pallial parenchyme, in agreement with the expected neuronal fate of *her4*<sup>pos</sup> cells in which the transgene was induced prior to the 4-day chase. nlsRFP did not delimit nuclei as cleanly as in our previous work using *Hmgb1-mCherry* expression (mCherry fused with the nuclear High-mobility group box 1 protein) (Figure S2). Some Sox2<sup>pos</sup>,nlsRFP<sup>pos</sup> cells were at the ventricular surface, and their RFP nuclear signal intensity was weaker than the deeper RFP<sup>pos</sup> cells (Figure 26B,C).

I also imaged the midbrains of the treated larvae and I analyzed the zone between the medial tectal proliferation zone and the thalamus (see Figure 20D). nlsRFP<sup>pos</sup> cells were spread in the neuron layers and at the midline (Figure 27A). At the midline, RGs had a characteristic triangular shape, a flattened nucleus, and were GFP<sup>pos</sup> (Figure 27A). However, in the RFP<sup>pos</sup> RGs the nuclear GFP intensity seemed weaker than in the RFP<sup>neg</sup> RGs (Figure 27A).

**A**





**Figure 27: Validation of the *VhhGFP4-hSPOP-nls*-mediated N3ICD-GFP degradation in the 6 dpf midbrain radial glia**

(A) Horizontal optical sections of 6 dpf *notch3<sup>GFP/GFP</sup> Tg(bact2:loxP-stop-loxP-VhhGFP4-hSPOP-nls-P2A-nlsRFP; her4:ERT2CreERT2)* midbrain at 30.2  $\mu\text{m}$  from the ventricular surface, and *notch3<sup>GFP/+</sup> Tg(bact2:loxP-stop-loxP-VhhGFP4-hSPOP-nls-P2A-nlsRFP; her4:ERT2CreERT2)* midbrain at 35.7  $\mu\text{m}$  from the ventricular surface, both expressing *VhhGFP4-hSPOP-nls-P2A-nlsRFP*. The control midbrain corresponds to a 4-OHT treated *notch3<sup>GFP/GFP</sup> Tg(her4:ERT2CreERT2)* or not transgenic larvae. The scale bars represent 10  $\mu\text{m}$ .

(B) Pipeline for nuclei segmentation at the midbrain midline and quantification of nuclear GFP using Imaris and Prism. The first picture is a horizontal optical section in a 6 dpf *notch3<sup>GFP/GFP</sup> Tg(bact2:loxP-stop-loxP-VhhGFP4-hSPOP-nls-P2A-nlsRFP; her4:ERT2CreERT2)* midbrain. The scale bar represents 10  $\mu\text{m}$ . Mann Whitney test, \*\*\* $p < 0.0001$ . RFP<sup>neg</sup> n= 33, RFP<sup>pos</sup> n= 13.

(C) Nuclear mean GFP intensity in RFP<sup>pos</sup> and RFP<sup>neg</sup> radial glia cells in *notch3<sup>GFP/GFP</sup>* and *notch3<sup>GFP/+</sup>* midbrains. Each dot is one nucleus among 3 pooled brains per condition. Bar at median and bracket for interquartile range. Two way ANOVA, Sidak's multiple comparison test, \*\*\*\* $p < 0.0001$  (control vs. *notch3<sup>GFP/GFP</sup> RFP<sup>neg</sup>*), \*\*\*\* $p < 0.0001$  (*notch3<sup>GFP/GFP</sup> RFP<sup>neg</sup>* vs. *notch3<sup>GFP/GFP</sup> RFP<sup>pos</sup>*), \*\*\* $p = 0.001$  (*notch3<sup>GFP/+</sup> RFP<sup>neg</sup>* vs. *notch3<sup>GFP/+</sup> RFP<sup>pos</sup>*), \*\*\*\* $p < 0.0001$  (*notch3<sup>GFP/GFP</sup> RFP<sup>neg</sup>* vs. *notch3<sup>GFP/+</sup> RFP<sup>pos</sup>*). Number of cells: control n= 152, *notch3<sup>GFP/GFP</sup> RFP<sup>neg</sup>* n= 106, RFP<sup>pos</sup> n= 46, *notch3<sup>GFP/+</sup> RFP<sup>neg</sup>* n=107, RFP<sup>pos</sup> n=18.

The easy identification of NPs/RGs via their characteristic nuclear shape, and the absence of proliferation in this territory, led me to study N3ICD-GFP degradation in the midbrain. To circumvent the weak Sox2 signal defining the NSCs nucleus at the midline, I stained nuclei with 4',6-diamidino-2-phenylindole (DAPI) and used this signal to segment the flattened nuclei located at the midline in the region of interest (Figure 27A,B). Upon quantification, I found that nlsRFP<sup>pos</sup> nuclei has significantly lower N3ICD-GFP levels than nlsRFP<sup>neg</sup> RGs/NPs (Figure 27B,C). The difference was stronger in larvae homozygous for the KI compared to heterozygotes (Figure 27C).

These results validated the efficient *in vivo* degradation of nuclear N3ICD-GFP by *VhhGFP4-hSPOP-nls* when induced by conditional *Cre-loxP* recombination in *her4*-expressing RGs/NPs at 24 hpf.

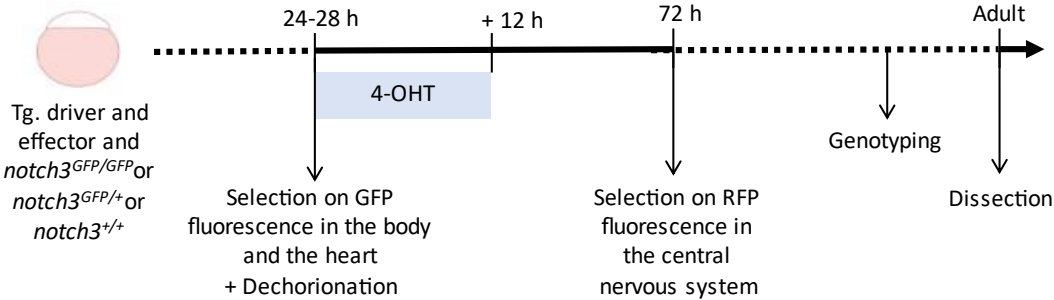
***Conditional and sporadic loss of Notch3-GFP in embryo creates clones in adult***

Because the absence of Notch3 before 7 dpf does not perturb brain development, we could induce Notch3 degradation at 24 hpf and isolate the phenotypes specific to Notch3 functions in the adult, by analyzing the grown fish. This would practically reveal Notch3 function from 7 dpf onwards. Due to the morphodynamics of the pallium, I expect the induced cells to form clones of neighboring cells in the adult.

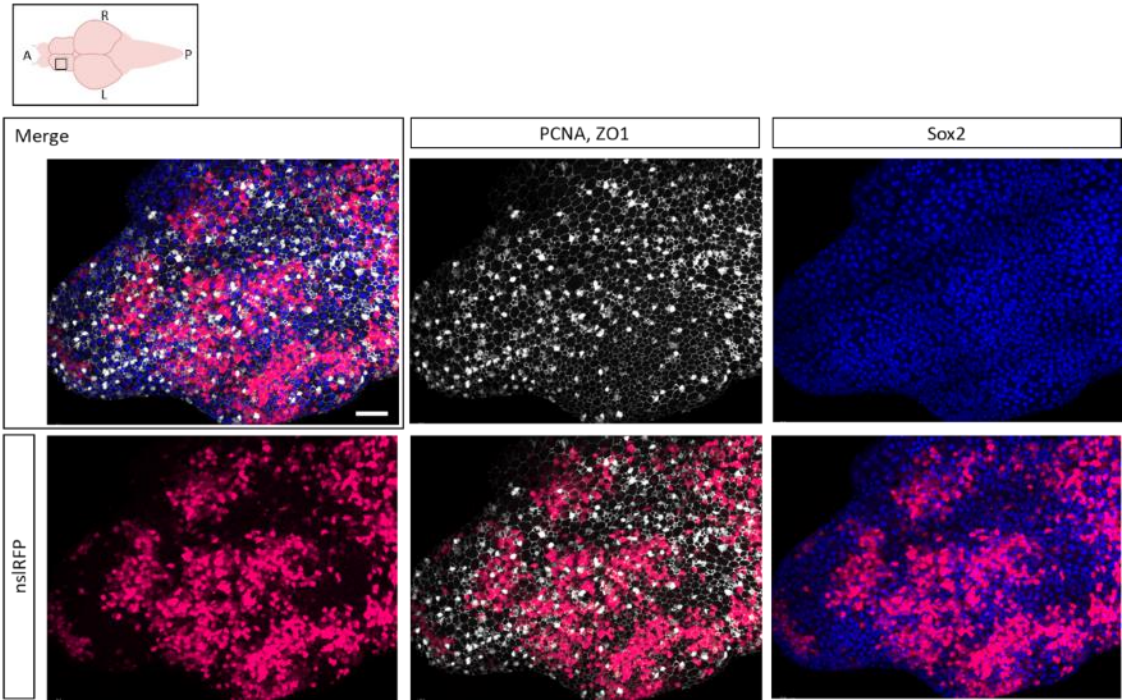
Thus, I induced the expression of *VhhGFP4-hSPOP-nls-P2A-nlsRFP* in 24 hpf driver/nanobody effector and/or KI embryos by bathing them in 4-OHT overnight, selecting the larvae with nlsRFP fluorescence at 72 hpf and growing the fish until adulthood. The induced

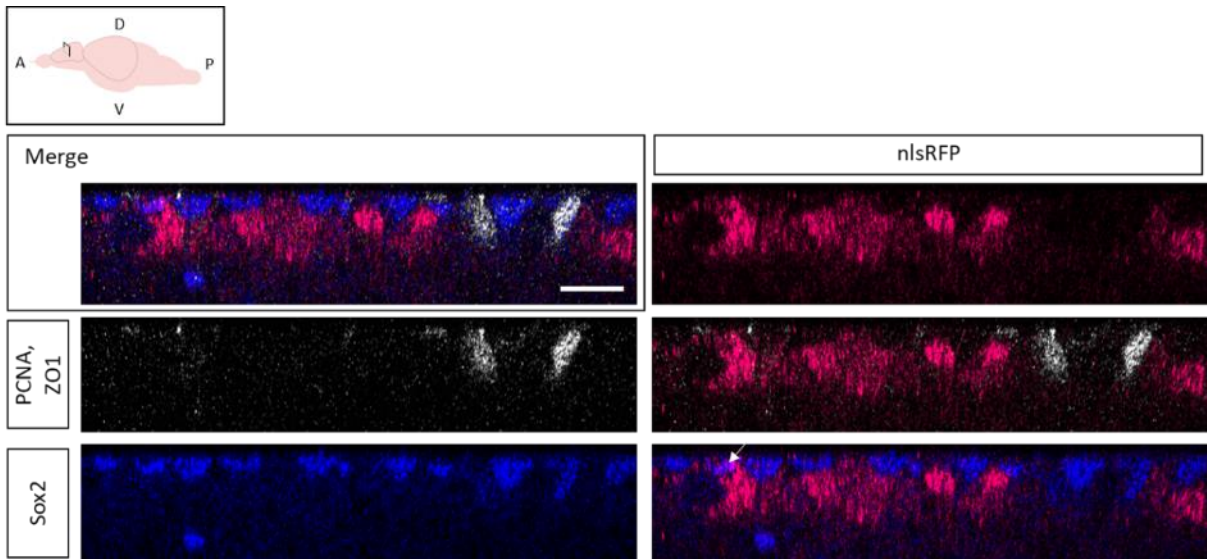
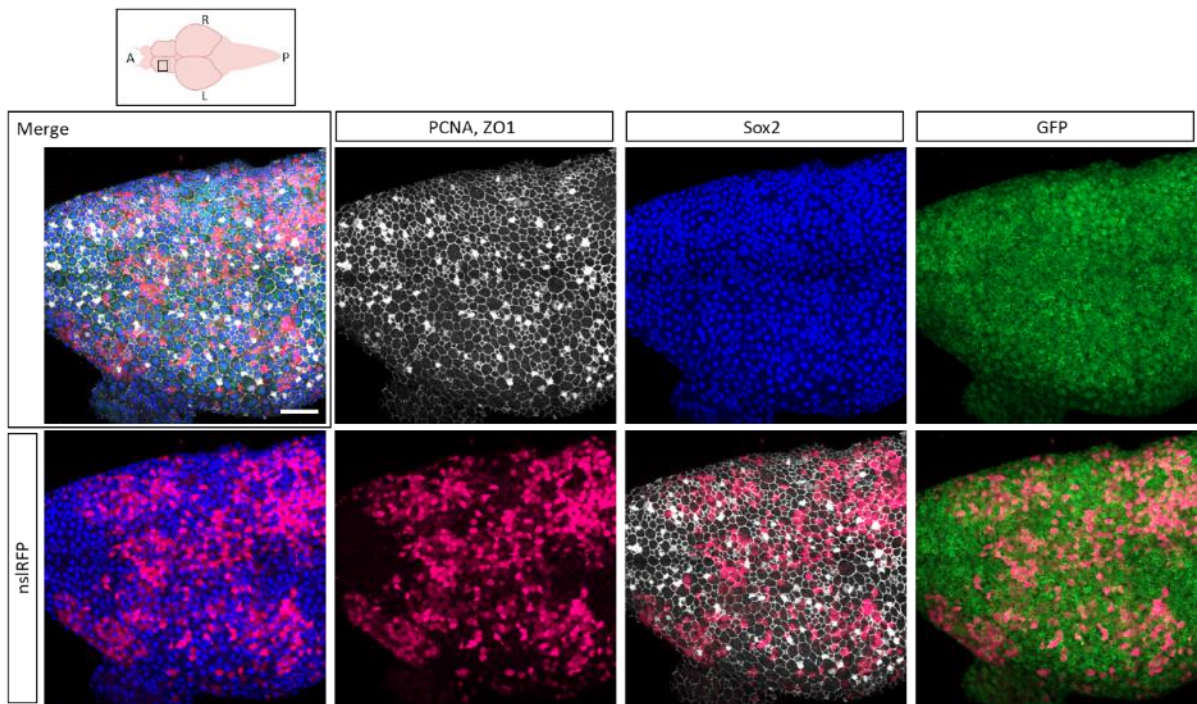
fish grew without any visible morphological phenotype (data not shown). The conditions of 4-OHT induction on 24 hpf embryos had already been improved for maximal recombination in another line with the same driver of expression. Analyzing the pallium 4 days after induction (i.e., at 6 dpf) in our line revealed that only a few RFP<sup>pos</sup> cells remain surface Sox2<sup>pos</sup> cells (Figure 26B,C). The few remaining Sox2<sup>pos</sup>RFP<sup>pos</sup> cells at 6 dpf are an advantage for the obtention of isolated cell clones in the grown brains.

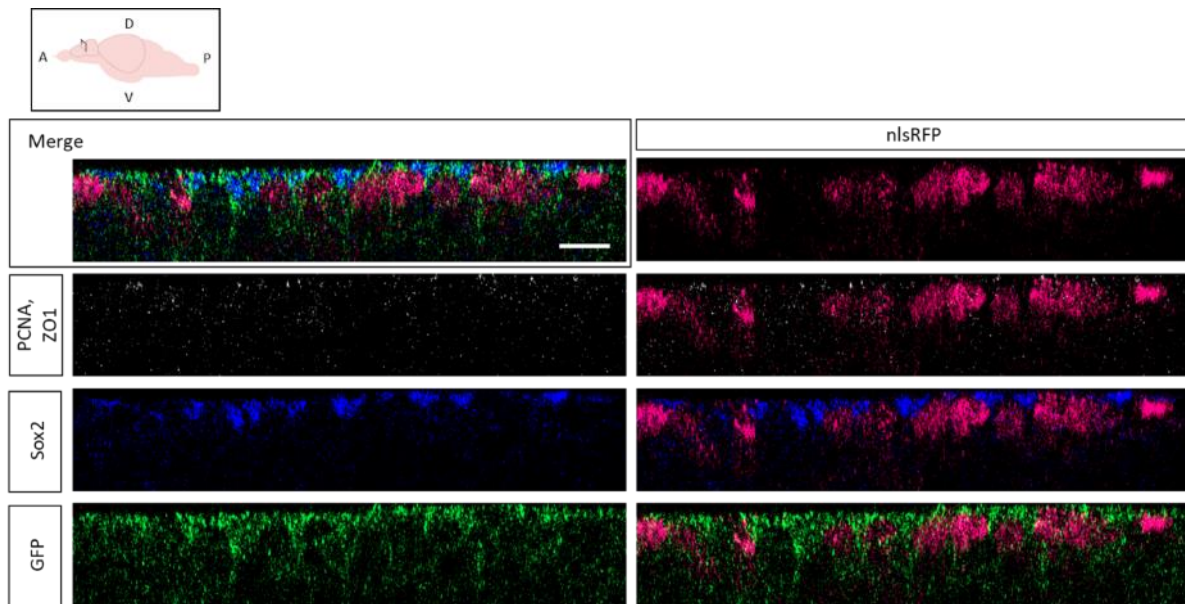
**A**



**B**



**C****D**

**E****Figure 28: Conditional and sporadic loss of Notch3-GFP in embryo creates clones in adult**

(A) Experimental design to induce the expression of *VhhGFP4-hSPOP-nls-P2A-nlsRFP* in the pallium of 24-28 hpf embryos with a 4-OHT treatment, and collect the resulting adult brains.

(B) Immunostaining on a resulting adult driver/nanobody effector control pallium. The picture is a Z projection over 28  $\mu\text{m}$ . The scale bar represents 50  $\mu\text{m}$ .

(C) Optical cross section in the resulting control pallium (25.2  $\mu\text{m}$  tissue deep). The arrow points to a  $\text{Sox2}^{\text{pos}}\text{RFP}^{\text{pos}}\text{PCNA}^{\text{neg}}$  nucleus. The scale bar represents 20  $\mu\text{m}$ .

(D) Immunostaining on a resulting adult driver/nanobody effector and *notch3*<sup>GFP/GFP</sup> pallium. The picture is a Z projection over 28  $\mu\text{m}$ . The scale bar represents 50  $\mu\text{m}$ .

(E) Optical cross section in the resulting control pallium (26  $\mu\text{m}$  tissue deep). The scale bar represents 20  $\mu\text{m}$ .

I first induced F2 embryos from founder D and imaged the pallia at 2 and 3 months post-fertilization (mpf). For control (no KI), and *notch3*<sup>GFP/GFP</sup> fish,  $\text{RFP}^{\text{pos}}$  cells were present at all parenchymal depths, forming clones of cells including cells located just below the NSCs layer, corresponding to recently delaminated neurons. Some  $\text{Sox2}^{\text{pos}}\text{RFP}^{\text{pos}}$  were present at the ventricular surface, but their RFP signal was weaker than the non-ventricular  $\text{RFP}^{\text{pos}}$  cells, similar to what I observed in induced larvae (data not shown). To know if this phenotype was founder-dependent, I tested F2 embryos from the EN founder and imaged the adult pallia at 4 mpf (Figure 28A-E). The overall brain morphology was similar in the two conditions, despite a lot of  $\text{PCNA}^{\text{pos}}$  cells in the control, but further analyses would be determinant. As in F2 from founder D, deep and large clones were present in the control (Figure 28B) and in the *notch3*<sup>GFP/GFP</sup> brains (Figure 28D). Most of the  $\text{RFP}^{\text{pos}}$  cells were in the brain parenchyma but some  $\text{Sox2}^{\text{pos}}\text{RFP}^{\text{pos}}$  were also present at the ventricular surface and had a weak RFP signal (Figure 28C,E). Because of this weak RFP intensity, the identification of  $\text{RFP}^{\text{pos}}$  NSCs and therefore the comparison of the number of clones still attached to the ventricular surface

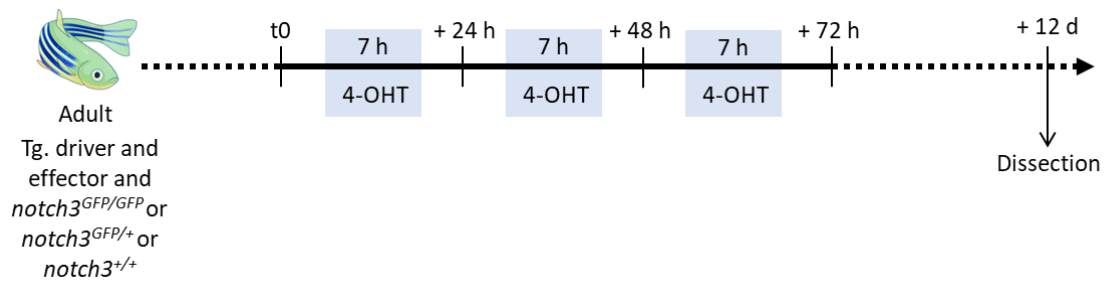
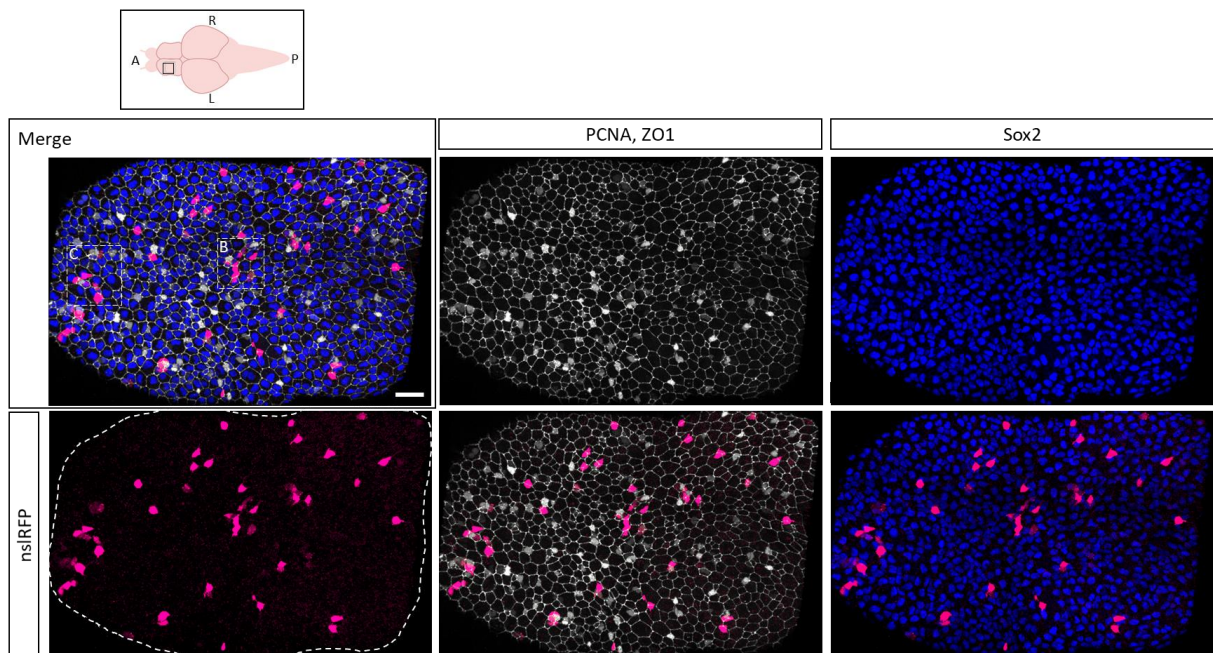
between conditions, and the analysis of the composition of the most superficial layers (accessible with optic microscopy) of the corresponding clones, is difficult.

Together, these results show that irrespective of the time of analysis (2, 3 or 4 mpf), clones generated at 24 hpf always distribute in the parenchyma until subventricular locations, and at least some include Sox2<sup>pos</sup> ventricular cells. This indicates that at least some induced NSC mothers generating these clones are still present at the ventricular surface. Indeed, if the mother NSCs had been lost, we should observe detached clones deeper into the parenchyma (Furlan et al., 2017).

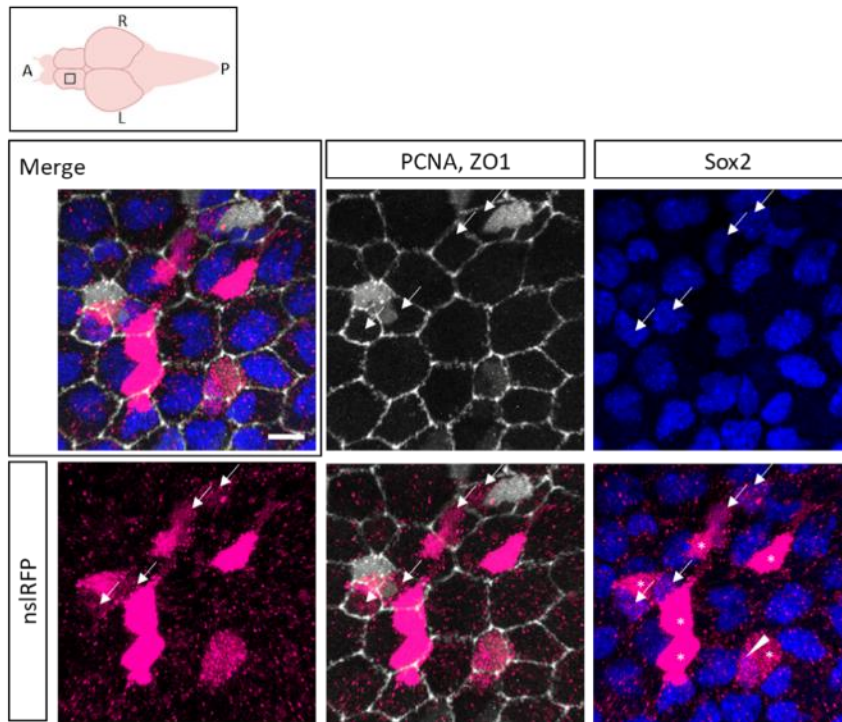
To conclude, I succeeded at inducing the expression of the degradation system and at forming clones of induced cells encompassing NSCs. As the weak RFP signal intensity appeared sufficient to sign an efficient degradation of N3ICD-GFP in larvae, the system could also be efficient in adults (this analysis is planned). However, if the system is working efficiently to induce a phenotype, whether long-term Notch3 KD in NPs/NSCs would induce a loss of NPs/NSCs (and more generally, which phenotype is triggered by long-term Notch3 KD) still needs to be assessed.

#### ***Conditional and sporadic expression of the degradation system in adults***

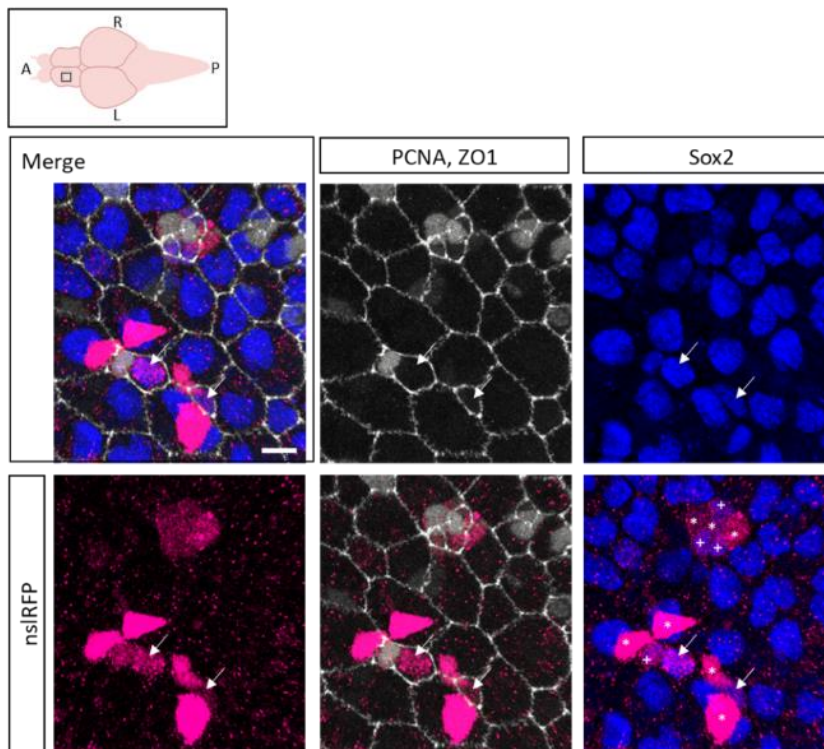
After the validation of Notch3-GFP degradation efficiency in larvae, and the possibility to express the system in adult NSCs, I aimed to study the functions of Notch3 signaling in adult NSCs. Due to the specific status of chromatin in pallial NSCs/NPs from embryo stages onwards, the recombination for the expression of the nanobody effector transgene can be challenging. I applied the 4-OHT treatment to 3-month-old adult fish to trigger the expression of the nanobody effector. To avoid 4-OHT toxicity in adult fish, I optimized the protocol by testing different concentrations and durations. I worked with F2 fish coming from different F1 from founder D, and one F2 from founder EN. The next results have been obtained in the latter background after a 4-OHT treatment applied three times for 7 hours at 5  $\mu$ M (Figure 29A).

**A****B**

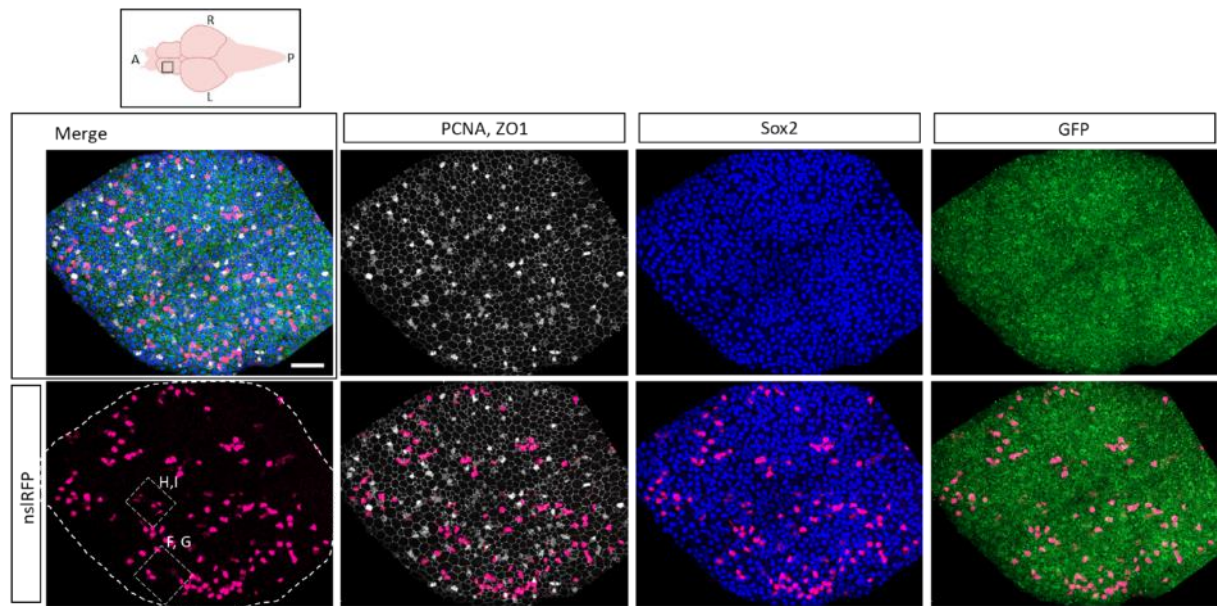
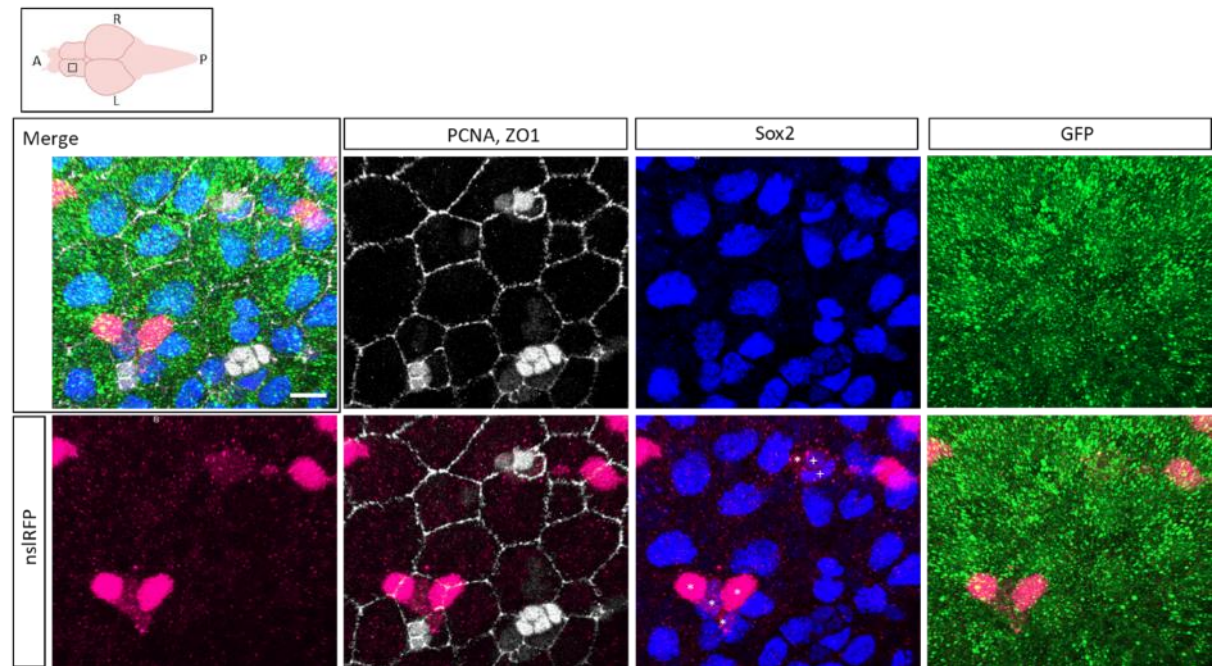
C

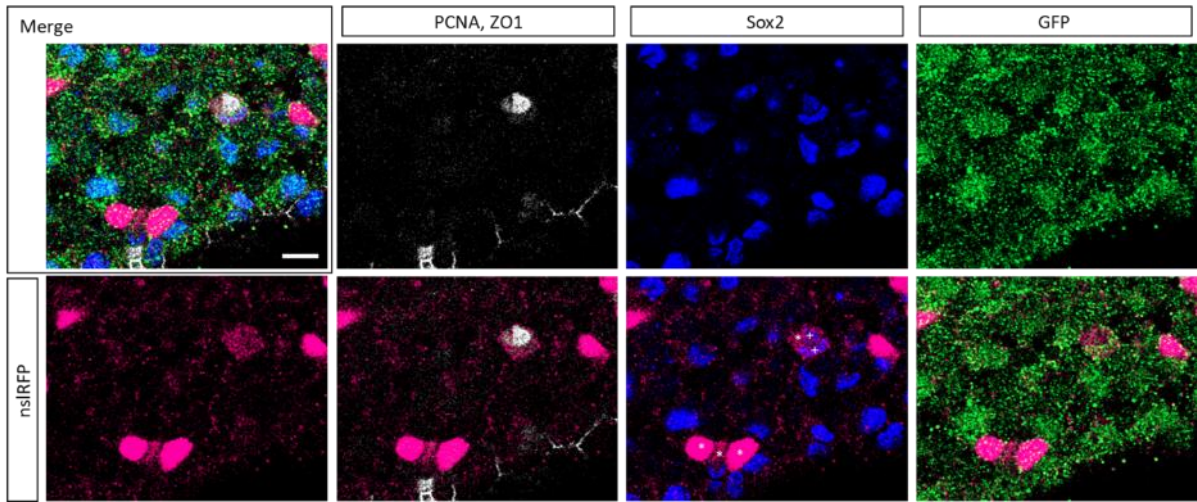
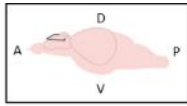
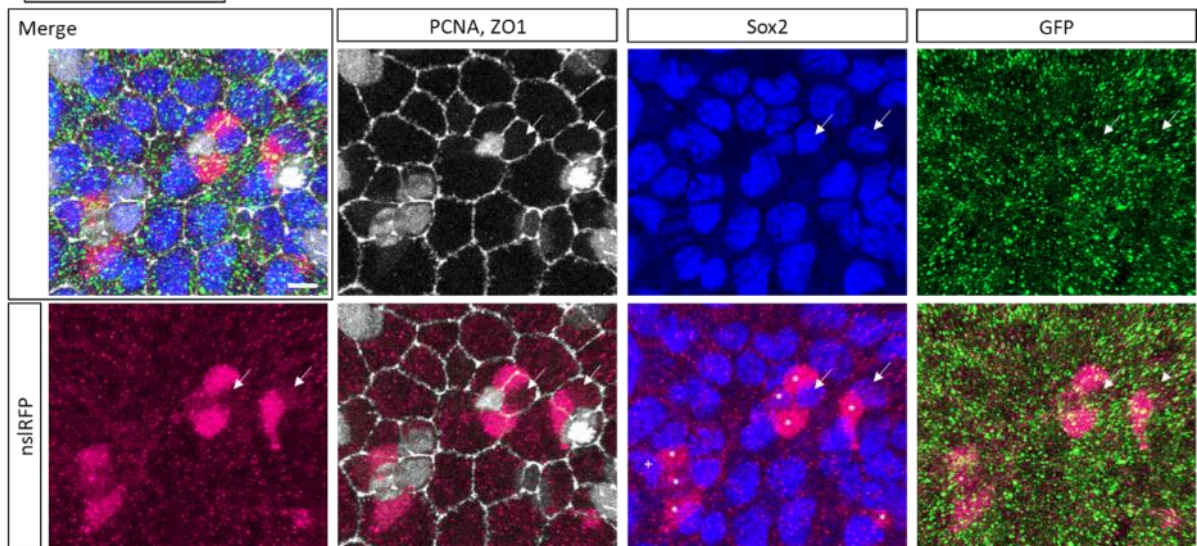
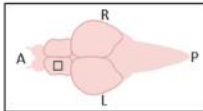


D





**E****F**

**G****H**

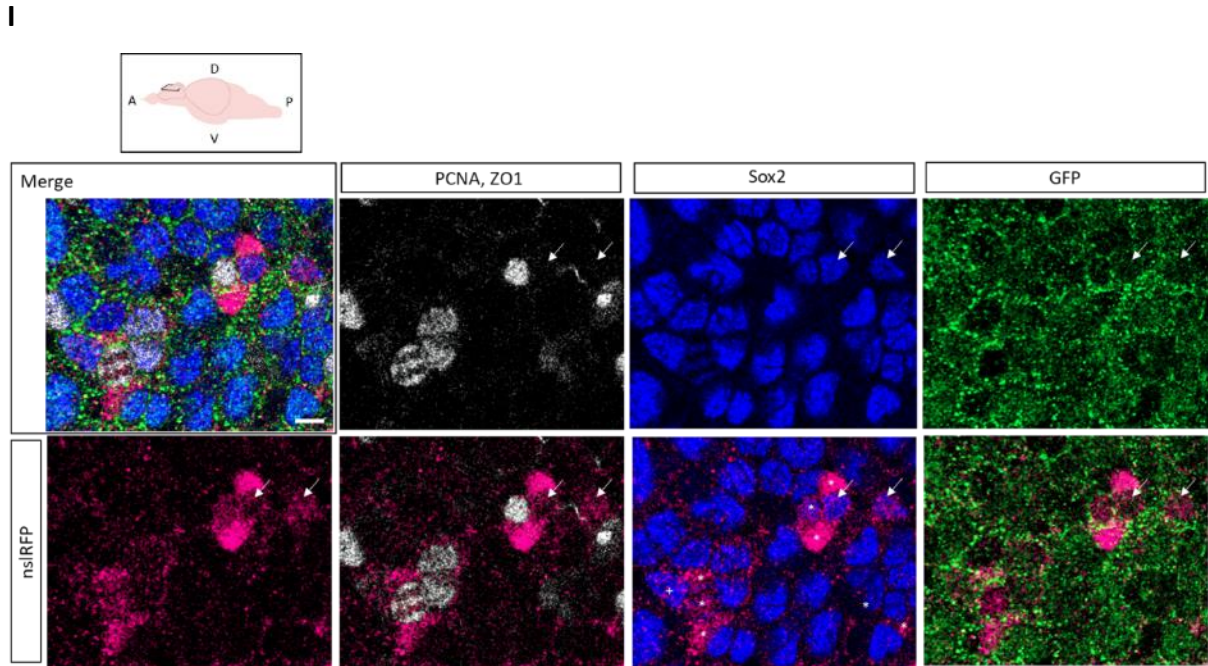


**Figure 29: Conditional and sporadic expression of the degradation system in adults**

(A) Experimental design to induce the expression of *VhhGFP4-hSPOP-nls-P2A-nlsRFP* in the adult brain with three successive 4-OHT treatments, and collect the resulting brains.

(B) Immunostaining on a resulting adult driver/nanobody effector control pallium. The picture is a Z projection over 12  $\mu\text{m}$ . The two dotted squares correspond to zooms in C and D. The scale bar represents 30  $\mu\text{m}$ .

(C,D) Zoomed pictures. The arrows point ventricular Sox2<sup>pos</sup>RFP<sup>pos</sup>PCNA<sup>neg</sup> cells, the plus (+) point ventricular Sox2<sup>pos</sup>RFP<sup>pos</sup>PCNA<sup>pos</sup> cells, and the stars (\*) point delaminated RFP<sup>pos</sup> cells. The scale bar represents 7  $\mu\text{m}$  in C and 10  $\mu\text{m}$  in D.

(E) Immunostaining on a resulting adult driver/nanobody effector and *notch3*<sup>GFP/GFP</sup> pallium. The picture is a Z projection over 14  $\mu\text{m}$ . The two dotted squares correspond to zooms in F to I. The scale bar represents 50  $\mu\text{m}$ .

(F,I) Zoomed pictures. (G,I) Horizontal optical sections of the zoomed pictures. The arrows point ventricular Sox2<sup>pos</sup>RFP<sup>pos</sup>PCNA<sup>neg</sup> cells, the plus (+) point ventricular Sox2<sup>pos</sup>RFP<sup>pos</sup>PCNA<sup>pos</sup> cells, and the stars (\*) point delaminated RFP<sup>pos</sup> cells. The scale bar represents 10  $\mu\text{m}$  in F and G, and 7  $\mu\text{m}$  in H and I.

The brains of the treated fish (n= 3 for control and *notch3*<sup>GFP/GFP</sup>) were analyzed 9 days after the treatment and all the dorsal regions of the pallium were screened for RFP<sup>pos</sup> cells (Figure 29B-I). The screened pallia had many induced cells, with some cells regrouping and forming clones (Figure 29B,E). In agreement with my previous results, the cells with the higher RFP signal were in the parenchyma, while the ventricular RFP<sup>pos</sup> cells had a weaker RFP signal. Focusing on clones, I identified some Sox2<sup>pos</sup>RFP<sup>pos</sup> cells in control and *notch3*<sup>GFP/GFP</sup> brains (Figure 29C,D,F-I). Some isolated Sox2<sup>pos</sup>RFP<sup>pos</sup> cells were also present (Figure 29B,E).

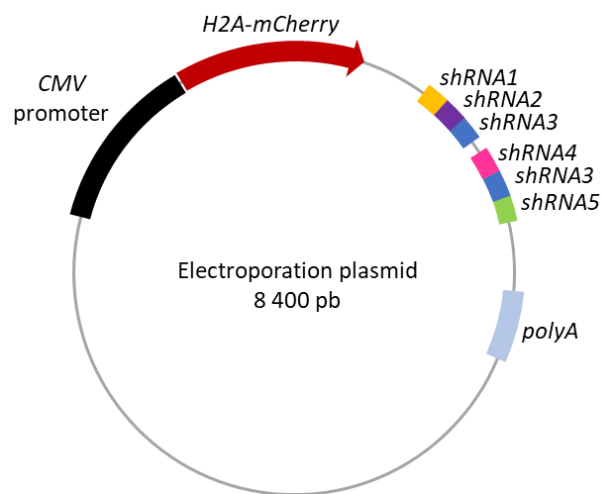
To conclude, I improved the induction efficiency in adult NSCs and I obtained clones of cells after 12 days of chase. Next, focusing on Sox2<sup>pos</sup>RFP<sup>pos</sup> cells in the induced *notch3*<sup>GFP/GFP</sup> brain, I will quantify the amount of nuclear N3ICD-GFP to validate the degradation efficiency in adult NSCs. After this validation, I will do the phenotypical analysis to test my hypotheses (see Introduction part 5.5, Hypotheses). However, together with the other results, the weak

expression of the transgene in NPs/NSCs could limit the degradation, and prevent the appearance of phenotypes.

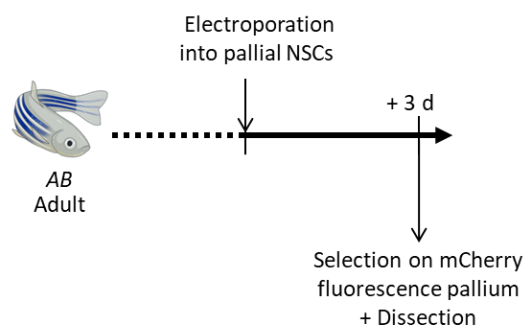
### *Conditional and sporadic loss of notch3 mRNA in adults*

To study Notch3 signaling functions in the adult NSCs, I also adapted to the study of *notch3* function an electroporation-mediated shRNA silencing method very recently set-up in the lab following the publication by J. Giacomotto (Giacomotto et al., 2015; Labusch et al., 2024). I built a plasmid containing five different shRNAs against the *notch3* 3'UTR region, transcribed under the control of the Human cytomegalovirus immediate early promoter (*CMV*), which also drives the expression of the *H2A-mCherry* sequence (Figure 30A). The histone H2A is one of the five main histone proteins involved in the structure of chromatin in eukaryotic cells. In our plasmid, *H2A*, fused to the mCherry fluorescent marker, is stably incorporated into the chromatin, allowing the selection of the electroporated cells and medium-term tracking.

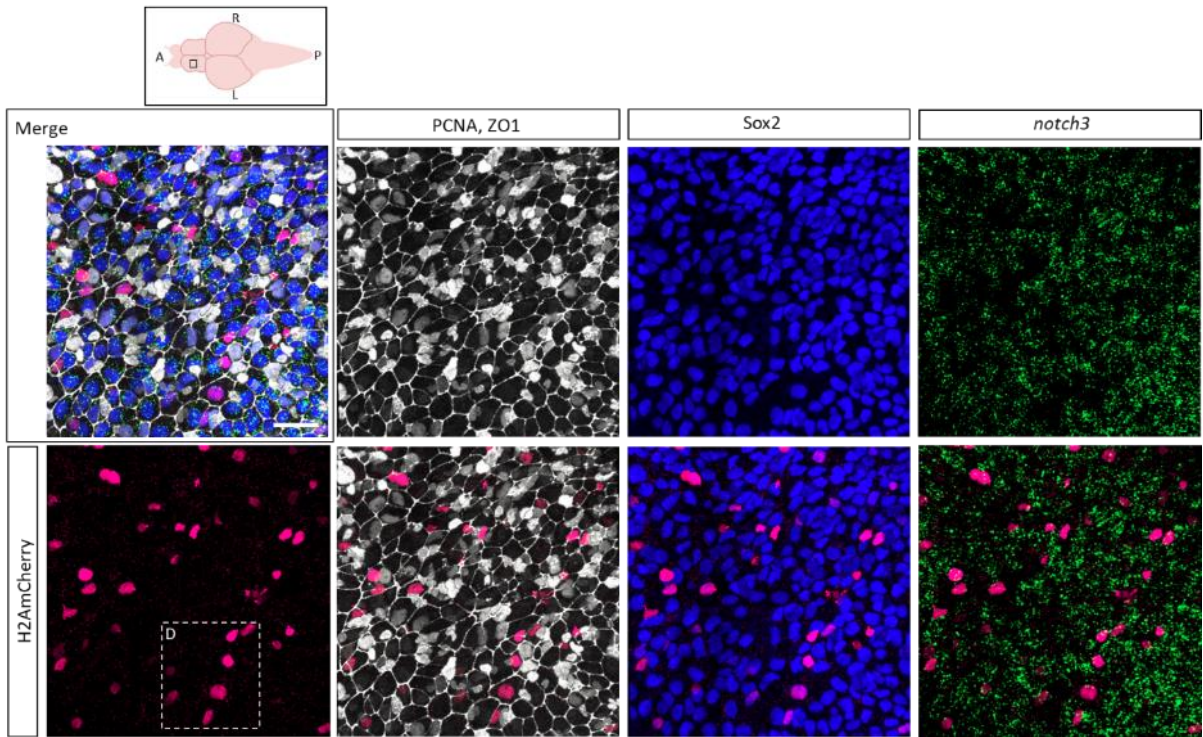
**A**



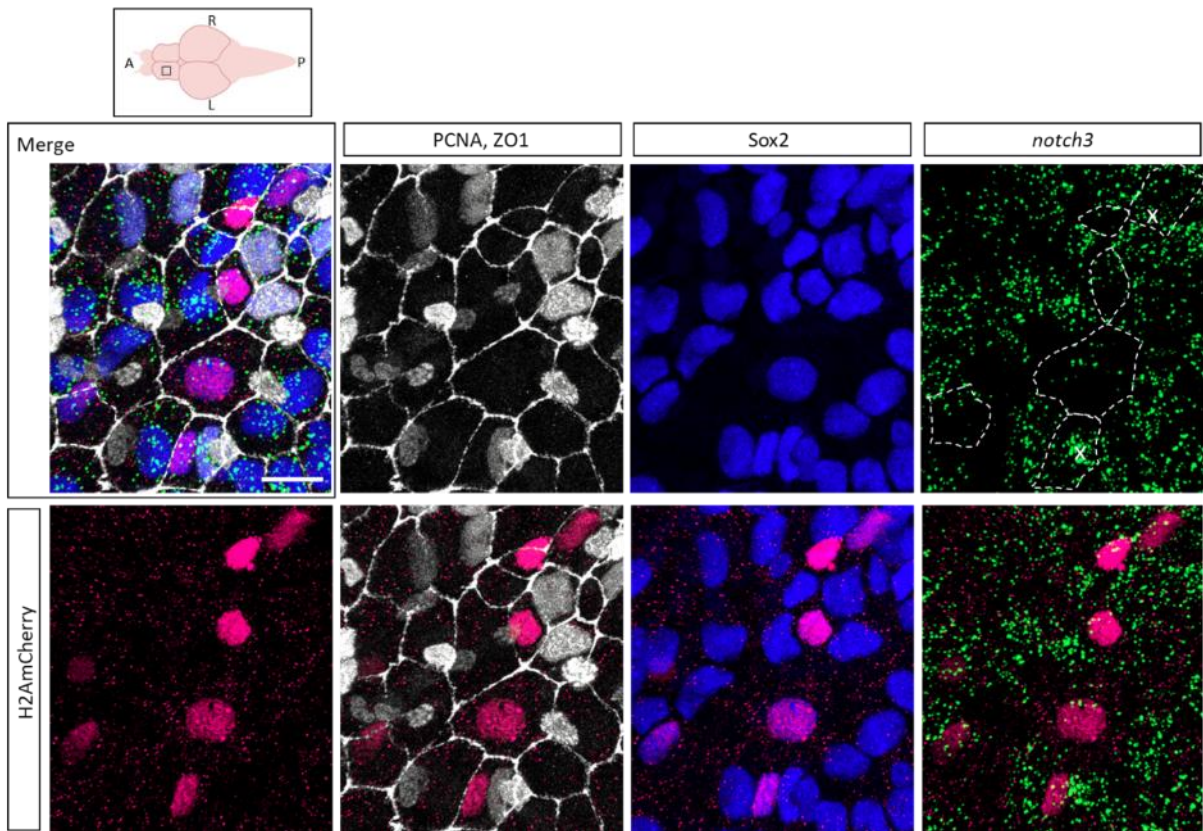
**B**



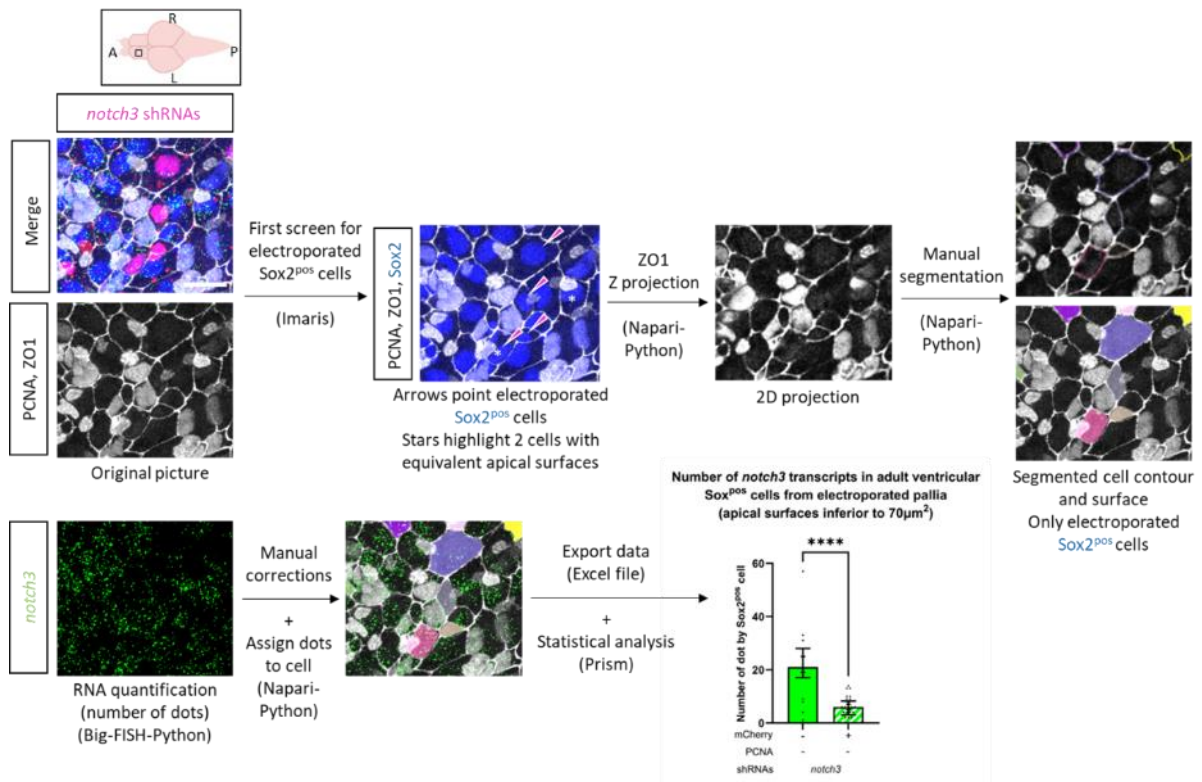
C



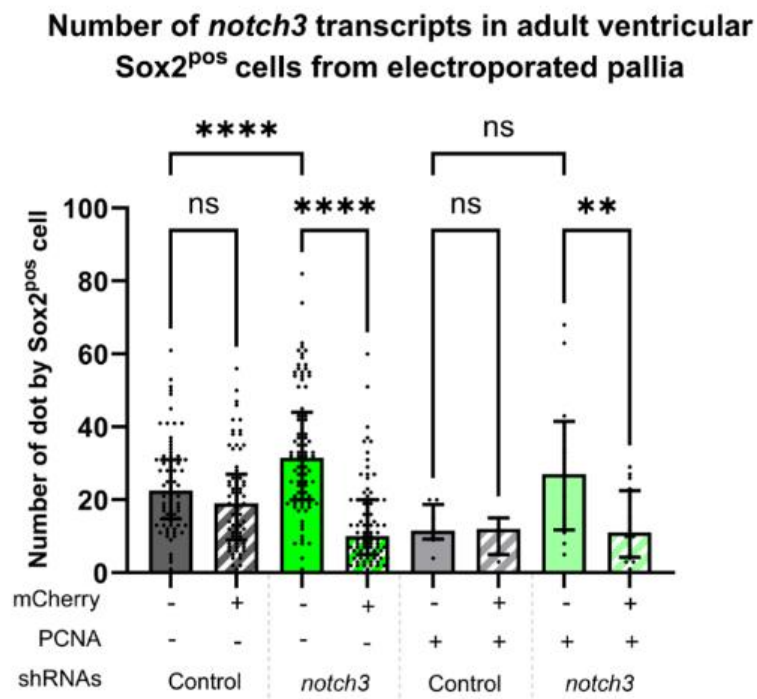
D



**E**

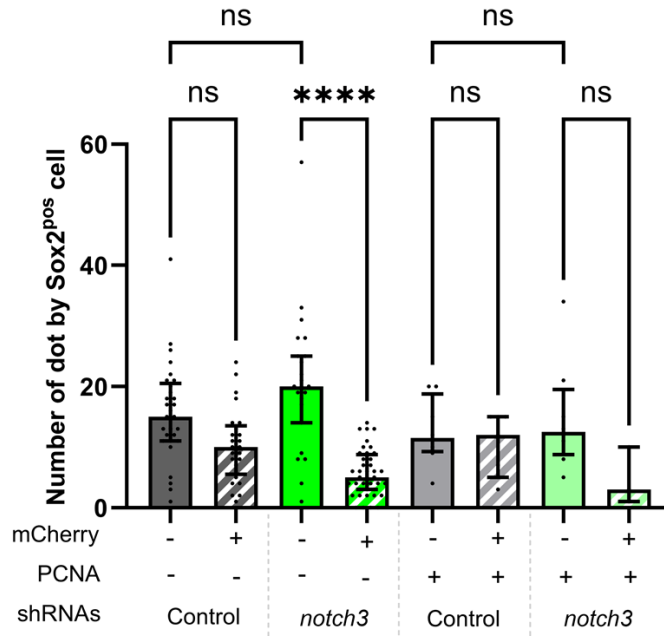


**F**



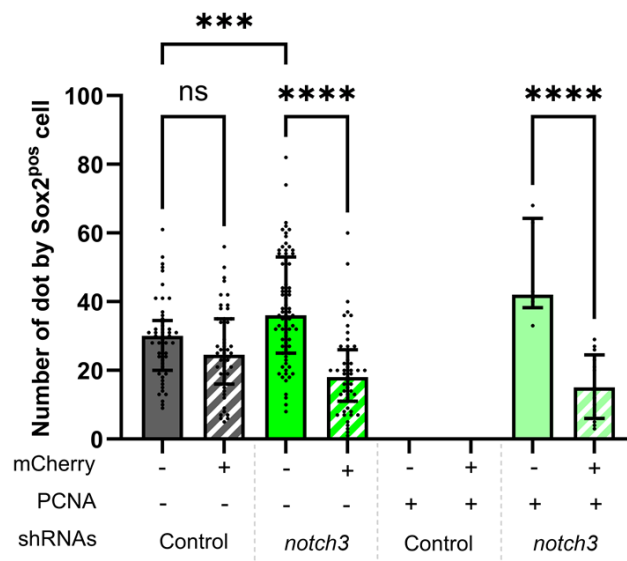
G

Number of *notch3* transcripts in adult ventricular Sox2<sup>pos</sup> cells from electroporated pallia (apical surfaces inferior to 70μm<sup>2</sup>)



H

Number of *notch3* transcripts in adult ventricular Sox2<sup>pos</sup> cells from electroporated pallia (apical surfaces superior to 70μm<sup>2</sup>)



**Percentage of proliferating cells among electroporated ventricular Sox2<sup>pos</sup> cells**

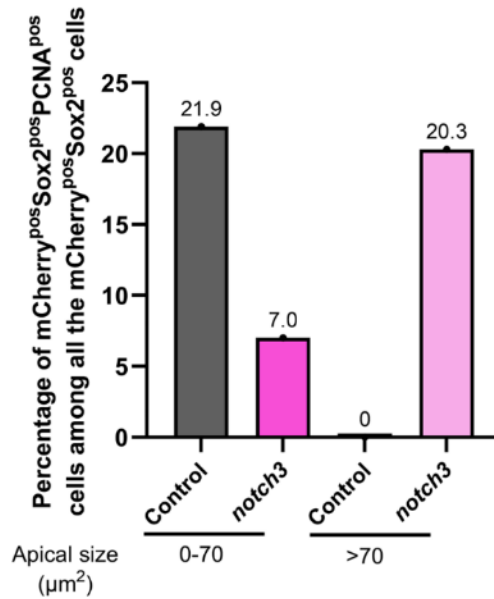


**Figure 30: Conditional and sporadic loss of *notch3* mRNA in adults**

(A) Schematic illustration of the electroporation plasmid.

(B) Experimental design to electroporate adult brains, and selection.

(C) *notch3* RNAscope smFISH and immunostaining on an AB fish. The picture is a Z projection over 16 μm. The dotted scare corresponds to zoom D. The scale bar represents 30 μm.

(D) Zoomed picture. The dotted lines correspond to contours of mCherry<sup>pos</sup>Sox2<sup>pos</sup>PCNA<sup>neg</sup> cell apical surfaces. The two crosses correspond to areas of the selected cells where RNAscope dots belong to neighboring cells. These dots are manually corrected during the analysis process. The scale bar represents 15 μm.

(E) Pipeline for quantification of the number of RNAscope dots in electroporated and non-electroporated Sox2<sup>pos</sup> cells. Along the process, Imaris, Napari-Python, Big-FISH-Python, and Prism are used. The first picture is a Z projection over 16 μm. The scale bar represents 20 μm. Mann Whitney test, \*\*\*\* p<0.0001. Data from one brain electroporated with *notch3* shRNAs. Number of cells: mCherry<sup>neg</sup> n= 19, mCherry<sup>pos</sup> n= 30.

(F) Number of *notch3* transcripts in adult ventricular Sox2<sup>pos</sup> cells from AB fish electroporated pallia. Data from two brains are pooled in the two conditions (control and *notch3* shRNAs). Each dot is one cell. Bar at median and bracket for interquartile range. Two way ANOVA, Sidak's multiple comparison test, \*\*\*\* p<0.0001 (mCherry<sup>neg</sup>PCNA<sup>neg</sup> cells vs. mCherry<sup>pos</sup>PCNA<sup>neg</sup> cells in the *notch3* shRNAs condition and mCherry<sup>neg</sup>PCNA<sup>neg</sup> cells in the control condition vs. in the *notch3* shRNAs condition), p= 0.0022 (mCherry<sup>neg</sup>PCNA<sup>pos</sup> cells vs. mCherry<sup>neg</sup>PCNA<sup>pos</sup> cells in the *notch3* shRNAs condition), p= 0.2732 (mCherry<sup>neg</sup>PCNA<sup>neg</sup> cells vs. mCherry<sup>pos</sup>PCNA<sup>neg</sup> cells in the control condition), p= 0.9998 (mCherry<sup>neg</sup>PCNA<sup>pos</sup> cells vs. mCherry<sup>pos</sup>PCNA<sup>pos</sup> cells in the control condition), p= 0.0809 (mCherry<sup>neg</sup>PCNA<sup>pos</sup> cells in the control condition vs. in the *notch3* shRNAs condition). Number of cells from the brains electroporated with *notch3* shRNAs: mCherry<sup>neg</sup>PCNA<sup>neg</sup> n= 94, mCherry<sup>pos</sup>PCNA<sup>neg</sup> n=91, mCherry<sup>neg</sup>PCNA<sup>pos</sup> n= 14, mCherry<sup>pos</sup>PCNA<sup>pos</sup> n= 16; from the control brains: mCherry<sup>neg</sup>PCNA<sup>neg</sup> n= 78, mCherry<sup>pos</sup>PCNA<sup>neg</sup> n=75, mCherry<sup>neg</sup>PCNA<sup>pos</sup> n= 8, mCherry<sup>pos</sup>PCNA<sup>pos</sup> n= 7.

(G) Number of *notch3* transcripts in adult ventricular Sox2<sup>pos</sup> cells from AB fish electroporated pallia (apical surfaces inferior to 70 μm<sup>2</sup>). Data from two brains are pooled in the two conditions (control and *notch3* shRNAs). Each dot is one cell. Bar at median and bracket for interquartile range. Two way ANOVA, Sidak's multiple comparison test, \*\*\*\* p<0.0001 (mCherry<sup>neg</sup>PCNA<sup>neg</sup> cells vs. mCherry<sup>pos</sup>PCNA<sup>neg</sup> cells in the *notch3* shRNAs condition), ns, not significant p= 0.0711 (mCherry<sup>neg</sup>PCNA<sup>neg</sup> cells vs. mCherry<sup>pos</sup>PCNA<sup>neg</sup> cells in the control condition), p= 0.0741 (mCherry<sup>neg</sup>PCNA<sup>neg</sup> cells in the control condition vs. the *notch3* shRNAs condition), p= 0.9981 (mCherry<sup>neg</sup>PCNA<sup>pos</sup> cells vs. mCherry<sup>pos</sup>PCNA<sup>pos</sup> cells in the control condition), p= 0.6855 (mCherry<sup>neg</sup>PCNA<sup>pos</sup> cells vs. mCherry<sup>pos</sup>PCNA<sup>pos</sup> cells in the *notch3* shRNAs condition), p= 0.9884 (mCherry<sup>neg</sup>PCNA<sup>pos</sup> cells in the control condition vs. the *notch3* shRNAs condition). Number of cells from the brains electroporated with *notch3* shRNAs: mCherry<sup>neg</sup>PCNA<sup>neg</sup> n= 23, mCherry<sup>pos</sup>PCNA<sup>neg</sup> n=40,



mCherry<sup>neg</sup>PCNA<sup>pos</sup> n= 8, mCherry<sup>neg</sup>PCNA<sup>pos</sup> n= 3; from the control brains: mCherry<sup>neg</sup>PCNA<sup>neg</sup> n= 29, mCherry<sup>pos</sup>PCNA<sup>neg</sup> n=25, mCherry<sup>neg</sup>PCNA<sup>pos</sup> n= 8, mCherry<sup>neg</sup>PCNA<sup>pos</sup> n= 7.

(H) Number of *notch3* transcripts in adult ventricular Sox2<sup>pos</sup> cells from AB fish electroporated pallia (apical surfaces superior to 70  $\mu\text{m}^2$ ). Data from two brains are pooled in the two conditions (control and *notch3* shRNAs). Each dot is one cell. Bar at median and bracket for interquartile range. Two way ANOVA, Sidak's multiple comparison test, \*\*\*\* p<0.0001 (mCherry<sup>neg</sup>PCNA<sup>neg</sup> cells vs. mCherry<sup>pos</sup>PCNA<sup>neg</sup> cells and mCherry<sup>neg</sup>PCNA<sup>pos</sup> cells vs. mCherry<sup>pos</sup>PCNA<sup>pos</sup> cells in the *notch3* shRNAs condition), p= 0.3683 (mCherry<sup>neg</sup>PCNA<sup>neg</sup> cells vs. mCherry<sup>pos</sup>PCNA<sup>neg</sup> cells in the control condition), p= 0.0002 (mCherry<sup>neg</sup>PCNA<sup>neg</sup> cells in the control condition vs. the *notch3* shRNAs condition). No cells are mCherry<sup>neg</sup>PCNA<sup>pos</sup> or mCherry<sup>pos</sup>PCNA<sup>pos</sup> in the control condition. Number of cells from the brains electroporated with *notch3* shRNAs: mCherry<sup>neg</sup>PCNA<sup>neg</sup> n= 71, mCherry<sup>pos</sup>PCNA<sup>neg</sup> n=51, mCherry<sup>neg</sup>PCNA<sup>pos</sup> n= 6, mCherry<sup>pos</sup>PCNA<sup>pos</sup> n= 13; from the control brains: mCherry<sup>neg</sup>PCNA<sup>neg</sup> n= 49, mCherry<sup>pos</sup>PCNA<sup>neg</sup> n=50.

(I) Percentage of proliferating cells among electroporated ventricular Sox2<sup>pos</sup> cells. Number of cells with apical surfaces between 0-70: control n= 32, *notch3* shRNAs n= 43; with apical surfaces >70: control n= 50, *notch3* shRNAs n= 64.

To validate the efficiency of the *notch3* shRNAs, adult AB fish were electroporated with the *notch3* shRNAs plasmid or with a control plasmid (directed against *GFP*), and were dissected at 3 dpe (Figure 30B). The pallia presenting a mCherry signal were selected at the fluorescence binocular and fixed for subsequent analyses. The efficiency of the electroporation, defined as the number of electroporated cells, was very variable from brain to brain. Selected brains were processed for an RNAscope single-molecule fluorescence *in situ* hybridization (smFISH) against *notch3*, to quantify *notch3* expression, and immunostained for mCherry for the identification of the electroporated cells, for ZO1 for the segmentation of the apical surfaces of the ventricular cells, and for Sox2 and PCNA, to identify the Sox2<sup>pos</sup> ventricular cells and their proliferative status (Figure 30C,D). The electroporated cells had variable nuclear sizes and mCherry signal intensities but were easily identified (Figure 30C). The *notch3* signal was widespread in the ventricular cells yet heterogeneous (Figure 30C). Moreover, the number of PCNA<sup>pos</sup> cells was increased in *notch3* shRNAs electroporated pallia similarly to in control pallia, suggesting that this effect was a consequence of the manipulation and not the activity of the *notch3* shRNAs (not quantified). Focusing on ventricular Sox2<sup>pos</sup> cells, the number of RNAscope dots, corresponding to *notch3* mRNA molecules, was variable between cells, but in mCherry<sup>pos</sup>Sox2<sup>pos</sup>, the tendency was less *notch3* dots than in the non-electroporated ventricular Sox2<sup>pos</sup> cells (Figure 30D). The sizes of the apical surface of ventricular Sox2<sup>pos</sup> cells were variable (Figure 30D).

To quantify the *notch3* signal in Sox2<sup>pos</sup> cells, I processed the pallia pictures by segmenting the apical surface of the cells using the ZO1 signal, and assigning the RNAscope dots to the apical surface of their cell of origin (Figure 30E). I compared the number of dots in electroporated and non-electroporated cells (in the same pallial region but not in direct contact) (Figure 30F).

Moreover, less *notch3* signal is expected in PCNA<sup>pos</sup> cells, therefore we also added PCNA expression to the analysis. Ventricular PCNA<sup>pos</sup>Sox2<sup>pos</sup> represent a minority of Sox2<sup>pos</sup> cells, and therefore their number is also limited in the analysis. The number of *notch3* transcripts after the electroporation of *notch3* shRNAs, both in PCNA<sup>neg</sup> and PCNA<sup>pos</sup> cells, was decreased (Figure 30F). Previous studies showed that pallial ventricular cells with big apical surfaces correspond to qNSCs, which by definition, have higher Notch signaling activity (measuring Notch3 activity in big versus small cells using the Notch3-GFP line will be done). Their apical surfaces were around 70  $\mu\text{m}^2$  or superior, while the apical surfaces of aNSCs and IPs were inferior (Mancini et al., 2023). Therefore, I created two categories: apical surfaces inferior to 70  $\mu\text{m}^2$  or superior. For cells with apical surfaces inferior to 70  $\mu\text{m}^2$ , the only significant difference was in *notch3* shRNAs electroporated PCNA<sup>neg</sup> cells compared to non-electroporated PCNA<sup>neg</sup> cells (Figure 30G). In bigger cells, the results were significant in *notch3* shRNAs electroporated PCNA<sup>neg</sup> and PCNA<sup>pos</sup> cells (Figure 30H). Together, these results validate the efficiency of the *notch3* shRNAs.

To analyze whether a phenotype is induced by *notch3* shRNAs, I counted the percentage of proliferating ventricular mCherry<sup>pos</sup>Sox<sup>pos</sup> cells (Figure 30I). To not include IPs, that do not express *notch3*, I looked at cells with an apical surface superior to 70  $\mu\text{m}^2$ , where I expected more proliferation if electroporated with *notch3* shRNAs. These cells were all quiescent in the control, but in the presence of *notch3* shRNAs, 20.3% were proliferative (Figure 30I). In contrast, among the cells with an apical surface inferior to 70  $\mu\text{m}^2$ , fewer cells were proliferative in the presence of *notch3* shRNAs (Figure 30I). The result obtained in big cells confirmed Notch3 function as a quiescence-promoting factor.

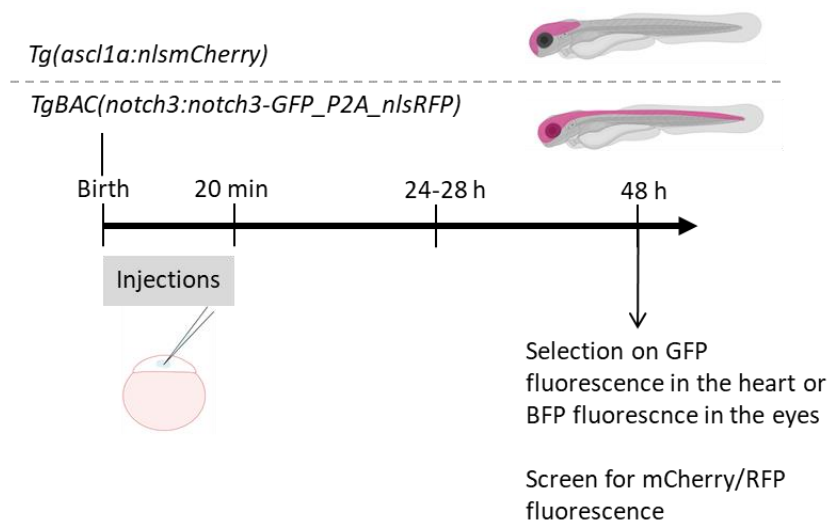
To conclude, I validated the *notch3* shRNAs efficiency and observed a phenotype in pallial Sox<sup>pos</sup> cells as early as three days after the electroporation. To reinforce these results, I will replicate the experiment.

## Supplementary Figures

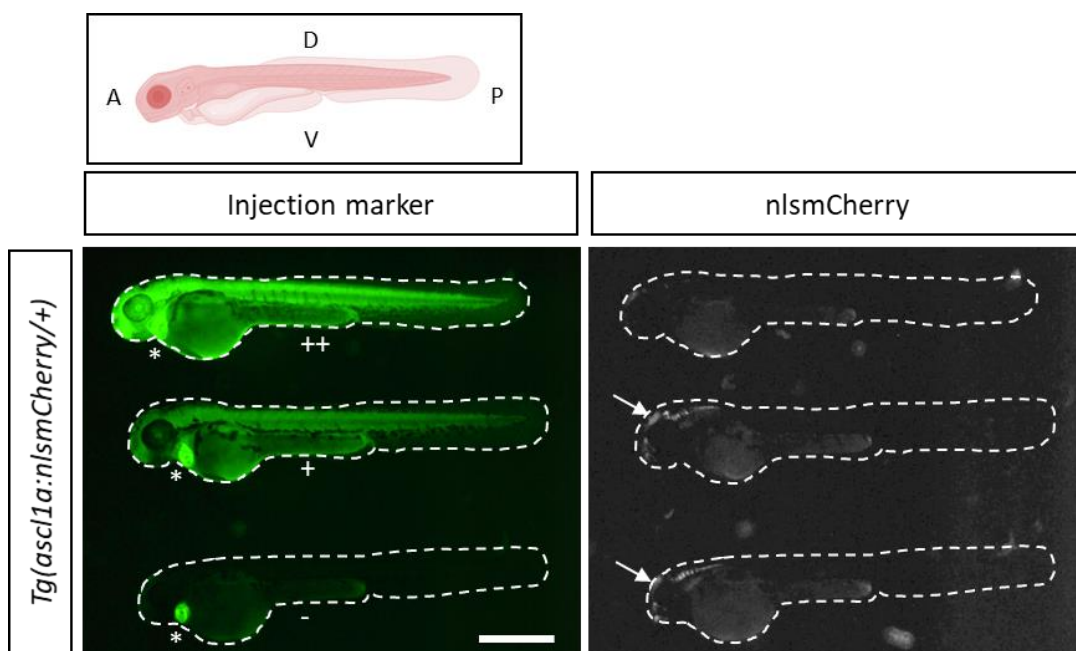
### *Validation of anti-RFP/mCherry nanobodies targeted to the nucleus for the selective degradation of nuclear RFP/mCherry protein in zebrafish embryos*

To enlarge our nanobody toolbox for future experiments, I also tested the RFP- and mCherry-specific nanobody LaM3 (Shin et al., unpublished) fused to hSPOPdelnls, by capped mRNA injections into one-cell stage transgenic embryos. The aim was to validate its functionality on nuclear proteins for the first time in zebrafish.

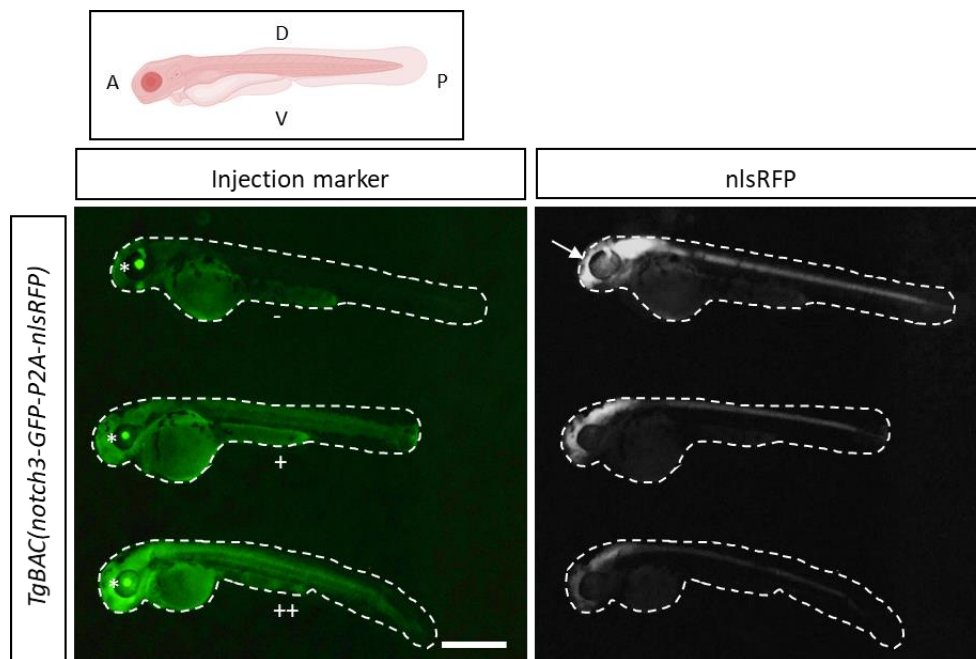
**A**



**B**



C



D

Test degradation	Transgenic line	Transgenics selection	Age for screen (hpf)	Control not injected, no red	Total injected	Injected, red	Injected, no/less red
<b>LaM3-hSPOPdelnls</b>							
nlsMCherry	<i>Tg(ascl1a:nlsMcherry)</i>	Green heart	48	52%	172	47	125 (73%)
nlsRFP	<i>TgBAC(notch3:notch3-GFP-P2A-nlsRFP)</i>	Blue eyes	48	50%	75	4	71 (95%)

**Figure S1: LaM3-hSPOPdelnls mediates degradation of nuclear mCherry and RFP in embryos**

(A) Experimental design to test the nanobody LaM3-hSPOPdelnls. *5'-cap\_LaM3-hSPOPdelnls* mRNA is injected with *5'-cap\_GFP* mRNA (injection marker) in embryos coming from crossings between AB and *Tg(ascl1a:nlsMCherry)* to test nuclear mCherry degradation, and AB and *TgBAC(notch3:notch3-GFP\_P2A\_nlsRFP)* to test nuclear RFP degradation.

(B) *Tg(ascl1a:nlsMCherry)* 48 hpf embryos injected (+++,+) or not injected (-) with *5'-cap\_LaM3-hSPOPdelnls*. The stars highlight the transgenic line selection marker: GFP fluorescence in the heart. The arrows point the mCherry fluorescence in the brain of low injected (+) and not injected embryos. The scale bar represents 500  $\mu$ m.

(C) *TgBAC(notch3:notch3-GFP\_P2A\_nlsRFP)* 48 hpf embryos injected (+++,+) or not injected (-) with *5'-cap\_LaM3-hSPOPdelnls*. The stars highlight the transgenic line selection marker: BFP fluorescence in the eyes (also visible in green). The arrow points the RFP fluorescence in the central nervous system in the absence of degradation. The scale bar represents 500  $\mu$ m.

(D) Results of the fluorescent screens at 48 hpf.

*Tg(ascl1:nlsMCherry)* (I. Foucher, unpub.) embryos from a cross between heterozygous parents and wildtype fish were injected and screened at 48 hpf (at 24 hpf, the nlsMCherry signal was too weak to separate the positive mCherry embryos from the others) (Figure S1A,B). In this fish line, *nlsMCherry* is expressed in the nucleus of NPs expressing the proneural gene *ascl1*, which is important for the regulation of neurogenesis and promotes progenitor proliferation, specification, and differentiation into neurons (Andersen et al., 2014). The percentage of nlsMCherry<sup>neg</sup> embryos was 73% in the injected clutch, against 52% in the non-injected clutch (Figure S1D). These results validate the capacity of LaM3-hSPOPdelnls to degrade

nlsmCherry, although at low efficiency. Different injection doses were also tested to identify the dose at which LaM3-hSPOPdelnls was the most efficient for the degradation of mCherry (Figure S1B). A dose effect was highlighted: with less capped mRNA injected, protein degradation was lower.

Next, to test the functionality of LaM3-hSPOPdelnls on nuclear RFP, *TgBAC(notch3:notch3-GFP-P2A-nlsRFP)* embryos were injected (Figure S1A,C). Because mCherry and RFP proteins are more than 90% identical, I expected the same efficiency of degradation. After unsuccessful injection assays of *LaM3-hSPOPdelnls* into embryos where no degradation activity was observed, it is only at double dose of capped mRNA that I obtained 95% of BAC-injected embryos that displayed, upon visual inspection, less nlsRFP signal than non-injected control embryos (figure S1D).

*ascl1* and *notch3* promoter activities are different in levels of expression and in number of expressing cells. The level of expression of mCherry being weaker than RFP (Figure S1B,C), I was not able to conclude on the difference of mCherry or RFP degradation efficiency by LaM3-hSPOPdelnls, but conclude that LaM3-hSPOPdelnls can degrade both mCherry and RFP nuclear proteins.

These results validated the efficient activity of LaM3-hSPOPdelnls for the degradation of mCherry and RFP nuclear proteins, and opened the possibility of studying proteins tagged not only with GFP, but also with mCherry and RFP.

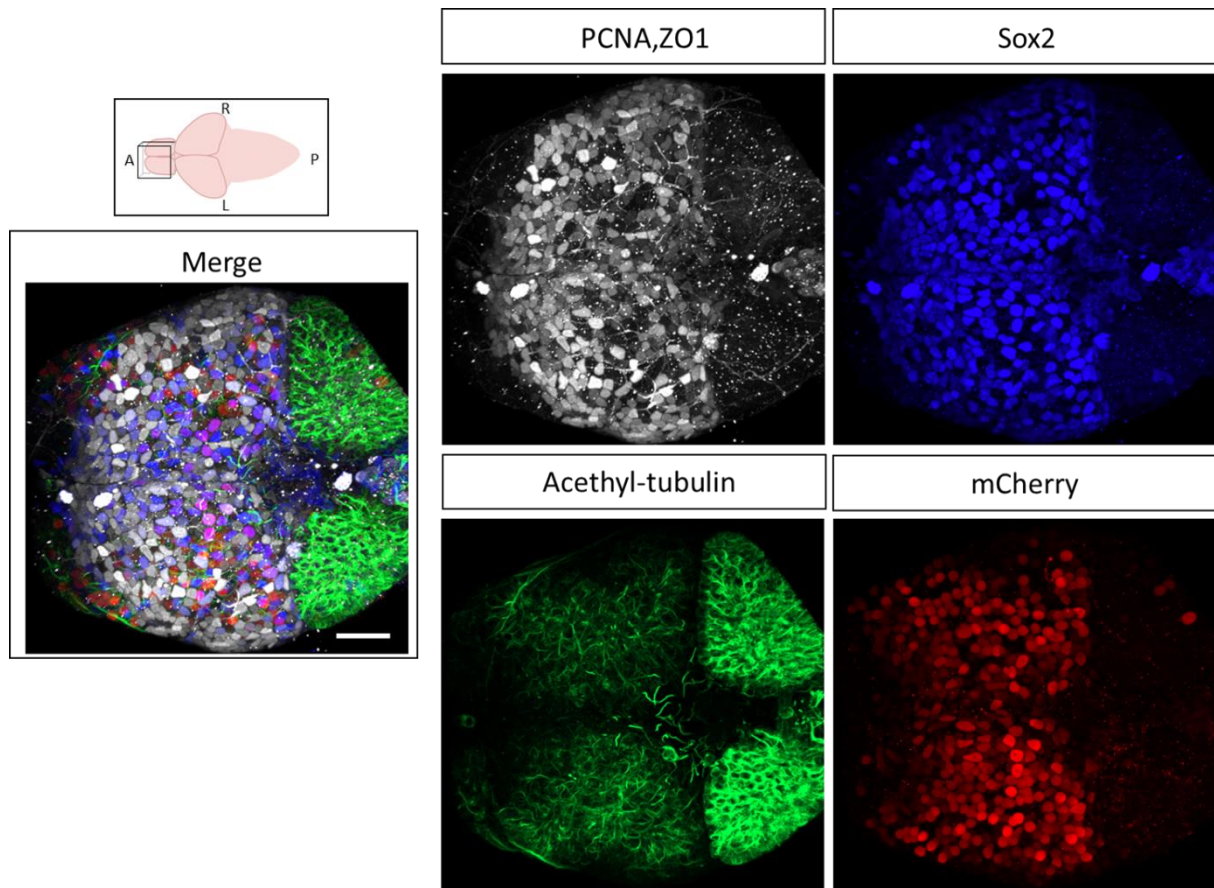


**Figure S2: Expression of *Hmgb1-mCherry* upon *loxP-stop-loxP* recombination**

*Tg(her4:ERT2CreERT2)* fish were crossed with *Tg(bact2:loxP-stop-loxP-hmgb1-mCherry)*. After dechoriation, at 24 hpf, the embryos were treated with 4-OHT for 12 h. At 72 hpf, larvae were selected on the presence of mCherry fluorescence. The larvae were dissected at 6 dpf and immunostained for PCNA, ZO1, Sox2, mCherry and the neuronal marker acetyl-tubulin. The scale bar represents 10  $\mu$ m.

# Materials and Methods

## *Zebrafish husbandry and strains*

All procedures for zebrafish (*Danio rerio*) care and treatment were conducted following the directive 2010/63/EU of the European Parliament and were approved by the CETEA (Pasteur Institute Ethics Committee). Adult fish were maintained in 27.8°C water at pH 7.5 and fed 3 times by day with GEMMA Micro (Skretting). Juveniles until 6 days were maintained in E3 embryo medium at 28°C. All fish were kept on a 14-hour light/10-hour dark cycle.

The fish lines used in this study were AB, *casper* (White et al., 2008), *Tg(gfap:nlsGFP)* (Bernardos et al., 2007), *Tg(gfap:GFP)* (Bernardos and Raymond, 2006), *Tg(deltaA:GFP)* (Christie et al., 2006), *Tg(ascl1a:nlsmCherry)* (Bally-Cuif, unpublished), *TgBAC(miR9-6:nlsGFP-P2A-mCherry-PEST-CG2)* (Bally-Cuif, unpublished), *TgBAC(notch3:notch3-GFP\_P2A\_nlsRFP)* (Ortica et al., in prep.), *Tg(her4.1:ERT2CreERT2)* (Boniface et al., 2009), *Tg(bact2:loxP-stop-loxP-hmgb1-mCherry)* (Wang et al., 2011), *Tg(bact2:loxP-stop-loxP-VhhGFP4-hSPOP-nls-P2A-nlsRFP)* (this study), *notch3<sup>GFP/GFP</sup>* (this study). Combined transgenic/KI lines were generated by crossing.

## *Generation of pXT7\_Nfbxw11b-VhhGFP4*

The *Nfbxw11b-VhhGFP4* sequence (also called *zGrad*) was amplified by PCR from *pDestTol2-hsp70l-zGrad-IRES-H2A-TagBFP* (Yamaguchi et al., 2019) with the following primers, designed to introduce KpnI and BglII restriction sites (underlined):

KpnI\_fwd: 5'- GATCGGTACCATGGAGACGGAGATGGAGGAC -3'

rev\_BglII: 5'- GATCAGATCTTTAGCTGGAGACGGTGACCTG -3'

The PCR product was cloned into pXT7 after digestion by KpnI and BglII and ligation using InstantStickyEnds (NEB).

## *Capped mRNA for embryonic microinjections*

The capped mRNAs were transcribed with mMACHINE<sup>®</sup> (ThermoFisher) according to Table 1. 1 nl of a mix containing nanobody capped mRNA at 100 ng/μl and the injection markers capped mRNA (*GFP* or *kusabira orange*) at 10 ng/μl was injected into one-cell stage embryos from crosses between transgenic and AB or *casper* fish. Non-injected embryos were kept as negative control.

**Table 1: Capped mRNA for embryonic microinjections**

mRNA for microinjections	Origin plasmid	Lab of origin	Linearization	Polymerase
<i>GFP</i>	pCS2_GFP	Charles River	XbaI (FastDigest, ThermoFisher)	SP6
<i>kusabira-orange</i>	pXT7_sgGFP1-P2A-kusabira-orange-pA	Laure Bally-Cuif	NdeI (Promega)	T7
<i>VhhGFP4-hSPOpdeINLS</i>	pCS2_Flag-VhhGFP4-hSPOpdeINLS	Byungjoon Hwang	NotI (FastDigest, ThermoFisher)	SP6
<i>VhhGFP4mut-hSPOpdeINLS</i>	pCS2_Flag-VhhGFP4mut-hSPOpdeINLS	Byungjoon Hwang	NotI (FastDigest, ThermoFisher)	SP6
<i>VhhGFP4-hSPOPnLS</i>	pCS2_Flag-VhhGFP4-hSPOPnLS	Byungjoon Hwang	NotI (FastDigest, ThermoFisher)	SP6
<i>Nfbxw11b-VhhGFP4</i>	pXT7_Nfbxw11b-VhhGFP4	Laure Bally-Cuif	XbaI (FastDigest, ThermoFisher)	T7
<i>LaM3-hSPOpdeINLS</i>	pCS2_Flag-LaM3-hSPOpdeINLS	Byungjoon Hwang	NotI (FastDigest, ThermoFisher)	SP6

Transgenic embryos were selected by their transgenic selection marker. In transgenic embryos devoid of a transgenic selection marker, the nanobody activity was determined by counting the percentage of non-fluorescent embryos following injection compared with control embryos.

### ***Generation of zebrafish transgenic line *bact2:loxP-stop-loxP-VhhGFP4-hSPOP-nls-P2A-nlsRFP****

The following sequences were amplified by PCR: *bact2* promoter using *p5E-bactin2* (tol2kit, #299), *loxP-stop-loxP* using *pENTR5'\_hsp70l:loxP-stop-loxP* (Kirchgeorg et al., 2018), *VhhGFP4-hSPOP-nls* using *pCS2\_Flag-VhhGFP4-hSPOP-nls* (Shin et al., 2015), *P2A-nlsRFP* using *pCS2-GVG-eGFP-P2A-nlsRFP* (Ortica et al., in prep.). All the PCR products were cloned by Gibson into pDestTol2CG2 (tol2kit, #395), previously digested by KpnI and SalI, and purified on gel.

For transgenics screening, the expression vector pEX*bact2:loxP-stop-loxP-VhhGFP4-hSPOP-nls-P2A-nlsRFP* (14527 base pairs) also contains another GFP sequence expressed under the control of the cardiac-specific promoter *cmlc2*. The sequence of the expression vector was verified by different PCR reactions (Table 2).

The pEX*bact2:loxP-stop-loxP-VhhGFP4-hSPOP-nls-P2A-nlsRFP* plasmid (also called Tol2 plasmid) and the *tol2 transposase* mRNA (transcribed from *pCS2+ TP* (provided by Koichi Kawakami), previously digested by NotI) were mixed (final concentration of 60 ng/μL each) and 1nL was injected into early 1-cell stage AB embryos.



**Table 2: PCR primers for cloning, sequencing and genotyping**

Objective	Sequence amplified by PCR	Forward primer sequence (5' -> 3')	Reverse primer sequence (5' -> 3')
Cloning	<i>Beta-actin</i>	AACACAACATATCCAGTCACTATGGTCGACCGTTAACGCTACCATGGAG	TCGACGGTATCGATCGGCTGAACGTAAAAGAAAGG
	<i>loxP-stop-loxP</i>	TTTTACAGTTCAGCCGATCGATACCGTCGACTC	TTGGACTTGATCCATCAAACCTGGGTCGAATTCG
	<i>vhhGFP4-hSPOP-nls</i>	TTCGACCAAGTTTGATGGATCAAGTCCAAGTGG	AGTAGCTCCGCTCCGGATTGCTTCAGGCGTTTG
	<i>P2A-nlsRFP</i>	CGCCTGAAGCAATCCGGAAGCGGAGCTACTAATTC	TATCATGCTGGATCATCATCGATGGTACCTTAGGCCCGGGAGTG
	pDONOR backbone + linker	GTACAAGTAAGCGGAGTGCATTACCCAC	CCTTGCTCAGGAATCTGAACCTCCACCTCC
	<i>GFP</i>	TTCAGAATTCGTGAGCAAGGGCGAGGAG	TGCACCTCGCCTTACTGTACAGCTCGTCATG
	Sequencing	<i>Beta-actin (partial) (*)</i>	TGGATGTGGCAGGTGAGAAT
<i>loxP-stop-loxP (*)</i>		GGGGACAAGTTTGTACAAAAAAGCAGGCTTACCGTCGACTCTAGAGGATCA	GGGGACCACTTTGTACAAGAAAGCTGGGTAACCTGGGTCGAATTCGCCCTTG
<i>vhhGFP4-hSPOP-nls (*)</i>		GGGGACAGCTTTCTGTACAAAGTGATGGATCAAGTCCAAGTGGTGG	TGAAGTTAGTAGCTCCGCTCCGGATTGCTTCAGGCGTTTTC
Junction <i>Beta-actin/loxP-stop-loxP (*)</i>		GTGTAATTGATCGCAGGCGAG	GATCGATCCGGAACCTTAA
Junction <i>loxP-stop-loxP/vhhGFP4-hSPOP-nls (*)</i>		GGGGACAAGTTTGTACAAAAAAGCAGGCTTACCGTCGACTCTAGAGGATCA	TGAAGTTAGTAGCTCCGCTCCGGATTGCTTCAGGCGTTTTC
Junction <i>vhhGFP4-hSPOP-nls/P2A-nlsRFP (*)</i>		GGCCGTGTATTACTGTAATGTG	CTCGTACTGTTCCACGATGGTG
<i>Kl linker-GFP (**)</i>		CATGGACAGACTCCCTCGAG	GCGGATACCGCAGATGG
<i>5' Kl linker-GFP (**)</i>		CATGGACAGACTCCCTCGAG	CCAGCAGGACCATGTGATC
<i>3' Kl linker-GFP (**)</i>		GCACAAGCTGGAAGTACAACACTAC	GCGGATACCGCAGATGG
<i>vhhGFP4-hSPOP-nls</i>		GGGGACAAGTTTGTACAAAAAAGCAGGCTTACCGTCGACTCTAGAGGATCA	GGGGACCACTTTGTACAAGAAAGCTGGGTAACCTGGGTCGAATTCGCCCTTG
Genotyping	<i>Kl linker-GFP</i>	CATGGACAGACTCCCTCGAG	GCGGATACCGCAGATGG
	<i>ERT2-Cre-ERT2</i>	GACCCCTCATGATCAGGTCCACC	GACCGTGGCAGGGAACCCCTCTG

(\*) refers to the sequencing for the transgenic line *Beta-actin:loxP-stop-loxP-vhhGFP4-hSPOP-nls-P2A-nlsRFP* and (\*\*) for the sequencing for the knock-in line *notch3-linkerGFP*.

Three different steps of screening were needed for the validation of the transgenic line, for:

- 1) The integration of the transgene into the genome: embryos containing the plasmid were selected at 24 hpf by their green heart and were grown until adulthood. The adults were sequenced to validate the correct integration and the sequence of the transgene (Table 2).
- 2) The transmission of the transgene to the offspring: transgenic adults were crossed with AB fish and the offsprings' hearts were screened. Some of the transgenic offsprings were kept to generate a stable transgenic line.
- 3) The efficient recombination of the stop cassette: some transgenic offsprings were bath into 4-OHT and screened for red fluorescence in the central nervous system (see '4-hydroxytamoxifen treatment' part).

### ***Generation of pXT7-VhhGFP4-hSPOP-nls-P2A-nlsRFP***

*VhhGFP4-hSPOP-nls-P2A-nlsRFP* sequence was amplified from *pEXbact2:loxP-stop-loxP-VhhGFP4-hSPOP-nls-P2A-nlsRFP* with the following primers, designed to introduce KpnI and BglII restriction sites (underlined):

KpnI\_fwd: 5'- ATCGGGTACCCGACCCAAGTTTGATGGATC -3'

rev\_BglII: 5'- ATCGAGATCTCATCGATGGTACTTAGGCGC -3'

The PCR product was cloned into pXT7 after the digestion of both by KpnI and BglII and the ligation using InstantStickyEnds (NEB).

*VhhGFP4-hSPOP-nls-P2A-nlsRFP* capped mRNA was transcribed by T7 with mMESSAGE mMACHINE® (ThermoFisher) and injected at one-cell stage in *notch3<sup>GFP/GFP</sup>* embryos.

### ***Generation of zebrafish knock-in line notch3<sup>GFP/GFP</sup>***

The following sequences were amplified by PCR: the plasmid backbone using *pDONOR-left\_arm-linker-AzamiGreen-P2A-nlsRFP-right\_arm* (Ortica et al., in prep.) to conserve the two homology arms (left: 892 aa; right: 800 aa) and the linker (GGAGGAGGTGGTTCAGGTGGTGGAGGATCTGGAGGTGGAGGTTCA; Hisano et al., 2015), and *eGFP* (714 aa) using *pCS2-GVG-eGFP-P2A-nlsRFP* (Ortica et al., in prep.). The PCR products were cloned together by Gibson to obtain *pDONOR-left\_arm-linker-GFP-right\_arm* (measuring 5225 base pairs) and the plasmid was sequenced (Table 2).

Target-specific Alt-R CRISPR-Cas9 crRNA and common Alt-R CRISPR-Cas9 tracrRNA were designed on CRISPOR (crispor.tefor.net) (Ortica et al., in prep.) and ordered on IDT (eu.idtdna.com). The crRNA target sequence, located in the *notch3* exon 32 among 32, was 5'-GGGGTAATCCTCTGGGCCTG[CGG]-3' ([PAM]). Each RNA was dissolved in Duplex Buffer (IDT) as 120  $\mu$ M stock solution and stored at -20°C. The crRNA:tracrRNA duplex was prepared by mixing the stock solutions on a 1:1 ratio, heating at 95°C for 5min and letting to cool down slowly for the annealing. The 60  $\mu$ M crRNA:tracrRNA duplex stock solution was stored at -20°C.

Cas9 protein (wild type, active) was ordered on LabOmics-Toolgen (www.labomics.com), dissolved in 2 M KCl, H<sub>2</sub>O and 50% glycerol for final concentrations of 30  $\mu$ M of Cas9 protein and 750 mM of KCl, and stored at -80°C.

On the injection day, the ribonucleoprotein (RNP) complex was assembled by mixing 2  $\mu$ L of 30  $\mu$ M Cas9 protein, 1  $\mu$ L of 60  $\mu$ M crRNA:tracrRNA duplex and 2  $\mu$ L H<sub>2</sub>O. The RNP was incubated at 37°C for 5 min and then kept on ice before the injections of 1 nL into 1-cell stage embryos.

The crRNA:tracrRNA duplex efficiency was previously validated in the team (Ortica et al., in prep.).

At 48 hpf, injected embryos were screened by PCR to verify the presence of the KI and the sequence of the 5' and the 3' extremities of the KI cassette (Table 2). Other injected embryos were grown until adulthood, sequenced, and screened for germline transmission by crossing with AB fish. The F1 KI embryos were selected by the green fluorescence of their body at 24 hpf and grew to create a stable KI line.

### RNAi-mediated gene silencing

*notch3* 3'UTR region was previously sequenced (Ortica et al., in prep.). To design shRNA, the BLOCK-iT™ RNAi Designer (ThermoFisher) was used, and the corresponding double-strand gBlocks® Gene Fragments with surrounding sequences containing restricting sites matching the entry plasmid *p3E\_INTRON-EmptyRNAi* (Giacomotto's lab (unpublished)), were ordered in IDT (Table 3).

**Table 3: gBlocks® Gene Fragments**

	Double-strand gBlock with iRNA SEQUENCE (5' -> 3')
<i>notch3-01</i>	atcgggatcctggaggcttgcgaaggctgtaTGCTGAACACAAGCCCTAGAGTGACGGTTTTGGCCACTGACTGACCGTCACTCGGGCTTG TGTTcaggacacaaggcctgttactagcactcacatggaacaaatggcccagatctggccgactcgagatcg
<i>notch3-02</i>	atcgggatcctggaggcttgcgaaggctgtaTGCTGAAATCTTGGAAATGGGCTGACGTTTTGGCCACTGACTGACGTCAGCCCTTCCAAG ATTTcaggacacaaggcctgttactagcactcacatggaacaaatggcccagatctggccgactcgagatcg
<i>notch3-03</i>	atcgggatcctggaggcttgcgaaggctgtaTGCTGTTCTTTCTGCGGATACCGGCAGTTTTGGCCACTGACTGACTGCCGGTACGCAGAA AGAAcaggacacaaggcctgttactagcactcacatggaacaaatggcccagatctggccgactcgagatcg
<i>notch3-04</i>	atcgggatcctggaggcttgcgaaggctgtaTGCTGATCTGTGACAGAAATGCTTACGTTTTGGCCACTGACTGACGTAAGACACTGTAC AGATcaggacacaaggcctgttactagcactcacatggaacaaatggcccagatctggccgactcgagatcg
<i>notch3-05</i>	atcgggatcctggaggcttgcgaaggctgtaTGCTGAAACAAGTCCATCTGTGACAGGTTTTGGCCACTGACTGACCTGTACATGGACTT GTTTcaggacacaaggcctgttactagcactcacatggaacaaatggcccagatctggccgactcgagatcg

Each DNA fragments were cloned into *pCR™ 2.1-TOPO™* (TOPO™ TA Cloning™ Kit, Invitrogen), then digested by XhoI and BamHI and sub-cloned by T4 ligation into *p3E\_INTRON-EmptyRNAi*, previously digested by BglII and XhoI. Then, other DNA fragments were integrated into *p3E\_INTRON-fragmentx* by the same digestion and ligation steps until the generation of a *p3E\_INTRON-6shRNAnotch3*, containing 6 sequences of shRNA.

The electroporation plasmid was built by Gateway cloning of *p3E\_INTRON-6shRNAnotch3* with the following plasmids: *p5E-CMV/SP6* (tol2kit, #382), *pME-H2AmCherry* (#234), and *pDestTol2pA2* (#394).

The expression vector *pEXCMV:H2Amcherry-6shRNAnotch3* or the control *pEXCMV:H2Amcherry-6shRNAGFP* were electroporated into adult zebrafish brains (anesthetized in water containing 0.01% of Tricaine methanesulfonate (MS222; Sigma-Aldrich), drilled, injected with a solution at 1 µg/µL, and electrocuted (4 × 1sec, 50 V)), and the efficiency of the shRNA was validated by RNAscope smFISH (bio-technique) on *notch3*.

### ***Genotyping***

Genomic DNA was recovered from the tail of zebrafish embryos or adults, and processed with the Phire Animal Tissue Direct PCR Kit (ThermoFisher) according to the manufacturer's instructions.

The presence of the *bact2:loxP-stop-loxP-VhhGFP4-hSPOP-nls-P2A-nlsRFP* transgene was verified by the amplification of 1029 bp, containing the sequence *VhhGFP4-hSPOP-nls*, and the presence of the *her4.1:ERT2CreERT2* transgene was verified by an amplification of 676 bp (described in Than-Trong et al., 2020).

The locus of the *linker-GFP* KI was amplified with a forward primer outside the left homology arm and a reverse primer inside the right homology arm, to form amplicons of 2322 bp if the KI is present or 1552 bp if it is absent.

### ***LY treatment***

*notch3<sup>GFP/GFP</sup>* adults and embryos were bathed for 24 hours in fish water or E3 medium containing 10  $\mu$ M of LY411575 (Sigma-Aldrich) diluted in 0.01% DMSO (Sigma-Aldrich), or 0.01% of DMSO. Fish were immediately dissected after the treatment.

### ***4-hydroxytamoxifen treatment***

#### ***Induction in embryos***

At 24 hpf, dechorionated *bact2:loxP-stop-loxP-VhhGFP4-hSPOP-nls-P2A-nlsRFP; her4.1:ERT2CreERT2* and *notch3<sup>GFP/GFP</sup>* transgenic embryos were bathed into E3 medium containing 10  $\mu$ M of 4-OHT (Sigma-Aldrich, T176) and kept in the dark overnight. The treatment was replaced by a new E3 medium, and at 72 hpf, treated embryos were screened for red fluorescence in their central nervous system. At 6 dpf, larvae were dissected (the brain was used for IHC and the tails for genotyping), or kept and grown until adulthood. The grown-induced adult fish were genotyped and dissected at 4 months for analysis.

#### ***Induction in adults***

Genotyped *bact2:loxP-stop-loxP-VhhGFP4-hSPOP-nls-P2A-nlsRFP; her4.1:ERT2CreERT2* and *notch3<sup>GFP/GFP</sup>*, *notch3<sup>GFP/+</sup>* or *notch3<sup>+/+</sup>* transgenic adult (3 to 4 months old) were bathed three consecutive days for 7 hours in fish water containing 5  $\mu$ M of 4-OHT and kept in the dark. Each fish was treated in a 50 mL total volume and rinsed for 48 hours before going back to the fish facility. At 9 dpi, fish brains were dissected and analyzed.

### ***Immunohistochemistry***

Brains were dissected in cold PBS (Fisher Bioreagents) and directly transferred to a 4% PFA solution in PBT for fixation. They were fixed for 2h at room temperature (RT) or overnight at 4°C under permanent agitation. After 3 washes in PBT, brains were dehydrated through a series of 25, 50, 75, 100% methanol and kept in 100% methanol at -20°C. Following rehydration, brains were processed for whole-mount immunohistochemistry. An antigen retrieval step of 1h in HistoVT One (Nacalai Tesque) was performed at 65°C. Brains were washed in PBT and bleached for 15min at RT under white light in an H<sub>2</sub>O<sub>2</sub> solution. After other washing, brains were pre-incubated for 2h at RT in a blocking buffer (4% Normal goat serum, 0.1% DMSO, 0.1% Triton (Sigma-Aldrich, X-100), 20 mM Glycine (Sigma-Aldrich, G7126) in PBS), and incubated overnight at 4°C under agitation in the primary antibodies diluted in the blocking buffer (Table 4). Brains were then washed with PBT and processed the same way for the secondary antibodies (Table 4). Before imaging, brains were kept in the dark at 4°C in PBT complemented with 0.02% sodium azide.

**Table 4: Antibodies**

Type of antibody	Antigen	Species of origin	Isotype	Dilution	Source	Reference	Fluorochrome
Primary	PCNA	Mouse	IgG2a	1:200	Santa Cruz Biotechnology	Sc56 (PC10)	
	GFP	Chicken	IgY	1:250	Aves Labs	GFP-1020	
	ZO1-647	Mouse	IgG1	1:500	Invitrogen	MA3-39100-A647	
	Sox2	Rabbit	IgG	1:250	Abcam	Ab97959	
	RFP	Rat	IgG2a	1:250	Chromotek	5F8	
	RFP	Rabbit	IgG	1:250	Abcam	Ab28664	
	Rab7	Mouse	IgG2b	1:200	Sigma-Aldrich	R8779	
	Sox2	Mouse	IgG1	1:200	Abcam	Ab171380	
	Rab5	Rabbit	IgG	1:200	Santa Cruz Biotechnology	Sc2850	
	Rab11	Rabbit	IgG	1:200	GeneTex	GTX127328	
	Lamp1	Rabbit	IgG	1:100	Abcam	Ab24170	
	Secondary	Chicken IgY (H+L)	Goat	IgG	1:1000	Invitrogen	A-11039
Rabbit IgG (H+L)		Goat	IgG	1:1000	Invitrogen	A-31556	Alexa Fluor 405
Rabbit IgG (H+L)		Goat	IgG	1:1000	Invitrogen	A-11010	Alexa Fluor 546
Mouse IgG2a		Goat	IgG	1:1000	Invitrogen	A-21136	Alexa Fluor 633
Rat IgG2a		Goat	IgG	1:1000	Invitrogen	A-11081	Alexa Fluor 546
Mouse IgG1		Goat	IgG	1:1000	BioLegend	409109	Alexa Fluor 405
Mouse IgG2b		Goat	IgG	1:1001	Invitrogen	A-21045	Alexa Fluor 546

Larval brains were incubated with DAPI overnight at 4°C and mounted on glass slides, using 2 overlaid reinforcement rings (3L Office) as spacers. Adult brains were mounted using iSpacer 0.5 mm (IS017, SunJin Lab Co.).

### ***RNAscope smFISH against notch3***

The RNAscope experiment was done before the immunostaining. The first steps are the same as for immunohistochemistry, but after rehydration, brains were directly bleached. They were washed in PBT and pre-incubated in Probe Diluent for at least 1 h at 40°C under permanent

agitation. The Diluent was then replaced by the prewarmed Probes and the brains were incubated overnight at 40°C under permanent agitation. Brains were then washed in Wash Buffer at RT and incubated in AMP1 and AMP2 for 30 min at 40°C, and AMP3 for 15 min at 40°C. After each amplification step, brains were washed in Wash Buffer at RT. Brains were incubated with Multiplex FL v2 HRP-C1 (for *notch3*) for 15 min at 40°C and washed with TSA Buffer for 10 min at RT. The Buffer was replaced by OPAL-520 diluted in TSA Buffer (1:500) and incubated for 30 min at 40°C. Brains were washed in Wash Buffer at RT and incubated in HRP Blocker for 15 min at 40°C. Finally, brains were washed in Wash Buffer at RT. For the following immunohistochemistry, the HistoVT One solution was not used, but the other steps were similar.

### ***Image acquisition, processing and cell counting***

The whole embryos and larvae were screened and imaged with an Olympus SZX16 stereomicroscope equipped with an Olympus DP73 camera. For the measurements of embryonic lengths, pictures of larvae and scale bars were done with a Leica M80 stereomicroscope and the Leica IC80 HD camera, and larval lengths were measured manually from the front of the head to the end of the pigments of the tail (corresponding to the standard length).

Immunostained brain pictures were acquired on a confocal microscope (LSM 980, Zeiss) using 40X oil objective. They were converted into Imaris files for their analysis on Imaris Software (version 10).

For the nuclear segmentation in the DMSO versus LY treated brains, a part of the Dm area was chosen and new surfaces were created on the Sox2 channel using the menu Surfaces and Automatic creation, followed by manual corrections.

For nuclear segmentation in the midbrain of 6 dpf larvae, the menu Surfaces and Edit Manually was used for each nucleus. The contour of each cell was drawn on the upper and the lower stack where the cell appears and in 2-3 stacks in between, and the surface covering the area was created. The data coming from the different segmentations were extracted in Excel tables and statistically analyzed on Prism.

For the co-localization analyses, the Coloc tool was applied to the RNAscope and GFP channels and a threshold was manually defined for signal selection.

For RNAscope smFISH quantification, pictures were processed in two Python libraries: Napari for Z-projection and cell annotations, and Big-FISH for analysis of single-molecule FISH.

Figures were created in PowerPoint (Microsoft) or BioRender (<https://www.biorender.com/>).

***Statistical analysis***

Statistical analysis was performed using GraphPad Prism 10.2.2.

## Discussion

This work lays the foundations for detailed conditional analyses of Notch3 signaling functions in zebrafish NPs/NSCs *in vivo*. Specifically, I developed two methods of KD to understand the precise mechanisms of action and the middle- to long-term effects of Notch3 invalidation *in vivo* in NPs/NSCs. The first method consisted of tagging endogenous Notch3 with GFP, which became a target for degradation in the presence of specific nanobodies. In parallel, I created the nanobody tool selective for nuclear GFP fusion proteins and conditionally activatable in NPs/NSCs. The alternative method, usable for middle-term *notch3* KD, consisted of adapting the shRNA method to the study of *notch3*: I created an electroporation plasmid containing *notch3* shRNAs and validated its efficiency post-electroporation into adult pallial NSCs *in vivo*.

To generate the *notch3<sup>GFP</sup>* line, I tagged the N3ICD domain of the endogenous Notch3 protein with a GFP by CRISPR-Cas9 KI (Figure 16). In the fusion protein, I validated that GFP could be used as a tracer for *notch3* expression, and validated Notch3 functionality by assessing the correct growth of the larvae and the percentage of proliferating cells in the adult pallium of *notch3<sup>GFP/GFP</sup>* fish compared to control (Figure 17). Then, I used this new line to follow Notch3 signaling, by localizing Notch3-GFP protein and its transcriptionally active form N3ICD-GFP in Sox2<sup>pos</sup> adult and larvae pallial cells (Figure 18-20). As expected, the GFP signal was high at the plasma membrane, in cytoplasmic vesicles, where it co-localized with recycling endosomes and lysosomes, and in the nucleus at a lower intensity level (Ilagan et al., 2011; Fryer et al., 2004). I quantified nuclear GFP signal intensity in Sox2<sup>pos</sup> cells in pallia treated with the  $\alpha$ -secretase inhibitor LY and obtained a significant decrease in GFP intensity compared to the control. I demonstrated that the Notch3-GFP line offers the possibility of measuring Notch3 signaling *in situ*.

Before generating the nanobody line, I tested the efficiency of anti-GFP nanobody tools in transgenic embryos expressing GFP or GFP-tagged proteins and I validated VhhGFP4-hSPOP-nls efficiency and specificity for nuclear protein degradation (Shin et al., 2015) (Figure 21). Then, at the cellular level, I validated the efficiency of VhhGFP4-hSPOP-nls in *notch3<sup>GFP/GFP</sup>* larvae (Figure 23). I also verified the efficiency of the *loxP-stop-loxP* recombination in the presence of Cre recombinase for the conditional expression of the



nanobody tool (Figure 24). Afterward, by *tol2*-transposase transgenesis, I generated *Tg(bact2:loxP-stop-loxP-VhhGFP4-hSPOP-nls-P2A-nlsRFP)* fish conditionally expressing the nanobody tool and a fluorescent marker of expression, and I selected four different founders on their abilities to transmit the transgene to their offspring (Figure 22).

By successive crossings, I created a fish line containing the conditional nanobody effector *bact2:loxP-stop-loxP-VhhGFP4-hSPOP-nls-P2A-nlsRFP*, the KI *notch3<sup>GFP/GFP</sup>*, and the genetic expression driver *her4.1:ERT2CreERT2*, which is specific to NPs/NSCs (Yeo et al., 2007) (Figure 25). In F2 embryos, I demonstrated that the expression of the degradation system was inducible. Above all, I validated the efficiency of *in vivo* N3ICD-GFP degradation in RGs/NPs nuclei of induced larvae midbrains (Figure 27). I also let some induced *notch3<sup>GFP/GFP</sup>* fish grow until adulthood where I observed large and deep “attached” cell clones encompassing some Sox2<sup>pos</sup> cells (Furlan et al., 2017) (Figure 28). I showed the possibility of forming adult KD cell clones from *her4.1<sup>pos</sup>* cells in the embryo.

After that, I validated the possibility of directly inducing the expression of the degradation system in adult NSCs of *notch3<sup>GFP/GFP</sup>* fish (Figure 29). Twelve days after the induction, I observed isolated superficial cells or cell clones of a few cells, some containing Sox2<sup>pos</sup> cells, in the adult pallium. Therefore, I validated the inducibility of the system expression directly in adults.

The second method of KD consisted of electroporating *notch3* shRNAs into the adult pallium (Labusch et al., 2020) (Figure 30). I confirmed the efficiency of the shRNAs by the decreased number of *notch3* transcripts in electroporated Sox2<sup>pos</sup> cells. Focusing on cells of large apical area, which are NSCs and characterized by deep/long quiescence, I further showed that the *notch3* shRNAs increased the percentage of proliferating cells. This is the expected phenotype of blocking Notch3 signaling (Alunni et al., 2013; Campbell et al., 2022; Hernández-Núñez et al., 2021; Basak et al., 2012; Ehret et al., 2015; Kawai et al., 2017), confirming the role of Notch3 as a promoter of NSC quiescence and concomitantly validating the shRNA approach.

By the conclusion of my PhD, I had reached a stage where I could begin investigating the role of Notch3 in NPs/NSCs. In this discussion, I will explore the future potential of the methods developed in this work. The discussion is structured into three key sections, each building on findings from the results: the creation of the *notch3<sup>GFP</sup>* line, the development of the

nanobody tool, and the design of the *notch3* shRNAs tool. I will then outline the specific phenotypes and research questions I intend to address shortly using these tools.

### **The *notch3*<sup>GFP</sup> line: a multifunctional tool for studying the Notch3 signaling pathway**

A main advantage of the *notch3*<sup>GFP</sup> line is the possibility to follow, at the cellular level, Notch3 protein in its full-length form and its effector form (N3ICD-GFP), to study Notch3 signaling dynamics. The GFP tag provides a domain to the fusion protein for spotting Notch3 when a working antibody against Notch3 is lacking -which is our case in zebrafish-. Equivalent lines with tagged intracellular receptor domains have been successfully used to characterize Notch signaling in *Drosophila* (Kawahashi and Hayashi, 2010; Couturier et al., 2012; Pinot and Le Borgne, 2024; Loubéry et al., 2014; Trylinski et al., 2017; Couturier et al., 2013; Couturier et al., 2014).

In Figure 18A,B, immunostained *notch3*<sup>GFP</sup> pallial cells had a dotted GFP signal aligned to the apical ZO1 signal, which I identified as a membrane signal. This signal was stronger a few micrometers below the ZO1 level in some ventricular cells, in a region where I considered that their soma are still in contact. I did not use a marker for membranes (e.g. N-cadherin (Lui et al., 2001; Nagashima et al., 2013; Harrington et al., 2007; Raymond et al., 2006; Liu et al., 2003), or LLGL scribble cell polarity complex component 2 (Llg12) (Kujawski et al., 2019)), therefore the localization of these accumulations of Notch3 receptors at the membrane is difficult to determine with precision. Moreover, because of the juxtaposition of NSCs, the GFP signal which seems to belong to one cell may belong to the neighboring cell. Due to the dense packing of cells in the zebrafish pallium, a basolateral marker signal would be difficult to read except if it is expressed in isolated NSCs. Indeed, we still do not know at which basolateral level of the cell are happening the main Notch interactions. In *Drosophila*, the question is debated. In SOPs, two pools of Notch receptors are present in the basal and the apical pIIa-pIIb interface, and their relative contribution to the signaling might be context-dependent (Bellec et al., 2021; Houssin et al., 2021; Trylinski et al., 2017). Indeed, Notch activation can take place basally as well as apically (Trylinski et al., 2017; Bellec et al., 2021), but the minor contribution of the apical pool of receptors to the Notch activation described in the control situation (Trylinski et al., 2017) suggests that apical activation may become preponderant when a given threshold of Notch and Delta is reached (Bellec et al., 2021). The differences between apical

and basal Notch signaling are unknown. However, due to a shorter distance to the nucleus, the time between NICD production and the transcriptional response could be decreased for basal signaling compared to apical (Bellec et al., 2021).

To characterize the localization of membrane Notch3 receptors in adult NSCs, I could electroporate a plasmid expressing a fluorescent membrane marker following intracerebral injection into the *notch3<sup>GFP</sup>* adult pallium (Alunni et al., 2013). To study Notch3 receptors in embryonic and larval NPs, I could transplant AB embryos with cells from *notch3<sup>GFP</sup>* embryos and work on isolated NPs in larvae pallia (Kemp et al., 2009; Gansner et al., 2017; Li et al., 2011).

In Figure 18A-H, the immunostaining on adult *notch3<sup>GFP</sup>* pallium also highlighted the presence of GFP signals inside the cytoplasm of ventricular cells, which I characterized as endosomes and lysosomes. Endocytosis is a known regulator of Notch signaling activity by regulating the number of receptors at the membrane (and by providing a cleavage compartment) (Zhou et al., 2022a; Coumailleau et al., 2009; Kressmann et al., 2015; Loubéry et al., 2014). As expected, many GFP signals were co-localized with recycling endosomes (Rab11<sup>POS</sup>), formed from early endosomes to target Notch3 receptors to the membrane. Similarly, many GFP signals co-localized with lysosomes (LAMP1<sup>POS</sup>). This result was unexpected because, in acidic environments, the GFP signal is normally quenched (Couturier et al., 2014). However, only weak co-localizations were observed with a few small early and late endosomes. I hypothesized that if the number of Rab proteins present in early and late endosomes is low, all the endosomes are not necessarily visible because of the limited size of the signals. The solution would be to increase picture resolution. In confocal microscopy, the best resolution that can be obtained is generally around 0.2  $\mu\text{m}$  laterally and 0.6  $\mu\text{m}$  axially (Elliott et al., 2020), however, using super-resolution microscopes would increase the resolution to 0.1  $\mu\text{m}$  laterally and 0.2  $\mu\text{m}$  axially (Wu et al., 2021). Another explanation would be that proteins only transit in early and late endosomes, and are stocked for longer times in recycling endosomes and lysosomes.

To validate the pattern of endosomes and lysosomes in NSCs, I could redo the immunostainings on AB fish. IHC experiments on *ex vivo* mouse SVZ NSCs, using the lysosomal marker LAMP2 and the LysoTracker, showed that qNSCs contain many lysosomes with big lumen, especially when compared to aNSCs (Leeman et al., 2018). LAMP2 and LAMP1 share similar patterns in the nervous system (Cheng et al., 2018), however, their

accuracy for assessing lysosome distribution and trafficking have been questioned because they are also distributed in other endosomal compartments (Cheng et al., 2018). The LysoTracker is a diffusible marker that stains acidic cell compartments. Therefore, it is not specific to lysosomes (Podinovskaia and Spang, 2018). It also stains endosomes, GA, secretory vesicles, and phagosomes (Podinovskaia and Spang, 2018; Kellokumpu et al., 2019; Morris, 2020; Yu et al., 2022). The solution would be to combine lysosomal hydrolase markers, autophagic and endo-lysosomal markers (Cheng et al., 2018). I would then quantify the co-localizations of these markers with the GFP signal from the *notch3<sup>GFP</sup>* line to determine Notch3 recycling activity. However, this experiment would not address Notch3 recycling dynamics. To do so, I could take advantage of the transparency of zebrafish embryos and do live imaging on *notch3<sup>GFP</sup>* embryos carrying fluorescent membrane, endosomal, and lysosomal markers (expressed from injected plasmids or transgenes) (Dong et al., 2011; McIntosh et al., 2017).

In Figure 18A,B and 19C-I, I also verified the presence of a GFP signal in NSCs nuclei. This nuclear GFP signal was the effector N3ICD-GFP in cells where Notch3 signaling was active. In parallel, I could easily identify cells with small apical surfaces that did not accumulate N3ICD-GFP in their nuclei. These cells were more proliferative than the bigger cells, and based on their small apical area size, I assumed that they were a mix of IPs and NSCs. Using LY-mediated inhibition of Notch signaling, I verified that the measurement of Notch3 signaling activity via the level of nuclear N3ICD-GFP was quantitative (Figure 19). For the quantification, I included all the ventricular Sox2<sup>pos</sup> cells i.e., a combination of IPs, that express less *notch3*, and NSCs. To focus the analysis on NSCs, I could use an NSC marker instead of Sox2, such as GS. In parallel to the decreased N3ICD-GFP signal in the nuclei of pallial NSCs treated 24 h with LY, the GFP signal at the membrane, which reflected the amount of Notch3 receptors at the membrane, was increased. In the LY condition, the interactions between the Notch3 receptor and its ligands are not interrupted, however, the absence of S3 and S4 cleavages anchor N3EXT-GFP at the membrane (Zhou et al., 2022a; Zhang et al., 2014). At least for 24 h, N3EXT-GFP is maintained at the membrane and is not recycled. Blocking  $\alpha$ -secretase activity is the only way to observe the N3EXT fragments because they are short-lived under normal circumstances (Mumm et al., 2000; van Tetering et al., 2009; Groot and Vooijs, 2014). In addition to the lack of Notch3 activity in the nucleus, this accumulation could also impact possible non-canonical Notch3 activities, such as cytoskeleton interaction and remodeling, which depend on the transmembrane and intracellular domains of the receptor

(Polacheck et al., 2017; White et al., 2023). Although equivalent percentages of proliferating cells were observed in control and LY brains (Figure 19B), the structure of the epithelium was already different. Indeed, arrangements of cells with very large apical areas, surrounded by cells of smaller apical area, were present in the LY condition compared to the control (not quantified). I also noted that some Sox2<sup>pos</sup> cells did not respond to LY treatment by decreasing the nuclear GFP signal and increasing the membrane signal. These cells could be more resistant to Notch inhibition. This result is in agreement with the observation that not all the qNSCs responded to Notch3 inhibition by reactivation (Alunni et al., 2013, Than-Trong et al., 2018). Moreover, one cluster of adult pallial qNSCs, identified by single-cell RNAseq (Morizet et al., 2024; Morizet et al., in prep.) was insensitive to an 24 h LY treatment.

I also tested the localization of Notch3-GFP and N3ICD-GFP in NPs of larvae treated with LY (Figure 20A-C). Similarly to the adult pallium, the nuclear GFP signal was reduced in treated larvae. The membrane GFP signal was still visible but at a lower level than in control brains. Another validation of the tight link between the intensity of GFP signal and the amount of tagged protein was given in Figure 27A: in *notch3*<sup>GFP/+</sup> midbrains, the general level of GFP signal in RGs was inferior to the control *notch3*<sup>GFP/GFP</sup> midbrains.

Moreover, while the number of Sox2<sup>pos</sup> cells and the intensity of the Sox2 signal were not modified in treated adults, they were modified in larvae. I concluded that this phenotype reflected the progressive differentiation of NPs that lose their progenitor features. To reinforce this interpretation, Sox2<sup>pos</sup> cells exited the ventricular layer, which is the NPs niche, and the ventricular cells lost the ZO1 signal e.g. their apicobasal polarity, which confirms the loss of neuroepithelium integrity. These phenotypes were also visible in the midbrain of the treated larvae. In the adult pallium, the effect of the treatment is reversible after a chase period of a few days (Alunni et al., 2013), however, the effects were more impacting in the larvae, and I did not study the survival or the reversibility of the induced phenotypes.

In the *notch3*<sup>GFP</sup> line, the GFP signal pattern was comparable to the AzamiGreen pattern in *notch3*<sup>AzamiGreen</sup> line (Ortica et al., in prep.), however, no other zebrafish KI lines were published for further comparisons.

Another future application of the *notch3*<sup>GFP</sup> line would be the identification of direct effectors of Notch3 signaling in NPs and NSCs, taking advantage of the GFP antibody to do chromatin immunoprecipitation sequencing (ChIP-Seq). I could first verify the direct N3ICD

targets included in the zebrafish Notch3 downstream genes that had been identified in a previous study by comparing RNAseq data obtained from 7 dpf *notch3*<sup>+/+</sup> and *notch1*<sup>fh332/fh332</sup> larval heads (Than-Trong et al., 2018), such as *her4.1* and *hey1*. ChIP-Seq experiment using N1ICD and RBP-Jκ precipitation and performed on adult hippocampal NSCs provided evidence for the fact that *Sox2* is a direct target of Notch signaling (Ehm et al., 2010). In neurospheres grown from adult mouse SVZ cells, N1ICD and RBP-Jκ precipitation were also used to provide evidence for three other target genes: *Hes1*, *Egfr* and *Gfap* (Andreu-Agulló et al., 2009). In cells from mouse embryo pituitary gland, RBP-Jκ precipitation highlighted the target gene *Prophet of PIT-1 (Prop1)* (Zhu et al., 2006).

### **The nanobody tool: a promising method for analyzing the nuclear functions of Notch3 protein and many other proteins**

During the preliminary validation of the nanobody tool efficiency for N3ICD-GFP degradation in the *notch3*<sup>GFP</sup> line (Figure 23A-D), I injected the capped mRNA of the nanobody tool in *notch3*<sup>GFP/GFP</sup> embryos and studied the 3 dpf pallium and midbrain. As expected, the nuclear N3ICD-GFP signal was absent from the cells expressing the nanobody. However, unexpectedly, and contrary to what we obtained after LY treatment, the membrane GFP signal was also absent in these cells. As these cells had a weaker Sox2 signal compared to their neighboring cells, I hypothesized that they were precociously differentiated. This result was encouraging for the next clonal analysis. However, I injected high concentrations of capped mRNA and I probably obtained an excess of functional nanobody tool proteins compared to what I could get with the transgenic line.

The nanobody effector sequence was cloned by using tol2-transposase transgenesis and therefore, I ignore where the sequence has been integrated. As the region where the transgene set is determining for the possibility of recombining the *loxP-stop-loxP* cassette, I first considered four founders. However, three of the four founders had multiple integrations of the transgene and this was a factor of variability in the offspring. Therefore, I chose to work with fish coming from the founder EN which has only one integration.

After the creation of the line containing the driver, the nanobody effector, and the KI, I induced the expression of the nanobody tool in embryos. The RFP fluorescence intensity and fluorescence spreading in the central nervous system were weak at 72 and 96 hpf (Figure 25C)

compared to what I got with larvae induced in the same condition and coming from crossings between *Tg(her4:ERT2CreERT2)* and *Tg(bact2:loxP-stop-loxP-hmgb1-mCherry)*, which use the same promoters (data not shown).

In the original paper (Shin et al., 2015), the Ab-SPOP tool was tested *in vivo* at the scale of whole zebrafish embryos for the disappearance of the fluorescent POI, and the appearance of abnormal phenotypes, reminiscent of the POI KD. However, they did not study the Ab-SPOP activity at the cellular level.

For the validation of the nanobody tool efficiency, I focused my study on 6 dpf larvae, i.e., 4 days after the end of the treatment period (Figure 26). A lot of induced cells were present in the larval pallia and midbrains. While the nlsRFP signal was expected only in nuclei, it also stained the cytoplasm. This result was unexpected because I used a *P2A-nlsRFP* sequence successfully highlighting the nuclei in another line (Ortica et al., in prep), and I sequenced the transgene cassette of the EN founder family. However, the nanobody tool also contains a *nls* sequence, and therefore, even if nlsRFP is not properly located, the nanobody should still be targeted to the nucleus. Finally, the number of RFP<sup>pos</sup>Sox2<sup>pos</sup> cells was limited.

For the validation of nuclear N3ICD-GFP degradation, I considered the previous results of the LY treatment on 3 dpf larvae which decreases the Sox2 signal intensity in pallial cells (Figure 20), and I looked at the Sox2 signal in RFP<sup>pos</sup> pallial NPs in the induced larvae (Figure 26B,C). I observed that many RFP<sup>pos</sup> cells had a lower Sox2 signal compared to neighboring RFP<sup>neg</sup> cells. This effect was accompanied by a decreased nuclear N3ICD-GFP signal. However, the fact that most ventricular cells were proliferating complicated the quantification of nuclear N3ICD-GFP. Therefore, I validated the nanobody efficiency in the midbrain of induced larvae by quantifying the nuclear GFP signal (Figure 27A-C).

As only a few NPs were RFP<sup>pos</sup> in the induced 6 dpf larvae, I decided to use the same induction parameters and grow the larvae to form isolated clones of cells in adults (Figure 28B-E). Dirian et al. had shown that conditional recombination of the *Zebrabow* transgene in *her4*-expressing NPs in 1 dpf embryos formed different types of clones in adults (Dirian et al., 2014). In control pallia, I was expecting many “attached” clones, i.e., clones that contain NSCs and still have a neurogenic potential, and more, or only, “detached” clones that have lost their neurogenic potential in *notch3<sup>GFP/GFP</sup>* pallia (Furlan et al., 2017) (Figure 31). I obtained big clones, but I was surprised to see a lot of RFP<sup>pos</sup> cells just below the Sox2<sup>pos</sup> nuclei or

intercalated between them in the control as well as in *notch3<sup>GFP/GFP</sup>* pallia. Due to the absence of cell migration in the adult pallium, these cells, which are PCNA<sup>neg</sup>, must correspond to young differentiated (or differentiating) neurons. Despite the size of the clones, only a few ventricular Sox2<sup>pos</sup> cells were also RFP<sup>pos</sup> in the control and the *notch3<sup>GFP/GFP</sup>* pallia. In future analyses, I will compare the two conditions for the number of “attached” clones. However, the analysis of clones has limitations for three different reasons: first, the clones are deep and prevent the analysis of all the cells; second, the clones are large, possibly overlapping, and make difficult the identification of each clone; third, the immunostaining was done on whole-mount brains and therefore the penetration of antibodies is limited to the more superficial cell layers. For the latter issue, the immunostaining could be done after whole-brain clearing (Furlan et al., 2017). A solution to the big size of the clones will be to induce the expression of the nanobody tool later during development or in adults. To limit the number of differentiated cells to count inside deep clones, I could focus on a defined parenchymal layer below the NSC layer, corresponding to e.g., two or three weeks of neurogenesis. To visualize this territory, I could pulse 5'-bromo-2'-deoxyuridine (BrdU) 2-3 weeks before the dissection, which would label, in the parenchyma, the layer of neurons born at that time. I would then only consider RFP<sup>pos</sup> cells within the territory delimited by this BrdU<sup>pos</sup> layer and the ventricular zone.

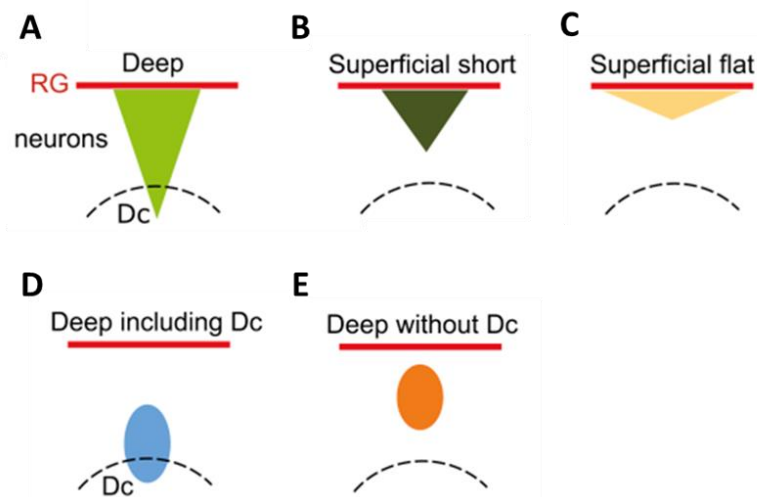


**Figure 31: Individual *her4*-positive pallial RGs are neurogenic throughout life (from Furlan et al., 2017)**

*Tg(her4:ERT2CreERT2;ubi:Zebrabow)* embryos were treated at 1 dpf with 4-OHT for 1 h at 5  $\mu$ M. The corresponding adult telencephalons were imaged and cell clones were distributed in 5 different categories. First, clones that still contain RGs, are “attached” to the pallial VZ (A-C), while clones empty of RGs are “detached” from the pallial VZ (D,E). Second, clones contributing to deep territories (A,D,E) were separated from clones confined to more superficial layers (B,C). Among the 34 clones studied (from 4 brains), 27 were “attached”, while 7 were “detached”. Dc, dorso-central pallium, RG, radial glia.



Directly in adults, I validated the inducibility of the nanobody tool and the generation of cell clones 9 days after the induction (Figure 29B-I). In adult zebrafish, the published 4-OHT condition for *switch* reporter clonal recombination in *Tg(her4.1:ERT2CreERT2; ubi:switch)* was 10 min in water containing 0.5  $\mu$ M 4-OHT, and 7 h in five consecutive days at 2  $\mu$ M 4-OHT for maximal recombination (Than-Trong et al., 2020). These conditions turned out not to be optimal in my case, as I only obtained a few to no induced cells. Therefore, I optimized the treatment to get a minimum number of isolated induced cells by pallium in a more reproducible manner. Finally, I chose a treatment of 7 h in three consecutive days at 5  $\mu$ M 4-OHT (Figure 29). In the future, to count the number of induced cells by pallium to have a reference point for the control and *notch3<sup>GFP/GFP</sup>* conditions before analyzing phenotypes, I would redo the treatment but sacrifice the fish sooner, e.g. at 3 dpi.

In control and *notch3<sup>GFP/GFP</sup>* pallia, 9 days after the treatment, many clones had been generated, and no obvious differences were observed between them (Figure 29B-I). However, further analyses will be conducted to characterize the number of isolated cells, the number of cells by clones, and the composition of the clones. If the nanobody tool does not impact the proliferation rate but the fate of the generated cells, I could study the identity of the clonal cells. First, I could identify NSCs and IPs by using a stem cell marker, such as GS on top of the Sox2 marker, and neuronal markers specific to different neuronal maturation or different neuron types. The nanobody tool could also have an impact on the tissue scale. For example, if the clonal NSCs are more proliferative than the non-clonal cells, I hypothesized that the cells around could compensate by being less proliferative to maintain tissue homeostasis. Therefore, I would study the percentage of proliferating NSCs outside the clones and the shape of the NSCs (e.g. apical surface...) in the epithelium.

The common issue of the different experiments in larvae pallia and midbrains, and adult pallia was the weak RFP signal intensity in Sox2<sup>pos</sup> cells compared to cells downstream in the neurogenic lineage (Sox2<sup>neg</sup>) (Figure 26C, 27A, 28C, 29C,D,F,G,H,I). This indicated that the expression of the transgene was induced in some NPs or NSCs, although at much lower levels than in their offspring. A similarly weak RFP signal was obtained from the 3 other nanobody tool founders. I hypothesized that in NPs/NSCs, either the degradation of the fluorescent marker is increased, or the transgene expression is abnormally low. To test if the quantity of nanobody was also weaker in NPs/NSCs, I tested two different antibodies against the nanobody. Unfortunately, I failed to validate a working antibody. However, in the laboratory, lower

transgene expression levels are observed in NSCs compared to other cells of the lineage in many other transgenic lines. The weak fluorescent marker intensity in Sox2<sup>Pos</sup> cells is therefore very likely to also reflect this particularity of NPs/NSCs. The chromatin state of NSCs, which is nevertheless crucial for the maintenance of adult neurogenesis (Kunoh et al., 2024), possibly limits transgenes expression.

This problem is inherent to the transgenesis methods that randomly integrate DNA into the genome because the integration position influences the transgene activity. In mouse, the ROSA26 locus is often used for controlled insertion and ubiquitous expression of transgenes (Bouabe and Okkenhaug, 2013). Recently, two universal landing sites, allowing consistent and uniform expression of transgenes over development and over generations, have been identified (Lalonde et al., 2024). These sites are located in chromosomes 14 and 24 where *attP* sites have been integrated. The targeted integration works by injecting into one-cell stage zebrafish embryos a vector containing the transgene and an *attB* site simultaneously as *phiC3 integrase* mRNA. They also established that *loxP*-based switch reporters showed sensitive and reproducible Cre-mediated recombination when integrated at these sites. Using this method for integrating the nanobody tool transgene in the zebrafish genome is a perspective to improve the concentration of nanobody tools in NPs/NSCs.

The development of the *in vivo* nanobody tool enables the study of Notch3 functions and opens the possibility of studying many other GFP or GFP derivatives-tagged nuclear proteins. By taking advantage of the already existing GFP-tagged proteins library, this method should be relatively fast to implement for addressing nuclear protein functions. Moreover, the nanobody tool could also be a tool for *in vivo* imaging. In adults, the pigments of the AB background prevent *in vivo* imaging of the zebrafish brain, however, obtaining the *notch3*<sup>GFP</sup> line in a *casper* background (White et al., 2008) would create a tool for Notch3 KD *in vivo* in adults (Mancini et al., 2023; Dray et al., 2015; Barbosa et al., 2015). However, this method requires multicolor two-photon microscopy (Mancini et al., 2023), which is not available in the laboratory.

### **The *notch3* shRNA: an alternative method targeting all Notch3 functions in isolated cells or clones**

I created an electroporation plasmid that contains five different shRNA targeting *notch3* 3'UTR (Figure 30A). Indeed, only these five shRNA were recovered by following Giacomotto

et al. method for the design of shRNA (Giacomotto et al., 2015). However, an increased number of different shRNA increases the efficiency of the tool. As an example, Labusch et al. used nine different shRNA to efficiently target *psap* in adult NSCs (Labusch et al., 2024). However, I validated the efficiency of the *notch3* shRNAs at the molecular level (Figure 30E-G). To reinforce this result, I would redo the experiment on more than two brains by condition. To test the duration of the shRNAs activity, I would also sacrifice electroporated fish at 15 dpe and 30 dpe and verify the presence of the electroporation marker mCherry and the impact on the *notch3* transcripts. After these validations, I could analyze the induced phenotypes and compare them with the ones obtained with the nanobody tool. The induced phenotypes could be different between the two methods because they do not impact the Notch3 pathway to the same extent; the nanobody tool only targets the nuclear functions while the shRNAs target all cellular functions.

The main limitation of the shRNAs is the necessity of using electroporation. This invasive method could impact tissue homeostasis at each step: creating a hole in the zebrafish skull, injecting the plasmid solution, and using an electric pulse to open the cell membranes. Indeed, in both control and *notch3<sup>GFP/GFP</sup>* electroporated pallia that I used for the analyses in Figure 30, many more proliferating cells were present than in non-electroporated pallia. This phenotype was not localized in specific regions but was broad, and I hypothesized that it was a consequence of tissue stress. Another limitation of electroporation is the variability of its efficiency. A significant number of electroporated fish die after the procedure or do not wake up from the anesthesia. Moreover, even when coming from the same session of electroporations, some pallia have many electroporated cells, some have only a few, and others are not electroporated.

An alternative method to electroporation is the lipofection. This method employs charged liposomes (Lipofectamine) that encapsulate the plasmid and rely on endocytosis for delivery into the cells. It is successfully used in zebrafish embryos (Terzi et al., 2024; bioRxiv preprint). However, in the laboratory, lipofection has been tested and was not efficient (Ortica, not published).

## Conclusion

This work led us to the point where we can begin questioning Notch3 functions in the zebrafish NSPCs with the newly created tools. Shortly, I will test my hypotheses (Figure 32) on the phenotypes induced by conditional Notch3 KD in the adult pallium by using the nanobody tool and the shRNAs. In particular, I will analyze the impacts of Notch3 loss-of-function in isolated NSCs or cell clones (Figure 32).

A better understanding of Notch3 functions in NSCs can enhance our knowledge of NSCs maintenance and behavior. It may also help understand the impact of NOTCH3 activity in brain tumors such as glioblastoma, and the effect of mutations such as those reported in CADASIL or Sneddon patients.

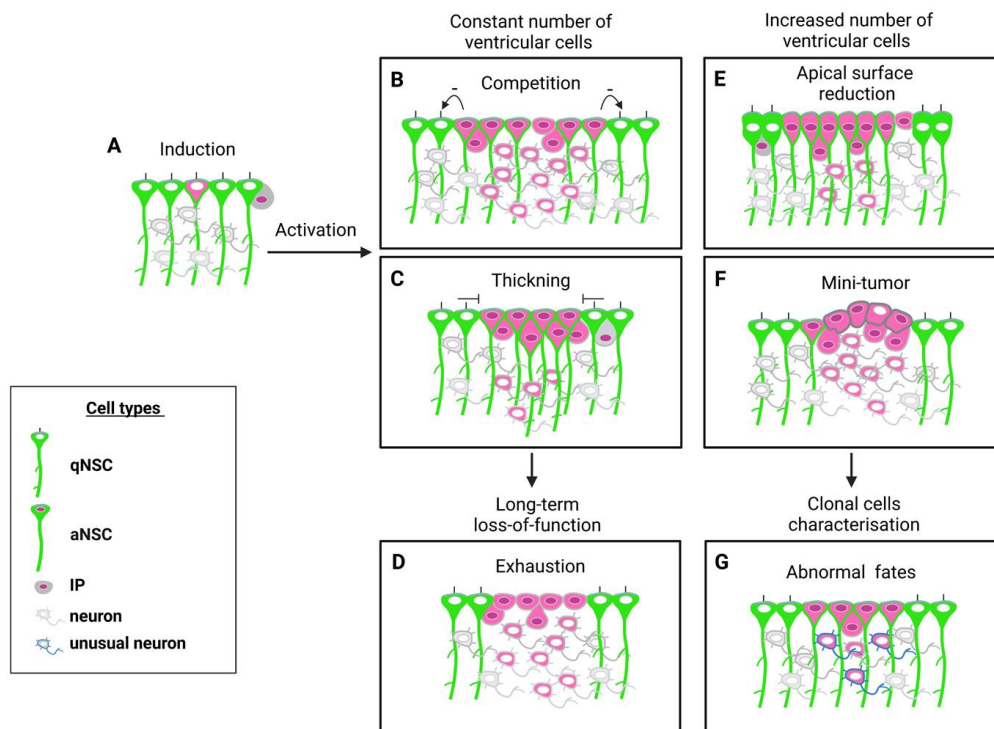


**Figure 32: Hypotheses on the phenotypes induced by Notch3 KD in adult clonal NSCs**

(A) After the induction of the nanobody tool expression in isolated NSCs (pink) of *notch3<sup>GFP/GFP</sup> Tg(bact2:lox-STOP-lox-VhhGFP4-hSPOP-nls-P2A-nlsRFP; her4:ERT2CreERT2)* adult pallia, I hypothesize that these cells will be activated and divide without entering quiescence (see Introduction part 5.5). I postulate that the surface area of the ventricular zone will not be increased by the divisions. After this, there are several possibilities.

(B,C) If the number of ventricular cells stays constant, then either clonal cells (pink) will enter competition with non-clonal cells (green) by proliferating and reducing the proliferation of the non-clonal cells or increasing non-clonal cells differentiation (B), or the longitudinal expansion of clonal cells will be blocked by non-clonal neighboring cells, and therefore NSCs will expand vertically, forming multiple layers of NSCs (C).

(D) After weeks, I hypothesize that continuously activated NSCs will be exhausted and differentiated.

(E,F) If the number of ventricular cells is increased, then either pallial NSCs will reduce their apical surface to fit in the unchanged ventricular surface area (E), or the clones will formed mini-tumors, losing cellular junction and breaking tissue homeostasis (F).

(G) Then, I also hypothesize that the fate of the daughter cells will be biased. Clonal cells are represented with a pink cytoplasm. aNSC, activated neural stem cell, IP, intermediate progenitor, qNSC, quiescent neural stem cell.

## **Annex**

### **Review article**

During my PhD, I had the chance to participate, together with Dr. Laure Bally-Cuif, in the writing of a review requested by the French Academy of Sciences, in which we compared embryo and adult neurogenesis in zebrafish and mammalian models.

In the review, we focused on Neural progenitor cells (2), Lineages and niches (3), Embryonic and adult neurogenesis cascade(s) (4), Division modes or how to balance progenitor maintenance and recruitment (5), Lineage progression, conserved and changing progenitor properties over time (6), Environmental/systemic/large-scale populational regulation (7).

I collaborated on the reflections that guided the writing on Notch signaling pathway, and the construction of Figures 2, 4, 5, and 6.



ACADÉMIE  
DES SCIENCES  
INSTITUT DE FRANCE

# *Comptes Rendus*

---

## *Biologies*


Mathilde Chouly and Laure Bally-Cuif

**Generating neurons in the embryonic and adult brain: compared principles and mechanisms**

Volume 347 (2024), p. 199-221

Online since: 13 November 2024

<https://doi.org/10.5802/crbio.167>

 This article is licensed under the  
CREATIVE COMMONS ATTRIBUTION 4.0 INTERNATIONAL LICENSE.  
<http://creativecommons.org/licenses/by/4.0/>



*The Comptes Rendus. Biologies are a member of the  
Mersenne Center for open scientific publishing*  
[www.centre-mersenne.org](http://www.centre-mersenne.org) — e-ISSN : 1768-3238



Review article

# Generating neurons in the embryonic and adult brain: compared principles and mechanisms

Mathilde Chouly<sup>a,b</sup> and Laure Bally-Cuif<sup>\*,a</sup>

<sup>a</sup> Institut Pasteur, Université Paris Cité, CNRS UMR3738, Zebrafish Neurogenetics Unit, F-75015 Paris, France

<sup>b</sup> Sorbonne Université, Collège doctoral, 75005 Paris, France  
E-mail: [laure.bally-cuif@pasteur.fr](mailto:laure.bally-cuif@pasteur.fr) (L. Bally-Cuif)

**Abstract.** Neurogenesis is a lifelong process, generating neurons in the right amount, time and place and with the correct identity to permit the growth, function, plasticity and repair of the nervous system, notably the brain. Neurogenesis originates from neural progenitor cells (NPs), endowed with the capacity to divide, renew to maintain the progenitor population, or commit to engage in the neurogenesis process. In the adult brain, these progenitors are classically called neural stem cells (NSCs). We review here the commonalities and differences between NPs and NSCs, in their cellular and molecular attributes but also in their potential, regulators and lineage, in the embryonic and adult brains. Our comparison is based on the two most studied model systems, namely the telencephalon of the zebrafish and mouse. We also discuss how the population of embryonic NPs gives rise to adult NSCs, and outstanding questions pertaining to this transition.

**Keywords.** Neural progenitor, Neural stem cell, Zebrafish, Mouse, Pallium, Notch signaling.

**Funding.** ANR (Labex Revive), La Ligue Nationale Contre le Cancer (LNCC EL2019 BALLY-CUIF), Fondation pour la Recherche Médicale (EQU202203014636), CNRS, INSERM, Institut Pasteur, European Research Council (ERC) (SyG 101071786 - PEPS), ED Complexité du Vivant, Sorbonne Université, LabEx Revive.

*Manuscript received 31 August 2024, revised 6 October 2024, accepted 9 October 2024.*

## 1. Introduction

There are an estimated 100 billion neurons in the adult human brain, 70 million in the adult mouse, 10 million in the adult zebrafish [1, 2]. Brain neurons control most body activities, including sensory, motor, autonomic, emotional and executive functions. How were they generated, and when? Are there common rules?

The generation of neurons, referred to as neurogenesis, is a multistep and gradual process that originates from a neural progenitor cell and ends with the formation of a mature cell capable of network

communication, the neuron. Along the way will occur cell divisions, commitment to a neuronal fate, entry into the postmitotic state, detachment and migration away from the progenitor territory, and the acquisition of neuronal characteristics such as electrical excitability, neurotransmitter(s) synthesis, an elaborated polar morphology including axon and dendrites, and connectivity with other cells (Figure 1A). The sequential order of these steps is not fixed, and the neurons generated are highly diverse, in identity, morphology, plasticity, circuit and function. Increasing this diversity, neurogenesis is a lifelong process, taking place from embryo to adult. As such, acquiring a comprehensive understanding of neurogenesis regulation is an immense task (for recent reviews, see [3–5]).

\* Corresponding author



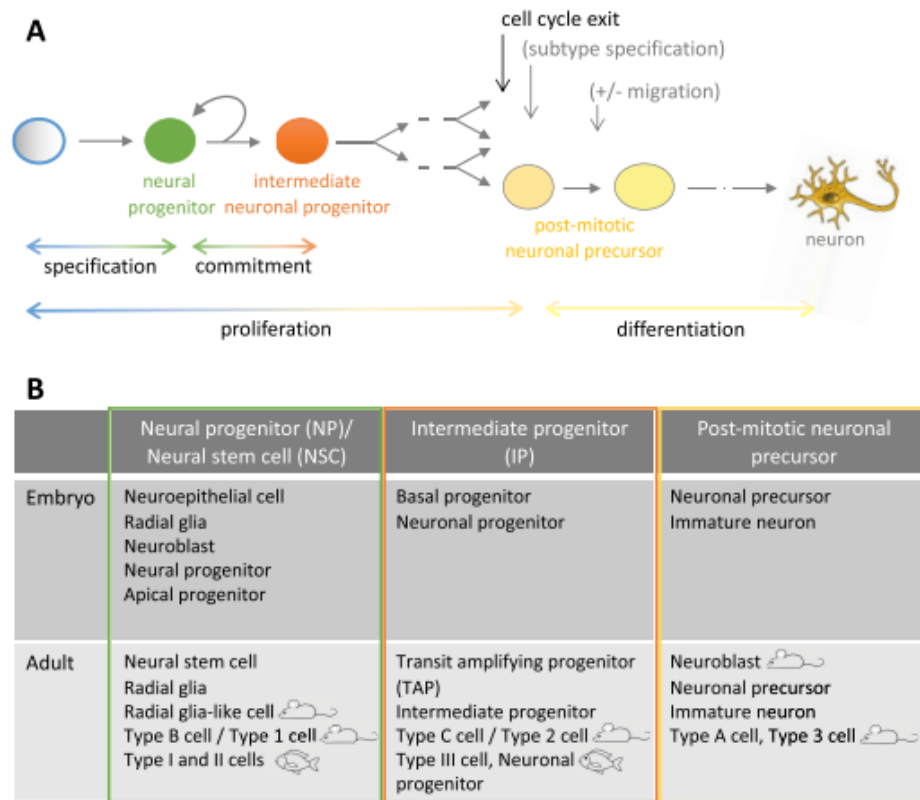


**Figure 1.** Neurogenesis steps and nomenclature. (A) Progression of neural progenitors along the neurogenic lineage (from left to right). The relative order of cell cycle exit and neuronal subtype specification is not fixed. (B) Cell types encompassed by the nomenclature NP/NSCs, IPs and precursors in the embryonic vs. adult brain and in mouse vs. zebrafish.

The present review will focus on the early steps of the neurogenesis process, which cover the transition from a progenitor to the post-mitotic and committed neuronal precursor. These initial events largely control the location, timing and extent of neuronal generation. As a driving thread, this review is also a comparative analysis of embryonic and adult neurogenesis processes, with focus on Notch signaling, the major regulatory pathway controlling neurogenesis during a lifetime [4, 6]. This is because general principles are better extracted from comparisons, and also because current translational research places high hopes in the manipulation of neural progenitors or in vitro models of embryonic characteristics to understand or ameliorate adult pathologies of neurons

loss. Finally, it will largely make use of knowledge gained from the teleost fish model *Danio rerio* (zebrafish) which, among other practicalities, offers the unequalled possibility to film neurogenesis “in situ” in vivo in both the embryonic and adult brain under fully non-invasive conditions, thanks to the transparency of its embryos and of some pigmentation-deficient adults [7–11]. We will, of course, refer to other models, in particular the mouse, when the latter led to the principles discovery or when interspecies comparisons add to the extraction of principles. As much as extracting shared and divergent neurogenesis principles between the embryonic and adult brain, we will aim to identify remaining key questions in the field.

## 2. Neural progenitor cells

### 2.1. Definitions

There is extensive work, associated with diverse and sometimes subtle nomenclature differences, to characterize the progenitors at the origin of neurons in diverse brain locations, time points or species. For clarity, we will adopt a simple rule here, which essentially reflects time, during life or along lineage progression. This nomenclature is placed alongside others in Figure 1B. In sum, we will refer to neural progenitors (NPs) when cells can generate both neurons and glial cells and their long-term neuron-generation potential is either limited (typically a few weeks in a vertebrate model species such as zebrafish or mouse) or unknown, to neural stem cells (NSCs) when cells can generate both neurons and glial cells but their long-term potential is extensive (typically a few months or more), and to intermediate neuronal progenitors (IPs) for the proliferating progeny of NPs or NSCs, that will exclusively generate neurons and will exhaust at short term. With this nomenclature, neurogenesis occurs in the order NP > IP > neuron or NSC > IP > neuron, and typically, NSCs are an adult cell type, while NPs refer to neural progenitors in the embryo. Indeed, even if some NPs have been shown to give rise to adult NSCs and are therefore long-lived (see below), not all of them do, and it is generally impossible to distinguish between these fates at the time of observation.

### 2.2. Neuroepithelial cells and radial glia

#### 2.2.1. Neural progenitors of the embryonic neural tube

Neural progenitors (NPs) of the embryonic neural tube are apico-basally polarized cells arranged in a monolayer bordering the neural tube lumen (ventricle) (Figure 2A,B) (reviewed in [12, 13]). Their apical membrane, in contact with the cerebrospinal fluid, is characterized by several specialized structures, such as a primary cilium pointing into the lumen, a Cadherin ring, and junctional complexes [14–17]. The latter include tight junctions marked by the Zona Occludens 1 (ZO1) protein that connect with adjacent progenitors at their apico-basal interface and seal the neural tube lumen. Their basolateral membrane is elongated and connects with the pial surface of the neural tube. At early developmental stages

(tail bud to a few somite-stage in zebrafish, E7-E8 in mouse), neural progenitors are neuroepithelial cells (NE) (Figure 2A), readily specified from the neuroectoderm. They express transcription factors that sign both their neural and their progenitor states, such as Sox2 or Hairy/Enhancer-of-Split (Hes/Her) family members [18–20]. As neurons become generated and the neural tube thickens, the basolateral membrane of progenitors elongates. The acquired radial morphology is associated with the expression of astroglial markers in addition to progenitor markers, hence the name of radial glia (RG) (Figure 2B). These markers include intermediate filaments (Vimentin; Glial fibrillary acidic protein, GFAP) and the Brain lipid binding protein (BLBP). Both NE and RG cells are actively dividing and exhibit the characteristic feature of interkinetic nuclear migration (INM), where the nucleus transits from apical to basal positions and back within the cell body as a function of cell cycle phases [12, 21]. Cytokinesis events occur apically along the ventricular plane, and INM is believed to avoid steric hindrance in this location for progenitor division to take place. Embryonic NE and RG are very similar between species, although, compared to mouse, zebrafish NE polarize relatively late and express glial markers almost from their onset [22], the transition from NE to RG is therefore blurred.

#### 2.2.2. Neural stem cells of the adult brain

Niches of constitutive neurogenesis have been identified in the adult brain in all vertebrates studied to date (with ongoing controversies for the human brain), although major differences exist in their location and extent, activity, and lifetime. For example, these niches are restricted to the forebrain in mouse, with three major sites described that are especially active in the young adult: the ventricular-subventricular zone of the lateral ventricle (vSVZ, also called sub-ependymal zone, SEZ) (Figure 2C), the sub-granular zone of the dentate gyrus of the hippocampus (SGZ), and the ventricular wall of the hypothalamus [23–25]. In contrast, neurogenic niches exist in all brain subdivisions in the adult zebrafish as well as in the retina and are active until a comparably late age (considering the fact that the two species have the same lifespan) [26–28]. A major niche that has been extensively studied is located in the pallium (dorsal telencephalon) (Figure 2D). We will restrict the following discussion to the forebrain.

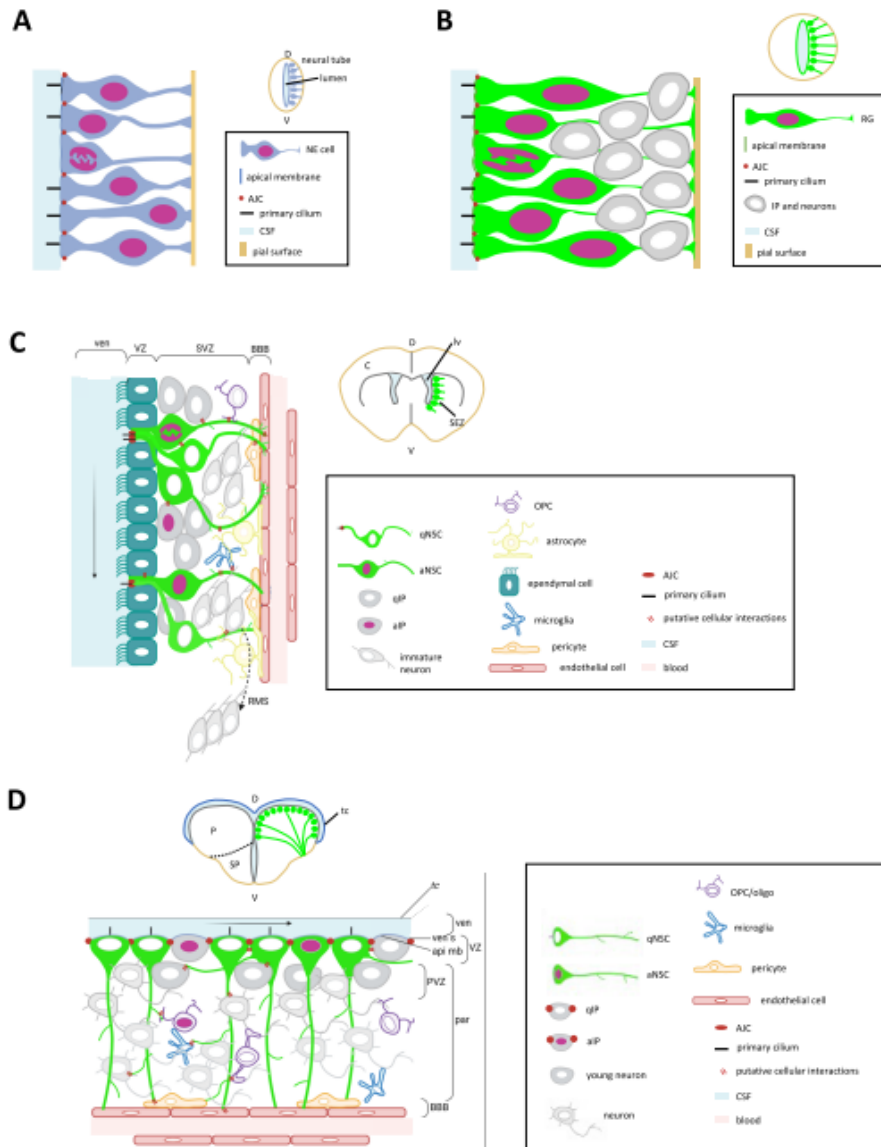


**Figure 2.** Morphology of NPs/NSCs and architecture of the neurogenic niches in the embryonic vs. adult brain and in mouse vs. zebrafish. (A–D) Schematic high magnification views of the cytoarchitecture of the ventricular zone when observed in cross sections (main panels), whole forebrain in cross-sections (small panels), and legends for colors and structures (boxed). (A,B) NPs at early embryonic stages (A) are neuroepithelial progenitors (NE), they transform into radial glia (RG) at later embryonic stages (B).

**Figure 2. (cont.)** (C,D) NSCs in the subependymal zone of the mouse adult brain (C) and in the zebrafish pallium (D) are RGs. Abbreviations: a, activated; AJC, apical junction complex; api mb, apical membrane; BBB, blood–brain barrier; C, cortex; CSF, cerebrospinal fluid; D, dorsal; IP, intermediate progenitor; lv, lateral ventricle; NE: neuroepithelial cell; OPS, oligodendrocyte progenitor cell; P, pallium; par, parenchyma; PVZ, periventricular zone; q, quiescent; RG: radial glia; RMS, rostral migratory stream; SEZ, subependymal zone; SP, subpallium; SVZ, subventricular zone; tc, tela choroidea; V, ventral; ven, ventricle; ven s, ventricular surface; VZ, ventricular zone.

The majority of NSCs across species are radial astroglia, frequently referred to as RG-like cells [29]. In most niches except the SGZ, which is not ventricular, they maintain an apical contact with the brain ventricle and cerebrospinal fluid. During interphase, this apical membrane bears a primary cilium. The RG basal process contacts the pial brain surface (in the case of small-sized brain territories) or blood vessels at specific interfaces contributing to the blood–brain barrier yet permitting systemic communication to NSCs [7,30]. This basal process is generally extensive and highly branched sub-apically or deeper into the parenchyma. Non-radial astroglial NSCs also coexist with radial NSCs in the SGZ, in slightly lower proportions [31, 32]. Finally, like in the embryo, NE-like cells with long-lasting neurogenic capacity, hence NSCs, have also been described in the adult zebrafish brain. These different NSC subtypes share expression of generic progenitor markers (e.g., Sox2) with variations for others [33,34]. Astroglial markers, such as cytoskeletal elements (Glial Fibrillary Acidic Protein, GFAP; Nestin; S100beta in zebrafish), Fatty Acid Binding Proteins (e.g., Brain Lipid Binding Protein, BLBP), or metabolic enzymes (e.g., Glutamine Synthase, GS) also characterize RG-like and non-radial glial NSCs, with some regional differences [35]. It is important to note, however, that these markers are often shared between physiologically neurogenic vs. non-neurogenic cells types (e.g., between RG-like cells and astrocytes in mouse) and should be associated with functional assays assessing self-renewal and neurogenesis potential, at least at the population level, to be conclusive.

### 2.2.3. Markers and properties

The overlaps and specificities of markers of NPs, NSCs and NEs are listed in Figure 3. The glial markers expressed by embryonic RGs encode factors relevant for known astroglial functions, such as glutamate synthesis and metabolism. This suggests that

embryonic RGs may exert such roles in addition to their progenitor properties. This point becomes very relevant when considering adult NSCs, as a major functional difference is observed in adult forebrain astroglia between zebrafish and mouse. The zebrafish adult forebrain is devoid of parenchymal astrocytes [36,37]. As a counterpart, radial glia NSCs do express markers of mature astroglia, suggesting that they also are endowed with the dual properties of progenitor cells and astroglia [38]. In contrast, these functions are split between NSCs and parenchymal astrocytes, respectively, in the adult mouse forebrain. Hence, zebrafish NSCs appear multifunctional while mouse NSCs are specialized stem cells. It should be noted that several observations argue against the fact that zebrafish RG NSCs would simply correspond to RGs at an intermediate state of maturation, which would not have chosen yet between the NSC and astrocytic fates. First, adult zebrafish RG do exhibit adult-specific features such as a long quiescence phase (see below). Second, their markers of astrocytic functions are not or lowly expressed in RG at juvenile stages, attesting to a maturation since that stage [39]. Third, the choice towards an astrocytic fate in fact occurs at a relatively early stage of mouse embryonic development [40,41]. Extramural parenchymal astrocytes in the adult mouse striatum can however be recruited for neurogenesis following stroke or lesion, showing that astrocytes have conserved some neurogenic capacity although not under physiological conditions [42–44].

### 2.3. Take home message

The characterization of neural progenitor subtypes and their comparison in the embryonic and adult brain lead to a refined understanding of the NE to RG transition. NE and RG progenitors co-exist in the embryonic brain, as this transition affects most, but not all, NEs. They also co-exist at least in the zebrafish brain where they can still be observed at adulthood.

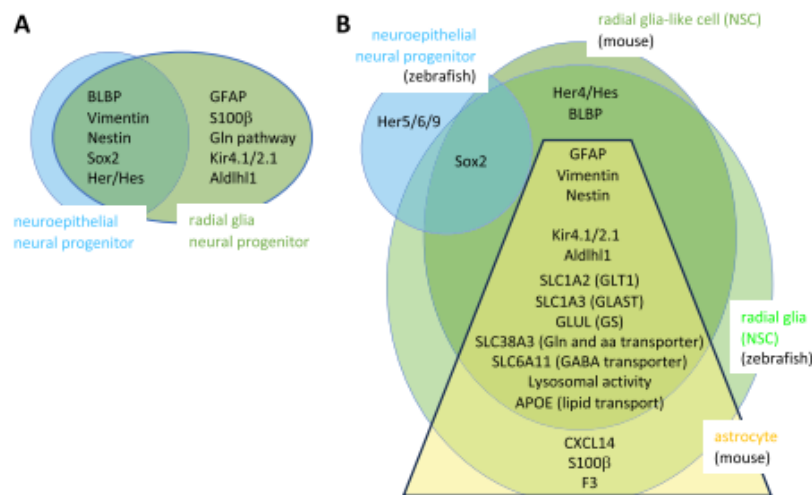


**Figure 3.** Radial glia markers in the embryonic and adult brain compared to other progenitors and astroglia in zebrafish and mouse. (A–B) Distribution of marker proteins between the different neuroepithelial and astroglial cell types in the embryo (A) and adult (B) in zebrafish and mouse (no species indicated when the markers are shared in both species). In B, the yellow trapeze including astrocyte genes in mouse reflects the expression gradient (low expression to high expression from top to bottom) of the encoded factors between radial glia-like cells (bona fide NSCs) and astrocytes (which are not neurogenic under physiological conditions).

Instead of RG, the adult mouse brain hosts specialized NSCs (RG-like cells) and parenchymal astrocytes. Counterintuitively, zebrafish RG NSCs express markers of mature astroglial function, which are the attribute of astrocytes but not RG-like NSCs in mouse.

### 3. Lineages and niches

Genetic tracing studies indicate that adult NSCs originate from embryonic NPs, as opposed to, for example, the dedifferentiation of mature neurons or glial cells in the adult brain. However, while embryonic NPs distribute broadly along the neural tube ventricle, in a pattern similar between vertebrate embryos in different species, adult NSCs are restricted to niches and display a species-specific distribution, much broader in zebrafish than in mouse. Furthermore, at both embryonic and adult stages, NE and RG cells occupy selective and exclusive locations. How are these patterns generated and their temporal evolution controlled between embryo and adult stages?

#### 3.1. A (constitutively) neurogenic lineage from radial glia

Embryonic RG give rise to adult RG NSCs in the adult forebrain of mouse and zebrafish (Figure 4). Specific embryonic RG have been traced genetically using Cre-lox recombination, for example using as drivers the *Gli1*, *Hopx* or *Nestin* promoters for SGZ precursors [45–48], promoters such as *Gli1*, *Hopx* (from post-natal day 1 onwards), *Gfap* or *Nestin* for SEZ precursors [45, 49–53], and the *her4* promoter for RG of the zebrafish adult pallium [33]. The question of whether embryonic RG NPs maintain, or not, a sustained neurogenic activity during the transition from embryo to juvenile to adult has been addressed recently. The use of conditional recombination in zebrafish, together with the fact that the neurons generated in the pallium over a lifetime neither migrate nor die at a detectable rate, made it possible to observe that neuronal clones issued from individual embryonic RG can expand continuously across the pallial parenchyme. These results demonstrate

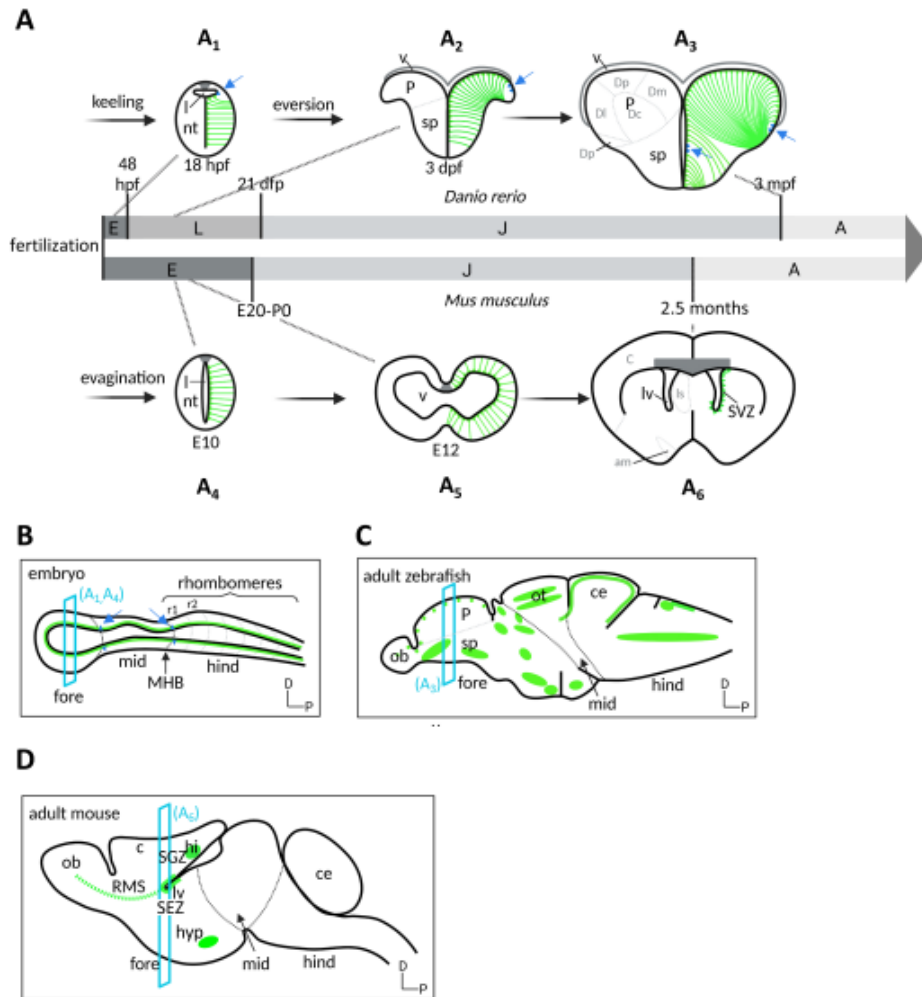


**Figure 4.** Embryonic to adult neurogenesis in zebrafish and mouse. (A) Temporal progression of neuroepithelial progenitors (NEs, blue), and radial glia NPs and NSCs (green), represented on schematic cross-sections (dorsal up) of the forebrain of zebrafish ( $A_1$ – $A_3$ , top) and mouse ( $A_4$ – $A_6$ , bottom) over a lifetime. Temporal nomenclature: E, embryo; L, larva; J, juvenile; A, adult; hpf, hours post-fertilization; dpf, days post-fertilization; E, embryonic day post-fertilization. In the zebrafish telencephalon, the formation of an initially compact neural rod (process referred to as “keeling”) is then followed by the lateral expansion of the dorsal neural territories and tela choroidea (process referred to as “eversion”). In contrast, evagination takes place in mouse to create the central canal. (B–D) Location of neurogenic niches (RG, green; NE: blue triangles, also indicated by blue arrows) on schematic sagittal sections of the brain in a prototypical mouse or zebrafish embryo at mid-embryogenesis (B) and in the zebrafish (C) and mouse (D) adult brains (anterior left, dorsal up). Section planes (blue) correspond to the cross-sections in A.

**Figure 4. (cont.)** Territorial nomenclature: am, amygdala; c, cortex; ce: cerebellum; Dc, central pallium; Dd, dorsal pallium; Dl, lateral pallium; Dm, medial pallium; Dp, posterior pallium; hi, hippocampus; hyp, hypothalamus; l, lumen; lv, lateral ventricle; mid: midbrain; MHB: midbrain–hindbrain boundary; fore: forebrain; hind: hindbrain; nt, neural tube; P, pallium; ob: olfactory bulb; ot: optic tectum; r1/2, rhombomeres 1 and 2; sp, subpallium; RMS, rostral migratory stream; SEZ, subependymal zone; SGZ, subgranular zone; v, ventricle.

the existence of RGs that maintain *her4* expression from embryo to adult and are continuously neurogenic, showing that a continuous neurogenic lineage ensures the transition from embryonic RG NPs to adult RGL NSCs [33, 54]. The same conclusion was later reached in the mouse dentate gyrus for SGZ NSCs [50]. The SEZ appears to contrast with this situation, as embryonic RG along the 4th ventricle and destined to populate the SEZ enter quiescence at an early stage [51, 52, 55]. Whether this reflects a bona fide interruption of neurogenesis between embryonic stages and adulthood, a heterochronic quiescence entry between brain territories, or an RG behavior that may have been missed in other brain territories, remains to be assessed precisely.

### 3.2. An embryonic to adult NE lineage at the origin of radial glia, neurons and growth

NE populations are positioned at the boundary between neural tube subdivisions at mid- to late embryogenesis (Figure 4B) [56]. A few of them have been reliably traced in the zebrafish using genetic Cre-lox labeling, and shown to contribute to the persisting NE NSC populations identified in the juvenile or adult zebrafish brain. For example, the small *her9/her6*-positive NE population located on the dorsal midline at the tel-diencephalic junction in the 24-h embryo contributes to the NE population found along the postero-lateral edge of the adult pallium (Figure 4C) [33]. Considering the morphogenetic eversion of the pallium taking place in teleosts [57], this location in the adult telencephalon does indeed correspond to the remnants of the dorsal midline, at the junction with the choroid plexus. In the adult pallium, this NE pool expresses *her9*, is highly proliferative, generates neurons and more of itself by amplification as well as neurogenic RG NSCs that leave the NE zone to contribute to the progressive enlargement of the RG population of the pallial ventricle [33]. A similar scenario was described

for *her5*-positive NE progenitors at the midbrain–hindbrain boundary: embryonic NE progenitors located at the MHB contribute to the NE NSC pool at the adult MHB, which generates neurons and neurogenic RG NSCs that settle away from the NE pool in an age-dependent order [34]. As such, embryonic and adult NEs are lineage related, and play multiple functions: they are neurogenic lifelong generators of RG NSCs, and amplification centers that act as growth zones. While NE pools are also found in the mouse embryonic neural tube [58], their adult equivalents have not been analyzed as such. The cortical hem, however, is in a homologous location to the tel-diencephalic dorsal NE pool in zebrafish, and contributes neurons and scaffold glial cells to the hippocampus [5, 59]. Whether a NE remnant can also be found in this location has not been studied.

### 3.3. Sculpting NP and NSC niches

In the embryonic neural tube, RG and NE NP populations occupy alternating domains along the antero-posterior axis (and along the dorso-ventral axis in the hindbrain and spinal cord), with RG pools located in the center of neural tube subdivisions while NE pools are located at neural tube boundaries [56]. This organization corresponds to an alternation between actively neurogenic (RG) domains and domains of delayed neurogenesis (NEs) which in fact already pre-exists in the very early neural plate, prior to the NE > RG transition that affects most NEs at mid-embryogenesis and is prefigured in the expression domains of *her/Hes* genes. As such, NP activity becomes patterned according to the general vertebrate body plan, contributing to the generation of the segmented embryonic neuronal scaffold of the larva, which controls early larval functions.

As discussed above, the lineage relation between embryonic and adult RGs on the one hand, and embryonic and adult NEs on the other hand, imparts a spatial organization to NSC niches in the adult

brain. In addition, in mouse, many RG populations become exhausted due to terminal differentiation, leading RGL NSCs to persist in even more restricted locations (Figure 4D). A typical example is that of the cortex: embryonic RG NPs terminate neurogenesis and terminally differentiate into astrocytes around E18 [60], and this contributes to isolating the SEZ and SGZ and non-contiguous neurogenic niches in the forebrain. Together, the spatial organization of adult NSC niches in the adult brain appears in part inherited from the lineage relation between NPs and NSCs, plus an exhaustion of some RGL pools between embryo and adult. This exhaustion varies between species, it is prominent in mouse and restricted in zebrafish. Of course, positive local cues (the so-called “niche”) also promote the persistence of adult neurogenic niches, such as in the SGZ and SEZ [61].

### 3.4. *Take home message*

NSCs are progeny cells of embryonic NPs. A comparative view of NP spatial organization in the embryo and adult sheds an ontological perspective on the spatial pattern of adult neurogenic niches, showing that it integrates a combination of events: spatial events that pattern the embryonic neural tube and impart progenitor properties that have long-term consequences on their progeny NSCs, and species-specific temporal events of local progenitor exhaustion, that further refine NSC niches to restricted domains in the adult brain.

## 4. The embryonic and adult neurogenesis cascade(s)

A primary molecular cascade controlling neurogenesis commitment is Notch signaling. It has been extensively studied and reviewed, in particular for its universal impact on embryonic neurogenesis [4, 54, 55]. The idea here is to mostly highlight its shared and divergent features between embryonic and adult neurogenesis, and to stress unknowns.

### 4.1. *Neurogenesis drivers*

In embryonic NPs, major neurogenesis drivers are basic Helix-Loop-Helix (bHLH) transcription factors of the Neurogenin (Neurog), Atonal (Ato), Achaete-Scute (Ascl) and NeuroD (specifically Neurod4)

families [62]. These factors trigger the expression of a cascade of differentiation factors (such as Neurod1, 2 or 6) and effectors of neuronal functionality or identity (cytoskeletal elements, axonal differentiation, synaptic components, neurotransmitters etc) [63–66]. Importantly, they are also the prime activators of expression of Notch ligand genes, thereby triggering Notch signaling [67]. Expression of proneural transcription factors is itself driven by neural Sox proteins such as Sox4 and Sox11, themselves signing neuronal engagement within permissive domains positive for Sox2 [68, 69]. Key parameters of this transcription factors cascade are its timing and tempo relative to other events such as cell cycle exit, progenitor delamination from the neural tube ventricle, and migration. The activity of proneural proteins is also modulated by phosphorylation, which can involve Cyclin-dependent kinases (Cdk) and hence be linked with cell cycle length. In particular, lower Cdk levels and cell cycle lengthening with age as embryogenesis progresses provide a window of opportunity for lower proneural protein phosphorylation levels and increased neurogenic efficiency [70]. In addition, proneural proteins are important counteractors of Notch signaling, discussed below.

### 4.2. *Notch signaling principles, actors and effectors*

Notch signaling is a cell–cell communication cascade, the outcome of which is to jointly regulate the state or fate of communicating cells. It is based on the interaction between a set of transmembrane receptors (Notch proteins [Notch1–4 in mammals, Notch1a, 1b, 2 and 3 in zebrafish]) and transmembrane ligands (Delta proteins [Dll1–4 in mammals, Delta-Delta in zebrafish] and Jagged proteins [Jag1–2 in mammals, Jag1a, 1b and 2 in zebrafish]). When expressed by contacting cells, the interaction between Notch and its ligand triggers the transmembrane cleavage of Notch to generate an intracellular fragment (NICD) that translocates to the nucleus, binds its interactor RBPj, and regulates transcription. This pathway has been extensively reviewed (for example: [71–74]).

Multiple levels of regulation exist that involve post-translational modifications of Notch and its ligands, intracellular trafficking, degradations and recycling, and mechanical forces, that have been



reviewed [75–78]. An important feature here is that transcriptional Notch signaling is direct and non-amplified, i.e., the receptor itself serves as the transcriptional regulator, and one molecule of engaged receptor generates one molecule of NICD. Variations in the outcome are encoded by the Notch receptor used, the specific ligand–receptor pair that is engaged (see example below), the levels of available receptors and ligands, the specific dynamics of NICD interactions with the chromatin, and the cellular context (for example, the RBPJ-bound loci open in a particular cell state, or the set of interactors available for Notch signaling targets). Another important feature of the pathway is that Notch signaling is an auto-consolidating system, as one output of signaling is to (directly or indirectly) enhance the expression of the receptor and ligand themselves.

General NICD/RBPJ transcriptional targets are genes encoding transcription factors of the E(spl)/Hairy family (Hes and Hey in mammals, Her and Hey in zebrafish). These are basic helix–loop–helix (bHLH) transcriptional inhibitors that dimerize or pair with the ubiquitous bHLH protein E42 to downregulate target genes at E-boxes (CANNTG sequences) [63, 79, 80]. They themselves are among their main targets, thus terminating signaling. Some NICD/RBPJ bound sites have been identified in mouse; in the context of embryonic NPs, they also include microRNA miR-9, itself an inhibitor of the neural progenitor state [81]; in adult NSCs, they include the progenitor gene Sox2 [82]. In the context of embryonic NPs and neurogenesis, Hes/Her themselves also inhibit expression of proneural genes. Because proneural proteins also positively control the expression of Notch ligands, this contributes to the consolidation of unidirectional Notch signaling. It is to note that, among all these interactions, very few direct transcriptional regulations have been formally demonstrated.

The main process involving trans interaction of Notch and a ligand is lateral inhibition [83, 84]. In embryonic NPs, it is classically initiated by the expression of a proneural factor, which upregulates expression of a Notch ligand. Signaling to a contacting Notch-expressing NP drives Hes/Her expression which in turn down-regulates expression of proneural and Notch ligand genes. This regulatory mechanism imparts and stabilizes distinct committed vs. progenitor fates to the Notch signaling vs. receiv-

ing cells, respectively. A contrasting trans-regulatory process, lateral induction, has also been described in embryonic NPs [85, 86]. There, Notch signaling in the receiving cell triggers expression of a Notch ligand, which propagates signaling to the neighboring cell, and so on from one cell to the next. This regulatory mechanism propagates a cell state across a cell population and has been described for example to define proneural domains of the embryonic inner ear [87]. Classically, lateral induction involves the Jagged ligand and an Hey1 effector, while lateral inhibition preferably relies on Delta ligands and Hes/Her. Finally, Notch and its ligands can also interact in cis, i.e., when expressed in the same cell [88]. Cis interactions decrease the number of receptors or ligands free to engage in trans interaction, thereby regulating the directionality and intensity of trans signaling.

#### 4.3. Embryonic and adult neurogenesis: Notch signaling compared

Neurogenesis proper, i.e., the generation of a non-stem committed progenitor that further progresses towards the neuronal fate, is a transient event in the life of an adult NSC, which spends most of its time in quiescence (Figure 5A). Neurogenesis commitment can take place in association with NSC activation and division (in one or both daughter cells from a mother NSC), or independently of division. The latter case has been described in the zebrafish adult pallium where quiescent NSCs were observed to lose their astroglial character, delaminate from the ventricular zone and directly differentiate into neurons [10, 11, 89]. The mechanisms of direct differentiation remain unknown, and we will focus here on the generation of IPs from NSCs post-division.

Embryonic RG NPs use Notch signaling when engaged in neurogenesis. The main proneural factors used in the forebrain are Neurog1 (ventrally) and Ascl1 (dorsally), and the main signaling players recruited are Notch1, DeltaA and Her4 in zebrafish (and Notch1, Dll1 and Hes1 in mouse). Other pathway members can be co-expressed, with partially redundant roles. For example, in the mouse embryo, it is necessary to knock-out the three genes *Hes1*, 3 and 5 to fully block neurogenesis [91]. Likewise, in the zebrafish embryo, single mutants have partial phenotypes (e.g., [92, 93]). In adult neurogenic niches, dividing NSCs express Notch1 and Her/Hes factors,

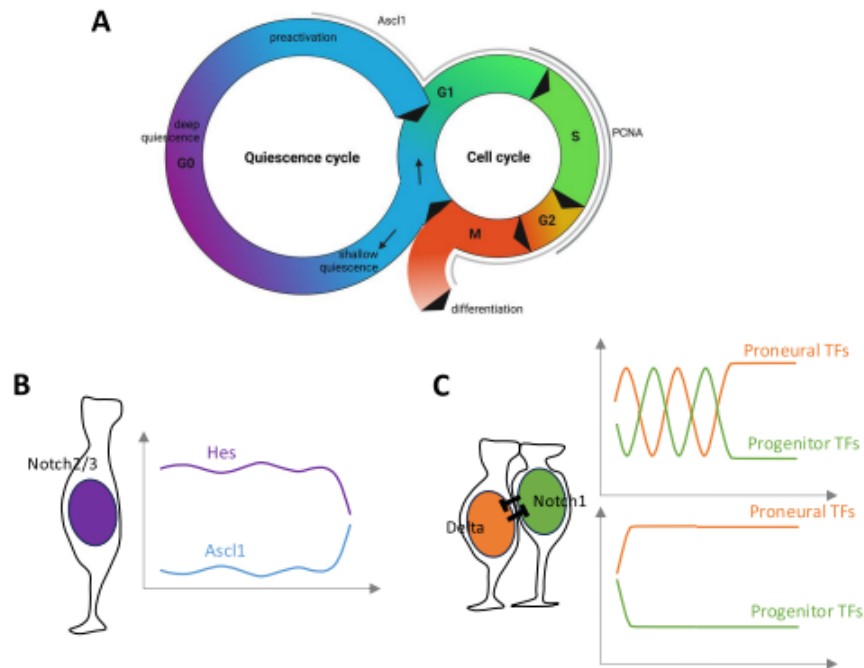


**Figure 5.** Cycling states, Notch signaling and fate choices during embryonic and adult neurogenesis (A). Quiescence (G0) and mitotic (G1-S-G2-M) cycles in neural progenitors. In the embryo, NPs are constantly cycling. In the adult brain, NSCs spend most of their time in quiescence and only infrequently activate to enter the mitotic cycle. (B) Adult NSC in quiescence, and levels of Hes and Ascl1 proteins (after [90]); quiescence is promoted by Notch2/3 signaling. (C) Fate choice in embryonic NPs or activated NSCs post-division. These choices involve Notch/Delta signaling where Notch1 is the primary Notch receptor. Signaling can be oscillating (top) or, as is probably the case for intralinear inhibition, directly oriented (bottom).

and the conditional invalidation of *Notch1* or *RBPj* in adult NSCs in the mouse SEZ and SGZ leads to NSC loss and differentiation [82,94,95]. Likewise, invalidation of *notch1b* in the zebrafish adult pallium leads to a loss of dividing NSCs and an increased production of neurons [96]. The key proneural factor expressed in the adult mouse SGZ and SEZ in dividing NSCs is *Ascl1*, and its direct requirement for the acquisition of the neuronal fate is discussed (see below). In the adult zebrafish telencephalon, where neurogenesis is found both in the subpallium and pallium, expression of *neurog1* and *ascl1a* is found in subpallial and pallial NSCs [97–100]. Thus, NPs and NSCs engaged in neurogenesis largely use

similar neurogenesis pathway components, suggesting that the neurogenesis process involved during terminal division in NSCs mimics the one at play in embryonic NPs.

In addition, NPs and NSCs of the embryonic and adult brain rely on the molecular oscillatory properties of the Notch pathway to promote the generation of committed progenitors (Figure 5B,C) (recently reviewed in [101, 102]). Molecular oscillations are primarily driven by the self-inhibition of Her/Hes proteins, which inhibit their own transcription. In embryonic NPs, this leads to an oscillatory production of Her/Hes proteins with a period of ~2–3 h. In turn, these oscillations drive offset oscillations of

proneural factors. Current evidence in the mouse and zebrafish embryos suggests that these oscillations of antagonistic fate drivers maintain NP in a plastic state poised for a fate decision, whether to remain an NP by stabilizing Notch signaling, or to commit to neurogenesis by stabilizing proneural expression. Several mechanisms have been postulated to underlie this final choice. Among them, microRNA-9 (miR-9), itself in a negative transcriptional feedback loop with Her/Hes factors but whose stability permits accumulation, may serve as a dose-dependent “clock” mechanism that will tilt the equilibrium towards neuronal commitment when above a threshold [103]. Another parameter is cell cycle length, which increases with time thereby allowing changes in the activity of proneural factors and/or cell cycle exit decisions (see below).

Most interestingly, alternating oscillations of Hes1 and Ascl1 proteins have also been observed (by means of Hes1-Venus and Ascl1-Venus fusion proteins using the endogenous *Hes1* and *Ascl1* loci) in dividing adult NSCs of the mouse SGZ [90, 104, 105]. The experimental induction of Ascl1 oscillations drives NSCs to enter the cell cycle and permits neurogenesis, and Ascl1 itself is absolutely required for NSC proliferation [106, 107]. Compared to embryonic NPs, it is less clear in adult NSCs whether Ascl1 itself encodes the neuronal fate, given that it appears very transiently expressed in IPs [31, 108], and that its overexpression rather induces oligodendrogenesis [109, 110]. It also remains unclear how oscillations drive proliferation, and how they are initiated and stopped. Regarding proliferation, the co-expression of Ascl1 and NICD may render the regulatory elements of proliferation genes accessible to Ascl1, as observed in embryos [111]. Regarding the initiation of oscillations, it was noted that the *Ascl1* mRNA is in fact expressed at low levels in most NSCs but is not productive due to post-translational destabilization of the Ascl1 protein [107]. This block is relieved pre-division, and this release may be sufficient to initiate a default oscillatory behavior. Finally, it is interesting to note that Notch1 seems to be the primary Notch receptor involved in progenitor maintenance during the activated phase of adult NSCs, both in mouse and zebrafish [96, 112]. Together, these observations highlight similarities between embryonic NPs and the activated and neurogenic state of adult NSCs.

#### 4.4. Cell cycle length and cell cycle exit

In embryonic NPs, neuronal commitment and cell cycle exit are not necessarily concomitant but are coupled in several ways. First, the progressive lengthening of the cell cycle and decreased Cdk activity during embryogenesis permit the accumulation of non-phosphorylated Sox2 (less active) [113] and proneural proteins (more active) [70], thereby promoting the switch from the progenitor to the differentiated state. Cell cycle lengthening itself depends on a Cdk-independent function of mitosis phosphatases such as Cdc25b [114]. In turn, proneural proteins, in addition to commitment, can control the expression of cell cycle components. This is the case of Ascl1 in mouse NPs in culture where, depending on the presence or absence of Notch signaling in its expressing cell, it can activate the expression of cell cycle-promoting genes (e.g., *CyclinD1*) or of genes inhibiting cell proliferation [111]. Second, Cyclins can also participate in transcription complexes and/or directly bind DNA to control the expression or activity of commitment proteins. For example, CyclinD1 can associate with (and inhibit) NeuroD [115].

In adult NSCs, direct neuronal differentiation events from quiescent NSCs have been observed [10, 11, 89]. The mechanisms of this fate decision, which temporally uncouples commitment from cell cycle exit, remain to be identified. For IP-generating NSC divisions, daughter cell fate choice is generally not made between cycling and commitment, but rather between quiescence (G0) and commitment. We note, in the mouse SEZ, the important role of two Cyclin-dependent kinase inhibitors, p21 and p27. p21<sup>Cip</sup>, in addition to its cell cycle-related function, inhibits expression of *BMP2* and *Sox2*, preventing the exhaustion of SEZ NSCs otherwise taking place through excessive expansion or astrocytic differentiation, respectively [116, 117]. These inhibitions involve Cdk-independent functions of p21, including direct binding to the *Sox2* enhancer. In epithelial cells in culture, endogenous p21 levels, which accumulate in G2, bias the fate of daughter cells towards G0 vs. G1 [118, 119]. So far however, this was not reported in adult NSCs. In the SGZ, p27 is necessary for NSC quiescence and for cell cycle exit of IPs through its regulation of the cell cycle [120], but it also directly binds to (and inhibits)

the *Sox2* promoter to promote the transition of IPs to differentiation [121].

In the context of the relation between cell cycle components and commitment, one key issue in both embryonic NPs and adult NSCs is to understand how a different choice between commitment and progenitor NP/NSC maintenance can be imparted in sister cells, in the case of asymmetric divisions. Rather than driving self-renewal or commitment, the factors above may open susceptibility states prone to fate choices, which are then made in daughter cells following intralineaage or environmental cues (see below).

#### 4.5. *Take home message*

Notch signaling, Hairy/E(Spl) factors and proneural proteins are major determinants of the choice between progenitor maintenance and neurogenesis progression in both embryonic NPs and active adult NSCs. These pathways are intertwined with cell cycle regulatory components to coordinate cell cycle exit and lineage progression. The quiescence state of adult NSCs complexifies this regulation by introducing a triple choice post-division: to re-divide, to re-enter quiescence, or to commit.

### 5. Division modes or how to balance progenitor maintenance and recruitment

#### 5.1. *Division modes in embryonic NPs and adult NSCs*

We will consider here divisions relative to the generation of IPs (or neurons when there are no intermediates). Hence, NSC/NSC and NP/NP divisions will be called symmetric amplifying, NSC/IP or NP/IP asymmetric, and IP/IP symmetric differentiative.

In the embryo, NP divisions of the three types above were reported *in vivo* (Figure 6A). Typically, NE progenitors divide in a symmetric amplifying manner, enlarging the NP pool. In contrast, RG NPs divide asymmetrically to generate one RG and one IP or neuron [60, 122]. In the zebrafish embryo, this process has been filmed in the telencephalon and hind-brain [123, 124]. In addition, at early stages, at least in zebrafish, some NPs divide following a symmetric differentiative mode, generating two neurons used to build the first larval neuronal scaffold [125]. The corresponding NPs are therefore lost in the process.

Likewise, the three division modes take place in adult NSCs, in both the mouse and zebrafish fore-brain (Figure 6B) (reviewed in [27]). They have been directly observed using intravital imaging in the adult mouse SGZ and zebrafish pallium [10, 11, 89, 126–128]. Modeling clonal dynamics in the zebrafish adult pallium predicts that NSCs choose stochastically between these division modes, in specific proportions [89]. Intravital imaging tracking validated these predictions, both regarding proportions and the apparently random order in which symmetric amplifying and asymmetric divisions occurred in tracks with multiple divisions [126]. In contrast, in the adult mouse SGZ, intravital imaging revealed non-stochastic choices, e.g., the fact that symmetric amplifying divisions never followed asymmetric divisions [128].

#### 5.2. *Population vs. intralineaage fate regulations, and implications*

Daughter cell fate choices can be imparted by the mother cell (e.g., through the partitioning of fate determinants), organized between daughter cells post-division through intralineaage interactions, or biased in a non-cell autonomous manner by the surrounding cells or niche. To distinguish between these regulations, it is necessary to trace individual NPs/NSCs *in situ* and modify their signal sending or receiving properties. A major cell–cell signaling pathway involved is Notch.

In the embryonic neural tube, the division of individual NE progenitors has not been tracked; however, the fact that Notch signaling—at least in the mouse neural tube—becomes active at a relatively late stage, after the initial NE amplification phase, strongly suggests that a lateral inhibition process takes place between adjacent NEs irrespective of the closeness of their relationship (Figure 5C, top, and Figure 6A) [129]. At the RG stage, blocking DeltaA expression in individual RG of the telencephalon leads to neuronal differentiation of all cells in each clone after just a few divisions, while control clones maintain a RG identity [123]. This approach prevents Notch signaling from occurring between clonally related cells but not with their non-clonally related neighbors (which express Delta, while cells of the clone express Notch), allowing to conclude that division asymmetry results from Notch signaling preferentially occurring

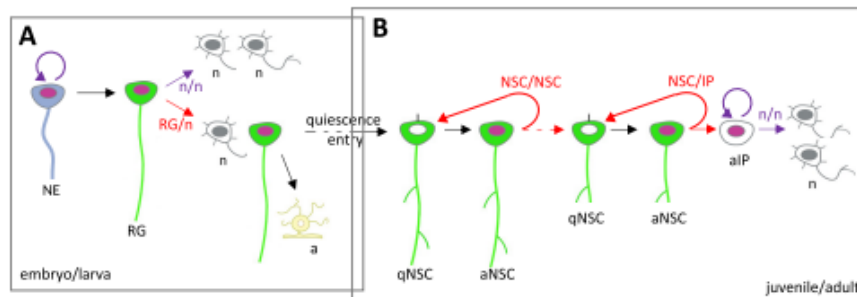


**Figure 6.** Lineage progression and division modes during embryonic and adult neurogenesis. (A) In the early embryo, NEs divide symmetrically, while the predominant division mode of RGs is asymmetric self-renewing to generate one RG and an IP or a neuron daughter. At late embryogenesis in the mouse, most RGs differentiate into astrocytes, and some enter quiescence to give rise to adult NSCs. In zebrafish, it is believed that most neurogenic RGs transit to the NSC state. (B) In the adult, NSCs undergo NSC/NSC-generating divisions. NSCs also progressively commit to give rise to NSCs that will generate IPs and, in turn, neurons. In the zebrafish adult pallium, an upstream self-renewing and asymmetric NSC/NSC division has been identified [126], likely responsible for the homeostatic maintenance of the NSC population. Symmetric divisions are drawn in purple, asymmetric divisions in red. Abbreviations: a, astrocyte; IP, intermediate progenitor; n, neuron; NE, neuroepithelial progenitor; aNSC, activated neural stem cell; qNSC, quiescent neural stem cell; RG, radial glia.

between sister cells. This has been called “intralineage regulation” (Figure 5C, bottom, and Figure 6A). It is likely also taking place in the embryonic hindbrain. Further functional assays demonstrated that it requires the asymmetric distribution of the Delta ubiquitin ligase Mindbomb (Mib), itself permitted by the asymmetric distribution of Par3 at division [123], which follows DeltaD-carrying recycling endosomes, in a complex that necessitates the centrosomal and endosomal protein PCM1 [130, 131]. In zebrafish (but not in mouse), Mib and Par3 are inherited by the future neuron. In a parallel set of studies, asymmetric distribution of DeltaD between sister cells was observed during RG division in the embryonic zebrafish hindbrain. DeltaD is transported by Sara endosomes, which are themselves partitioned unequally at division [132]. What prevents cells from interacting with their non-lineage related neighbors is not clear. It could be that the mechanisms involved in partitioning Notch–Delta signaling components between sisters at division dominate, in strength or speed, the establishment of other interactions. Asymmetric distribution of Dll1 protein was also observed (on static preparations using immunostaining) in dividing RGs of the mouse embryonic cortex.

The mechanisms that account for terminal division asymmetry (NSC/IP or NSC/neuron) in the adult brain have not been studied *in vivo* to date. In cell pair assays *in vitro*, asymmetric Notch signaling levels can be observed between mouse SEZ NSC daughters. This study identified that Pigment epithelium-derived factor (PEDF), possibly released by endothelial and ependymal cells of the niche, induces NFκB activation, which itself leads to release of inhibition at Hes1 and EGFR promoters, permitting Notch signaling and EGFR expression [133]. This mechanism, where differential proximity to PEDF might introduce asymmetries between sisters, is superimposed on the effect of the Dyrk phosphatase, which affects the stability of EGFR and decreases self-renewal [134]. In a possible link with this, asymmetric distribution of the Dll1 protein was observed in GFAP+ NSCs of the mouse SEZ [135]. In Dll1+ dividing mother cells (at pre-cytokinesis stages), an asymmetric distribution of Dll1 was seen in a majority of cases.

### 5.3. Take home message

The control of the NSC/NP division mode (in relation with the generation, or not, of an IP or neuron) re-

lies on a combination of intrinsic determinants, privileged sister-sister interactions or more general local cues. Notch signaling is an important regulatory pathway in all scenarios. Its implication in the control of division modes in adult NSCs *in vivo* remains to be formally demonstrated.

## 6. Lineage progression, conserved and changing progenitor properties over time

### 6.1. Commitment status along lineage progression during adult neurogenesis

Our recent work based on intravital imaging to track NSC behavior in the adult zebrafish pallium points to another level of complexity in the control of the NSC division mode. Indeed, symmetric NSC/NSC divisions were observed to generate differently fated NSC daughters (Figure 6B). Specifically, NSCs negative for the expression of the Notch ligand DeltaA ( $\Delta A^{neg}$ ) divide to generate one  $\Delta A^{neg}$  daughter NSC seemingly identical to its mother, and one daughter that switches on expression of deltaA ( $\Delta A^{pos}$ ) and will further divide at higher frequency to finally generate IPs [126]. The divisions of  $\Delta A^{neg}$  NSCs are therefore asymmetric in terms of NSC fate, splitting daughter NSCs between self-renewal and lineage progression. The mechanisms controlling this asymmetric division mode remain unknown. Furthermore, the division of  $\Delta A^{pos}$  NSCs was seen to generate daughters with progressively increasing levels of  $\Delta A$  expression, possibly indicating progressive neurogenesis commitment during divisions. These levels could differ between daughters, which may also signify different commitment levels. Although our understanding remains very limited, and heavily relies on our limited readouts of cell state or identity, these observations together raise the fundamental question of whether bona fide symmetric NSC divisions exist at all during adult neurogenesis.

### 6.2. The notion of self-renewal

The notion of self-renewal is associated with the definition of a NSC, hence largely with the adult context. Probing for it is however limited by our experimental readouts. Whether molecular, cellular or functional, these readouts are only very partial accounts of a cell's state. It is within the frame of these technical

limitations that  $\Delta A^{neg}$  NSCs of the adult zebrafish pallium are currently considered to self-renew (Figure 6B) [126], but more precise analyses of these cells in the long-term would be needed. In this context, ageing is an interesting aspect to study. Zebrafish pallial NSCs are described to activate less frequently in aged animals [136, 137], but NSC state under precise ageing conditions remains largely unexplored at the molecular level. Changes in activation frequency and potential have also been reported in aged NSCs in mouse [138–141]. However, self-renewal proper has not been studied in either species.

Embryonic NPs, except for those that will ultimately give rise to adult NSCs, are bound to exhaust after the generation of neurons. This can occur after a fixed number of asymmetric divisions, as described in the mouse embryonic cortex where RG undergo on average 8 divisions to generate 8–9 neurons [142]. It is difficult to imagine that daughter RGs arising at each division are strictly identical to their mother until the end, as some mechanism must register each round of cell division, and in fact, the duration of the cell cycle increases over time. In the mouse embryonic cortex and retina, the transcription factors expressed by NPs also change over time and divisions [143, 144], akin to the transcription factor series deployed to generate different neuronal subtypes during nerve cord or optic lobe neurogenesis during fly development [145, 146].

### 6.3. Quiescence and quiescence instatement

A striking feature of adult NSCs, compared to embryonic NPs, is their prolonged quiescence (Figure 5A) [147]. Thus, to initiate the neurogenesis process, adult NSCs first need to exit the quiescence state, and their quiescence/activation balance is an additional level of control compared to embryonic neurogenesis.

Adult NSCs are stalled in G<sub>0</sub>, in which they spend most of their time. In the adult mouse SGZ for example, tracing RG-like NSCs shows a mean duration between two cell cycles (for dividing NSCs) varying between 1 and 90 days [128], and this amounts to a doubling time of 124 days for the highly quiescent NSC subpopulation in the zebrafish pallium [126]. Several pathways were identified to control the quiescence/activation balance, among which Notch2/3 signaling, BMP signaling, and Id factors

promote quiescence [96, 148–153], while mTORC1 and EGF signaling and the transcription factor Ascl1 promote activation [107, 154–157]. In detail, the Notch ligand DeltaA is expressed by IPs in the adult zebrafish pallial niche, and IPs signal via Notch to prevent activation in contacting NSCs [158, 159]. As mentioned above, *deltaA* is also expressed in the subpopulation of NSCs engaged in neurogenesis, and these cells also maintain their quiescence via Notch signaling, possibly tempered by a cis-regulation by DeltaA [126]. In zebrafish, BMP4, produced by pallial neurons, acts in concert with Notch, possibly via the induction of expression of Id1 [150]. Id4 plays a similar role in mouse [149]. Notch signaling and Ascl1 are particularly interesting to consider in the context of this review, as they have been extensively studied in embryonic progenitors and permit a direct comparison. While Notch2/3 maintain quiescence, Notch1 is expressed in activated NSCs and maintains their progenitor potential, as the selective abrogation of Notch1 function triggers neuronal differentiation [94]. In parallel, low levels of Ascl1 transcription are found in quiescent NSCs, while higher and oscillatory expression of Ascl1 is sufficient to trigger activation [90, 106, 128]. Because the involvement of Notch1 and Ascl1 oscillations are reminiscent of neurogenesis control in embryonic NPs, these observations suggest that, at adult stage, activated NSCs engaged in neurogenesis recapitulate an embryonic process, and that new regulators have been superimposed on this initial embryonic regulatory cascade to encode the quiescence state in adult NSCs.

Quiescence duration is highly variable between NSCs, with overall much longer doubling times for NSCs of the *deltaA*<sup>neg</sup> self-renewing pool (123 days) than for the *deltaA*<sup>pos</sup> neurogenic pool (28 days) in the adult zebrafish pallium [126]. In addition, NSCs activate more or less rapidly upon Notch blockade, suggesting the existence of different quiescence depths [96]. Thus, compared to embryonic NPs, adult NSCs not only display a quiescence phase but different quiescence durations and/or depths. The regulation of this heterogeneity is only beginning to be unraveled. It is a complex task given that, in vivo, quiescence parameters such as duration are linked with NSC progression along the lineage, hence these aspects are difficult to disentangle.

Finally, it remains important to understand how quiescence is instated in NPs that transit to NSCs

during life. Classically, quiescence is measured at the population level as the proportion of NPs found in the non-activated state (PCNA<sup>neg</sup> or MCM2/5<sup>neg</sup>) at any given time within a population. With such measurements, quiescence became detectable between larval day 5 and 8 in the zebrafish pallium (50% PCNA<sup>neg</sup> RGs) to progressively increase during the juvenile period to finally reach adult levels (typically 5% of PCNA<sup>neg</sup> or MCM2/5<sup>neg</sup> NSCs) [160]. Individual NPs/NSCs have not been tracked, however, and they divide asynchronously. Thus, whether the increased proportion of PCNA<sup>neg</sup> or MCM2/5<sup>neg</sup> NSCs with age reflects the progressive increase of quiescence duration in each cell over time, or the asynchronous entry of individual cells into an adult-like duration of quiescence, cannot be concluded at this point. If, as suggested above, quiescence is the result of the recruitment over time of an additional molecular pathway (such as Notch2/3) by NPs, another open question is what triggers the expression of this pathway.

#### 6.4. *Take home message*

Lineage progression involves intrinsic changes in NP/NSC properties, affecting their commitment level, the identity of the neurons they generate, or, in the adult brain, the depth or duration of quiescence. These changes occur concomitantly and are experimentally difficult to disentangle. Another question that remains open is their relationship with cell division. Steps in lineage progression are often observed to take place concomitantly with cell division, e.g., with at least one daughter appearing to differ from its mother. However, whether lineage progression also occurs between cell divisions remains to be studied.

### 7. Environmental/systemic/large-scale population regulation

NPs/NSCs and the neurogenesis process are controlled by cell-intrinsic molecular and cellular events, as well as local cell–cell interactions, as discussed until now. On a larger spatial scale, NPs/NSCs are also embedded in a niche, which is a key regulator of their fate.

An important component contacting NPs and NSCs in both embryos and adults is the cerebrospinal fluid, largely produced by the choroid plexuses and

containing a spatially heterogeneous mix of bioactive molecules (notably hormones and growth factors), peptides and neurotransmitters that are either filtered from the blood or secreted by the choroid plexuses themselves, the supracommissural organ, tanycytes, or neurons. NPs/NSCs themselves release factors or vesicles into the CSF [161–163]. Many of these factors, whether brain-borne or blood-borne, in turn impact the proliferation or commitment of NPs/NSCs or downstream steps of the neurogenesis process. Steroid hormones, thyroid hormone, insulin, cortisol, growth hormone, FGF/EGF etc, have been the focus of intense study in this context. Hormones vary between the embryonic and adult contexts, also because in embryos some are mother-derived (released during pregnancy in mammals, or deposited in the oocytes in fish for example). They will not be discussed here as they do not affect the principles of neuron generation as such, but they are clear modulators of neurogenesis at the systemic level.

Additional to this external, systemic niche, our recent work in the zebrafish adult pallium led us to postulate the existence of a medium-scale “intrinsic niche” created, via spatiotemporal feedbacks, by NSCs and IPs [164]. By restricting NSC activation in the vicinity of lineage intermediates (IPs), a specific number of activated NSCs is permitted at any given time, and is positioned in physical space within the NSC population. Spatial modeling suggests that this regulation is important to avoid spatial drifts in neuronal production in the long-term [159]. At this point, the demonstrated interactions are local, and whether and how they propagate across the NSC population is expected to depend on the relation between the frequency and duration of NSC states competent for activation and the half-life of IPs. Long sub-apical protrusions have also been observed in *deltaA<sup>pos</sup>* cells that could signal at a distance [126]. An interesting aspect of these findings is that spatial signaling is temporally linked with lineage progression. Thus, in the asynchronous adult NSC population where IPs are also short-lived (and leave the germinal population upon differentiation), this allows a self-perpetuating system to emerge where lineage termination allows lineage initiation from another NSC. The spatio-temporal coordination of NSC fate decisions, other than their activation, remains to be tested, as well as the relevance of other signaling

pathways, whether relying on cell–cell interactions, reaction–diffusion processes, or mechanical information. Finally, in addition to this spatio-temporal regulation at the individual cell level, it is interesting to wonder whether the intrinsic niche also includes spatio-temporal feedbacks at a clonal level. Such regulations akin to competition processes have been described in non-follicular epidermal SCs of the mouse adult skin [165].

In the embryonic central nervous system, the occurrence of cross-interactions between NPs to control the position of neuron generation in physical space is a well-known property of lateral inhibition. In contrast to the adult pallial NSC pools, obviously, it affects neurogenesis commitment rather than quiescence exit. In addition, Notch-Delta signaling via horizontal protrusions exhibited by NPs were recently described to space out neuronal differentiation in the zebrafish embryonic hindbrain, showing that lateral inhibition can also generate longer-distance patterns [166].

### 7.1. *Take home message*

In addition to systemic or local signals from non-NPs/NSCs, the fact that NPs/NSCs are often found in groups allows inter-progenitor interactions. This “intrinsic niche” is responsible for the organization of neurogenesis progression in physical space over time.

## 8. Conclusion

The core principles and molecular regulators of neurogenesis are shared between the embryonic and adult central nervous systems, with some adaptations in spatial organization and speed. The latter is much slower in the adult compared to the embryonic brain, due to a number of factors including the existence of an NSC quiescence phase and a lengthened progenitor commitment phase. Overall, the neurogenesis process is better understood, because experimentally more easily tractable, in the embryonic than in the adult brain. But the next step and recurrent remaining issue is to understand transitions: how are cell identities gradually changed, how is cycling behavior modified (to introduce quiescence), how are lineages prolonged (to introduce transient progenitor states) in the transition from embryo and adult?



Are these transitions abrupt or gradual, what are their regulators, and how is a new equilibrium reached that will characterize the adult stage? Future work along these lines will be highly informative for understanding how dynamic pattern and tissue generation concert over time to result in tissue homeostasis.

### Abbreviations

bHLH	Basic helix-loop-helix domain
BLBP	Brain Lipid-Binding Protein
BMP	Bone morphogenetic protein
Cdk	Cyclin-dependent kinase
CSF	Cerebrospinal fluid
Dll1	Delta-like 1
EGF	Epidermal growth factor
EGFR	Epidermal growth factor receptor
FGF	Fibroblast growth factor
GFAP	Glial fibrillary acidic protein
GS	Glutamine synthase
Hes/Her	Hairy/Enhancer-or-Split transcription factor
INM	Interkinetic nuclear migration
IP	Intermediate neuronal progenitor
MHB	Midbrain-hindbrain boundary
NE	Neuroepithelial cell
NICD	Notch intracellular domain
NP	Neural progenitor
NSC	Neural stem cell
PEDF	Pigment epithelium-derived factor
RG	Radial glia
SEZ	Sub-ependymal zone of the lateral ventricle
SGZ	Sub-granular zone of the dentate gyrus of the hippocampus
ZO1	Zona Occludens 1

### Methods

Images in Figures 2, 4, 5 and 6 were generated using BioRender (with a license from Institut Pasteur).

### Declaration of interests

The authors do not work for, advise, own shares in, or receive funds from any organization that could benefit from this article, and have declared no affiliations other than their research organizations.

### Author contributions

Conceptualization and writing—original draft—: LB-C; review & editing: MC, LB-C; illustrations: MC.

### Funding

Work in the LB-C laboratory was funded by the ANR (Labex Revive), La Ligue Nationale Contre le Cancer (LNCC EL2019 BALLY-CUIF), the Fondation pour la Recherche Médicale (EQU202203014636), CNRS, INSERM, Institut Pasteur and the European Research Council (ERC) (SyG 101071786 - PEPS). MC was a recipient of a 3-year PhD student fellowship from ED Complexité du Vivant, Sorbonne Université, Paris, complemented for one year by LabEx Revive.

### Acknowledgments

We thank the ZEN team for generating some of the important scientific data mentioned in this review, and for regular discussions.

### References

- [1] K. Hirsch, G. K. H. Zupanc, "Generation and long-term persistence of new neurons in the adult zebrafish brain: a quantitative analysis", *Neuroscience* **146** (2007), p. 679-696.
- [2] S. Herculano-Houzel, "The human brain in numbers: a linearly scaled-up primate brain", *Front. Hum. Neurosci.* **3** (2009), article no. 31.
- [3] H. Mira, J. Morante, "Neurogenesis from embryo to adult—lessons from flies and mice", *Front. Cell Dev. Biol.* **8** (2020), article no. 533.
- [4] A. Engler, R. Zhang, V. Taylor, "Notch and neurogenesis", *Adv. Exp. Med. Biol.* **1066** (2018), p. 223-234.
- [5] N. Urbán, F. Guillemot, "Neurogenesis in the embryonic and adult brain: same regulators, different roles", *Front. Cell. Neurosci.* **8** (2014), article no. 396.
- [6] A. Lampada, V. Taylor, "Notch signaling as a master regulator of adult neurogenesis", *Front. Neurosci.* **17** (2023), article no. 1179011.
- [7] N. Jurisch-Yaksi, E. Yaksi, C. Kizil, "Radial glia in the zebrafish brain: Functional, structural, and physiological comparison with the mammalian glia", *Glia* **68** (2020), p. 2451-2470.
- [8] R. Schmidt, U. Strähle, S. Scholpp, "Neurogenesis in zebrafish—from embryo to adult", *Neural Dev.* **8** (2013), article no. 3.
- [9] A. B. Chitnis, I. B. Dawid, "Chapter 20 neurogenesis in zebrafish embryos", in *Methods in Cell Biology* (H. W. Detrich, M. Westerfield, L. I. Zon, eds.), Elsevier, 1998, p. 367-386.
- [10] J. S. Barbosa, R. Sanchez-Gonzalez, R. Di Gialmo, E. V. Baumgart, F. J. Theis, M. Götz, J. Ninkovic, "Neurodevelopment. Live imaging of adult neural stem cell behavior in the intact and injured zebrafish brain", *Science* **348** (2015), p. 789-793.

- [11] N. Dray, S. Bedu, N. Vuillemin *et al.*, "Large-scale live imaging of adult neural stem cells in their endogenous niche", *Development* **142** (2015), p. 3592-3600.
- [12] E. Taverna, M. Götz, W. B. Huttner, "The cell biology of neurogenesis: toward an understanding of the development and evolution of the neocortex", *Annu. Rev. Cell Dev. Biol.* **30** (2014), p. 465-502.
- [13] A. Alunni, M. Coolen, I. Foucher, L. Bally-Cuif, "Chapter 26—Neurogenesis in zebrafish", in *Patterning and Cell Type Specification in the Developing CNS and PNS (Second Edition)* (J. Rubenstein, P. Rakic, B. Chen, K. Y. Kwan, eds.), Academic Press, 2020, p. 643-697.
- [14] V. Marthiens, C. French Constant, "Adherens junction domains are split by asymmetric division of embryonic neural stem cells", *EMBO Rep.* **10** (2009), p. 515-520.
- [15] E. Peyre, X. Morin, "An oblique view on the role of spindle orientation in vertebrate neurogenesis", *Dev. Growth Differ.* **54** (2012), p. 287-305.
- [16] D. Zaidi, K. Chinnappa, F. Francis, "Primary cilia influence progenitor function during cortical development", *Cells* **11** (2022), article no. 2895.
- [17] E.-S. Chou, R. Li, P.-S. Wang, "Molecular components and polarity of radial glial cells during cerebral cortex development", *Cell Mol. Life Sci.* **75** (2018), p. 1027-1041.
- [18] R. Catena, C. Tiveron, A. Ronchi *et al.*, "Conserved POU binding DNA sites in the Sox2 upstream enhancer regulate gene expression in embryonic and neural stem cells", *J. Biol. Chem.* **279** (2004), p. 41846-41857.
- [19] M. Ishibashi, K. Moriyoshi, Y. Sasaki, K. Shiota, S. Nakanishi, R. Kageyama, "Persistent expression of helix-loop-helix factor HES-1 prevents mammalian neural differentiation in the central nervous system", *EMBO J.* **13** (1994), p. 1799-1805.
- [20] T. Ohtsuka, M. Ishibashi, G. Gradwohl, S. Nakanishi, F. Guillemot, R. Kageyama, "Hes1 and Hes5 as Notch effectors in mammalian neuronal differentiation", *EMBO J.* **18** (1999), p. 2196-2207.
- [21] P. J. Strzyz, M. Matejczak, C. Norden, in *International Review of Cell and Molecular Biology* (K. W. Jeon, ed.), Academic Press, 2016, p. 89-118.
- [22] B. Thisse, S. Pflumio, M. Fürthauer *et al.*, "Expression of the zebrafish genome during embryogenesis (NIH R01 RR15402)", 2001, ZFIN Direct Data Submission, <http://zfin.org>.
- [23] S. Yoo, S. Blackshaw, "Regulation and function of neurogenesis in the adult mammalian hypothalamus", *Prog. Neurobiol.* **170** (2018), p. 53-66.
- [24] K. Obernier, A. Alvarez-Buylla, "Neural stem cells: origin, heterogeneity and regulation in the adult mammalian brain", *Development* **146** (2019), article no. dev156059.
- [25] T. Toda, F. H. Gage, "Review: adult neurogenesis contributes to hippocampal plasticity", *Cell Tissue Res.* **373** (2018), p. 693-709.
- [26] B. W. Lindsey, Z. J. Hall, A. Heuzé, J.-S. Joly, V. Tropepe, J. Kaslin, "The role of neuro-epithelial-like and radial-glia stem and progenitor cells in development, plasticity, and repair", *Prog. Neurobiol.* **170** (2018), p. 99-114.
- [27] M. Labusch, L. Mancini, D. Morizet, L. Bally-Cuif, "Conserved and divergent features of adult neurogenesis in zebrafish", *Front. Cell Dev. Biol.* **8** (2020), article no. 525.
- [28] N. Diotel, L. Lübke, U. Strähle, S. Rastegar, "Common and distinct features of adult neurogenesis and regeneration in the telencephalon of zebrafish and mammals", *Front. Neurosci.* **14** (2020), article no. 568930.
- [29] S. Falk, M. Götz, "Glial control of neurogenesis", *Curr. Opin. Neurobiol.* **47** (2017), p. 188-195.
- [30] J. Moss, E. Gebara, E. A. Bushong *et al.*, "Fine processes of Nestin-GFP-positive radial glia-like stem cells in the adult dentate gyrus ensheath local synapses and vasculature", *Proc. Natl Acad. Sci. USA* **113** (2016), p. E2536-E2545.
- [31] J. Andersen, N. Urbán, A. Achimastou *et al.*, "A transcriptional mechanism integrating inputs from extracellular signals to activate hippocampal stem cells", *Neuron* **83** (2014), p. 1085-1097.
- [32] H. Suh, A. Consiglio, J. Ray, T. Sawai, K. A. D'Amour, F. H. Gage, "In vivo fate analysis reveals the multipotent and self-renewal capacities of Sox2+ neural stem cells in the adult hippocampus", *Cell Stem Cell* **1** (2007), p. 515-528.
- [33] L. Dirian, S. Galant, M. Coolen, W. Chen, S. Bedu, C. Houart, L. Bally-Cuif, I. Foucher, "Spatial regionalization and heterochrony in the formation of adult pallial neural stem cells", *Dev. Cell* **30** (2014), p. 123-136.
- [34] S. Galant, G. Furlan, M. Coolen, L. Dirian, I. Foucher, L. Bally-Cuif, "Embryonic origin and lineage hierarchies of the neural progenitor subtypes building the zebrafish adult mid-brain", *Dev. Biol.* **420** (2016), p. 120-135.
- [35] E. Than-Trong, L. Bally-Cuif, "Radial glia and neural progenitors in the adult zebrafish central nervous system", *Glia* **63** (2015), p. 1406-1428.
- [36] J. Chen, K. E. Poskanzer, M. R. Freeman, K. R. Monk, "Live-imaging of astrocyte morphogenesis and function in zebrafish neural circuits", *Nat. Neurosci.* **23** (2020), p. 1297-1306.
- [37] Y. Mu, D. V. Bennett, M. Rubinov *et al.*, "Glia accumulate evidence that actions are futile and suppress unsuccessful behavior", *Cell* **178** (2019), p. 27-43, e19.
- [38] D. Morizet, I. Foucher, A. Alunni, L. Bally-Cuif, "Reconstruction of macroglia and adult neurogenesis evolution through cross-species single-cell transcriptomic analyses", *Nat. Commun.* **15** (2024), article no. 3306.
- [39] B. Raj, D. E. Wagner, A. McKenna, S. Pandey, A. M. Klein, J. Shendure, J. A. Gagnon, A. F. Schier, "Simultaneous single-cell profiling of lineages and cell types in the vertebrate brain", *Nat. Biotechnol.* **36** (2018), p. 442-450.
- [40] S. Magavi, D. Friedmann, G. Banks, A. Stolfi, C. Lois, "Coincident generation of pyramidal neurons and protoplasmic astrocytes in neocortical columns", *J. Neurosci.* **32** (2012), p. 4762-4772.
- [41] K. A. Burns, B. Murphy, S. C. Danzer, C.-Y. Kuan, "Developmental and post-injury cortical gliogenesis: a genetic fate-mapping study with nestin-CreER mice", *Glia* **57** (2009), p. 1115-1129.
- [42] J. P. Magnusson, C. Göritz, J. Tatarishvili, D. O. Dias, E. M. K. Smith, O. Lindvall, Z. Kokaia, J. Frisén, "A latent neurogenic program in astrocytes regulated by Notch signaling in the mouse", *Science* **346** (2014), p. 237-241.
- [43] J. P. Magnusson, M. Zamboni, G. Santopolo, J. E. Mold, M. Barrientos-Somarrivas, C. Talavera-Lopez, B. Andersson, J. Frisén, "Activation of a neural stem cell transcriptional

- program in parenchymal astrocytes", *Elife* **9** (2020), article no. e59733.
- [44] G. Nato, A. Caramello, S. Trova *et al.*, "Striatal astrocytes produce neuroblasts in an excitotoxic model of Huntington's disease", *Development* **142** (2015), p. 840-845.
- [45] S. Ahn, A. L. Joyner, "In vivo analysis of quiescent adult neural stem cells responding to Sonic hedgehog", *Nature* **437** (2005), p. 894-897.
- [46] F. Balordi, G. Fishell, "Hedgehog signaling in the subventricular zone is required for both the maintenance of stem cells and the migration of newborn neurons", *J. Neurosci.* **27** (2007), p. 5936-5947.
- [47] M. A. Bonaguidi, M. A. Wheeler, J. S. Shapiro, R. P. Stadel, G. J. Sun, G. Ming, H. Song, "In vivo clonal analysis reveals self-renewing and multipotent adult neural stem cell characteristics", *Cell* **145** (2011), p. 1142-1155.
- [48] D. A. Berg, Y. Su, D. Jimenez-Cyrus *et al.*, "A common embryonic origin of stem cells drives developmental and adult neurogenesis", *Cell* **177** (2019), p. 654-668, e15.
- [49] S. Zweifel, G. Marcy, Q. Lo Guidice, D. Li, C. Heinrich, K. Azim, O. Raineteau, "HOPX defines heterogeneity of postnatal subventricular zone neural stem cells", *Stem Cell Rep.* **11** (2018), p. 770-783.
- [50] K. Obernier, A. Cebrian-Silla, M. Thomson, J. I. Parraguez, R. Anderson, C. Guinto, J. Rodas Rodriguez, J.-M. Garcia-Verdugo, A. Alvarez-Buylla, "Adult neurogenesis is sustained by symmetric self-renewal and differentiation", *Cell Stem Cell* **22** (2018), p. 221-234, e8.
- [51] L. C. Fuentealba, S. B. Rompani, J. I. Parraguez, K. Obernier, R. Romero, C. L. Cepko, A. Alvarez-Buylla, "Embryonic origin of postnatal neural stem cells", *Cell* **161** (2015), p. 1644-1655.
- [52] S. Furutachi, H. Miya, T. Watanabe *et al.*, "Slowly dividing neural progenitors are an embryonic origin of adult neural stem cells", *Nat. Neurosci.* **18** (2015), p. 657-665.
- [53] S. A. Redmond, M. Figueres-Oñate, K. Obernier, M. A. Nascimto, J. I. Parraguez, L. López-Mascaraque, L. C. Fuentealba, A. Alvarez-Buylla, "Development of ependymal and postnatal neural stem cells and their origin from a common embryonic progenitor", *Cell Rep.* **27** (2019), p. 429-441, e3.
- [54] G. Furlan, V. Cuccioli, N. Vüllemin *et al.*, "Life-long neurogenic activity of individual neural stem cells and continuous growth establish an outside-in architecture in the teleost pallium", *Curr. Biol.* **27** (2017), p. 3288-3301, e3.
- [55] S. Furutachi, A. Matsumoto, K. I. Nakayama, Y. Gotoh, "p57 controls adult neural stem cell quiescence and modulates the pace of lifelong neurogenesis", *EMBO J.* **32** (2013), p. 970-981.
- [56] C. Stigloher, P. Chapouton, B. Adolf, L. Bally-Cuif, "Identification of neural progenitor pools by E(Spl) factors in the embryonic and adult brain", *Brain Res. Bull.* **75** (2008), p. 266-273.
- [57] M. Folgueira, P. Bayley, P. Navratilova, T. S. Becker, S. W. Wilson, J. D. W. Clarke, "Morphogenesis underlying the development of the everted teleost telencephalon", *Neural Dev.* **7** (2012), article no. 32.
- [58] J. H. Baek, J. Hatakeyama, S. Sakamoto, T. Ohtsuka, R. Kageyama, "Persistent and high levels of Hes1 expression regulate boundary formation in the developing central nervous system", *Development* **133** (2006), p. 2467-2476.
- [59] A. Caramello, C. Gallchet, K. Rizzoti, R. Lovell-Badge, "Dentate gyrus development requires a cortical hem-derived astrocytic scaffold", *eLife* **10** (2021), article no. e63904.
- [60] M. Götz, W. B. Huttner, "The cell biology of neurogenesis", *Nat. Rev. Mol. Cell Biol.* **6** (2005), p. 777-788.
- [61] J. Ninkovic, M. Götz, "Signaling in adult neurogenesis: from stem cell niche to neuronal networks", *Curr. Opin. Neurobiol.* **17** (2007), p. 338-344.
- [62] N. E. Baker, N. L. Brown, "All in the family: proneural bHLH genes and neuronal diversity", *Development* **145** (2018), article no. dev159426.
- [63] N. Bertrand, D. S. Castro, F. Guillemot, "Proneural genes and the specification of neural cell types", *Nat. Rev. Neurosci.* **3** (2002), p. 517-530.
- [64] F. Guillemot, B. A. Hassan, "Beyond proneural: emerging functions and regulations of proneural proteins", *Curr. Opin. Neurobiol.* **42** (2017), p. 93-101.
- [65] G. Wilkinson, D. Dennis, C. Schuurmans, "Proneural genes in neocortical development", *Neurosci.* **253** (2013), p. 256-273.
- [66] D. J. Dennis, G. Wilkinson, S. Li *et al.*, "Neurog2 and Ascl1 together regulate a postmitotic derepression circuit to govern laminar fate specification in the murine neocortex", *Proc. Natl. Acad. Sci. USA* **114** (2017), p. E4934-E4943.
- [67] F. F. Vasconcelos, D. S. Castro, "Transcriptional control of vertebrate neurogenesis by the proneural factor Ascl1", *Front. Cell. Neurosci.* **8** (2014), article no. 412.
- [68] M. Stevanovic, D. Drakulic, A. Ladic, D. S. Ninkovic, M. Schwirtlich, M. Mojsin, "SOX transcription factors as important regulators of neuronal and glial differentiation during nervous system development and adult neurogenesis", *Front. Mol. Neurosci.* **14** (2021), article no. 654031.
- [69] A. Kavyanifar, S. Turan, D. C. Lie, "SoxC transcription factors: multifunctional regulators of neurodevelopment", *Cell Tissue Res.* **371** (2018), p. 91-103.
- [70] A.-M. Oproescu, S. Han, C. Schuurmans, "New insights into the intricacies of proneural gene regulation in the embryonic and adult cerebral cortex", *Front. Mol. Neurosci.* **14** (2021), article no. 642016.
- [71] K. Hori, A. Sen, S. Artavanis-Tsakonas, "Notch signaling at a glance", *J. Cell Sci.* **126** (2013), p. 2135-2140.
- [72] R. Zhang, A. Engler, V. Taylor, "Notch: an interactive player in neurogenesis and disease", *Cell Tissue Res.* **371** (2018), p. 73-89.
- [73] J. Reichrath, S. Reichrath, "A snapshot of the molecular biology of Notch signaling: challenges and promises", *Adv. Exp. Med. Biol.* **1227** (2020), p. 1-7.
- [74] C. Siebel, U. Lendahl, "Notch signaling in development, tissue homeostasis, and disease", *Physiol. Rev.* **97** (2017), p. 1235-1294.
- [75] B. M. Harvey, R. S. Haltiwanger, "Regulation of Notch function by O-glycosylation", *Adv. Exp. Med. Biol.* **1066** (2018), p. 59-78.
- [76] P. A. Handford, B. Korona, R. Suckling, C. Redfield, S. M. Lea, "Structural insights into Notch receptor-ligand interactions", *Adv. Exp. Med. Biol.* **1066** (2018), p. 33-46.
- [77] R. A. Kovall, B. Gebelein, D. Sprinzak, R. Kopan, "The canon-

- ical Notch signaling pathway: structural and biochemical insights into shape, sugar, and force", *Dev. Cell* **41** (2017), p. 228-241.
- [78] D. Sprinzak, S. C. Blacklow, "Biophysics of Notch signaling", *Annu. Rev. Biophys.* **50** (2021), p. 157-189.
- [79] C. Huang, J. A. Chan, C. Schuurmans, "Proneural bHLH genes in development and disease", *Curr. Top. Dev. Biol.* **110** (2014), p. 75-127.
- [80] C. Delidakis, M. Monastirioti, S. S. Magadi, "E(spl): genetic, developmental, and evolutionary aspects of a group of invertebrate Hes proteins with close ties to Notch signaling", *Curr. Top. Dev. Biol.* **110** (2014), p. 217-262.
- [81] B. Roesse-Koerner, L. Stappert, O. Brüstle, "Notch/Hes signaling and miR-9 engage in complex feedback interactions controlling neural progenitor cell proliferation and differentiation", *Neurogenesis* **4** (2017), article no. e1313647.
- [82] O. Ehm, C. Göritz, M. Covic *et al.*, "RBPJkappa-dependent signaling is essential for long-term maintenance of neural stem cells in the adult hippocampus", *J. Neurosci.* **30** (2010), p. 13794-13807.
- [83] J. Lewis, "Notch signalling and the control of cell fate choices in vertebrates", *Semin. Cell Dev. Biol.* **9** (1998), p. 583-589.
- [84] F. Bocci, J. N. Onuchic, M. K. Jolly, "Understanding the principles of pattern formation driven by Notch signaling by integrating experiments and theoretical models", *Front. Physiol.* **11** (2020), article no. 929.
- [85] J. Neves, G. Abelló, J. Petrovic, F. Giraldez, "Patterning and cell fate in the inner ear: a case for Notch in the chicken embryo", *Dev. Growth Differ.* **55** (2013), p. 96-112.
- [86] M. Sjöqvist, E. R. Andersson, "Do as I say, Not(ch) as I do: Lateral control of cell fate", *Dev. Biol.* **447** (2019), p. 58-70.
- [87] J. Petrovic, H. Gálvez, J. Neves, G. Abelló, F. Giraldez, "Differential regulation of Hes/Hey genes during inner ear development", *Dev. Neurobiol.* **75** (2015), p. 703-720.
- [88] D. del Álamo, H. Rouault, F. Schweisguth, "Mechanism and significance of cis-inhibition in Notch signalling", *Curr. Biol.* **21** (2011), p. R40-R47.
- [89] E. Than-Trong, B. Kiani, N. Dray, S. Ortica, B. Simons, S. Rulands, A. Alunni, L. Bally-Cuif, "Lineage hierarchies and stochasticity ensure the long-term maintenance of adult neural stem cells", *Sci. Adv.* **6** (2020), article no. eaaz5424.
- [90] R. Sueda, I. Imayoshi, Y. Harima, R. Kageyama, "High Hes1 expression and resultant Ascl1 suppression regulate quiescent vs. active neural stem cells in the adult mouse brain", *Genes Dev.* **33** (2019), p. 511-523.
- [91] I. Imayoshi, T. Shimagori, T. Ohtsuka, R. Kageyama, "Hes genes and neurogenin regulate non-neural versus neural fate specification in the dorsal telencephalic midline", *Development* **135** (2008), p. 2531-2541.
- [92] Y.-J. Jiang, M. Brand, C.-P. Heisenberg *et al.*, "Mutations affecting neurogenesis and brain morphology in the zebrafish, *Danio rerio*", *Development* **123** (1996), p. 205-216.
- [93] M. Gray, C. B. Moens, S. L. Amacher, J. S. Eisen, C. E. Beattie, "Zebrafish *deadly seven* Functions in Neurogenesis", *Dev. Biol.* **237** (2001), p. 306-323.
- [94] J. L. Ables, N. A. Decarolis, M. A. Johnson *et al.*, "Notch1 is required for maintenance of the reservoir of adult hippocampal stem cells", *J. Neurosci.* **30** (2010), p. 10484-10492.
- [95] I. Imayoshi, M. Sakamoto, M. Yamaguchi, K. Mori, R. Kageyama, "Essential roles of Notch signaling in maintenance of neural stem cells in developing and adult brains", *J. Neurosci.* **30** (2010), p. 3489-3498.
- [96] A. Alunni, M. Krecsmarik, A. Bosco, S. Galant, L. Pan, C. B. Moens, L. Bally-Cuif, "Notch3 signaling gates cell cycle entry and limits neural stem cell amplification in the adult pallium", *Development* **140** (2013), p. 3335-3347.
- [97] B. Adolf, P. Chapouton, C. S. Lam, S. Topp, B. Tannhäuser, U. Strähle, M. Götz, L. Bally-Cuif, "Conserved and acquired features of adult neurogenesis in the zebrafish telencephalon", *Dev. Biol.* **295** (2006), p. 278-293.
- [98] P. Chapouton, K. J. Webb, C. Stigloher *et al.*, "Expression of hairy/enhancer of split genes in neural progenitors and neurogenesis domains of the adult zebrafish brain", *J. Comp. Neurol.* **519** (2011), p. 1748-1769.
- [99] N. Kishimoto, K. Shimizu, K. Sawamoto, "Neuronal regeneration in a zebrafish model of adult brain injury", *Dis. Model Mech.* **5** (2012), p. 200-209.
- [100] S. Topp, C. Stigloher, A. Z. Komisarczuk, B. Adolf, T. S. Becker, L. Bally-Cuif, "Fgf signaling in the zebrafish adult brain: association of Fgf activity with ventricular zones but not cell proliferation", *J. Comp. Neurol.* **510** (2008), p. 422-439.
- [101] H. Shimojo, R. Kageyama, "Oscillatory control of Delta-like1 in somitogenesis and neurogenesis: A unified model for different oscillatory dynamics", *Semin. Cell Dev. Biol.* **49** (2016), p. 76-82.
- [102] I. Imayoshi, R. Kageyama, "Oscillatory control of bHLH factors in neural progenitors", *Trends Neurosci.* **37** (2014), p. 531-538.
- [103] B. Bonev, P. Stanley, N. Papalopulu, "MicroRNA-9 Modulates Hes1 ultradian oscillations by forming a double-negative feedback loop", *Cell Rep.* **2** (2012), p. 10-18.
- [104] R. Sueda, R. Kageyama, "Regulation of active and quiescent somatic stem cells by Notch signaling", *Dev. Growth Differ.* **62** (2020), p. 59-66.
- [105] L. Harris, F. Guillemot, "HES1, two programs: promoting the quiescence and proliferation of adult neural stem cells", *Genes Dev.* **33** (2019), p. 479-481.
- [106] I. M. Blomfield, B. Rocamonde, M. D. M. Masdeu *et al.*, "Id4 promotes the elimination of the pro-activation factor Ascl1 to maintain quiescence of adult hippocampal stem cells", *Elife* **8** (2019), article no. e48561.
- [107] N. Urbán, D. L. C. van den Berg, A. Forget, J. Andersen, J. A. A. Demmers, C. Hunt, O. Ayrault, F. Guillemot, "Return to quiescence of mouse neural stem cells by degradation of a proactivation protein", *Science* **353** (2016), p. 292-295.
- [108] E. J. Kim, J. L. Ables, L. K. Dickel, A. J. Eisch, J. E. Johnson, "Ascl1 (Mash1) defines cells with long-term neurogenic potential in subgranular and subventricular zones in adult mouse brain", *PLoS One* **6** (2011), article no. e18472.
- [109] C. M. Perras, C. Hunt, M. Sugimori, M. Nakafuku, D. Rowitch, F. Guillemot, "The proneural gene Mash1 specifies an early population of telencephalic oligodendrocytes", *J. Neurosci.* **27** (2007), p. 4233-4242.
- [110] S. Jessberger, N. Toni, G. D. Clemenson, J. Ray, F. H. Gage, "Directed differentiation of hippocampal stem/progenitor cells in the adult brain", *Nat. Neurosci.* **11** (2008), p. 888-893.
- [111] D. S. Castro, B. Martynoga, C. Perras *et al.*, "A novel function of the proneural factor Ascl1 in progenitor proliferation

- identified by genome-wide characterization of its targets", *Genes Dev.* **25** (2011), p. 930-945.
- [112] O. Basak, C. Giachino, E. Fiorini, H. R. Macdonald, V. Taylor, "Neurogenic subventricular zone stem/progenitor cells are Notch1-dependent in their active but not quiescent state", *J. Neurosci.* **32** (2012), p. 5654-5666.
- [113] S. Lim, A. Bhinge, S. Bragado Alonso *et al.*, "Cyclin-dependent kinase-dependent phosphorylation of Sox2 at Serine 39 regulates neurogenesis", *Mol. Cell Biol.* **37** (2017), article no. e00201-17.
- [114] M. Roussat, T. Jungas, C. Audouard *et al.*, "Control of G2 phase duration by CDC25B modulates the switch from direct to indirect neurogenesis in the neocortex", *J. Neurosci.* **43** (2023), p. 1154-1165.
- [115] C. Ratineau, M. W. Petry, H. Mutoh, A. B. Leiter, "Cyclin D1 represses the basic helix-loop-helix transcription factor, BETA2/NeuroD", *J. Biol. Chem.* **277** (2002), p. 8847-8853.
- [116] M. Marqués-Torrejón, C. A. C. Williams, B. Southgate *et al.*, "LRIG1 is a gatekeeper to exit from quiescence in adult neural stem cells", *Nat. Commun.* **12** (2021), article no. 2594.
- [117] E. Portlan, J. M. Morante-Redolat, M. Á. Marqués-Torrejón *et al.*, "Transcriptional repression of Bmp2 by p21(Waf1/Cip1) links quiescence to neural stem cell maintenance", *Nat. Neurosci.* **16** (2013), p. 1567-1575.
- [118] S. L. Spencer, S. D. Cappell, F.-C. Tsai, K. W. Overton, C. L. Wang, T. Meyer, "The proliferation-quiescence decision is controlled by a bifurcation in CDK2 activity at mitotic exit", *Cell* **155** (2013), p. 369-383.
- [119] K. W. Overton, S. L. Spencer, W. L. Noderer, T. Meyer, C. L. Wang, "Basal p21 controls population heterogeneity in cycling and quiescent cell cycle states", *Proc. Natl. Acad. Sci. USA* **111** (2014), p. E4386-E4393.
- [120] Z. Andreu, M. A. Khan, P. González-Gómez *et al.*, "The cyclin-dependent kinase inhibitor p27kip1 regulates radial stem cell quiescence and neurogenesis in the adult hippocampus", *Stem Cells* **33** (2015), p. 219-229.
- [121] A. Domingo-Muelas, J. M. Morante-Redolat, V. Moncho-Amor *et al.*, "The rates of adult neurogenesis and oligodendrogenesis are linked to cell cycle regulation through p27-dependent gene repression of SOX2", *Cell Mol. Life Sci.* **80** (2023), article no. 36.
- [122] A. Uzquiano, I. Gladwyn-Ng, L. Nguyen, O. Reiner, M. Götz, E. Matsuzaki, F. Francis, "Cortical progenitor biology: key features mediating proliferation versus differentiation", *J. Neurochem.* **146** (2018), p. 500-525.
- [123] Z. Dong, N. Yang, S.-Y. Yeo, A. Chitnis, S. Guo, "Intralineage directional Notch signaling regulates self-renewal and differentiation of asymmetrically dividing radial glia", *Neuron* **74** (2012), p. 65-78.
- [124] P. Alexandre, A. M. Reugels, D. Barker, E. Blanc, J. D. W. Clarke, "Neurons derive from the more apical daughter in asymmetric divisions in the zebrafish neural tube", *Nat. Neurosci.* **13** (2010), p. 673-679.
- [125] D. A. Lyons, A. T. Guy, J. D. W. Clarke, "Monitoring neural progenitor fate through multiple rounds of division in an intact vertebrate brain", *Development* **130** (2003), p. 3427-3436.
- [126] L. Mancini, B. Guirao, S. Ortica *et al.*, "Apical size and deltaA expression predict adult neural stem cell decisions along lineage progression", *Sci. Adv.* **9** (2023), no. 35, article no. eadg7519.
- [127] G.-A. Pilz, S. Bottes, M. Betizeau, D. J. Jörg, S. Carta, B. D. Simons, F. Helmchen, S. Jessberger, "Live imaging of neurogenesis in the adult mouse hippocampus", *Science* **359** (2018), p. 658-662.
- [128] S. Bottes, B. N. Jaeger, G.-A. Pilz *et al.*, "Long-term self-renewing stem cells in the adult mouse hippocampus identified by intravital imaging", *Nat. Neurosci.* **24** (2021), p. 225-233.
- [129] J. Hatakeyama, Y. Bessho, K. Katoh, S. Ookawara, M. Fujioka, F. Guillemot, R. Kageyama, "Hes genes regulate size, shape and histogenesis of the nervous system by control of the timing of neural stem cell differentiation", *Development* **131** (2004), p. 5539-5550.
- [130] X. Zhao, J. Q. Garcia, K. Tong *et al.*, "Polarized endosome dynamics engage cytoplasmic Par-3 that recruits dynein during asymmetric cell division", *Sci. Adv.* **7** (2021), article no. eabg1244.
- [131] X. Zhao, Y. Wang, V. Mouilleau *et al.*, "PCM1 conveys centrosome asymmetry to polarized endosome dynamics in regulating daughter cell fate", 2024, bioRxiv, <https://doi.org/10.1101/2024.06.17.599416>.
- [132] S. Kressmann, C. Campos, I. Castanon, M. Fürthauer, M. González-Gaitán, "Directional Notch trafficking in Sara endosomes during asymmetric cell division in the spinal cord", *Nat. Cell Biol.* **17** (2015), p. 333-339.
- [133] C. Andreu-Agulló, J. M. Morante-Redolat, A. C. Delgado, I. Fariñas, "Vascular niche factor PEDF modulates Notch-dependent stemness in the adult subependymal zone", *Nat. Neurosci.* **12** (2009), p. 1514-1523.
- [134] S. R. Ferron, N. Pozo, A. Laguna *et al.*, "Regulated segregation of kinase Dyrk1A during asymmetric neural stem cell division is critical for EGFR-mediated biased signaling", *Cell Stem Cell* **7** (2010), p. 367-379.
- [135] D. Kawaguchi, S. Furutachi, H. Kawai, K. Hozumi, Y. Gotoh, "Dil1 maintains quiescence of adult neural stem cells and segregates asymmetrically during mitosis", *Nat. Commun.* **4** (2013), article no. 1880.
- [136] J. Obermann, F. Wagner, A. Kociaj, A. Zambusi, J. Ninkovic, S. M. Hauck, P. Chapouton, "The surface proteome of adult neural stem cells in Zebrafish unveils long-range cell-cell connections and age-related changes in responsiveness to IGF", *Stem Cell Rep.* **12** (2019), p. 258-273.
- [137] K. Edelmann, L. Glashauser, S. Sprungala, B. Hesi, M. Fritschle, J. Ninkovic, L. Godinho, P. Chapouton, "Increased radial glia quiescence, decreased reactivation upon injury and unaltered neuroblast behavior underlie decreased neurogenesis in the aging zebrafish telencephalon", *J. Comp. Neurol.* **521** (2013), p. 3099-3115.
- [138] G. Kalamakis, D. Brüne, S. Ravichandran *et al.*, "Quiescence modulates stem cell maintenance and regenerative capacity in the aging brain", *Cell* **176** (2019), p. 1407-1419, e14.
- [139] D. S. Leeman, K. Hebestreit, T. Ruetz *et al.*, "Lysosome activation clears aggregates and enhances quiescent neural stem cell activation during aging", *Science* **359** (2018), p. 1277-1283.
- [140] V. Capilla-Gonzalez, A. Cebrian-Silla, H. Guerrero-Cazares,

- J. M. Garcia-Verdugo, A. Quiñones-Hinojosa, "Age-related changes in astrocytic and ependymal cells of the subventricular zone", *Glia* **62** (2014), p. 790-803.
- [141] C. Giachino, O. Basak, S. Lugert *et al.*, "Molecular diversity subdivides the adult forebrain neural stem cell population", *Stem Cells* **32** (2014), p. 70-84.
- [142] P. Gao, M. P. Postiglione, T. G. Krieger *et al.*, "Deterministic progenitor behavior and unitary production of neurons in the neocortex", *Cell* **159** (2014), p. 775-788.
- [143] L. Telley, G. Agirman, J. Prados *et al.*, "Temporal patterning of apical progenitors and their daughter neurons in the developing neocortex", *Science* **364** (2019), article no. eaav2522.
- [144] P. Lyu, T. Hoang, C. P. Santiago *et al.*, "Gene regulatory networks controlling temporal patterning, neurogenesis, and cell-fate specification in mammalian retina", *Cell Rep.* **37** (2021), article no. 109994.
- [145] A. M. Rossi, S. Jafari, C. Desplan, "Integrated patterning programs during drosophila development generate the diversity of neurons and control their mature properties", *Annu. Rev. Neurosci.* **44** (2021), p. 153-172.
- [146] C. Q. Doe, S. Thor, "40 years of homeodomain transcription factors in the Drosophila nervous system", *Development* **151** (2024), article no. dev202910.
- [147] N. Urbán, I. M. Blomfield, F. Guillemot, "Quiescence of adult mammalian neural stem cells: a highly regulated rest", *Neuron* **104** (2019), p. 834-848.
- [148] H. Mira, Z. Andreu, H. Suh *et al.*, "Signaling through BMPRIA regulates quiescence and long-term activity of neural stem cells in the adult hippocampus", *Cell Stem Cell* **7** (2010), p. 78-89.
- [149] R. Zhang, M. Boareto, A. Engler, A. Louvi, C. Giachino, D. Iber, V. Taylor, "Id4 downstream of Notch2 maintains neural stem cell quiescence in the adult hippocampus", *Cell Rep.* **28** (2019), p. 1485-1498, e6.
- [150] G. Zhang, M. Ferg, L. Lübke *et al.*, "Bone morphogenetic protein signaling regulates Id1-mediated neural stem cell quiescence in the adult zebrafish brain via a phylogenetically conserved enhancer module", *Stem Cells* **38** (2020), no. 7, p. 875-889.
- [151] R. Rodriguez Viales, N. Diotel, M. Ferg *et al.*, "The helix-loop-helix protein id1 controls stem cell proliferation during regenerative neurogenesis in the adult zebrafish telencephalon", *Stem Cells* **33** (2015), p. 892-903.
- [152] A. Engler, C. Rolando, C. Giachino *et al.*, "Notch2 signaling maintains NSC quiescence in the murine ventricular-subventricular zone", *Cell Rep.* **22** (2018), p. 992-1002.
- [153] H. Kawai, D. Kawaguchi, B. D. Kuebrich, T. Kitamoto, M. Yamaguchi, Y. Gotoh, S. Furutachi, "Area-specific regulation of quiescent neural stem cells by Notch3 in the adult mouse subependymal zone", *J. Neurosci.* **37** (2017), p. 11867-11880.
- [154] T. Zhang, H. Ding, Y. Wang, Z. Yuan, Y. Zhang, G. Chen, Y. Xu, L. Chen, "Akt3-mTOR regulates hippocampal neurogenesis in adult mouse", *J. Neurochem.* **159** (2021), p. 498-511.
- [155] D. Carvajal Ibañez, M. Skabkin, J. Hooli *et al.*, "Interferon regulates neural stem cell function at all ages by orchestrating mTOR and cell cycle", *EMBO Mol. Med.* **15** (2023), article no. e16434.
- [156] Y. Zhou, A. M. Bond, J. E. Shade *et al.*, "Autocrine Mfge8 signaling prevents developmental exhaustion of the adult neural stem cell pool", *Cell Stem Cell* **23** (2018), p. 444-452, e4.
- [157] L. M. Cochard, L.-C. Levros, S. E. Joppé, F. Pratesi, A. Aumont, K. J. L. Fernandes, "Manipulation of EGFR-induced signaling for the recruitment of quiescent neural stem cells in the adult mouse forebrain", *Front. Neurosci.* **15** (2021), article no. 621076.
- [158] P. Chapouton, P. Skupien, B. Hesl *et al.*, "Notch activity levels control the balance between quiescence and recruitment of adult neural stem cells", *J. Neurosci.* **30** (2010), p. 7961-7974.
- [159] N. Dray, L. Mancini, U. Binshok *et al.*, "Dynamic spatiotemporal coordination of neural stem cell fate decisions occurs through local feedback in the adult vertebrate brain", *Cell Stem Cell* **28** (2021), no. 8, p. 1457-1472, e12.
- [160] E. Than-Trong, S. Ortica-Gatti, S. Mella, C. Nepal, A. Alunni, L. Bally-Cuif, "Neural stem cell quiescence and stemness are molecularly distinct outputs of the Notch3 signalling cascade in the vertebrate adult brain", *Development* **145** (2018), article no. dev161034.
- [161] V. Silva-Vargas, E. E. Crouch, F. Doetsch, "Adult neural stem cells and their niche: a dynamic duo during homeostasis, regeneration, and aging", *Curr. Opin. Neurobiol.* **23** (2013), p. 935-942.
- [162] Z. Chaker, E. Makarouni, F. Doetsch, "The organism as the niche: physiological states crack the code of adult neural stem cell heterogeneity", *Annu. Rev. Cell Dev. Biol.* **40** (2024), no. 1, p. 381-406.
- [163] G. F. Valamparamban, P. Spéder, "Homemade: building the structure of the neurogenic niche", *Front. Cell Dev. Biol.* **11** (2023), article no. 1275963.
- [164] N. Dray, E. Than-Trong, L. Bally-Cuif, "Neural stem cell pools homeostasis in the vertebrate adult brain: cell-autonomous decisions or community rules?", *BioEssays* **43** (2021), article no. e2000228.
- [165] N. Liu, H. Matsumura, T. Kato *et al.*, "Stem cell competition orchestrates skin homeostasis and ageing", *Nature* **568** (2019), p. 344-350.
- [166] Z. Hadjivasiliou, R. E. Moore, R. McIntosh, G. L. Galea, J. D. W. Clarke, P. Alexandre, "Basal protrusions mediate spatiotemporal patterns of spinal neuron differentiation", *Dev. Cell* **49** (2019), p. 907-919, e10.

## References

- Ables, J.L., Decarolis, N.A., Johnson, M.A., Rivera, P.D., Gao, Z., Cooper, D.C., Radtke, F., Hsieh, J., Eisch, A.J., 2010. Notch1 is required for maintenance of the reservoir of adult hippocampal stem cells. *J Neurosci* 30, 10484–10492. <https://doi.org/10.1523/JNEUROSCI.4721-09.2010>
- Acar, A., Hidalgo-Sastre, A., Leverentz, M.K., Mills, C.G., Woodcock, S., Baron, M., Collu, G.M., Brennan, K., 2021. Inhibition of Wnt signalling by Notch via two distinct mechanisms. *Sci Rep* 11, 9096. <https://doi.org/10.1038/s41598-021-88618-5>
- Adolf, B., Chapouton, P., Lam, C.S., Topp, S., Tannhäuser, B., Strähle, U., Götz, M., Bally-Cuif, L., 2006. Conserved and acquired features of adult neurogenesis in the zebrafish telencephalon. *Dev Biol* 295, 278–293. <https://doi.org/10.1016/j.ydbio.2006.03.023>
- Akdemir, E.S., Huang, A.Y.-S., Deneen, B., 2020. Astrocytogenesis: where, when, and how. *F1000Res* 9, F1000 Faculty Rev-233. <https://doi.org/10.12688/f1000research.22405.1>
- Altman, J., 1969. Autoradiographic and histological studies of postnatal neurogenesis. IV. Cell proliferation and migration in the anterior forebrain, with special reference to persisting neurogenesis in the olfactory bulb. *J Comp Neurol* 137, 433–457. <https://doi.org/10.1002/cne.901370404>
- Altman, J., 1963. Autoradiographic investigation of cell proliferation in the brains of rats and cats. *Anat Rec* 145, 573–591. <https://doi.org/10.1002/ar.1091450409>
- Altman, J., Das, G.D., 1965. Autoradiographic and histological evidence of postnatal hippocampal neurogenesis in rats. *J Comp Neurol* 124, 319–335. <https://doi.org/10.1002/cne.901240303>
- Alunni, A., Krecsmarik, M., Bosco, A., Galant, S., Pan, L., Moens, C.B., Bally-Cuif, L., 2013. Notch3 signaling gates cell cycle entry and limits neural stem cell amplification in the adult pallium. *Development* 140, 3335–3347. <https://doi.org/10.1242/dev.095018>
- Alvarez-Buylla, A., Garcia-Verdugo, J.M., 2002. Neurogenesis in adult subventricular zone. *J Neurosci* 22, 629–634. <https://doi.org/10.1523/JNEUROSCI.22-03-00629.2002>
- Andersen, J., Urbán, N., Achimastou, A., Ito, A., Simic, M., Ullom, K., Martynoga, B., Lebel, M., Göritz, C., Frisén, J., Nakafuku, M., Guillemot, F., 2014. A transcriptional mechanism integrating inputs from extracellular signals to activate hippocampal stem cells. *Neuron* 83, 1085–1097. <https://doi.org/10.1016/j.neuron.2014.08.004>
- Andersen, P., Uosaki, H., Shenje, L.T., Kwon, C., 2012. Non-canonical Notch signaling: emerging role and mechanism. *Trends Cell Biol* 22, 257–265. <https://doi.org/10.1016/j.tcb.2012.02.003>
- Ando, K., Wang, W., Peng, D., Chiba, A., Lagendijk, A.K., Barske, L., Crump, J.G., Stainier, D.Y.R., Lendahl, U., Koltowska, K., Hogan, B.M., Fukuhara, S., Mochizuki, N., Betsholtz, C., 2019. Peri-arterial specification of vascular mural cells from naïve mesenchyme requires Notch signaling. *Development* 146, dev165589. <https://doi.org/10.1242/dev.165589>
- Andreu-Agulló, C., Morante-Redolat, J.M., Delgado, A.C., Fariñas, I., 2009. Vascular niche factor PEDF modulates Notch-dependent stemness in the adult subependymal zone. *Nat Neurosci* 12, 1514–1523. <https://doi.org/10.1038/nn.2437>
- Anneser, L., Satou, C., Hotz, H.-R., Friedrich, R.W., 2024. Molecular organization of neuronal cell types and neuromodulatory systems in the zebrafish telencephalon. *Curr Biol* 34, 298–312.e4. <https://doi.org/10.1016/j.cub.2023.12.003>
- Appel, B., Givan, L.A., Eisen, J.S., 2001. Delta-Notch signaling and lateral inhibition in zebrafish spinal cord development. *BMC Dev Biol* 1, 13. <https://doi.org/10.1186/1471-213x-1-13>

- Araki, T., Ikegaya, Y., Koyama, R., 2021. The effects of microglia- and astrocyte-derived factors on neurogenesis in health and disease. *Eur J Neurosci* 54, 5880–5901. <https://doi.org/10.1111/ejn.14969>
- Azzarelli, R., Simons, B.D., Philpott, A., 2018. The developmental origin of brain tumours: a cellular and molecular framework. *Development* 145, dev162693. <https://doi.org/10.1242/dev.162693>
- Bahrami, N., Childs, S.J., 2018. Pericyte Biology in Zebrafish. *Adv Exp Med Biol* 1109, 33–51. [https://doi.org/10.1007/978-3-030-02601-1\\_4](https://doi.org/10.1007/978-3-030-02601-1_4)
- Bahrampour, S., Thor, S., 2020. The Five Faces of Notch Signalling During *Drosophila melanogaster* Embryonic CNS Development. *Adv Exp Med Biol* 1218, 39–58. [https://doi.org/10.1007/978-3-030-34436-8\\_3](https://doi.org/10.1007/978-3-030-34436-8_3)
- Baker, N.E., Brown, N.L., 2018. All in the family: proneural bHLH genes and neuronal diversity. *Development* 145, dev159426. <https://doi.org/10.1242/dev.159426>
- Barbosa, J.S., Sanchez-Gonzalez, R., Di Giaimo, R., Baumgart, E.V., Theis, F.J., Götz, M., Ninkovic, J., 2015. Neurodevelopment. Live imaging of adult neural stem cell behavior in the intact and injured zebrafish brain. *Science* 348, 789–793. <https://doi.org/10.1126/science.aaa2729>
- Bard, J.A.M., Goodall, E.A., Greene, E.R., Jonsson, E., Dong, K.C., Martin, A., 2018. Structure and Function of the 26S Proteasome. *Annu Rev Biochem* 87, 697–724. <https://doi.org/10.1146/annurev-biochem-062917-011931>
- Basak, O., Giachino, C., Fiorini, E., Macdonald, H.R., Taylor, V., 2012. Neurogenic subventricular zone stem/progenitor cells are Notch1-dependent in their active but not quiescent state. *J Neurosci* 32, 5654–5666. <https://doi.org/10.1523/JNEUROSCI.0455-12.2012>
- Basak, O., Krieger, T.G., Muraro, M.J., Wiebrands, K., Stange, D.E., Frias-Aldeguer, J., Rivron, N.C., van de Wetering, M., van Es, J.H., van Oudenaarden, A., Simons, B.D., Clevers, H., 2018. Troy+ brain stem cells cycle through quiescence and regulate their number by sensing niche occupancy. *Proc Natl Acad Sci U S A* 115, E610–E619. <https://doi.org/10.1073/pnas.1715911114>
- Basak, O., Taylor, V., 2007. Identification of self-replicating multipotent progenitors in the embryonic nervous system by high Notch activity and Hes5 expression. *European Journal of Neuroscience* 25, 1006–1022. <https://doi.org/10.1111/j.1460-9568.2007.05370.x>
- Batista, M.R., Diniz, P., Torres, A., Murta, D., Lopes-da-Costa, L., Silva, E., 2020. Notch signaling in mouse blastocyst development and hatching. *BMC Dev Biol* 20, 9. <https://doi.org/10.1186/s12861-020-00216-2>
- Baye, L.M., Link, B.A., 2007. Interkinetic nuclear migration and the selection of neurogenic cell divisions during vertebrate retinogenesis. *J Neurosci* 27, 10143–10152. <https://doi.org/10.1523/JNEUROSCI.2754-07.2007>
- Bellec, K., Pinot, M., Gicquel, I., Le Borgne, R., 2021. The Clathrin adaptor AP-1 and Stratum act in parallel pathways to control Notch activation in *Drosophila* sensory organ precursors cells. *Development* 148, dev191437. <https://doi.org/10.1242/dev.191437>
- Belmonte-Mateos, C., Meister, L., Pujades, C., 2023. Hindbrain rhombomere centers harbor a heterogenous population of dividing progenitors which rely on Notch signaling. *Front Cell Dev Biol* 11, 1268631. <https://doi.org/10.3389/fcell.2023.1268631>
- Berger, T., Lee, H., Young, A.H., Aarsland, D., Thuret, S., 2020. Adult Hippocampal Neurogenesis in Major Depressive Disorder and Alzheimer’s Disease. *Trends Mol Med* 26, 803–818. <https://doi.org/10.1016/j.molmed.2020.03.010>
- Bernardos, R.L., Barthel, L.K., Meyers, J.R., Raymond, P.A., 2007. Late-stage neuronal progenitors in the retina are radial Müller glia that function as retinal stem cells. *J*



- Neurosci 27, 7028–7040. <https://doi.org/10.1523/JNEUROSCI.1624-07.2007>
- Bernardos, R.L., Raymond, P.A., 2006. GFAP transgenic zebrafish. *Gene Expr Patterns* 6, 1007–1013. <https://doi.org/10.1016/j.modgep.2006.04.006>
- Bertrand, N., Castro, D.S., Guillemot, F., 2002. Proneural genes and the specification of neural cell types. *Nat Rev Neurosci* 3, 517–530. <https://doi.org/10.1038/nrn874>
- Bian, W., Jiang, H., Yao, L., Hao, W., Wu, L., Li, X., 2023. A spatially defined human Notch receptor interaction network reveals Notch intracellular storage and Ataxin-2-mediated fast recycling. *Cell Rep* 42, 112819. <https://doi.org/10.1016/j.celrep.2023.112819>
- Bill, B.R., Petzold, A.M., Clark, K.J., Schimmenti, L.A., Ekker, S.C., 2009. A primer for morpholino use in zebrafish. *Zebrafish* 6, 69–77. <https://doi.org/10.1089/zeb.2008.0555>
- Blomfield, I.M., Rocamonde, B., Masdeu, M.D.M., Mulugeta, E., Vaga, S., van den Berg, D.L., Huillard, E., Guillemot, F., Urbán, N., 2019. Id4 promotes the elimination of the pro-activation factor *Ascl1* to maintain quiescence of adult hippocampal stem cells. *Elife* 8, e48561. <https://doi.org/10.7554/eLife.48561>
- Boareto, M., 2020. Patterning via local cell-cell interactions in developing systems. *Dev Biol* 460, 77–85. <https://doi.org/10.1016/j.ydbio.2019.12.008>
- Bonaguidi, M.A., Wheeler, M.A., Shapiro, J.S., Stadel, R.P., Sun, G.J., Ming, G., Song, H., 2011. In vivo clonal analysis reveals self-renewing and multipotent adult neural stem cell characteristics. *Cell* 145, 1142–1155. <https://doi.org/10.1016/j.cell.2011.05.024>
- Bond, A.M., Ming, G.-L., Song, H., 2015. Adult Mammalian Neural Stem Cells and Neurogenesis: Five Decades Later. *Cell Stem Cell* 17, 385–395. <https://doi.org/10.1016/j.stem.2015.09.003>
- Boniface, E.J., Lu, J., Victoroff, T., Zhu, M., Chen, W., 2009. FLEX-based transgenic reporter lines for visualization of Cre and Flp activity in live zebrafish. *genesis* 47, 484–491. <https://doi.org/10.1002/dvg.20526>
- Borggreffe, T., Lauth, M., Zwijsen, A., Huylebroeck, D., Oswald, F., Giaimo, B.D., 2016. The Notch intracellular domain integrates signals from Wnt, Hedgehog, TGF $\beta$ /BMP and hypoxia pathways. *Biochim Biophys Acta* 1863, 303–313. <https://doi.org/10.1016/j.bbamcr.2015.11.020>
- Borggreffe, T., Oswald, F., 2009. The Notch signaling pathway: transcriptional regulation at Notch target genes. *Cell Mol Life Sci* 66, 1631–1646. <https://doi.org/10.1007/s00018-009-8668-7>
- Bottes, S., Jaeger, B.N., Pilz, G.-A., Jörg, D.J., Cole, J.D., Kruse, M., Harris, L., Korobeynyk, V.I., Mallona, I., Helmchen, F., Guillemot, F., Simons, B.D., Jessberger, S., 2021. Long-term self-renewing stem cells in the adult mouse hippocampus identified by intravital imaging. *Nat Neurosci* 24, 225–233. <https://doi.org/10.1038/s41593-020-00759-4>
- Bouabe, H., Okkenhaug, K., 2013. Gene Targeting in Mice: a Review. *Methods Mol Biol* 1064, 315–336. [https://doi.org/10.1007/978-1-62703-601-6\\_23](https://doi.org/10.1007/978-1-62703-601-6_23)
- Bray, S., 1998. Notch signalling in *Drosophila*: three ways to use a pathway. *Semin Cell Dev Biol* 9, 591–597. <https://doi.org/10.1006/scdb.1998.0262>
- Bray, S.J., 2016. Notch signalling in context. *Nat Rev Mol Cell Biol* 17, 722–735. <https://doi.org/10.1038/nrm.2016.94>
- Bray, S.J., Gomez-Lamarca, M., 2018. Notch after cleavage. *Curr Opin Cell Biol* 51, 103–109. <https://doi.org/10.1016/j.ceb.2017.12.008>
- Bringuier, C.M., Noristani, H.N., Perez, J.-C., Cardoso, M., Goze-Bac, C., Gerber, Y.N., Perrin, F.E., 2023. Up-Regulation of Astrocytic *Fgfr4* Expression in Adult Mice after Spinal Cord Injury. *Cells* 12, 528. <https://doi.org/10.3390/cells12040528>
- Buckley, C.E., Marguerie, A., Alderton, W.K., Franklin, R.J.M., 2010. Temporal dynamics of myelination in the zebrafish spinal cord. *Glia* 58, 802–812.

- <https://doi.org/10.1002/glia.20964>
- Bueno, D., Parvas, M., Nabiuni, M., Miyan, J., 2020. Embryonic cerebrospinal fluid formation and regulation. *Semin Cell Dev Biol* 102, 3–12. <https://doi.org/10.1016/j.semcdb.2019.09.006>
- Bultje, R.S., Castaneda-Castellanos, D.R., Jan, L.Y., Jan, Y.-N., Kriegstein, A.R., Shi, S.-H., 2009. Mammalian Par3 regulates progenitor cell asymmetric division via notch signaling in the developing neocortex. *Neuron* 63, 189–202. <https://doi.org/10.1016/j.neuron.2009.07.004>
- Byrd, C.A., Brunjes, P.C., 2001. Neurogenesis in the olfactory bulb of adult zebrafish. *Neuroscience* 105, 793–801. [https://doi.org/10.1016/s0306-4522\(01\)00215-9](https://doi.org/10.1016/s0306-4522(01)00215-9)
- Byrd, C.A., Brunjes, P.C., 1998. Addition of new cells to the olfactory bulb of adult zebrafish. *Ann N Y Acad Sci* 855, 274–276. <https://doi.org/10.1111/j.1749-6632.1998.tb10582.x>
- Cahoy, J.D., Emery, B., Kaushal, A., Foo, L.C., Zamanian, J.L., Christopherson, K.S., Xing, Y., Lubischer, J.L., Krieg, P.A., Krupenko, S.A., Thompson, W.J., Barres, B.A., 2008. A transcriptome database for astrocytes, neurons, and oligodendrocytes: a new resource for understanding brain development and function. *J Neurosci* 28, 264–278. <https://doi.org/10.1523/JNEUROSCI.4178-07.2008>
- Calzolari, F., Michel, J., Baumgart, E.V., Theis, F., Götz, M., Ninkovic, J., 2015. Fast clonal expansion and limited neural stem cell self-renewal in the adult subependymal zone. *Nat Neurosci* 18, 490–492. <https://doi.org/10.1038/nn.3963>
- Campbell, L.J., Hobgood, J.S., Jia, M., Boyd, P., Hipp, R.I., Hyde, D.R., 2021. Notch3 and DeltaB maintain Müller glia quiescence and act as negative regulators of regeneration in the light-damaged zebrafish retina. *Glia* 69, 546–566. <https://doi.org/10.1002/glia.23912>
- Campbell, L.J., Levendusky, J.L., Steines, S.A., Hyde, D.R., 2022. Retinal regeneration requires dynamic Notch signaling. *Neural Regen Res* 17, 1199–1209. <https://doi.org/10.4103/1673-5374.327326>
- Cardozo, M.J., Mysiak, K.S., Becker, T., Becker, C.G., 2017. Reduce, reuse, recycle - Developmental signals in spinal cord regeneration. *Dev Biol* 432, 53–62. <https://doi.org/10.1016/j.ydbio.2017.05.011>
- Carney, T.J., Mosimann, C., 2018. Switch and Trace: Recombinase Genetics in Zebrafish. *Trends Genet* 34, 362–378. <https://doi.org/10.1016/j.tig.2018.01.004>
- Casano, A.M., Peri, F., 2015. Microglia: multitasking specialists of the brain. *Dev Cell* 32, 469–477. <https://doi.org/10.1016/j.devcel.2015.01.018>
- Castel, D., Mourikis, P., Bartels, S.J.J., Brinkman, A.B., Tajbakhsh, S., Stunnenberg, H.G., 2013. Dynamic binding of RBPJ is determined by Notch signaling status. *Genes Dev* 27, 1059–1071. <https://doi.org/10.1101/gad.211912.112>
- Caussinus, E., Kanca, O., Affolter, M., 2011. Fluorescent fusion protein knockout mediated by anti-GFP nanobody. *Nat Struct Mol Biol* 19, 117–121. <https://doi.org/10.1038/nsmb.2180>
- Chapouton, P., Skupien, P., Hesl, B., Coolen, M., Moore, J.C., Madelaine, R., Kremmer, E., Faus-Kessler, T., Blader, P., Lawson, N.D., Bally-Cuif, L., 2010. Notch activity levels control the balance between quiescence and recruitment of adult neural stem cells. *J Neurosci* 30, 7961–7974. <https://doi.org/10.1523/JNEUROSCI.6170-09.2010>
- Chapouton, P., Webb, K.J., Stigloher, C., Alunni, A., Adolf, B., Hesl, B., Topp, S., Kremmer, E., Bally-Cuif, L., 2011. Expression of hairy/enhancer of split genes in neural progenitors and neurogenesis domains of the adult zebrafish brain. *J Comp Neurol* 519, 1748–1769. <https://doi.org/10.1002/cne.22599>
- Chen, C., Fingerhut, J.M., Yamashita, Y.M., 2016. The ins(ide) and outs(ide) of asymmetric stem cell division. *Curr Opin Cell Biol* 43, 1–6.

- <https://doi.org/10.1016/j.ceb.2016.06.001>
- Chen, Y., Li, H., Yi, T.-C., Shen, J., Zhang, J., 2023. Notch Signaling in Insect Development: A Simple Pathway with Diverse Functions. *Int J Mol Sci* 24, 14028. <https://doi.org/10.3390/ijms241814028>
- Cheng, X.-T., Xie, Y.-X., Zhou, B., Huang, N., Farfel-Becker, T., Sheng, Z.-H., 2018. Revisiting LAMP1 as a marker for degradative autophagy-lysosomal organelles in the nervous system. *Autophagy* 14, 1472–1474. <https://doi.org/10.1080/15548627.2018.1482147>
- Cheng, Y.-C., Amoyel, M., Qiu, X., Jiang, Y.-J., Xu, Q., Wilkinson, D.G., 2004. Notch activation regulates the segregation and differentiation of rhombomere boundary cells in the zebrafish hindbrain. *Dev Cell* 6, 539–550. [https://doi.org/10.1016/s1534-5807\(04\)00097-8](https://doi.org/10.1016/s1534-5807(04)00097-8)
- Cheung, T.H., Rando, T.A., 2013. Molecular regulation of stem cell quiescence. *Nat Rev Mol Cell Biol* 14, 329–340. <https://doi.org/10.1038/nrm3591>
- Christie, S.B., Li, R.-W., Miralles, C.P., Yang, B.-Y., De Blas, A.L., 2006. Clustered and non-clustered GABAA receptors in cultured hippocampal neurons. *Mol Cell Neurosci* 31, 1–14. <https://doi.org/10.1016/j.mcn.2005.08.014>
- Conlon, R.A., Reaume, A.G., Rossant, J., 1995. Notch1 is required for the coordinate segmentation of somites. *Development* 121, 1533–1545. <https://doi.org/10.1242/dev.121.5.1533>
- Coolen, M., Thieffry, D., Drivenes, Ø., Becker, T.S., Bally-Cuif, L., 2012. miR-9 controls the timing of neurogenesis through the direct inhibition of antagonistic factors. *Dev Cell* 22, 1052–1064. <https://doi.org/10.1016/j.devcel.2012.03.003>
- Cosacak, M.I., Bhattarai, P., Reinhardt, S., Petzold, A., Dahl, A., Zhang, Y., Kizil, C., 2019. Single-Cell Transcriptomics Analyses of Neural Stem Cell Heterogeneity and Contextual Plasticity in a Zebrafish Brain Model of Amyloid Toxicity. *Cell Rep* 27, 1307–1318.e3. <https://doi.org/10.1016/j.celrep.2019.03.090>
- Coumailleau, F., Fürthauer, M., Knoblich, J.A., González-Gaitán, M., 2009. Directional Delta and Notch trafficking in Sara endosomes during asymmetric cell division. *Nature* 458, 1051–1055. <https://doi.org/10.1038/nature07854>
- Couturier, L., Mazouni, K., Schweisguth, F., 2013. Numb Localizes at Endosomes and Controls the Endosomal Sorting of Notch after Asymmetric Division in *Drosophila*. *Current Biology* 23, 588–593. <https://doi.org/10.1016/j.cub.2013.03.002>
- Couturier, L., Trylinski, M., Mazouni, K., Darnet, L., Schweisguth, F., 2014. A fluorescent tagging approach in *Drosophila* reveals late endosomal trafficking of Notch and Sanpodo. *J Cell Biol* 207, 351–363. <https://doi.org/10.1083/jcb.201407071>
- Couturier, L., Vodovar, N., Schweisguth, F., 2012. Endocytosis by Numb breaks Notch symmetry at cytokinesis. *Nat Cell Biol* 14, 131–139. <https://doi.org/10.1038/ncb2419>
- Dambroise, E., Simion, M., Bourquard, T., Bouffard, S., Rizzi, B., Jaszczyszyn, Y., Bourge, M., Affaticati, P., Heuzé, A., Jouralet, J., Edouard, J., Brown, S., Thermes, C., Poupon, A., Reiter, E., Sohm, F., Bourrat, F., Joly, J.-S., 2017. Postembryonic Fish Brain Proliferation Zones Exhibit Neuroepithelial-Type Gene Expression Profile. *Stem Cells* 35, 1505–1518. <https://doi.org/10.1002/stem.2588>
- Dang, L., Yoon, K., Wang, M., Gaiano, N., 2006. Notch3 signaling promotes radial glial/progenitor character in the mammalian telencephalon. *Dev Neurosci* 28, 58–69. <https://doi.org/10.1159/000090753>
- Das, R.M., Storey, K.G., 2014. Apical abscission alters cell polarity and dismantles the primary cilium during neurogenesis. *Science* 343, 200–204. <https://doi.org/10.1126/science.1247521>
- de la Pompa, J.L., Wakeham, A., Correia, K.M., Samper, E., Brown, S., Aguilera, R.J., Nakano,

- T., Honjo, T., Mak, T.W., Rossant, J., Conlon, R.A., 1997. Conservation of the Notch signalling pathway in mammalian neurogenesis. *Development* 124, 1139–1148. <https://doi.org/10.1242/dev.124.6.1139>
- Deasy, B., 2009. Asymmetric Behavior in Stem Cells. pp. 13–26. [https://doi.org/10.1007/978-1-60327-227-8\\_2](https://doi.org/10.1007/978-1-60327-227-8_2)
- Del Bene, F., Wehman, A.M., Link, B.A., Baier, H., 2008. Regulation of neurogenesis by interkinetic nuclear migration through an apical-basal notch gradient. *Cell* 134, 1055–1065. <https://doi.org/10.1016/j.cell.2008.07.017>
- Delgado, A.C., Maldonado-Soto, A.R., Silva-Vargas, V., Mizrak, D., von Känel, T., Tan, K.R., Paul, A., Madar, A., Cuervo, H., Kitajewski, J., Lin, C.-S., Doetsch, F., 2021. Release of stem cells from quiescence reveals gliogenic domains in the adult mouse brain. *Science* 372, 1205–1209. <https://doi.org/10.1126/science.abg8467>
- Demmerle, J., Hao, S., Cai, D., 2023. Transcriptional condensates and phase separation: condensing information across scales and mechanisms. *Nucleus* 14, 2213551. <https://doi.org/10.1080/19491034.2023.2213551>
- Dennis, D.J., Wilkinson, G., Li, S., Dixit, R., Adnani, L., Balakrishnan, A., Han, S., Kovach, C., Gruenig, N., Kurrasch, D.M., Dyck, R.H., Schuurmans, C., 2017. Neurog2 and Ascl1 together regulate a postmitotic derepression circuit to govern laminar fate specification in the murine neocortex. *Proc Natl Acad Sci U S A* 114, E4934–E4943. <https://doi.org/10.1073/pnas.1701495114>
- D’Gama, P.P., Qiu, T., Cosacak, M.I., Rayamajhi, D., Konac, A., Hansen, J.N., Ringers, C., Acuña-Hinrichsen, F., Hui, S.P., Olstad, E.W., Chong, Y.L., Lim, C.K.A., Gupta, A., Ng, C.P., Nilges, B.S., Kashikar, N.D., Wachten, D., Liebl, D., Kikuchi, K., Kizil, C., Yaksi, E., Roy, S., Jurisch-Yaksi, N., 2021. Diversity and function of motile ciliated cell types within ependymal lineages of the zebrafish brain. *Cell Rep* 37, 109775. <https://doi.org/10.1016/j.celrep.2021.109775>
- Dho, S.E., Silva-Gagliardi, N., Morgese, F., Coyaud, E., Lamoureux, E., Berry, D.M., Raught, B., McGlade, C.J., 2019. Proximity interactions of the ubiquitin ligase Mind bomb 1 reveal a role in regulation of epithelial polarity complex proteins. *Sci Rep* 9, 12471. <https://doi.org/10.1038/s41598-019-48902-x>
- Dias, T.B., Yang, Y.-J., Ogai, K., Becker, T., Becker, C.G., 2012. Notch signaling controls generation of motor neurons in the lesioned spinal cord of adult zebrafish. *J Neurosci* 32, 3245–3252. <https://doi.org/10.1523/JNEUROSCI.6398-11.2012>
- Diotel, N., Lübke, L., Strähle, U., Rastegar, S., 2020. Common and Distinct Features of Adult Neurogenesis and Regeneration in the Telencephalon of Zebrafish and Mammals. *Front Neurosci* 14, 568930. <https://doi.org/10.3389/fnins.2020.568930>
- Dirian, L., Galant, S., Coolen, M., Chen, W., Bedu, S., Houart, C., Bally-Cuif, L., Foucher, I., 2014. Spatial regionalization and heterochrony in the formation of adult pallial neural stem cells. *Dev Cell* 30, 123–136. <https://doi.org/10.1016/j.devcel.2014.05.012>
- Doetsch, F., Caillé, I., Lim, D.A., García-Verdugo, J.M., Alvarez-Buylla, A., 1999. Subventricular zone astrocytes are neural stem cells in the adult mammalian brain. *Cell* 97, 703–716. [https://doi.org/10.1016/s0092-8674\(00\)80783-7](https://doi.org/10.1016/s0092-8674(00)80783-7)
- Dong, Z., Yang, N., Yeo, S.-Y., Chitnis, A., Guo, S., 2012. Intralineaage directional Notch signaling regulates self-renewal and differentiation of asymmetrically dividing radial glia. *Neuron* 74, 65–78. <https://doi.org/10.1016/j.neuron.2012.01.031>
- Dong, Z., Wagle, M., Guo, S., 2011. Time-lapse live imaging of clonally related neural progenitor cells in the developing zebrafish forebrain. *J Vis Exp* 2594. <https://doi.org/10.3791/2594>
- Doostdar, P., Hawley, J., Chopra, K., Marinopoulou, E., Lea, R., Arashvand, K., Biga, V., Papalopulu, N., Soto, X., 2024. Cell coupling compensates for changes in single-cell

- Her6 dynamics and provides phenotypic robustness. *Development* 151, dev202640. <https://doi.org/10.1242/dev.202640>
- Dray, N., Bedu, S., Vuillemin, N., Alunni, A., Coolen, M., Krecsmarik, M., Supatto, W., Beaurepaire, E., Bally-Cuif, L., 2015. Large-scale live imaging of adult neural stem cells in their endogenous niche. *Development* 142, 3592–3600. <https://doi.org/10.1242/dev.123018>
- Dray, N., Mancini, L., Binshtok, U., Cheysson, F., Supatto, W., Mahou, P., Bedu, S., Ortica, S., Than-Trong, E., Krecsmarik, M., Herbert, S., Masson, J.-B., Tinevez, J.-Y., Lang, G., Beaurepaire, E., Sprinzak, D., Bally-Cuif, L., 2021. Dynamic spatiotemporal coordination of neural stem cell fate decisions occurs through local feedback in the adult vertebrate brain. *Cell Stem Cell* 28, 1457-1472.e12. <https://doi.org/10.1016/j.stem.2021.03.014>
- D'Souza, B., Meloty-Kapella, L., Weinmaster, G., 2010. Canonical and non-canonical Notch ligands. *Curr Top Dev Biol* 92, 73–129. [https://doi.org/10.1016/S0070-2153\(10\)92003-6](https://doi.org/10.1016/S0070-2153(10)92003-6)
- Dubreuil, V., Marzesco, A.-M., Corbeil, D., Huttner, W.B., Wilsch-Bräuninger, M., 2007. Midbody and primary cilium of neural progenitors release extracellular membrane particles enriched in the stem cell marker prominin-1. *J Cell Biol* 176, 483–495. <https://doi.org/10.1083/jcb.200608137>
- Dulken, B.W., Leeman, D.S., Boutet, S.C., Hebestreit, K., Brunet, A., 2017. Single-Cell Transcriptomic Analysis Defines Heterogeneity and Transcriptional Dynamics in the Adult Neural Stem Cell Lineage. *Cell Rep* 18, 777–790. <https://doi.org/10.1016/j.celrep.2016.12.060>
- Dvorianchikova, G., Perea-Martinez, I., Pappas, S., Barry, A.F., Danek, D., Dvorianchikova, X., Pelaez, D., Ivanov, D., 2015. Molecular Characterization of Notch1 Positive Progenitor Cells in the Developing Retina. *PLoS One* 10, e0131054. <https://doi.org/10.1371/journal.pone.0131054>
- Edelmann, K., Glashauser, L., Sprungala, S., Hesl, B., Fritschle, M., Ninkovic, J., Godinho, L., Chapouton, P., 2013. Increased radial glia quiescence, decreased reactivation upon injury and unaltered neuroblast behavior underlie decreased neurogenesis in the aging zebrafish telencephalon. *J Comp Neurol* 521, 3099–3115. <https://doi.org/10.1002/cne.23347>
- Ehm, O., Göritz, C., Covic, M., Schäffner, I., Schwarz, T.J., Karaca, E., Kempkes, B., Kremmer, E., Pfrieger, F.W., Espinosa, L., Bigas, A., Giachino, C., Taylor, V., Frisén, J., Lie, D.C., 2010. RBPJkappa-dependent signaling is essential for long-term maintenance of neural stem cells in the adult hippocampus. *J Neurosci* 30, 13794–13807. <https://doi.org/10.1523/JNEUROSCI.1567-10.2010>
- Ehret, F., Vogler, S., Pojar, S., Elliott, D.A., Bradke, F., Steiner, B., Kempermann, G., 2015. Mouse model of CADASIL reveals novel insights into Notch3 function in adult hippocampal neurogenesis. *Neurobiol Dis* 75, 131–141. <https://doi.org/10.1016/j.nbd.2014.12.018>
- El-Brolosy, M.A., Kontarakis, Z., Rossi, A., Kuenne, C., Günther, S., Fukuda, N., Kikhi, K., Boezio, G.L.M., Takacs, C.M., Lai, S.-L., Fukuda, R., Gerri, C., Giraldez, A.J., Stainier, D.Y.R., 2019. Genetic compensation triggered by mutant mRNA degradation. *Nature* 568, 193–197. <https://doi.org/10.1038/s41586-019-1064-z>
- El-Brolosy, M.A., Stainier, D.Y.R., 2017. Genetic compensation: A phenomenon in search of mechanisms. *PLoS Genet* 13, e1006780. <https://doi.org/10.1371/journal.pgen.1006780>
- Elliott, A.D., 2020. Confocal Microscopy: Principles and Modern Practices. *Curr Protoc Cytom* 92, e68. <https://doi.org/10.1002/cpcy.68>
- Encinas, J.M., Michurina, T.V., Peunova, N., Park, J.-H., Tordo, J., Peterson, D.A., Fishell, G.,

- Koulakov, A., Enikolopov, G., 2011. Division-coupled astrocytic differentiation and age-related depletion of neural stem cells in the adult hippocampus. *Cell Stem Cell* 8, 566–579. <https://doi.org/10.1016/j.stem.2011.03.010>
- Encinas, J.M., Sierra, A., 2012. Neural stem cell deforestation as the main force driving the age-related decline in adult hippocampal neurogenesis. *Behav Brain Res* 227, 433–439. <https://doi.org/10.1016/j.bbr.2011.10.010>
- Engler, A., Rolando, C., Giachino, C., Saotome, I., Erni, A., Brien, C., Zhang, R., Zimmer-Strobl, U., Radtke, F., Artavanis-Tsakonas, S., Louvi, A., Taylor, V., 2018a. Notch2 Signaling Maintains NSC Quiescence in the Murine Ventricular-Subventricular Zone. *Cell Rep* 22, 992–1002. <https://doi.org/10.1016/j.celrep.2017.12.094>
- Engler, A., Zhang, R., Taylor, V., 2018b. Notch and Neurogenesis, in: Borggreffe, T., Giaimo, B.D. (Eds.), *Molecular Mechanisms of Notch Signaling*. Springer International Publishing, Cham, pp. 223–234. [https://doi.org/10.1007/978-3-319-89512-3\\_11](https://doi.org/10.1007/978-3-319-89512-3_11)
- Falo-Sanjuan, J., Bray, S.J., 2021. Membrane architecture and adherens junctions contribute to strong Notch pathway activation. *Development* 148, dev199831. <https://doi.org/10.1242/dev.199831>
- Farmer, W.T., Murai, K., 2017. Resolving Astrocyte Heterogeneity in the CNS. *Front Cell Neurosci* 11, 300. <https://doi.org/10.3389/fncel.2017.00300>
- Faucherre, A., Moha Ou Maati, H., Nasr, N., Pinard, A., Theron, A., Odelin, G., Desvignes, J.-P., Salgado, D., Collod-Bérout, G., Avierinos, J.-F., Lebon, G., Zaffran, S., Jopling, C., 2020. Piezo1 is required for outflow tract and aortic valve development. *J Mol Cell Cardiol* 143, 51–62. <https://doi.org/10.1016/j.yjmcc.2020.03.013>
- Felker, A., Mosimann, C., 2016. Contemporary zebrafish transgenesis with Tol2 and application for Cre/lox recombination experiments. *Methods Cell Biol* 135, 219–244. <https://doi.org/10.1016/bs.mcb.2016.01.009>
- Feng, M., Santhanam, R.K., Xing, H., Zhou, M., Jia, H., 2024. Inhibition of  $\gamma$ -secretase/Notch pathway as a potential therapy for reversing cancer drug resistance. *Biochem Pharmacol* 220, 115991. <https://doi.org/10.1016/j.bcp.2023.115991>
- Fischer, A., Gessler, M., 2007. Delta-Notch--and then? Protein interactions and proposed modes of repression by Hes and Hey bHLH factors. *Nucleic Acids Res* 35, 4583–4596. <https://doi.org/10.1093/nar/gkm477>
- Folgueira, M., Bayley, P., Navratilova, P., Becker, T.S., Wilson, S.W., Clarke, J.D.W., 2012. Morphogenesis underlying the development of the everted teleost telencephalon. *Neural Dev* 7, 32. <https://doi.org/10.1186/1749-8104-7-32>
- Fontán-Lozano, Á., Morcuende, S., Davis-López de Carrizosa, M.A., Benítez-Temiño, B., Mejías, R., Matarredona, E.R., 2020. To Become or Not to Become Tumorigenic: Subventricular Zone Versus Hippocampal Neural Stem Cells. *Front Oncol* 10, 602217. <https://doi.org/10.3389/fonc.2020.602217>
- Fousse, J., Gautier, E., Patti, D., Dehay, C., 2019. Developmental changes in interkinetic nuclear migration dynamics with respect to cell-cycle progression in the mouse cerebral cortex ventricular zone. *J Comp Neurol* 527, 1545–1557. <https://doi.org/10.1002/cne.24641>
- Frith, T.J.R., Briscoe, J., Boezio, G.L.M., 2024. From signalling to form: the coordination of neural tube patterning. *Curr Top Dev Biol* 159, 168–231. <https://doi.org/10.1016/bs.ctdb.2023.11.004>
- Fryer, C.J., White, J.B., Jones, K.A., 2004. Mastermind recruits CycC:CDK8 to phosphorylate the Notch ICD and coordinate activation with turnover. *Mol Cell* 16, 509–520. <https://doi.org/10.1016/j.molcel.2004.10.014>
- Fuentealba, L.C., Obernier, K., Alvarez-Buylla, A., 2012. Adult neural stem cells bridge their niche. *Cell Stem Cell* 10, 698–708. <https://doi.org/10.1016/j.stem.2012.05.012>

- Fuentealba, L.C., Rompani, S.B., Parraguez, J.I., Obernier, K., Romero, R., Cepko, C.L., Alvarez-Buylla, A., 2015. Embryonic Origin of Postnatal Neural Stem Cells. *Cell* 161, 1644–1655. <https://doi.org/10.1016/j.cell.2015.05.041>
- Furlan, G., Cuccioli, V., Vuillemin, N., Dirian, L., Muntasell, A.J., Coolen, M., Dray, N., Bedu, S., Houart, C., Beaurepaire, E., Foucher, I., Bally-Cuif, L., 2017. Life-Long Neurogenic Activity of Individual Neural Stem Cells and Continuous Growth Establish an Outside-In Architecture in the Teleost Pallium. *Curr Biol* 27, 3288–3301.e3. <https://doi.org/10.1016/j.cub.2017.09.052>
- Fürthauer, M., González-Gaitán, M., 2009. Endocytic regulation of notch signalling during development. *Traffic* 10, 792–802. <https://doi.org/10.1111/j.1600-0854.2009.00914.x>
- Furutachi, S., Miya, H., Watanabe, T., Kawai, H., Yamasaki, N., Harada, Y., Imayoshi, I., Nelson, M., Nakayama, K.I., Hirabayashi, Y., Gotoh, Y., 2015. Slowly dividing neural progenitors are an embryonic origin of adult neural stem cells. *Nat Neurosci* 18, 657–665. <https://doi.org/10.1038/nn.3989>
- Gaiano, N., Nye, J.S., Fishell, G., 2000. Radial glial identity is promoted by Notch1 signaling in the murine forebrain. *Neuron* 26, 395–404. [https://doi.org/10.1016/s0896-6273\(00\)81172-1](https://doi.org/10.1016/s0896-6273(00)81172-1)
- Galant, S., Furlan, G., Coolen, M., Dirian, L., Foucher, I., Bally-Cuif, L., 2016. Embryonic origin and lineage hierarchies of the neural progenitor subtypes building the zebrafish adult midbrain. *Dev Biol* 420, 120–135. <https://doi.org/10.1016/j.ydbio.2016.09.022>
- Gansner, J.M., Dang, M., Ammerman, M., Zon, L.I., 2017. Transplantation in zebrafish. *Methods Cell Biol* 138, 629–647. <https://doi.org/10.1016/bs.mcb.2016.08.006>
- Ganz, J., Kaslin, J., Hochmann, S., Freudenreich, D., Brand, M., 2010. Heterogeneity and Fgf dependence of adult neural progenitors in the zebrafish telencephalon. *Glia* 58, 1345–1363. <https://doi.org/10.1002/glia.21012>
- Ganz, J., Kroehne, V., Freudenreich, D., Machate, A., Geffarth, M., Braasch, I., Kaslin, J., Brand, M., 2014. Subdivisions of the adult zebrafish pallium based on molecular marker analysis. *F1000Res* 3, 308. <https://doi.org/10.12688/f1000research.5595.2>
- Gao, H., Bu, Y., Wu, Q., Wang, X., Chang, N., Lei, L., Chen, S., Liu, D., Zhu, X., Hu, K., Xiong, J.-W., 2015. Mecp2 regulates neural cell differentiation by suppressing the Id1 to Her2 axis in zebrafish. *J Cell Sci* 128, 2340–2350. <https://doi.org/10.1242/jcs.167874>
- Gao, Z., Ure, K., Ables, J.L., Lagace, D.C., Nave, K.-A., Goebbels, S., Eisch, A.J., Hsieh, J., 2009. Neurod1 is essential for the survival and maturation of adult-born neurons. *Nat Neurosci* 12, 1090–1092. <https://doi.org/10.1038/nn.2385>
- Gazdik, T.R., Crow, J.J., Lawton, T., Munroe, C.J., Theriault, H., Wood, T.M., Albig, A.R., 2024. Notch intracellular domains form transcriptionally active heterodimeric complexes on sequence-paired sites. *Sci Rep* 14, 218. <https://doi.org/10.1038/s41598-023-50763-4>
- Giacomotto, J., Rinkwitz, S., Becker, T.S., 2015. Effective heritable gene knockdown in zebrafish using synthetic microRNAs. *Nat Commun* 6, 7378. <https://doi.org/10.1038/ncomms8378>
- Götz, M., Huttner, W.B., 2005. The cell biology of neurogenesis. *Nat Rev Mol Cell Biol* 6, 777–788. <https://doi.org/10.1038/nrm1739>
- Götz, M., Nakafuku, M., Petrik, D., 2016. Neurogenesis in the Developing and Adult Brain-Similarities and Key Differences. *Cold Spring Harb Perspect Biol* 8, a018853. <https://doi.org/10.1101/cshperspect.a018853>
- Granados, A.A., Kanrar, N., Elowitz, M.B., 2024. Combinatorial expression motifs in signaling pathways. *Cell Genom* 4, 100463. <https://doi.org/10.1016/j.xgen.2023.100463>
- Grandel, H., Kaslin, J., Ganz, J., Wenzel, I., Brand, M., 2006. Neural stem cells and neurogenesis in the adult zebrafish brain: origin, proliferation dynamics, migration and

- cell fate. *Dev Biol* 295, 263–277. <https://doi.org/10.1016/j.ydbio.2006.03.040>
- Gray, M., Moens, C.B., Amacher, S.L., Eisen, J.S., Beattie, C.E., 2001. Zebrafish deadly seven functions in neurogenesis. *Dev Biol* 237, 306–323. <https://doi.org/10.1006/dbio.2001.0381>
- Groot, A.J., Vooijs, M.A., 2012. The Role of Adams in Notch Signaling. *Adv Exp Med Biol* 727, 15–36. [https://doi.org/10.1007/978-1-4614-0899-4\\_2](https://doi.org/10.1007/978-1-4614-0899-4_2)
- Guillemot, F., Hassan, B.A., 2017. Beyond proneural: emerging functions and regulations of proneural proteins. *Curr Opin Neurobiol* 42, 93–101. <https://doi.org/10.1016/j.conb.2016.11.011>
- Guo, R., Han, D., Song, X., Gao, Y., Li, Z., Li, X., Yang, Z., Xu, Z., 2023. Context-dependent regulation of Notch signaling in glial development and tumorigenesis. *Sci Adv* 9, eadi2167. <https://doi.org/10.1126/sciadv.adi2167>
- Gupta-Rossi, N., Le Bail, O., Gonen, H., Brou, C., Logeat, F., Six, E., Ciechanover, A., Israël, A., 2001. Functional interaction between SEL-10, an F-box protein, and the nuclear form of activated Notch1 receptor. *J Biol Chem* 276, 34371–34378. <https://doi.org/10.1074/jbc.M101343200>
- Hamada, Y., Kadokawa, Y., Okabe, M., Ikawa, M., Coleman, J.R., Tsujimoto, Y., 1999. Mutation in ankyrin repeats of the mouse Notch2 gene induces early embryonic lethality. *Development* 126, 3415–3424. <https://doi.org/10.1242/dev.126.15.3415>
- Handford, P.A., Korona, B., Suckling, R., Redfield, C., Lea, S.M., 2018. Structural Insights into Notch Receptor-Ligand Interactions. *Adv Exp Med Biol* 1066, 33–46. [https://doi.org/10.1007/978-3-319-89512-3\\_2](https://doi.org/10.1007/978-3-319-89512-3_2)
- Harada, Y., Yamada, M., Imayoshi, I., Kageyama, R., Suzuki, Y., Kuniya, T., Furutachi, S., Kawaguchi, D., Gotoh, Y., 2021. Cell cycle arrest determines adult neural stem cell ontogeny by an embryonic Notch-nonoscillatory Hey1 module. *Nat Commun* 12, 6562. <https://doi.org/10.1038/s41467-021-26605-0>
- Harbuzariu, A., Oprea-Ilieș, G.M., Gonzalez-Perez, R.R., 2018. The Role of Notch Signaling and Leptin-Notch Crosstalk in Pancreatic Cancer. *Medicines (Basel)* 5, 68. <https://doi.org/10.3390/medicines5030068>
- Harder, B., Schomburg, A., Pflanz, R., Küstner, K., Gerlach, N., Schuh, R., 2008. TEV protease-mediated cleavage in *Drosophila* as a tool to analyze protein functions in living organisms. *Biotechniques* 44, 765–772. <https://doi.org/10.2144/000112884>
- Harmand, T.J., Islam, A., Pishesha, N., Ploegh, H.L., n.d. Nanobodies as in vivo, non-invasive, imaging agents. *RSC Chem Biol* 2, 685–701. <https://doi.org/10.1039/d1cb00023c>
- Harris, L., Rigo, P., Stiehl, T., Gaber, Z.B., Austin, S.H.L., Masdeu, M.D.M., Edwards, A., Urbán, N., Marciniak-Czochra, A., Guillemot, F., 2021. Coordinated changes in cellular behavior ensure the lifelong maintenance of the hippocampal stem cell population. *Cell Stem Cell* 28, 863–876.e6. <https://doi.org/10.1016/j.stem.2021.01.003>
- Harrington, M.J., Hong, E., Fasanmi, O., Brewster, R., 2007. Cadherin-mediated adhesion regulates posterior body formation. *BMC Developmental Biology* 7, 130. <https://doi.org/10.1186/1471-213X-7-130>
- Hartsock, A., Nelson, W.J., 2008. Adherens and tight junctions: structure, function and connections to the actin cytoskeleton. *Biochim Biophys Acta* 1778, 660–669. <https://doi.org/10.1016/j.bbamem.2007.07.012>
- Hatakeyama, J., Tomita, K., Inoue, T., Kageyama, R., 2001. Roles of homeobox and bHLH genes in specification of a retinal cell type. *Development* 128, 1313–1322. <https://doi.org/10.1242/dev.128.8.1313>
- Henrique, D., Schweisguth, F., 2019. Mechanisms of Notch signaling: a simple logic deployed in time and space. *Development* 146, dev172148. <https://doi.org/10.1242/dev.172148>
- Hermkens, D.M.A., van Impel, A., Urasaki, A., Bussmann, J., Duckers, H.J., Schulte-Merker,



- S., 2015. Sox7 controls arterial specification in conjunction with hey2 and efnb2 function. *Development* 142, 1695–1704. <https://doi.org/10.1242/dev.117275>
- Hernández-Núñez, I., Quelle-Regaldie, A., Sánchez, L., Adrio, F., Candal, E., Barreiro-Iglesias, A., 2021. Decline in Constitutive Proliferative Activity in the Zebrafish Retina with Ageing. *Int J Mol Sci* 22, 11715. <https://doi.org/10.3390/ijms222111715>
- Hevia, C.F., Engel-Pizcueta, C., Udina, F., Pujades, C., 2022. The neurogenic fate of the hindbrain boundaries relies on Notch3-dependent asymmetric cell divisions. *Cell Rep* 39, 110915. <https://doi.org/10.1016/j.celrep.2022.110915>
- Hirai, S., Harada, T., 2004. Morphological comparison of apoptotic with non-apoptotic dying cells in the developing inner ear of mouse embryos. *Hear Res* 198, 41–47. <https://doi.org/10.1016/j.heares.2004.07.012>
- Hisano, Y., Sakuma, T., Nakade, S., Ohga, R., Ota, S., Okamoto, H., Yamamoto, T., Kawahara, A., 2015. Precise in-frame integration of exogenous DNA mediated by CRISPR/Cas9 system in zebrafish. *Sci Rep* 5, 8841. <https://doi.org/10.1038/srep08841>
- Hoffman, R.M., 2018. Fluorescent Proteins as Sensors for Cellular Behavior in Mice. *Prog Mol Biol Transl Sci* 160, 29–45. <https://doi.org/10.1016/bs.pmbts.2018.09.005>
- Holley, S.A., Geisler, R., Nüsslein-Volhard, C., 2000. Control of her1 expression during zebrafish somitogenesis by a delta-dependent oscillator and an independent wave-front activity. *Genes Dev* 14, 1678–1690.
- Hounjet, J., Vooijs, M., 2021. The Role of Intracellular Trafficking of Notch Receptors in Ligand-Independent Notch Activation. *Biomolecules* 11, 1369. <https://doi.org/10.3390/biom11091369>
- Houssin, E., Pinot, M., Bellec, K., Le Borgne, R., 2021. Par3 cooperates with Sanpodo for the assembly of Notch clusters following asymmetric division of Drosophila sensory organ precursor cells. *Elife* 10, e66659. <https://doi.org/10.7554/eLife.66659>
- Howe, K., Clark, M.D., Torroja, C.F., Torrance, J., Berthelot, C., Muffato, M., Collins, J.E., Humphray, S., McLaren, K., Matthews, L., McLaren, S., Sealy, I., Caccamo, M., Churcher, C., Scott, C., Barrett, J.C., Koch, R., Rauch, G.-J., White, S., Chow, W., Kilian, B., Quintais, L.T., Guerra-Assunção, J.A., Zhou, Y., Gu, Y., Yen, J., Vogel, J.-H., Eyre, T., Redmond, S., Banerjee, R., Chi, J., Fu, B., Langley, E., Maguire, S.F., Laird, G.K., Lloyd, D., Kenyon, E., Donaldson, S., Sehra, H., Almeida-King, J., Loveland, J., Trevanion, S., Jones, M., Quail, M., Willey, D., Hunt, A., Burton, J., Sims, S., McLay, K., Plumb, B., Davis, J., Clee, C., Oliver, K., Clark, R., Riddle, C., Elliot, D., Threadgold, G., Harden, G., Ware, D., Begum, S., Mortimore, B., Kerry, G., Heath, P., Phillimore, B., Tracey, A., Corby, N., Dunn, M., Johnson, C., Wood, J., Clark, S., Pelan, S., Griffiths, G., Smith, M., Glithero, R., Howden, P., Barker, N., Lloyd, C., Stevens, C., Harley, J., Holt, K., Panagiotidis, G., Lovell, J., Beasley, H., Henderson, C., Gordon, D., Auger, K., Wright, D., Collins, J., Raisen, C., Dyer, L., Leung, K., Robertson, L., Ambridge, K., Leongamornlert, D., McGuire, S., Gildershorp, R., Griffiths, C., Manthavadi, D., Nichol, S., Barker, G., Whitehead, S., Kay, M., Brown, J., Murnane, C., Gray, E., Humphries, M., Sycamore, N., Barker, D., Saunders, D., Wallis, J., Babbage, A., Hammond, S., Mashreghi-Mohammadi, M., Barr, L., Martin, S., Wray, P., Ellington, A., Matthews, N., Ellwood, M., Woodmansey, R., Clark, G., Cooper, J.D., Tromans, A., Grafham, D., Skuce, C., Pandian, R., Andrews, R., Harrison, E., Kimberley, A., Garnett, J., Fosker, N., Hall, R., Garner, P., Kelly, D., Bird, C., Palmer, S., Gehring, I., Berger, A., Dooley, C.M., Ersan-Ürün, Z., Eser, C., Geiger, H., Geisler, M., Karotki, L., Kirn, A., Konantz, J., Konantz, M., Oberländer, M., Rudolph-Geiger, S., Teucke, M., Lanz, C., Raddatz, G., Osoegawa, K., Zhu, B., Rapp, A., Widaa, S., Langford, C., Yang, F., Schuster, S.C., Carter, N.P., Harrow, J., Ning, Z., Herrero, J., Searle, S.M.J., Enright, A., Geisler, R., Plasterk, R.H.A., Lee, C., Westerfield, M.,

- de Jong, P.J., Zon, L.I., Postlethwait, J.H., Nüsslein-Volhard, C., Hubbard, T.J.P., Roest Crolius, H., Rogers, J., Stemple, D.L., 2013. The zebrafish reference genome sequence and its relationship to the human genome. *Nature* 496, 498–503. <https://doi.org/10.1038/nature12111>
- Hsiao, C.-D., You, M.-S., Guh, Y.-J., Ma, M., Jiang, Y.-J., Hwang, P.-P., 2007. A positive regulatory loop between foxi3a and foxi3b is essential for specification and differentiation of zebrafish epidermal ionocytes. *PLoS One* 2, e302. <https://doi.org/10.1371/journal.pone.0000302>
- Hu, N., Zou, L., 2022. Multiple functions of Hes genes in the proliferation and differentiation of neural stem cells. *Ann Anat* 239, 151848. <https://doi.org/10.1016/j.aanat.2021.151848>
- Huang, P., Xiong, F., Megason, S.G., Schier, A.F., 2012. Attenuation of Notch and Hedgehog signaling is required for fate specification in the spinal cord. *PLoS Genet* 8, e1002762. <https://doi.org/10.1371/journal.pgen.1002762>
- Ilagan, M.X.G., Lim, S., Fulbright, M., Piwnica-Worms, D., Kopan, R., 2011. Real-time imaging of notch activation with a luciferase complementation-based reporter. *Sci Signal* 4, rs7. <https://doi.org/10.1126/scisignal.2001656>
- Imayoshi, I., Isomura, A., Harima, Y., Kawaguchi, K., Kori, H., Miyachi, H., Fujiwara, T., Ishidate, F., Kageyama, R., 2013. Oscillatory control of factors determining multipotency and fate in mouse neural progenitors. *Science* 342, 1203–1208. <https://doi.org/10.1126/science.1242366>
- Imayoshi, I., Sakamoto, M., Yamaguchi, M., Mori, K., Kageyama, R., 2010. Essential roles of Notch signaling in maintenance of neural stem cells in developing and adult brains. *J Neurosci* 30, 3489–3498. <https://doi.org/10.1523/JNEUROSCI.4987-09.2010>
- Ito, Y., Tanaka, H., Okamoto, H., Ohshima, T., 2010. Characterization of neural stem cells and their progeny in the adult zebrafish optic tectum. *Dev Biol* 342, 26–38. <https://doi.org/10.1016/j.ydbio.2010.03.008>
- Jackson, A.L., Linsley, P.S., 2004. Noise amidst the silence: off-target effects of siRNAs? *Trends Genet* 20, 521–524. <https://doi.org/10.1016/j.tig.2004.08.006>
- Jacobo, A., Dasgupta, A., Erzberger, A., Siletti, K., Hudspeth, A.J., 2019. Notch-Mediated Determination of Hair-Bundle Polarity in Mechanosensory Hair Cells of the Zebrafish Lateral Line. *Curr Biol* 29, 3579–3587.e7. <https://doi.org/10.1016/j.cub.2019.08.060>
- Jacobs, C.T., Huang, P., 2019. Notch signalling maintains Hedgehog responsiveness via a Gli-dependent mechanism during spinal cord patterning in zebrafish. *Elife* 8, e49252. <https://doi.org/10.7554/eLife.49252>
- Jacobs, C.T., Kejrival, A., Kocha, K.M., Jin, K.Y., Huang, P., 2022. Temporal cell fate determination in the spinal cord is mediated by the duration of Notch signalling. *Dev Biol* 489, 1–13. <https://doi.org/10.1016/j.ydbio.2022.05.010>
- Jacobson, G.A., Rupprecht, P., Friedrich, R.W., 2018. Experience-Dependent Plasticity of Odor Representations in the Telencephalon of Zebrafish. *Curr Biol* 28, 1–14.e3. <https://doi.org/10.1016/j.cub.2017.11.007>
- James, A.C., Szot, J.O., Iyer, K., Major, J.A., Pursglove, S.E., Chapman, G., Dunwoodie, S.L., 2014. Notch4 reveals a novel mechanism regulating Notch signal transduction. *Biochim Biophys Acta* 1843, 1272–1284. <https://doi.org/10.1016/j.bbamcr.2014.03.015>
- Jiang, Y.J., Brand, M., Heisenberg, C.P., Beuchle, D., Furutani-Seiki, M., Kelsh, R.N., Warga, R.M., Granato, M., Haffter, P., Hammerschmidt, M., Kane, D.A., Mullins, M.C., Odenthal, J., van Eeden, F.J., Nüsslein-Volhard, C., 1996. Mutations affecting neurogenesis and brain morphology in the zebrafish, *Danio rerio*. *Development* 123, 205–216. <https://doi.org/10.1242/dev.123.1.205>
- Jin, M., Zhang, H., Xu, B., Li, Y., Qin, H., Yu, S., He, J., 2022. Jag2b-Notch3/1b-mediated

- neuron-to-glia crosstalk controls retinal gliogenesis. *EMBO reports* 23, e54922. <https://doi.org/10.15252/embr.202254922>
- Johnson, J.E., Macdonald, R.J., 2011. Notch-independent functions of CSL. *Curr Top Dev Biol* 97, 55–74. <https://doi.org/10.1016/B978-0-12-385975-4.00009-7>
- Joshi, M., Dey, P., De, A., 2023. Recent advancements in targeted protein knockdown technologies-emerging paradigms for targeted therapy. *Explor Target Antitumor Ther* 4, 1227–1248. <https://doi.org/10.37349/etat.2023.00194>
- Jülich, D., Hwee Lim, C., Round, J., Nicolaije, C., Schroeder, J., Davies, A., Geisler, R., Lewis, J., Jiang, Y.-J., Holley, S.A., Tübingen 2000 Screen Consortium, 2005. beamter/deltaC and the role of Notch ligands in the zebrafish somite segmentation, hindbrain neurogenesis and hypochord differentiation. *Dev Biol* 286, 391–404. <https://doi.org/10.1016/j.ydbio.2005.06.040>
- Jurisch-Yaksi, N., Yaksi, E., Kizil, C., 2020. Radial glia in the zebrafish brain: Functional, structural, and physiological comparison with the mammalian glia. *Glia* 68, 2451–2470. <https://doi.org/10.1002/glia.23849>
- Jussila, M., Boswell, C.W., Griffiths, N.W., Pumputis, P.G., Ciruna, B., 2022. Live imaging and conditional disruption of native PCP activity using endogenously tagged zebrafish sfGFP-Vangl2. *Nat Commun* 13, 5598. <https://doi.org/10.1038/s41467-022-33322-9>
- Kadokawa, Y., Marunouchi, T., 2002. Chimeric analysis of Notch2 function: a role for Notch2 in the development of the roof plate of the mouse brain. *Dev Dyn* 225, 126–134. <https://doi.org/10.1002/dvdy.10140>
- Kageyama, R., Isomura, A., Shimojo, H., 2023. Biological Significance of the Coupling Delay in Synchronized Oscillations. *Physiology (Bethesda)* 38, 0. <https://doi.org/10.1152/physiol.00023.2022>
- Kageyama, R., Ochi, S., Sueda, R., Shimojo, H., 2020. The significance of gene expression dynamics in neural stem cell regulation. *Proc Jpn Acad Ser B Phys Biol Sci* 96, 351–363. <https://doi.org/10.2183/pjab.96.026>
- Kageyama, R., Ohtsuka, T., Kobayashi, T., 2007. The Hes gene family: repressors and oscillators that orchestrate embryogenesis. *Development* 134, 1243–1251. <https://doi.org/10.1242/dev.000786>
- Kageyama, R., Shimojo, H., Isomura, A., 2018. Oscillatory Control of Notch Signaling in Development. *Adv Exp Med Biol* 1066, 265–277. [https://doi.org/10.1007/978-3-319-89512-3\\_13](https://doi.org/10.1007/978-3-319-89512-3_13)
- Kageyama, R., Shimojo, H., Ohtsuka, T., 2019. Dynamic control of neural stem cells by bHLH factors. *Neurosci Res* 138, 12–18. <https://doi.org/10.1016/j.neures.2018.09.005>
- Kaneko, N., Sawada, M., Sawamoto, K., 2017. Mechanisms of neuronal migration in the adult brain. *J Neurochem* 141, 835–847. <https://doi.org/10.1111/jnc.14002>
- Kasioulis, I., Storey, K.G., 2018. Cell biological mechanisms regulating chick neurogenesis. *Int J Dev Biol* 62, 167–175. <https://doi.org/10.1387/ijdb.170268ks>
- Kaslin, J., Brand, M., 2022. Cerebellar Development and Neurogenesis in Zebrafish, in: Manto, M.U., Gruol, D.L., Schmähmann, J.D., Koibuchi, N., Sillitoe, R.V. (Eds.), *Handbook of the Cerebellum and Cerebellar Disorders*. Springer International Publishing, Cham, pp. 1623–1646. [https://doi.org/10.1007/978-3-030-23810-0\\_63](https://doi.org/10.1007/978-3-030-23810-0_63)
- Kaslin, J., Ganz, J., Geffarth, M., Grandel, H., Hans, S., Brand, M., 2009. Stem cells in the adult zebrafish cerebellum: initiation and maintenance of a novel stem cell niche. *J Neurosci* 29, 6142–6153. <https://doi.org/10.1523/JNEUROSCI.0072-09.2009>
- Kaslin, J., Kroehne, V., Ganz, J., Hans, S., Brand, M., 2017. Distinct roles of neuroepithelial-like and radial glia-like progenitor cells in cerebellar regeneration. *Development* 144, 1462–1471. <https://doi.org/10.1242/dev.144907>
- Kaufman, M.H., 1992. *The Atlas of Mouse Development*. Elsevier Science.

- Kavyanifar, A., Turan, S., Lie, D.C., 2018. SoxC transcription factors: multifunctional regulators of neurodevelopment. *Cell Tissue Res* 371, 91–103. <https://doi.org/10.1007/s00441-017-2708-7>
- Kawahashi, K., Hayashi, S., 2010. Dynamic intracellular distribution of Notch during activation and asymmetric cell division revealed by functional fluorescent fusion proteins. *Genes Cells* 15, 749–759. <https://doi.org/10.1111/j.1365-2443.2010.01412.x>
- Kawaguchi, D., Furutachi, S., Kawai, H., Hozumi, K., Gotoh, Y., 2013. Dll1 maintains quiescence of adult neural stem cells and segregates asymmetrically during mitosis. *Nat Commun* 4, 1880. <https://doi.org/10.1038/ncomms2895>
- Kawaguchi, D., Yoshimatsu, T., Hozumi, K., Gotoh, Y., 2008. Selection of differentiating cells by different levels of delta-like 1 among neural precursor cells in the developing mouse telencephalon. *Development* 135, 3849–3858. <https://doi.org/10.1242/dev.024570>
- Kawai, H., Kawaguchi, D., Kuebrich, B.D., Kitamoto, T., Yamaguchi, M., Gotoh, Y., Furutachi, S., 2017. Area-Specific Regulation of Quiescent Neural Stem Cells by Notch3 in the Adult Mouse Subependymal Zone. *J Neurosci* 37, 11867–11880. <https://doi.org/10.1523/JNEUROSCI.0001-17.2017>
- Kawasoe, R., Shinoda, T., Hattori, Y., Nakagawa, M., Pham, T.Q., Tanaka, Y., Sagou, K., Saito, K., Katsuki, S., Kotani, T., Sano, A., Fujimori, T., Miyata, T., 2020. Two-photon microscopic observation of cell-production dynamics in the developing mammalian neocortex in utero. *Dev Growth Differ* 62, 118–128. <https://doi.org/10.1111/dgd.12648>
- Kellokumpu, S., 2019. Golgi pH, Ion and Redox Homeostasis: How Much Do They Really Matter? *Frontiers in Cell and Developmental Biology* 7. <https://doi.org/10.3389/fcell.2019.00093>
- Kemp, H.A., Carmany-Rampey, A., Moens, C., 2009. Generating chimeric zebrafish embryos by transplantation. *J Vis Exp* 1394. <https://doi.org/10.3791/1394>
- Kempermann, G., Gage, F.H., Aigner, L., Song, H., Curtis, M.A., Thuret, S., Kuhn, H.G., Jessberger, S., Frankland, P.W., Cameron, H.A., Gould, E., Hen, R., Abrous, D.N., Toni, N., Schinder, A.F., Zhao, X., Lucassen, P.J., Frisén, J., 2018. Human Adult Neurogenesis: Evidence and Remaining Questions. *Cell Stem Cell* 23, 25–30. <https://doi.org/10.1016/j.stem.2018.04.004>
- Kempermann, G., Song, H., Gage, F.H., 2015. Neurogenesis in the Adult Hippocampus. *Cold Spring Harb Perspect Biol* 7, a018812. <https://doi.org/10.1101/cshperspect.a018812>
- Khakh, B.S., Deneen, B., 2019. The Emerging Nature of Astrocyte Diversity. *Annu Rev Neurosci* 42, 187–207. <https://doi.org/10.1146/annurev-neuro-070918-050443>
- Kim, A.D., Melick, C.H., Clements, W.K., Stachura, D.L., Distel, M., Panáková, D., MacRae, C., Mork, L.A., Crump, J.G., Traver, D., 2014. Discrete Notch signaling requirements in the specification of hematopoietic stem cells. *EMBO J* 33, 2363–2373. <https://doi.org/10.15252/emboj.201488784>
- Kim, H., Kim, S., Chung, A.-Y., Bae, Y.-K., Hibi, M., Lim, C.S., Park, H.-C., 2008a. Notch-regulated perineurium development from zebrafish spinal cord. *Neurosci Lett* 448, 240–244. <https://doi.org/10.1016/j.neulet.2008.10.072>
- Kim, H., Shin, J., Kim, S., Poling, J., Park, H.-C., Appel, B., 2008b. Notch-regulated oligodendrocyte specification from radial glia in the spinal cord of zebrafish embryos. *Dev Dyn* 237, 2081–2089. <https://doi.org/10.1002/dvdy.21620>
- Kimmel, C.B., Ballard, W.W., Kimmel, S.R., Ullmann, B., Schilling, T.F., 1995. Stages of embryonic development of the zebrafish. *Dev Dyn* 203, 253–310. <https://doi.org/10.1002/aja.1002030302>
- Kimura, Y., Satou, C., Higashijima, S.-I., 2008. V2a and V2b neurons are generated by the final divisions of pair-producing progenitors in the zebrafish spinal cord. *Development* 135, 3001–3005. <https://doi.org/10.1242/dev.024802>

- Kirby, B.B., Takada, N., Latimer, A.J., Shin, J., Carney, T.J., Kelsh, R.N., Appel, B., 2006. In vivo time-lapse imaging shows dynamic oligodendrocyte progenitor behavior during zebrafish development. *Nat Neurosci* 9, 1506–1511. <https://doi.org/10.1038/nn1803>
- Kirchgeorg, L., Felker, A., van Oostrom, M., Chiavacci, E., Mosimann, C., 2018. Cre/lox-controlled spatiotemporal perturbation of FGF signaling in zebrafish. *Dev Dyn* 247, 1146–1159. <https://doi.org/10.1002/dvdy.24668>
- Kishimoto, N., Alfaro-Cervello, C., Shimizu, K., Asakawa, K., Urasaki, A., Nonaka, S., Kawakami, K., Garcia-Verdugo, J.M., Sawamoto, K., 2011. Migration of neuronal precursors from the telencephalic ventricular zone into the olfactory bulb in adult zebrafish. *J Comp Neurol* 519, 3549–3565. <https://doi.org/10.1002/cne.22722>
- Kitamoto, T., Takahashi, K., Takimoto, H., Tomizuka, K., Hayasaka, M., Tabira, T., Hanaoka, K., 2005. Functional redundancy of the Notch gene family during mouse embryogenesis: analysis of Notch gene expression in Notch3-deficient mice. *Biochem Biophys Res Commun* 331, 1154–1162. <https://doi.org/10.1016/j.bbrc.2005.03.241>
- Kizil, C., Kaslin, J., Kroehne, V., Brand, M., 2012. Adult neurogenesis and brain regeneration in zebrafish. *Dev Neurobiol* 72, 429–461. <https://doi.org/10.1002/dneu.20918>
- Kobayashi, T., Kageyama, R., 2021. Lysosomes and signaling pathways for maintenance of quiescence in adult neural stem cells. *FEBS J* 288, 3082–3093. <https://doi.org/10.1111/febs.15555>
- Kobayashi, T., Piao, W., Takamura, T., Kori, H., Miyachi, H., Kitano, S., Iwamoto, Y., Yamada, M., Imayoshi, I., Shioda, S., Ballabio, A., Kageyama, R., 2019. Enhanced lysosomal degradation maintains the quiescent state of neural stem cells. *Nat Commun* 10, 5446. <https://doi.org/10.1038/s41467-019-13203-4>
- Kopan, R., Ilagan, M.X.G., 2009. The canonical Notch signaling pathway: unfolding the activation mechanism. *Cell* 137, 216–233. <https://doi.org/10.1016/j.cell.2009.03.045>
- Kovall, R.A., Gebelein, B., Sprinzak, D., Kopan, R., 2017. The Canonical Notch Signaling Pathway: Structural and Biochemical Insights into Shape, Sugar, and Force. *Dev Cell* 41, 228–241. <https://doi.org/10.1016/j.devcel.2017.04.001>
- Kramer-Zucker, A.G., Olale, F., Haycraft, C.J., Yoder, B.K., Schier, A.F., Drummond, I.A., 2005. Cilia-driven fluid flow in the zebrafish pronephros, brain and Kupffer's vesicle is required for normal organogenesis. *Development* 132, 1907–1921. <https://doi.org/10.1242/dev.01772>
- Krebs, L.T., Xue, Y., Norton, C.R., Shutter, J.R., Maguire, M., Sundberg, J.P., Gallahan, D., Closson, V., Kitajewski, J., Callahan, R., Smith, G.H., Stark, K.L., Gridley, T., 2000. Notch signaling is essential for vascular morphogenesis in mice. *Genes Dev* 14, 1343–1352.
- Krebs, L.T., Xue, Y., Norton, C.R., Sundberg, J.P., Beatus, P., Lendahl, U., Joutel, A., Gridley, T., 2003. Characterization of Notch3-deficient mice: normal embryonic development and absence of genetic interactions with a Notch1 mutation. *Genesis* 37, 139–143. <https://doi.org/10.1002/gene.10241>
- Kressmann, S., Campos, C., Castanon, I., Fürthauer, M., González-Gaitán, M., 2015. Directional Notch trafficking in Sara endosomes during asymmetric cell division in the spinal cord. *Nat Cell Biol* 17, 333–339. <https://doi.org/10.1038/ncb3119>
- Kriegstein, A., Alvarez-Buylla, A., 2009. The glial nature of embryonic and adult neural stem cells. *Annu Rev Neurosci* 32, 149–184. <https://doi.org/10.1146/annurev.neuro.051508.135600>
- Kroehne, V., Freudenreich, D., Hans, S., Kaslin, J., Brand, M., 2011. Regeneration of the adult zebrafish brain from neurogenic radial glia-type progenitors. *Development* 138, 4831–4841. <https://doi.org/10.1242/dev.072587>
- Kuhn, S., Gritti, L., Crooks, D., Dombrowski, Y., 2019. Oligodendrocytes in Development,

- Myelin Generation and Beyond. *Cells* 8, 1424. <https://doi.org/10.3390/cells8111424>
- Kuintzle, R., Santat, L.A., Elowitz, M.B., 2024. Diversity in Notch ligand-receptor signaling interactions. *bioRxiv* 2023.08.24.554677. <https://doi.org/10.1101/2023.08.24.554677>
- Kujawski, S., Sonawane, M., Knust, E., 2019. *penner/lgl2* is required for the integrity of the photoreceptor layer in the zebrafish retina. *Biology Open* 8, bio041830. <https://doi.org/10.1242/bio.041830>
- Kunoh, S., Nakashima, H., Nakashima, K., 2024. Epigenetic Regulation of Neural Stem Cells in Developmental and Adult Stages. *Epigenomes* 8, 22. <https://doi.org/10.3390/epigenomes8020022>
- Labusch, M., Mancini, L., Morizet, D., Bally-Cuif, L., 2020. Conserved and Divergent Features of Adult Neurogenesis in Zebrafish. *Front Cell Dev Biol* 8, 525. <https://doi.org/10.3389/fcell.2020.00525>
- Labusch, M., Thetiot, M., Than-Trong, E., Morizet, D., Coolen, M., Varet, H., Legendre, R., Ortica, S., Mancini, L., Bally-Cuif, L., 2024. Prosaposin maintains adult neural stem cells in a state associated with deep quiescence. *Stem Cell Reports* 19, 515–528. <https://doi.org/10.1016/j.stemcr.2024.02.007>
- Lahne, M., Hyde, D.R., 2023. Live Cell Imaging of Dynamic Processes in Adult Zebrafish Retinal Cross-Section Cultures. *Methods Mol Biol* 2636, 367–388. [https://doi.org/10.1007/978-1-0716-3012-9\\_20](https://doi.org/10.1007/978-1-0716-3012-9_20)
- Lahne, M., Hyde, D.R., 2016. Interkinetic Nuclear Migration in the Regenerating Retina. *Adv Exp Med Biol* 854, 587–593. [https://doi.org/10.1007/978-3-319-17121-0\\_78](https://doi.org/10.1007/978-3-319-17121-0_78)
- Lalonde, R.L., Kemmler, C.L., Riemsdijk, F.W., Aman, A.J., Kresoja-Rakic, J., Moran, H.R., Nieuwenhuize, S., Parichy, D.M., Burger, A., Mosimann, C., 2022. Heterogeneity and genomic loci of ubiquitous transgenic Cre reporter lines in zebrafish. *Dev Dyn* 251, 1754–1773. <https://doi.org/10.1002/dvdy.499>
- Lampada, A., Taylor, V., 2023. Notch signaling as a master regulator of adult neurogenesis. *Front Neurosci* 17, 1179011. <https://doi.org/10.3389/fnins.2023.1179011>
- Lange, C., Rost, F., Machate, A., Reinhardt, S., Lesche, M., Weber, A., Kuscha, V., Dahl, A., Rulands, S., Brand, M., 2020. Single cell sequencing of radial glia progeny reveals the diversity of newborn neurons in the adult zebrafish brain. *Development* 147, dev185595. <https://doi.org/10.1242/dev.185595>
- Latimer, A.J., Dong, X., Markov, Y., Appel, B., 2002. Delta-Notch signaling induces hypochord development in zebrafish. *Development* 129, 2555–2563. <https://doi.org/10.1242/dev.129.11.2555>
- Leal-Galicia, P., Chávez-Hernández, M.E., Mata, F., Mata-Luévanos, J., Rodríguez-Serrano, L.M., Tapia-de-Jesús, A., Buenrostro-Jáuregui, M.H., 2021. Adult Neurogenesis: A Story Ranging from Controversial New Neurogenic Areas and Human Adult Neurogenesis to Molecular Regulation. *Int J Mol Sci* 22, 11489. <https://doi.org/10.3390/ijms222111489>
- Lee, K.-S., Wu, Z., Song, Y., Mitra, S.S., Feroze, A.H., Cheshier, S.H., Lu, B., 2013. Roles of PINK1, mTORC2, and mitochondria in preserving brain tumor-forming stem cells in a noncanonical Notch signaling pathway. *Genes Dev* 27, 2642–2647. <https://doi.org/10.1101/gad.225169.113>
- Leeman, D.S., Hebestreit, K., Ruetz, T., Webb, A.E., McKay, A., Pollina, E.A., Dulken, B.W., Zhao, X., Yeo, R.W., Ho, T.T., Mahmoudi, S., Devarajan, K., Passequé, E., Rando, T.A., Frydman, J., Brunet, A., 2018. Lysosome activation clears aggregates and enhances quiescent neural stem cell activation during aging. *Science* 359, 1277–1283. <https://doi.org/10.1126/science.aag3048>
- Lehtinen, M.K., Zappaterra, M.W., Chen, X., Yang, Y.J., Hill, A.D., Lun, M., Maynard, T., Gonzalez, D., Kim, S., Ye, P., D’Ercole, A.J., Wong, E.T., LaMantia, A.S., Walsh,

- C.A., 2011. The cerebrospinal fluid provides a proliferative niche for neural progenitor cells. *Neuron* 69, 893–905. <https://doi.org/10.1016/j.neuron.2011.01.023>
- Leung, L., Klopper, A.V., Grill, S.W., Harris, W.A., Norden, C., 2011. Apical migration of nuclei during G2 is a prerequisite for all nuclear motion in zebrafish neuroepithelia. *Development* 138, 5003–5013. <https://doi.org/10.1242/dev.071522>
- Li, P., White, R.M., Zon, L.I., 2011. Transplantation in zebrafish. *Methods Cell Biol* 105, 403–417. <https://doi.org/10.1016/B978-0-12-381320-6.00017-5>
- Li, W., Zhang, Yage, Han, B., Li, L., Li, M., Lu, X., Chen, C., Lu, M., Zhang, Yujie, Jia, X., Zhu, Z., Tong, X., Zhang, B., 2019. One-step efficient generation of dual-function conditional knockout and geno-tagging alleles in zebrafish. *Elife* 8, e48081. <https://doi.org/10.7554/eLife.48081>
- Li, X., Pu, W., Chen, S., Peng, Y., 2021. Therapeutic targeting of RNA-binding protein by RNA-PROTAC. *Mol Ther* 29, 1940–1942. <https://doi.org/10.1016/j.ymthe.2021.04.032>
- Li, X., Yan, X., Wang, Y., Kaur, B., Han, H., Yu, J., 2023. The Notch signaling pathway: a potential target for cancer immunotherapy. *J Hematol Oncol* 16, 45. <https://doi.org/10.1186/s13045-023-01439-z>
- Li, Y., Hibbs, M.A., Gard, A.L., Shylo, N.A., Yun, K., 2012. Genome-wide analysis of N1ICD/RBPJ targets in vivo reveals direct transcriptional regulation of Wnt, SHH, and hippo pathway effectors by Notch1. *Stem Cells* 30, 741–752. <https://doi.org/10.1002/stem.1030>
- Liang, S.-T., Chen, J.-R., Tsai, J.-J., Lai, Y.-H., Hsiao, C.-D., 2019. Overexpression of Notch Signaling Induces Hyperosteogeny in Zebrafish. *Int J Mol Sci* 20, 3613. <https://doi.org/10.3390/ijms20153613>
- Lim, D.A., Alvarez-Buylla, A., 2016. The Adult Ventricular-Subventricular Zone (V-SVZ) and Olfactory Bulb (OB) Neurogenesis. *Cold Spring Harb Perspect Biol* 8, a018820. <https://doi.org/10.1101/cshperspect.a018820>
- Lim, D.A., Alvarez-Buylla, A., 2014. Adult neural stem cells stake their ground. *Trends Neurosci* 37, 563–571. <https://doi.org/10.1016/j.tins.2014.08.006>
- Lindquist, J.A., Mertens, P.R., 2018. Cold shock proteins: from cellular mechanisms to pathophysiology and disease. *Cell Commun Signal* 16, 63. <https://doi.org/10.1186/s12964-018-0274-6>
- Liu, C., Li, R., Li, Young, Lin, X., Zhao, K., Liu, Q., Wang, S., Yang, X., Shi, X., Ma, Y., Pei, C., Wang, H., Bao, W., Hui, J., Yang, T., Xu, Z., Lai, T., Berberoglu, M.A., Sahu, S.K., Esteban, M.A., Ma, K., Fan, G., Li, Yuxiang, Liu, S., Chen, A., Xu, X., Dong, Z., Liu, L., 2022. Spatiotemporal mapping of gene expression landscapes and developmental trajectories during zebrafish embryogenesis. *Dev Cell* 57, 1284-1298.e5. <https://doi.org/10.1016/j.devcel.2022.04.009>
- Liu, J., Chen, H., Kaniskan, H.Ü., Xie, L., Chen, X., Jin, J., Wei, W., 2021. TF-PROTACs Enable Targeted Degradation of Transcription Factors. *J Am Chem Soc* 143, 8902–8910. <https://doi.org/10.1021/jacs.1c03852>
- Liu, K.S., Gray, M., Otto, S.J., Fetcho, J.R., Beattie, C.E., 2003. Mutations in *deadly seven/notch1a* reveal developmental plasticity in the escape response circuit. *J Neurosci* 23, 8159–8166. <https://doi.org/10.1523/JNEUROSCI.23-22-08159.2003>
- Liu, Q., Babb, S.G., Novince, Z.M., Doedens, A.L., Marrs, J., Raymond, P.A., 2001. Differential expression of cadherin-2 and cadherin-4 in the developing and adult zebrafish visual system. *Vis Neurosci* 18, 923–933.
- Liu, Q., Kerstetter, A. e., Azodi, E., Marrs, J. a., 2003. Cadherin-1, -2, and -11 expression and cadherin-2 function in the pectoral limb bud and fin of the developing zebrafish. *Developmental Dynamics* 228, 734–739. <https://doi.org/10.1002/dvdy.10401>

- Liu, Y., Pathak, N., Kramer-Zucker, A., Drummond, I.A., 2007. Notch signaling controls the differentiation of transporting epithelia and multiciliated cells in the zebrafish pronephros. *Development* 134, 1111–1122. <https://doi.org/10.1242/dev.02806>
- Llorens-Bobadilla, E., Zhao, S., Baser, A., Saiz-Castro, G., Zwadlo, K., Martin-Villalba, A., 2015. Single-Cell Transcriptomics Reveals a Population of Dormant Neural Stem Cells that Become Activated upon Brain Injury. *Cell Stem Cell* 17, 329–340. <https://doi.org/10.1016/j.stem.2015.07.002>
- Long, K.R., Huttner, W.B., 2019. How the extracellular matrix shapes neural development. *Open Biol* 9, 180216. <https://doi.org/10.1098/rsob.180216>
- Loras, A., Gonzalez-Bonet, L.G., Gutierrez-Arroyo, J.L., Martinez-Cadenas, C., Marques-Torrejon, M.A., 2023. Neural Stem Cells as Potential Glioblastoma Cells of Origin. *Life (Basel)* 13, 905. <https://doi.org/10.3390/life13040905>
- Loubéry, S., Seum, C., Moraleda, A., Daeden, A., Fürthauer, M., Gonzalez-Gaitan, M., 2014. Uninflatable and Notch control the targeting of Sara endosomes during asymmetric division. *Curr Biol* 24, 2142–2148. <https://doi.org/10.1016/j.cub.2014.07.054>
- Louvi, A., Grove, E.A., 2011. Cilia in the CNS: the quiet organelle claims center stage. *Neuron* 69, 1046–1060. <https://doi.org/10.1016/j.neuron.2011.03.002>
- Lugert, S., Basak, O., Knuckles, P., Haussler, U., Fabel, K., Götz, M., Haas, C.A., Kempermann, G., Taylor, V., Giachino, C., 2010. Quiescent and active hippocampal neural stem cells with distinct morphologies respond selectively to physiological and pathological stimuli and aging. *Cell Stem Cell* 6, 445–456. <https://doi.org/10.1016/j.stem.2010.03.017>
- Lugert, S., Vogt, M., Tchorz, J.S., Müller, M., Giachino, C., Taylor, V., 2012. Homeostatic neurogenesis in the adult hippocampus does not involve amplification of Ascl1(high) intermediate progenitors. *Nat Commun* 3, 670. <https://doi.org/10.1038/ncomms1670>
- Luo, Z., Mu, L., Zheng, Y., Shen, W., Li, J., Xu, L., Zhong, B., Liu, Y., Zhou, Y., 2020. NUMB enhances Notch signaling by repressing ubiquitination of NOTCH1 intracellular domain. *J Mol Cell Biol* 12, 345–358. <https://doi.org/10.1093/jmcb/mjz088>
- Lupo, G., Gioia, R., Nisi, P.S., Biagioni, S., Cacci, E., 2019. Molecular Mechanisms of Neurogenic Aging in the Adult Mouse Subventricular Zone. *J Exp Neurosci* 13, 1179069519829040. <https://doi.org/10.1177/1179069519829040>
- Lütolf, S., Radtke, F., Aguet, M., Suter, U., Taylor, V., 2002. Notch1 is required for neuronal and glial differentiation in the cerebellum. *Development* 129, 373–385. <https://doi.org/10.1242/dev.129.2.373>
- Lv, Y., Pang, X., Cao, Z., Song, C., Liu, B., Wu, W., Pang, Q., 2024. Evolution and Function of the Notch Signaling Pathway: An Invertebrate Perspective. *Int J Mol Sci* 25, 3322. <https://doi.org/10.3390/ijms25063322>
- Lyon, K.A., Allen, N.J., 2021. From Synapses to Circuits, Astrocytes Regulate Behavior. *Front Neural Circuits* 15, 786293. <https://doi.org/10.3389/fncir.2021.786293>
- Ma, M., Jiang, Y.-J., 2007. Jagged2a-notch signaling mediates cell fate choice in the zebrafish pronephric duct. *PLoS Genet* 3, e18. <https://doi.org/10.1371/journal.pgen.0030018>
- Ma, Z., Zhu, P., Shi, H., Guo, L., Zhang, Q., Chen, Y., Chen, S., Zhang, Z., Peng, J., Chen, J., 2019. PTC-bearing mRNA elicits a genetic compensation response via Upf3a and COMPASS components. *Nature* 568, 259–263. <https://doi.org/10.1038/s41586-019-1057-y>
- Magnusson, J.P., Göritz, C., Tatarishvili, J., Dias, D.O., Smith, E.M.K., Lindvall, O., Kokaia, Z., Frisén, J., 2014. A latent neurogenic program in astrocytes regulated by Notch signaling in the mouse. *Science* 346, 237–241. <https://doi.org/10.1126/science.346.6206.237>
- Mancini, L., Guirao, B., Ortica, S., Labusch, M., Cheysson, F., Bonnet, V., Phan, M.S., Herbert,



- S., Mahou, P., Menant, E., Bedu, S., Tinevez, J.-Y., Baroud, C., Beaurepaire, E., Bellaiche, Y., Bally-Cuif, L., Dray, N., 2023. Apical size and deltaA expression predict adult neural stem cell decisions along lineage progression. *Sci Adv* 9, eadg7519. <https://doi.org/10.1126/sciadv.adg7519>
- Marcus, R.C., Delaney, C.L., Easter, S.S., 1999. Neurogenesis in the visual system of embryonic and adult zebrafish (*Danio rerio*). *off. Vis Neurosci* 16, 417–424. <https://doi.org/10.1017/s095252389916303x>
- Marcy, G., Foucault, L., Babina, E., Capeliez, T., Texeraud, E., Zweifel, S., Heinrich, C., Hernandez-Vargas, H., Parras, C., Jabaudon, D., Raineteau, O., 2023. Single-cell analysis of the postnatal dorsal V-SVZ reveals a role for *Bmpr1a* signaling in silencing pallial germinal activity. *Sci Adv* 9, eabq7553. <https://doi.org/10.1126/sciadv.abq7553>
- Marinopoulou, E., Biga, V., Sabherwal, N., Miller, A., Desai, J., Adamson, A.D., Papalopulu, N., 2021. HES1 protein oscillations are necessary for neural stem cells to exit from quiescence. *iScience* 24, 103198. <https://doi.org/10.1016/j.isci.2021.103198>
- März, M., Chapouton, P., Diotel, N., Vaillant, C., Hesl, B., Takamiya, M., Lam, C.S., Kah, O., Bally-Cuif, L., Strähle, U., 2010a. Heterogeneity in progenitor cell subtypes in the ventricular zone of the zebrafish adult telencephalon. *Glia* 58, 870–888. <https://doi.org/10.1002/glia.20971>
- März, M., Schmidt, R., Rastegar, S., Strähle, U., 2010b. Expression of the transcription factor *Olig2* in proliferating cells in the adult zebrafish telencephalon. *Dev Dyn* 239, 3336–3349. <https://doi.org/10.1002/dvdy.22455>
- Mason, H.A., Rakowiecki, S.M., Gridley, T., Fishell, G., 2006. Loss of notch activity in the developing central nervous system leads to increased cell death. *Dev Neurosci* 28, 49–57. <https://doi.org/10.1159/000090752>
- Masson, M.-A., Nait-Oumesmar, B., 2023. Emerging concepts in oligodendrocyte and myelin formation, inputs from the zebrafish model. *Glia* 71, 1147–1163. <https://doi.org/10.1002/glia.24336>
- McGill, M.A., Dho, S.E., Weinmaster, G., McGlade, C.J., 2009. Numb regulates post-endocytic trafficking and degradation of Notch1. *J Biol Chem* 284, 26427–26438. <https://doi.org/10.1074/jbc.M109.014845>
- McGill, M.A., McGlade, C.J., 2003. Mammalian numb proteins promote Notch1 receptor ubiquitination and degradation of the Notch1 intracellular domain. *J Biol Chem* 278, 23196–23203. <https://doi.org/10.1074/jbc.M302827200>
- McIntosh, R., Norris, J., Clarke, J.D., Alexandre, P., 2017. Spatial distribution and characterization of non-apical progenitors in the zebrafish embryo central nervous system. *Open Biol* 7, 160312. <https://doi.org/10.1098/rsob.160312>
- McMenamin, S.K., Parichy, D.M., 2013. Metamorphosis in teleosts. *Curr Top Dev Biol* 103, 127–165. <https://doi.org/10.1016/B978-0-12-385979-2.00005-8>
- Megaly, Marvel, Turgambayeva, A., Hallam, R.D., Foran, G., Megaly, Mark, Necakov, A., 2024. Human Diseases Associated with Notch Signalling: Lessons from *Drosophila melanogaster*. *Front Biosci (Landmark Ed)* 29, 234. <https://doi.org/10.31083/j.fbl2906234>
- Miale, I.L., Sidman, R.L., 1961. An autoradiographic analysis of histogenesis in the mouse cerebellum. *Exp Neurol* 4, 277–296. [https://doi.org/10.1016/0014-4886\(61\)90055-3](https://doi.org/10.1016/0014-4886(61)90055-3)
- Ming, G.-L., Song, H., 2011. Adult neurogenesis in the mammalian brain: significant answers and significant questions. *Neuron* 70, 687–702. <https://doi.org/10.1016/j.neuron.2011.05.001>
- Mitic, N., Neuschulz, A., Spanjaard, B., Schneider, J., Fresmann, N., Novoselc, K.T., Strunk, T., Münster, L., Olivares-Chauvet, P., Ninkovic, J., Junker, J.P., 2024. Dissecting the spatiotemporal diversity of adult neural stem cells. *Mol Syst Biol* 20, 321–337.

- <https://doi.org/10.1038/s44320-024-00022-z>
- Miyata, T., Kawaguchi, A., Okano, H., Ogawa, M., 2001. Asymmetric inheritance of radial glial fibers by cortical neurons. *Neuron* 31, 727–741. [https://doi.org/10.1016/s0896-6273\(01\)00420-2](https://doi.org/10.1016/s0896-6273(01)00420-2)
- Miyata, T., Okamoto, M., Shinoda, T., Kawaguchi, A., 2014. Interkinetic nuclear migration generates and opposes ventricular-zone crowding: insight into tissue mechanics. *Front Cell Neurosci* 8, 473. <https://doi.org/10.3389/fncel.2014.00473>
- Mizoguchi, T., Togawa, S., Kawakami, K., Itoh, M., 2011. Neuron and sensory epithelial cell fate is sequentially determined by Notch signaling in zebrafish lateral line development. *J Neurosci* 31, 15522–15530. <https://doi.org/10.1523/JNEUROSCI.3948-11.2011>
- Mizrak, D., Levitin, H.M., Delgado, A.C., Crotet, V., Yuan, J., Chaker, Z., Silva-Vargas, V., Sims, P.A., Doetsch, F., 2019. Single-Cell Analysis of Regional Differences in Adult V-SVZ Neural Stem Cell Lineages. *Cell Rep* 26, 394–406.e5. <https://doi.org/10.1016/j.celrep.2018.12.044>
- Mizuguchi, R., Kriks, S., Cordes, R., Gossler, A., Ma, Q., Goulding, M., 2006. *Ascl1* and *Gsh1/2* control inhibitory and excitatory cell fate in spinal sensory interneurons. *Nat Neurosci* 9, 770–778. <https://doi.org/10.1038/nn1706>
- Morizet, D., Foucher, I., Alunni, A., Bally-Cuif, L., 2024. Reconstruction of macroglia and adult neurogenesis evolution through cross-species single-cell transcriptomic analyses. *Nat Commun* 15, 3306. <https://doi.org/10.1038/s41467-024-47484-1>
- Morris, J.F., 2020. Neurosecretory Vesicles: Structure, Distribution, Release and Breakdown, in: Lemos, J.R., Dayanithi, G. (Eds.), *Neurosecretion: Secretory Mechanisms*. Springer International Publishing, Cham, pp. 81–102. [https://doi.org/10.1007/978-3-030-22989-4\\_5](https://doi.org/10.1007/978-3-030-22989-4_5)
- Mosimann, C., Kaufman, C.K., Li, P., Pugach, E.K., Tamplin, O.J., Zon, L.I., 2011. Ubiquitous transgene expression and Cre-based recombination driven by the ubiquitin promoter in zebrafish. *Development* 138, 169–177. <https://doi.org/10.1242/dev.059345>
- Moulton, J.D., 2017. Using Morpholinos to Control Gene Expression. *Curr Protoc Nucleic Acid Chem* 68, 4.30.1–4.30.29. <https://doi.org/10.1002/cpnc.21>
- Mueller, T., Dong, Z., Berberoglu, M.A., Guo, S., 2011. The dorsal pallium in zebrafish, *Danio rerio* (Cyprinidae, Teleostei). *Brain Res* 1381, 95–105. <https://doi.org/10.1016/j.brainres.2010.12.089>
- Mumm, J.S., Schroeter, E.H., Saxena, M.T., Griesemer, A., Tian, X., Pan, D.J., Ray, W.J., Kopan, R., 2000. A ligand-induced extracellular cleavage regulates gamma-secretase-like proteolytic activation of Notch1. *Mol Cell* 5, 197–206. [https://doi.org/10.1016/s1097-2765\(00\)80416-5](https://doi.org/10.1016/s1097-2765(00)80416-5)
- Nagashima, M., Barthel, L.K., Raymond, P.A., 2013. A self-renewing division of zebrafish Müller glial cells generates neuronal progenitors that require N-cadherin to regenerate retinal neurons. *Development* 140, 4510–4521. <https://doi.org/10.1242/dev.090738>
- Nandi, D., Tahiliani, P., Kumar, A., Chandu, D., 2006. The ubiquitin-proteasome system. *J Biosci* 31, 137–155. <https://doi.org/10.1007/BF02705243>
- Navarro Negredo, P., Yeo, R.W., Brunet, A., 2020. Aging and Rejuvenation of Neural Stem Cells and Their Niches. *Cell Stem Cell* 27, 202–223. <https://doi.org/10.1016/j.stem.2020.07.002>
- Ncube, D., Tallafuss, A., Serafin, J., Bruckner, J., Farnsworth, D.R., Miller, A.C., Eisen, J.S., Washbourne, P., 2022. A conserved transcriptional fingerprint of multi-neurotransmitter neurons necessary for social behavior. *BMC Genomics* 23, 675. <https://doi.org/10.1186/s12864-022-08879-w>
- Neely, S.A., Lyons, D.A., 2021. Insights Into Central Nervous System Glial Cell Formation and Function From Zebrafish. *Front Cell Dev Biol* 9, 754606.

- <https://doi.org/10.3389/fcell.2021.754606>
- Nikolopoulou, E., Galea, G.L., Rolo, A., Greene, N.D.E., Copp, A.J., 2017. Neural tube closure: cellular, molecular and biomechanical mechanisms. *Development* 144, 552–566. <https://doi.org/10.1242/dev.145904>
- Nóbrega-Pereira, S., Marín, O., 2009. Transcriptional control of neuronal migration in the developing mouse brain. *Cereb Cortex* 19 Suppl 1, i107–113. <https://doi.org/10.1093/cercor/bhp044>
- Noctor, S.C., Martínez-Cerdeño, V., Ivic, L., Kriegstein, A.R., 2004. Cortical neurons arise in symmetric and asymmetric division zones and migrate through specific phases. *Nat Neurosci* 7, 136–144. <https://doi.org/10.1038/nn1172>
- Noorimotlagh, Z., Babaie, M., Safdarian, M., Ghadiri, T., Rahimi-Movaghar, V., 2017. Mechanisms of spinal cord injury regeneration in zebrafish: a systematic review. *Iran J Basic Med Sci* 20, 1287–1296. <https://doi.org/10.22038/IJBMS.2017.9620>
- Nyfeler, Y., Kirch, R.D., Mantei, N., Leone, D.P., Radtke, F., Suter, U., Taylor, V., 2005. Jagged1 signals in the postnatal subventricular zone are required for neural stem cell self-renewal. *EMBO J* 24, 3504–3515. <https://doi.org/10.1038/sj.emboj.7600816>
- Obernier, K., Alvarez-Buylla, A., 2019. Neural stem cells: origin, heterogeneity and regulation in the adult mammalian brain. *Development* 146, dev156059. <https://doi.org/10.1242/dev.156059>
- Obernier, K., Cebrian-Silla, A., Thomson, M., Parraguez, J.I., Anderson, R., Guinto, C., Rodas Rodriguez, J., Garcia-Verdugo, J.-M., Alvarez-Buylla, A., 2018. Adult Neurogenesis Is Sustained by Symmetric Self-Renewal and Differentiation. *Cell Stem Cell* 22, 221–234.e8. <https://doi.org/10.1016/j.stem.2018.01.003>
- O’Brown, N.M., Pfau, S.J., Gu, C., 2018. Bridging barriers: a comparative look at the blood-brain barrier across organisms. *Genes Dev* 32, 466–478. <https://doi.org/10.1101/gad.309823.117>
- Ohata, S., Aoki, R., Kinoshita, S., Yamaguchi, M., Tsuruoka-Kinoshita, S., Tanaka, H., Wada, H., Watabe, S., Tsuboi, T., Masai, I., Okamoto, H., 2011. Dual roles of Notch in regulation of apically restricted mitosis and apicobasal polarity of neuroepithelial cells. *Neuron* 69, 215–230. <https://doi.org/10.1016/j.neuron.2010.12.026>
- Oishi, K., Kamakura, S., Isazawa, Y., Yoshimatsu, T., Kuida, K., Nakafuku, M., Masuyama, N., Gotoh, Y., 2004. Notch promotes survival of neural precursor cells via mechanisms distinct from those regulating neurogenesis. *Dev Biol* 276, 172–184. <https://doi.org/10.1016/j.ydbio.2004.08.039>
- Oka, C., Nakano, T., Wakeham, A., de la Pompa, J.L., Mori, C., Sakai, T., Okazaki, S., Kawaichi, M., Shiota, K., Mak, T.W., Honjo, T., 1995. Disruption of the mouse RBP-J kappa gene results in early embryonic death. *Development* 121, 3291–3301. <https://doi.org/10.1242/dev.121.10.3291>
- Okigawa, S., Mizoguchi, T., Okano, M., Tanaka, H., Isoda, M., Jiang, Y.-J., Suster, M., Higashijima, S.-I., Kawakami, K., Itoh, M., 2014. Different combinations of Notch ligands and receptors regulate V2 interneuron progenitor proliferation and V2a/V2b cell fate determination. *Dev Biol* 391, 196–206. <https://doi.org/10.1016/j.ydbio.2014.04.011>
- Olsauskas-Kuprys, R., Zlobin, A., Osipo, C., 2013. Gamma secretase inhibitors of Notch signaling. *Onco Targets Ther* 6, 943–955. <https://doi.org/10.2147/OTT.S33766>
- Ortega-Campos, S.M., García-Heredia, J.M., 2023. The Multitasker Protein: A Look at the Multiple Capabilities of NUMB. *Cells* 12, 333. <https://doi.org/10.3390/cells12020333>
- Otsuki, L., Brand, A.H., 2018. Cell cycle heterogeneity directs the timing of neural stem cell activation from quiescence. *Science* 360, 99–102. <https://doi.org/10.1126/science.aan8795>

- Pagliaro, L., Sorrentino, C., Roti, G., 2020. Targeting Notch Trafficking and Processing in Cancers. *Cells* 9, 2212. <https://doi.org/10.3390/cells9102212>
- Pala, R., Alomari, N., Nauli, S.M., 2017. Primary Cilium-Dependent Signaling Mechanisms. *Int J Mol Sci* 18, 2272. <https://doi.org/10.3390/ijms18112272>
- Palmer, T.D., Willhoite, A.R., Gage, F.H., 2000. Vascular niche for adult hippocampal neurogenesis. *J Comp Neurol* 425, 479–494. [https://doi.org/10.1002/1096-9861\(20001002\)425:4<479::aid-cne2>3.0.co;2-3](https://doi.org/10.1002/1096-9861(20001002)425:4<479::aid-cne2>3.0.co;2-3)
- Pan, Y.A., Freundlich, T., Weissman, T.A., Schoppik, D., Wang, X.C., Zimmerman, S., Ciruna, B., Sanes, J.R., Lichtman, J.W., Schier, A.F., 2013. Zebrafish: multispectral cell labeling for cell tracing and lineage analysis in zebrafish. *Development* 140, 2835–2846. <https://doi.org/10.1242/dev.094631>
- Pandey, S., Moyer, A.J., Thyme, S.B., 2023. A single-cell transcriptome atlas of the maturing zebrafish telencephalon. *Genome Res* 33, 658–671. <https://doi.org/10.1101/gr.277278.122>
- Parichy, D.M., Elizondo, M.R., Mills, M.G., Gordon, T.N., Engeszer, R.E., 2009. Normal table of postembryonic zebrafish development: staging by externally visible anatomy of the living fish. *Dev Dyn* 238, 2975–3015. <https://doi.org/10.1002/dvdy.22113>
- Park, H.-C., Appel, B., 2003. Delta-Notch signaling regulates oligodendrocyte specification. *Development* 130, 3747–3755. <https://doi.org/10.1242/dev.00576>
- Park, H.-C., Mehta, A., Richardson, J.S., Appel, B., 2002. *olig2* is required for zebrafish primary motor neuron and oligodendrocyte development. *Dev Biol* 248, 356–368. <https://doi.org/10.1006/dbio.2002.0738>
- Park, H.-C., Shin, J., Roberts, R.K., Appel, B., 2007. An *olig2* reporter gene marks oligodendrocyte precursors in the postembryonic spinal cord of zebrafish. *Dev Dyn* 236, 3402–3407. <https://doi.org/10.1002/dvdy.21365>
- Parmigiani, E., Taylor, V., Giachino, C., 2020. Oncogenic and Tumor-Suppressive Functions of NOTCH Signaling in Glioma. *Cells* 9, 2304. <https://doi.org/10.3390/cells9102304>
- Pasini, A., Henrique, D., Wilkinson, D.G., 2001. The zebrafish Hairy/Enhancer-of-split-related gene *her6* is segmentally expressed during the early development of hindbrain and somites. *Mech Dev* 100, 317–321. [https://doi.org/10.1016/s0925-4773\(00\)00538-4](https://doi.org/10.1016/s0925-4773(00)00538-4)
- Patel, M., Anderson, J., Lei, S., Finkel, Z., Rodriguez, B., Esteban, F., Risman, R., Li, Y., Lee, K.-B., Lyu, Y.L., Cai, L., 2021. *Nkx6.1* enhances neural stem cell activation and attenuates glial scar formation and neuroinflammation in the adult injured spinal cord. *Exp Neurol* 345, 113826. <https://doi.org/10.1016/j.expneurol.2021.113826>
- Pellegrini, E., Mouriec, K., Anglade, I., Menuet, A., Le Page, Y., Gueguen, M.-M., Marmignon, M.-H., Brion, F., Pakdel, F., Kah, O., 2007. Identification of aromatase-positive radial glial cells as progenitor cells in the ventricular layer of the forebrain in zebrafish. *J Comp Neurol* 501, 150–167. <https://doi.org/10.1002/cne.21222>
- Penisson, M., Ladewig, J., Belvindrah, R., Francis, F., 2019. Genes and Mechanisms Involved in the Generation and Amplification of Basal Radial Glial Cells. *Front Cell Neurosci* 13, 381. <https://doi.org/10.3389/fncel.2019.00381>
- Pereira, M., Birtele, M., Rylander Ottosson, D., 2019. Direct reprogramming into interneurons: potential for brain repair. *Cell Mol Life Sci* 76, 3953–3967. <https://doi.org/10.1007/s00018-019-03193-3>
- Pérez-Domínguez, M., Tovar-Y-Romo, L.B., Zepeda, A., 2018. Neuroinflammation and physical exercise as modulators of adult hippocampal neural precursor cell behavior. *Rev Neurosci* 29, 1–20. <https://doi.org/10.1515/revneuro-2017-0024>
- Perez-Mockus, G., Schweisguth, F., 2017. Cell Polarity and Notch Signaling: Linked by the E3 Ubiquitin Ligase Neuralized? *Bioessays* 39. <https://doi.org/10.1002/bies.201700128>
- Pérez-Rodríguez, D.R., Blanco-Luquin, I., Mendioroz, M., 2021. The Participation of

- Microglia in Neurogenesis: A Review. *Brain Sci* 11, 658. <https://doi.org/10.3390/brainsci11050658>
- Petersen, P.H., Zou, K., Hwang, J.K., Jan, Y.N., Zhong, W., 2002. Progenitor cell maintenance requires numb and numbl like during mouse neurogenesis. *Nature* 419, 929–934. <https://doi.org/10.1038/nature01124>
- Pinot, M., Le Borgne, R., 2024. Spatio-Temporal Regulation of Notch Activation in Asymmetrically Dividing Sensory Organ Precursor Cells in *Drosophila melanogaster* Epithelium. *Cells* 13, 1133. <https://doi.org/10.3390/cells13131133>
- Pinto, L., Götz, M., 2007. Radial glial cell heterogeneity--the source of diverse progeny in the CNS. *Prog Neurobiol* 83, 2–23. <https://doi.org/10.1016/j.pneurobio.2007.02.010>
- Podinovskaia, M., Spang, A., 2018. The Endosomal Network: Mediators and Regulators of Endosome Maturation, in: Lamaze, C., Prior, I. (Eds.), *Endocytosis and Signaling*. Springer International Publishing, Cham, pp. 1–38. [https://doi.org/10.1007/978-3-319-96704-2\\_1](https://doi.org/10.1007/978-3-319-96704-2_1)
- Pogoda, H.-M., Sternheim, N., Lyons, D.A., Diamond, B., Hawkins, T.A., Woods, I.G., Bhatt, D.H., Franzini-Armstrong, C., Dominguez, C., Arana, N., Jacobs, J., Nix, R., Fetcho, J.R., Talbot, W.S., 2006. A genetic screen identifies genes essential for development of myelinated axons in zebrafish. *Dev Biol* 298, 118–131. <https://doi.org/10.1016/j.ydbio.2006.06.021>
- Polacheck, W.J., Kutys, M.L., Yang, J., Eyckmans, J., Wu, Y., Vasavada, H., Hirschi, K.K., Chen, C.S., 2017. A non-canonical Notch complex regulates adherens junctions and vascular barrier function. *Nature* 552, 258–262. <https://doi.org/10.1038/nature24998>
- Ponti, G., Obernier, K., Guinto, C., Jose, L., Bonfanti, L., Alvarez-Buylla, A., 2013. Cell cycle and lineage progression of neural progenitors in the ventricular-subventricular zones of adult mice. *Proc Natl Acad Sci U S A* 110, E1045-1054. <https://doi.org/10.1073/pnas.1219563110>
- Pontious, A., Kowalczyk, T., Englund, C., Hevner, R.F., 2008. Role of intermediate progenitor cells in cerebral cortex development. *Dev Neurosci* 30, 24–32. <https://doi.org/10.1159/000109848>
- Qi, Y., Rezaeian, A.-H., Wang, J., Huang, D., Chen, H., Inuzuka, H., Wei, W., 2024. Molecular insights and clinical implications for the tumor suppressor role of SCFFBXW7 E3 ubiquitin ligase. *Biochim Biophys Acta Rev Cancer* 1879, 189140. <https://doi.org/10.1016/j.bbcan.2024.189140>
- Qiu, X., Lim, C.-H., Ho, S.H.-K., Lee, K.-H., Jiang, Y.-J., 2009. Temporal Notch activation through Notch1a and Notch3 is required for maintaining zebrafish rhombomere boundaries. *Dev Genes Evol* 219, 339–351. <https://doi.org/10.1007/s00427-009-0296-6>
- Ramesh, P.S., Chu, L.-F., 2023. Species-specific roles of the Notch ligands, receptors, and targets orchestrating the signaling landscape of the segmentation clock. *Front Cell Dev Biol* 11, 1327227. <https://doi.org/10.3389/fcell.2023.1327227>
- Rao, D.D., Vorhies, J.S., Senzer, N., Nemunaitis, J., 2009. siRNA vs. shRNA: similarities and differences. *Adv Drug Deliv Rev* 61, 746–759. <https://doi.org/10.1016/j.addr.2009.04.004>
- Rasmussen, M.K., Mestre, H., Nedergaard, M., 2022. Fluid transport in the brain. *Physiol Rev* 102, 1025–1151. <https://doi.org/10.1152/physrev.00031.2020>
- Raymond, P.A., Barthel, L.K., Bernardos, R.L., Perkowski, J.J., 2006. Molecular characterization of retinal stem cells and their niches in adult zebrafish. *BMC Developmental Biology* 6, 36. <https://doi.org/10.1186/1471-213X-6-36>
- Reimer, M.M., Sörensen, I., Kuscha, V., Frank, R.E., Liu, C., Becker, C.G., Becker, T., 2008. Motor neuron regeneration in adult zebrafish. *J Neurosci* 28, 8510–8516.

- <https://doi.org/10.1523/JNEUROSCI.1189-08.2008>
- Richard, C.-A., Seum, C., Gonzalez-Gaitan, M., 2024. Microtubule polarity determines the lineage of embryonic neural precursor in zebrafish spinal cord. *Commun Biol* 7, 439. <https://doi.org/10.1038/s42003-024-06018-7>
- Riesenberg, A.N., Liu, Z., Kopan, R., Brown, N.L., 2009. Rbpj cell autonomous regulation of retinal ganglion cell and cone photoreceptor fates in the mouse retina. *J Neurosci* 29, 12865–12877. <https://doi.org/10.1523/JNEUROSCI.3382-09.2009>
- Robu, M.E., Larson, J.D., Nasevicius, A., Beiraghi, S., Brenner, C., Farber, S.A., Ekker, S.C., 2007. p53 activation by knockdown technologies. *PLoS Genet* 3, e78. <https://doi.org/10.1371/journal.pgen.0030078>
- Rodriguez Viales, R., Diotel, N., Ferg, M., Armant, O., Eich, J., Alunni, A., März, M., Bally-Cuif, L., Rastegar, S., Strähle, U., 2015. The helix-loop-helix protein id1 controls stem cell proliferation during regenerative neurogenesis in the adult zebrafish telencephalon. *Stem Cells* 33, 892–903. <https://doi.org/10.1002/stem.1883>
- Roschger, C., Cabrele, C., 2017. The Id-protein family in developmental and cancer-associated pathways. *Cell Commun Signal* 15, 7. <https://doi.org/10.1186/s12964-016-0161-y>
- Rossi, A., Kontarakis, Z., Gerri, C., Nolte, H., Hölper, S., Krüger, M., Stainier, D.Y.R., 2015. Genetic compensation induced by deleterious mutations but not gene knockdowns. *Nature* 524, 230–233. <https://doi.org/10.1038/nature14580>
- Rothbauer, U., Zolghadr, K., Muyldermans, S., Schepers, A., Cardoso, M.C., Leonhardt, H., 2008. A versatile nanotrap for biochemical and functional studies with fluorescent fusion proteins. *Mol Cell Proteomics* 7, 282–289. <https://doi.org/10.1074/mcp.M700342-MCP200>
- Rothenaigner, I., Krecsmarik, M., Hayes, J.A., Bahn, B., Lepier, A., Fortin, G., Götz, M., Jagasia, R., Bally-Cuif, L., 2011. Clonal analysis by distinct viral vectors identifies bona fide neural stem cells in the adult zebrafish telencephalon and characterizes their division properties and fate. *Development* 138, 1459–1469. <https://doi.org/10.1242/dev.058156>
- Rusanescu, G., Mao, J., 2017. Peripheral nerve injury induces adult brain neurogenesis and remodelling. *J Cell Mol Med* 21, 299–314. <https://doi.org/10.1111/jcmm.12965>
- Sachan, N., Sharma, V., Mutsuddi, M., Mukherjee, A., 2024. Notch signalling: multifaceted role in development and disease. *FEBS J* 291, 3030–3059. <https://doi.org/10.1111/febs.16815>
- Sahu, A., Devi, S., Jui, J., Goldman, D., 2021. Notch signaling via Hey1 and Id2b regulates Müller glia's regenerative response to retinal injury. *Glia* 69, 2882–2898. <https://doi.org/10.1002/glia.24075>
- Sakamoto, M., Hirata, H., Ohtsuka, T., Bessho, Y., Kageyama, R., 2003. The basic helix-loop-helix genes *Hesr1/Hey1* and *Hesr2/Hey2* regulate maintenance of neural precursor cells in the brain. *J Biol Chem* 278, 44808–44815. <https://doi.org/10.1074/jbc.M300448200>
- Samarasinghe, K.T.G., Jaime-Figueroa, S., Burgess, M., Nalawansa, D.A., Dai, K., Hu, Z., Bebenek, A., Holley, S.A., Crews, C.M., 2021. Targeted degradation of transcription factors by TRAFACs: TRAnscription Factor TArgeting Chimeras. *Cell Chem Biol* 28, 648–661.e5. <https://doi.org/10.1016/j.chembiol.2021.03.011>
- Sanalkumar, R., Indulekha, C.L., Divya, T.S., Divya, M.S., Anto, R.J., Vinod, B., Vidyanand, S., Jagatha, B., Venugopal, S., James, J., 2010. ATF2 maintains a subset of neural progenitors through CBF1/Notch independent *Hes-1* expression and synergistically activates the expression of *Hes-1* in Notch-dependent neural progenitors. *J Neurochem* 113, 807–818. <https://doi.org/10.1111/j.1471-4159.2010.06574.x>
- Satow, T., Bae, S.K., Inoue, T., Inoue, C., Miyoshi, G., Tomita, K., Bessho, Y., Hashimoto, N., Kageyama, R., 2001. The basic helix-loop-helix gene *hesr2* promotes gliogenesis in

- mouse retina. *J Neurosci* 21, 1265–1273. <https://doi.org/10.1523/JNEUROSCI.21-04-01265.2001>
- Schebesta, M., Serluca, F.C., 2009. *olig1* Expression identifies developing oligodendrocytes in zebrafish and requires hedgehog and notch signaling. *Dev Dyn* 238, 887–898. <https://doi.org/10.1002/dvdy.21909>
- Schier, A.F., Neuhauss, S.C., Harvey, M., Malicki, J., Solnica-Krezel, L., Stainier, D.Y., Zwartkruis, F., Abdelilah, S., Stemple, D.L., Rangini, Z., Yang, H., Driever, W., 1996. Mutations affecting the development of the embryonic zebrafish brain. *Development* 123, 165–178. <https://doi.org/10.1242/dev.123.1.165>
- Schmidt, R., Strähle, U., Scholpp, S., 2013. Neurogenesis in zebrafish - from embryo to adult. *Neural Dev* 8, 3. <https://doi.org/10.1186/1749-8104-8-3>
- Semple, B.D., Blomgren, K., Gimlin, K., Ferriero, D.M., Noble-Haeusslein, L.J., 2013. Brain development in rodents and humans: Identifying benchmarks of maturation and vulnerability to injury across species. *Prog Neurobiol* 106–107, 1–16. <https://doi.org/10.1016/j.pneurobio.2013.04.001>
- Seok, H., Lee, H., Jang, E.-S., Chi, S.W., 2018. Evaluation and control of miRNA-like off-target repression for RNA interference. *Cell Mol Life Sci* 75, 797–814. <https://doi.org/10.1007/s00018-017-2656-0>
- Seri, B., García-Verdugo, J.M., Collado-Morente, L., McEwen, B.S., Alvarez-Buylla, A., 2004. Cell types, lineage, and architecture of the germinal zone in the adult dentate gyrus. *Journal of Comparative Neurology* 478, 359–378. <https://doi.org/10.1002/cne.20288>
- Sharma, P., Saraswathy, V.M., Xiang, L., Fürthauer, M., 2019. Notch-mediated inhibition of neurogenesis is required for zebrafish spinal cord morphogenesis. *Sci Rep* 9, 9958. <https://doi.org/10.1038/s41598-019-46067-1>
- Shen, Q., Goderie, S.K., Jin, L., Karanth, N., Sun, Y., Abramova, N., Vincent, P., Pumiglia, K., Temple, S., 2004. Endothelial cells stimulate self-renewal and expand neurogenesis of neural stem cells. *Science* 304, 1338–1340. <https://doi.org/10.1126/science.1095505>
- Shi, Q., Xue, C., Zeng, Y., Yuan, X., Chu, Q., Jiang, S., Wang, J., Zhang, Y., Zhu, D., Li, L., 2024. Notch signaling pathway in cancer: from mechanistic insights to targeted therapies. *Signal Transduct Target Ther* 9, 128. <https://doi.org/10.1038/s41392-024-01828-x>
- Shimojo, H., Kageyama, R., 2016. Oscillatory control of Delta-like1 in somitogenesis and neurogenesis: A unified model for different oscillatory dynamics. *Semin Cell Dev Biol* 49, 76–82. <https://doi.org/10.1016/j.semcdb.2016.01.017>
- Shimojo, H., Masaki, T., Kageyama, R., 2024. The Neurog2-Tbr2 axis forms a continuous transition to the neurogenic gene expression state in neural stem cells. *Dev Cell* 59, 1913–1923.e6. <https://doi.org/10.1016/j.devcel.2024.04.019>
- Shin, J., Berg, D.A., Zhu, Y., Shin, J.Y., Song, J., Bonaguidi, M.A., Enikolopov, G., Nauen, D.W., Christian, K.M., Ming, G., Song, H., 2015. Single-Cell RNA-Seq with Waterfall Reveals Molecular Cascades underlying Adult Neurogenesis. *Cell Stem Cell* 17, 360–372. <https://doi.org/10.1016/j.stem.2015.07.013>
- Shin, J., Park, H.-C., Topczewska, J.M., Mawdsley, D.J., Appel, B., 2003. Neural cell fate analysis in zebrafish using *olig2* BAC transgenics. *Methods Cell Sci* 25, 7–14. <https://doi.org/10.1023/B:MICS.0000006847.09037.3a>
- Shin, J., Poling, J., Park, H.-C., Appel, B., 2007. Notch signaling regulates neural precursor allocation and binary neuronal fate decisions in zebrafish. *Development* 134, 1911–1920. <https://doi.org/10.1242/dev.001602>
- Shin, M., Yin, H.-M., Shih, Y.-H., Nozaki, T., Portman, D., Toles, B., Kolb, A., Luk, K., Isogai, S., Ishida, K., Hanasaka, T., Parsons, M.J., Wolfe, S.A., Burns, C.E., Burns, C.G., Lawson, N.D., 2023. Generation and application of endogenously floxed alleles for cell-

- specific knockout in zebrafish. *Dev Cell* 58, 2614-2626.e7. <https://doi.org/10.1016/j.devcel.2023.07.022>
- Shin, Y.J., Park, S.K., Jung, Y.J., Kim, Y.N., Kim, K.S., Park, O.K., Kwon, S.-H., Jeon, S.H., Trinh, L.A., Fraser, S.E., Kee, Y., Hwang, B.J., 2015. Nanobody-targeted E3-ubiquitin ligase complex degrades nuclear proteins. *Sci Rep* 5, 14269. <https://doi.org/10.1038/srep14269>
- Sidik, H., Talbot, W.S., 2015. A zinc finger protein that regulates oligodendrocyte specification, migration and myelination in zebrafish. *Development* 142, 4119–4128. <https://doi.org/10.1242/dev.128215>
- Siebel, C., Lendahl, U., 2017. Notch Signaling in Development, Tissue Homeostasis, and Disease. *Physiol Rev* 97, 1235–1294. <https://doi.org/10.1152/physrev.00005.2017>
- Sigloch, C., Spitz, D., Driever, W., 2023. A network of Notch-dependent and -independent her genes controls neural stem and progenitor cells in the zebrafish thalamic proliferation zone. *Development* 150, dev201301. <https://doi.org/10.1242/dev.201301>
- Singh, A., Tare, M., Puli, O.R., Kango-Singh, M., 2012. A glimpse into dorso-ventral patterning of the Drosophila eye. *Dev Dyn* 241, 69–84. <https://doi.org/10.1002/dvdy.22764>
- Singleman, C., Holtzman, N.G., 2014. Growth and maturation in the zebrafish, *Danio rerio*: a staging tool for teaching and research. *Zebrafish* 11, 396–406. <https://doi.org/10.1089/zeb.2014.0976>
- Sirerol-Piquer, M.S., Belenguer, G., Morante-Redolat, J.M., Duarte-Abadia, P., Perez-Villalba, A., Fariñas, I., 2019. Physiological Interactions between Microglia and Neural Stem Cells in the Adult Subependymal Niche. *Neuroscience* 405, 77–91. <https://doi.org/10.1016/j.neuroscience.2019.01.009>
- Skalska, L., Stojnic, R., Li, J., Fischer, B., Cerda-Moya, G., Sakai, H., Tajbakhsh, S., Russell, S., Adryan, B., Bray, S.J., 2015. Chromatin signatures at Notch-regulated enhancers reveal large-scale changes in H3K56ac upon activation. *EMBO J* 34, 1889–1904. <https://doi.org/10.15252/embj.201489923>
- Sokpor, G., Brand-Saberi, B., Nguyen, H.P., Tuoc, T., 2022. Regulation of Cell Delamination During Cortical Neurodevelopment and Implication for Brain Disorders. *Front Neurosci* 16, 824802. <https://doi.org/10.3389/fnins.2022.824802>
- Soto, X., Biga, V., Kursawe, J., Lea, R., Doostdar, P., Thomas, R., Papalopulu, N., 2020. Dynamic properties of noise and Her6 levels are optimized by miR-9, allowing the decoding of the Her6 oscillator. *EMBO J* 39, e103558. <https://doi.org/10.15252/embj.2019103558>
- Sowell, E.R., Thompson, P.M., Toga, A.W., 2004. Mapping changes in the human cortex throughout the span of life. *Neuroscientist* 10, 372–392. <https://doi.org/10.1177/1073858404263960>
- Spassky, N., Merkle, F.T., Flames, N., Tramontin, A.D., García-Verdugo, J.M., Alvarez-Buylla, A., 2005. Adult ependymal cells are postmitotic and are derived from radial glial cells during embryogenesis. *J Neurosci* 25, 10–18. <https://doi.org/10.1523/JNEUROSCI.1108-04.2005>
- Sprinzak, D., Blacklow, S.C., 2021. Biophysics of Notch Signaling. *Annu Rev Biophys* 50, 157–189. <https://doi.org/10.1146/annurev-biophys-101920-082204>
- Stachniak, T.J., Kastli, R., Hanley, O., Argunsah, A.Ö., van der Valk, E.G.T., Kanatouris, G., Karayannis, T., 2021. Postmitotic Prox1 Expression Controls the Final Specification of Cortical VIP Interneuron Subtypes. *J Neurosci* 41, 8150–8162. <https://doi.org/10.1523/JNEUROSCI.1021-21.2021>
- Stednitz, S.J., McDermott, E.M., Ncube, D., Tallafuss, A., Eisen, J.S., Washbourne, P., 2018. Forebrain Control of Behaviorally Driven Social Orienting in Zebrafish. *Curr Biol* 28, 2445-2451.e3. <https://doi.org/10.1016/j.cub.2018.06.016>



- Stednitz, S.J., Washbourne, P., 2020. Rapid Progressive Social Development of Zebrafish. *Zebrafish* 17, 11–17. <https://doi.org/10.1089/zeb.2019.1815>
- Stevanovic, M., Drakulic, D., Lazic, A., Ninkovic, D.S., Schwirtlich, M., Mojsin, M., 2021. SOX Transcription Factors as Important Regulators of Neuronal and Glial Differentiation During Nervous System Development and Adult Neurogenesis. *Front Mol Neurosci* 14, 654031. <https://doi.org/10.3389/fnmol.2021.654031>
- Sueda, R., Imayoshi, I., Harima, Y., Kageyama, R., 2019. High Hes1 expression and resultant Ascl1 suppression regulate quiescent vs. active neural stem cells in the adult mouse brain. *Genes Dev* 33, 511–523. <https://doi.org/10.1101/gad.323196.118>
- Sueda, R., Kageyama, R., 2020. Regulation of active and quiescent somatic stem cells by Notch signaling. *Dev Growth Differ* 62, 59–66. <https://doi.org/10.1111/dgd.12626>
- Sun, W., Kim, H., Moon, Y., 2010. Control of neuronal migration through rostral migration stream in mice. *Anat Cell Biol* 43, 269–279. <https://doi.org/10.5115/acb.2010.43.4.269>
- Swiatek, P.J., Lindsell, C.E., del Amo, F.F., Weinmaster, G., Gridley, T., 1994. Notch1 is essential for postimplantation development in mice. *Genes Dev* 8, 707–719. <https://doi.org/10.1101/gad.8.6.707>
- Tanaka, K., 2009. The proteasome: overview of structure and functions. *Proc Jpn Acad Ser B Phys Biol Sci* 85, 12–36. <https://doi.org/10.2183/pjab.85.12>
- Taverna, E., Huttner, W.B., 2010. Neural progenitor nuclei IN motion. *Neuron* 67, 906–914. <https://doi.org/10.1016/j.neuron.2010.08.027>
- Teoh, S.L., Das, S., 2018. Notch Signalling Pathways and Their Importance in the Treatment of Cancers. *Curr Drug Targets* 19, 128–143. <https://doi.org/10.2174/1389450118666170309143419>
- Than-Trong, E., Kiani, B., Dray, N., Ortica, S., Simons, B., Rulands, S., Alunni, A., Bally-Cuif, L., 2020. Lineage hierarchies and stochasticity ensure the long-term maintenance of adult neural stem cells. *Sci Adv* 6, eaaz5424. <https://doi.org/10.1126/sciadv.aaz5424>
- Than-Trong, E., Ortica-Gatti, S., Mella, S., Nepal, C., Alunni, A., Bally-Cuif, L., 2018. Neural stem cell quiescence and stemness are molecularly distinct outputs of the Notch3 signalling cascade in the vertebrate adult brain. *Development* 145, dev161034. <https://doi.org/10.1242/dev.161034>
- Tian, X., Zhou, B., 2021. Strategies for site-specific recombination with high efficiency and precise spatiotemporal resolution. *J Biol Chem* 296, 100509. <https://doi.org/10.1016/j.jbc.2021.100509>
- Toda, T., Gage, F.H., 2018. Review: adult neurogenesis contributes to hippocampal plasticity. *Cell Tissue Res* 373, 693–709. <https://doi.org/10.1007/s00441-017-2735-4>
- Toda, T., Parylak, S.L., Linker, S.B., Gage, F.H., 2019. The role of adult hippocampal neurogenesis in brain health and disease. *Mol Psychiatry* 24, 67–87. <https://doi.org/10.1038/s41380-018-0036-2>
- Tran, L.N., Loew, S.K., Franco, S.J., 2023. Notch Signaling Plays a Dual Role in Regulating the Neuron-to-Oligodendrocyte Switch in the Developing Dorsal Forebrain. *J Neurosci* 43, 6854–6871. <https://doi.org/10.1523/JNEUROSCI.0144-23.2023>
- Trylinski, M., Mazouni, K., Schweisguth, F., 2017. Intra-lineage Fate Decisions Involve Activation of Notch Receptors Basal to the Midbody in *Drosophila* Sensory Organ Precursor Cells. *Curr Biol* 27, 2239–2247.e3. <https://doi.org/10.1016/j.cub.2017.06.030>
- Tümpel, S., Rudolph, K.L., 2019. Quiescence: Good and Bad of Stem Cell Aging. *Trends Cell Biol* 29, 672–685. <https://doi.org/10.1016/j.tcb.2019.05.002>
- Urbán, N., Guillemot, F., 2014. Neurogenesis in the embryonic and adult brain: same regulators, different roles. *Front Cell Neurosci* 8, 396. <https://doi.org/10.3389/fncel.2014.00396>
- Uzman, L.L., 1960. The histogenesis of the mouse cerebellum as studied by its tritiated

- thymidine uptake. *J Comp Neurol* 114, 137–159. <https://doi.org/10.1002/cne.901140204>
- Valente, A., Huang, K.-H., Portugues, R., Engert, F., 2012. Ontogeny of classical and operant learning behaviors in zebrafish. *Learn Mem* 19, 170–177. <https://doi.org/10.1101/lm.025668.112>
- Van Eeden, F.J., Holley, S.A., Haffter, P., Nüsslein-Volhard, C., 1998. Zebrafish segmentation and pair-rule patterning. *Dev Genet* 23, 65–76. [https://doi.org/10.1002/\(SICI\)1520-6408\(1998\)23:1<65::AID-DVG7>3.0.CO;2-4](https://doi.org/10.1002/(SICI)1520-6408(1998)23:1<65::AID-DVG7>3.0.CO;2-4)
- Van Houcke, J., Mariën, V., Zandecki, C., Seuntjens, E., Ayana, R., Arckens, L., 2021. Modeling Neuroregeneration and Neurorepair in an Aging Context: The Power of a Teleost Model. *Front Cell Dev Biol* 9, 619197. <https://doi.org/10.3389/fcell.2021.619197>
- Van Tetering, G., van Diest, P., Verlaan, I., van der Wall, E., Kopan, R., Vooijs, M., 2009. Metalloprotease ADAM10 is required for Notch1 site 2 cleavage. *J Biol Chem* 284, 31018–31027. <https://doi.org/10.1074/jbc.M109.006775>
- Vasconcelos, F.F., Castro, D.S., 2014. Transcriptional control of vertebrate neurogenesis by the proneural factor *Ascl1*. *Front Cell Neurosci* 8, 412. <https://doi.org/10.3389/fncel.2014.00412>
- Vazdar, M., Heyda, J., Mason, P.E., Tessei, G., Allolio, C., Lund, M., Jungwirth, P., 2018. Arginine “Magic”: Guanidinium Like-Charge Ion Pairing from Aqueous Salts to Cell Penetrating Peptides. *Acc Chem Res* 51, 1455–1464. <https://doi.org/10.1021/acs.accounts.8b00098>
- Viswanathan, R., Necakov, A., Trylinski, M., Harish, R.K., Krueger, D., Esposito, E., Schweisguth, F., Neveu, P., De Renzis, S., 2019. Optogenetic inhibition of Delta reveals digital Notch signalling output during tissue differentiation. *EMBO Rep* 20, e47999. <https://doi.org/10.15252/embr.201947999>
- von Trotha, J.W., Vernier, P., Bally-Cuif, L., 2014. Emotions and motivated behavior converge on an amygdala-like structure in the zebrafish. *Eur J Neurosci* 40, 3302–3315. <https://doi.org/10.1111/ejn.12692>
- Wang, H., Zang, C., Taing, L., Arnett, K.L., Wong, Y.J., Pear, W.S., Blacklow, S.C., Liu, X.S., Aster, J.C., 2014. NOTCH1-RBPJ complexes drive target gene expression through dynamic interactions with superenhancers. *Proc Natl Acad Sci U S A* 111, 705–710. <https://doi.org/10.1073/pnas.1315023111>
- Wang, R., Zhao, C., Li, J., Li, Y., Liu, Y., Dong, H., Wang, D., Zhao, B., Zhang, X., Wang, S., Cui, F., Li, H., He, X., Qin, J., 2018. Notch1 promotes mouse spinal neural stem and progenitor cells proliferation via p-p38-pax6 induced cyclin D1 activation. *Exp Cell Res* 373, 80–90. <https://doi.org/10.1016/j.yexcr.2018.09.025>
- Wang, Y., Pan, L., Moens, C.B., Appel, B., 2014. Notch3 establishes brain vascular integrity by regulating pericyte number. *Development* 141, 307–317. <https://doi.org/10.1242/dev.096107>
- Wang, Y., Rovira, M., Yusuff, S., Parsons, M.J., 2011. Genetic inducible fate mapping in larval zebrafish reveals origins of adult insulin-producing  $\beta$ -cells. *Development* 138, 609–617. <https://doi.org/10.1242/dev.059097>
- Weller, M., Krautler, N., Mantei, N., Suter, U., Taylor, V., 2006. Jagged1 ablation results in cerebellar granule cell migration defects and depletion of Bergmann glia. *Dev Neurosci* 28, 70–80. <https://doi.org/10.1159/000090754>
- White, M.J., Jacobs, K.A., Singh, T., Mayo, L.N., Lin, A., Chen, C.S., Jun, Y.-W., Kutys, M.L., 2023. Notch1 cortical signaling regulates epithelial architecture and cell-cell adhesion. *J Cell Biol* 222, e202303013. <https://doi.org/10.1083/jcb.202303013>
- White, R.M., Sessa, A., Burke, C., Bowman, T., LeBlanc, J., Ceol, C., Bourque, C., Dovey, M.,

- Goessling, W., Burns, C.E., Zon, L.I., 2008. Transparent adult zebrafish as a tool for in vivo transplantation analysis. *Cell Stem Cell* 2, 183–189. <https://doi.org/10.1016/j.stem.2007.11.002>
- Wilkinson, G., Dennis, D., Schuurmans, C., 2013. Proneural genes in neocortical development. *Neuroscience* 253, 256–273. <https://doi.org/10.1016/j.neuroscience.2013.08.029>
- Winner, B., Kohl, Z., Gage, F.H., 2011. Neurodegenerative disease and adult neurogenesis. *Eur J Neurosci* 33, 1139–1151. <https://doi.org/10.1111/j.1460-9568.2011.07613.x>
- Wu, G., Lyapina, S., Das, I., Li, J., Gurney, M., Pauley, A., Chui, I., Deshaies, R.J., Kitajewski, J., 2001. SEL-10 is an inhibitor of notch signaling that targets notch for ubiquitin-mediated protein degradation. *Mol Cell Biol* 21, 7403–7415. <https://doi.org/10.1128/MCB.21.21.7403-7415.2001>
- Wu, Y., Han, X., Su, Y., Glidewell, M., Daniels, J.S., Liu, J., Sengupta, T., Rey-Suarez, I., Fischer, R., Patel, A., Combs, C., Sun, J., Wu, X., Christensen, R., Smith, C., Bao, L., Sun, Y., Duncan, L.H., Chen, J., Pommier, Y., Shi, Y.-B., Murphy, E., Roy, S., Upadhyaya, A., Colón-Ramos, D., La Riviere, P., Shroff, H., 2021. Multiview confocal super-resolution microscopy. *Nature* 600, 279–284. <https://doi.org/10.1038/s41586-021-04110-0>
- Wullmann, M.F., Mueller, T., 2002. Expression of Zash-1a in the postembryonic zebrafish brain allows comparison to mouse Mash1 domains. *Brain Res Gene Expr Patterns* 1, 187–192. [https://doi.org/10.1016/s1567-133x\(02\)00016-9](https://doi.org/10.1016/s1567-133x(02)00016-9)
- Xu, J., Deng, X., Gu, A., Cai, Y., Huang, Y., Zhang, W., Zhang, Y., Wen, W., Xie, Y., 2023. Ccdc85c-Par3 condensates couple cell polarity with Notch to control neural progenitor proliferation. *Cell Rep* 42, 112677. <https://doi.org/10.1016/j.celrep.2023.112677>
- Yamaguchi, N., Colak-Champollion, T., Knaut, H., 2019. zGrad is a nanobody-based degron system that inactivates proteins in zebrafish. *eLife* 8, e43125. <https://doi.org/10.7554/eLife.43125>
- Yamakawa, M., Santosa, S.M., Chawla, N., Ivakhnitskaia, E., Del Pino, M., Giakas, S., Nadel, A., Bontu, S., Tambe, A., Guo, K., Han, K.-Y., Cortina, M.S., Yu, C., Rosenblatt, M.I., Chang, J.-H., Azar, D.T., 2020. Transgenic models for investigating the nervous system: Currently available neurofluorescent reporters and potential neuronal markers. *Biochim Biophys Acta Gen Subj* 1864, 129595. <https://doi.org/10.1016/j.bbagen.2020.129595>
- Yang, X., Klein, R., Tian, X., Cheng, H.-T., Kopan, R., Shen, J., 2004. Notch activation induces apoptosis in neural progenitor cells through a p53-dependent pathway. *Dev Biol* 269, 81–94. <https://doi.org/10.1016/j.ydbio.2004.01.014>
- Yang, X., Tomita, T., Wines-Samuelson, M., Beglopoulos, V., Tansey, M.G., Kopan, R., Shen, J., 2006. Notch1 signaling influences v2 interneuron and motor neuron development in the spinal cord. *Dev Neurosci* 28, 102–117. <https://doi.org/10.1159/000090757>
- Yelle, N., Bakhshinyan, D., Venugopal, C., Singh, S.K., 2019. Introduction to Brain Tumor Stem Cells. *Methods Mol Biol* 1869, 1–9. [https://doi.org/10.1007/978-1-4939-8805-1\\_1](https://doi.org/10.1007/978-1-4939-8805-1_1)
- Yeo, S.-Y., Chitnis, A.B., 2007. Jagged-mediated Notch signaling maintains proliferating neural progenitors and regulates cell diversity in the ventral spinal cord. *Proc Natl Acad Sci U S A* 104, 5913–5918. <https://doi.org/10.1073/pnas.0607062104>
- Yeo, S.-Y., Kim, M., Kim, H.-S., Huh, T.-L., Chitnis, A.B., 2007. Fluorescent protein expression driven by her4 regulatory elements reveals the spatiotemporal pattern of Notch signaling in the nervous system of zebrafish embryos. *Dev Biol* 301, 555–567. <https://doi.org/10.1016/j.ydbio.2006.10.020>
- Yokota, Y., Eom, T.-Y., Stanco, A., Kim, W.-Y., Rao, S., Snider, W.D., Anton, E.S., 2010. Cdc42 and Gsk3 modulate the dynamics of radial glial growth, inter-radial glial interactions and polarity in the developing cerebral cortex. *Development* 137, 4101–

4110. <https://doi.org/10.1242/dev.048637>
- Yoon, K., Gaiano, N., 2005. Notch signaling in the mammalian central nervous system: insights from mouse mutants. *Nat Neurosci* 8, 709–715. <https://doi.org/10.1038/nn1475>
- Yoon, K., Nery, S., Rutlin, M.L., Radtke, F., Fishell, G., Gaiano, N., 2004. Fibroblast growth factor receptor signaling promotes radial glial identity and interacts with Notch1 signaling in telencephalic progenitors. *J Neurosci* 24, 9497–9506. <https://doi.org/10.1523/JNEUROSCI.0993-04.2004>
- Yoon, K.-J., Koo, B.-K., Im, S.-K., Jeong, H.-W., Ghim, J., Kwon, M.-C., Moon, J.-S., Miyata, T., Kong, Y.-Y., 2008. Mind bomb 1-expressing intermediate progenitors generate notch signaling to maintain radial glial cells. *Neuron* 58, 519–531. <https://doi.org/10.1016/j.neuron.2008.03.018>
- Yoshihara, M., Takahashi, S., 2023. Recent advances in in situ Notch signaling measurement. *Front Cell Dev Biol* 11, 1244105. <https://doi.org/10.3389/fcell.2023.1244105>
- You, M.-S., Wang, W.-P., Wang, J.-Y., Jiang, Y.-J., Chi, Y.-H., 2019. Sun1 Mediates Interkinetic Nuclear Migration and Notch Signaling in the Neurogenesis of Zebrafish. *Stem Cells Dev* 28, 1116–1127. <https://doi.org/10.1089/scd.2019.0063>
- Yu, Yanqi, Zhang, Z., Walpole, G.F.W., Yu, Yan, 2022. Kinetics of phagosome maturation is coupled to their intracellular motility. *Commun Biol* 5, 1–14. <https://doi.org/10.1038/s42003-022-03988-4>
- Yuan, L., Chen, X., Jankovic, J., Deng, H., 2024. CADASIL: A NOTCH3-associated cerebral small vessel disease. *J Adv Res* S2090-1232(24)00001–8. <https://doi.org/10.1016/j.jare.2024.01.001>
- Zada, S., Hwang, J.S., Lai, T.H., Pham, T.M., Ahmed, M., Elashkar, O., Kim, W., Kim, D.R., 2022. Autophagy-mediated degradation of NOTCH1 intracellular domain controls the epithelial to mesenchymal transition and cancer metastasis. *Cell Biosci* 12, 17. <https://doi.org/10.1186/s13578-022-00752-3>
- Zaucker, A., Mercurio, S., Sternheim, N., Talbot, W.S., Marlow, F.L., 2013. notch3 is essential for oligodendrocyte development and vascular integrity in zebrafish. *Dis Model Mech* 6, 1246–1259. <https://doi.org/10.1242/dmm.012005>
- Zhang, C., Li, Q., Lim, C.-H., Qiu, X., Jiang, Y.-J., 2007. The characterization of zebrafish antimorphic mib alleles reveals that Mib and Mind bomb-2 (Mib2) function redundantly. *Dev Biol* 305, 14–27. <https://doi.org/10.1016/j.ydbio.2007.01.034>
- Zhang, G., Ferg, M., Lübke, L., Takamiya, M., Beil, T., Gourain, V., Diotel, N., Strähle, U., Rastegar, S., 2020. Bone morphogenetic protein signaling regulates Id1-mediated neural stem cell quiescence in the adult zebrafish brain via a phylogenetically conserved enhancer module. *Stem Cells* 38, 875–889. <https://doi.org/10.1002/stem.3182>
- Zhang, G., Lübke, L., Chen, F., Beil, T., Takamiya, M., Diotel, N., Strähle, U., Rastegar, S., 2021. Neuron-Radial Glial Cell Communication via BMP/Id1 Signaling Is Key to Long-Term Maintenance of the Regenerative Capacity of the Adult Zebrafish Telencephalon. *Cells* 10, 2794. <https://doi.org/10.3390/cells10102794>
- Zhang, R., Boareto, M., Engler, A., Louvi, A., Giachino, C., Iber, D., Taylor, V., 2019. Id4 Downstream of Notch2 Maintains Neural Stem Cell Quiescence in the Adult Hippocampus. *Cell Rep* 28, 1485–1498.e6. <https://doi.org/10.1016/j.celrep.2019.07.014>
- Zhang, R., Engler, A., Taylor, V., 2018. Notch: an interactive player in neurogenesis and disease. *Cell Tissue Res* 371, 73–89. <https://doi.org/10.1007/s00441-017-2641-9>
- Zhang, X., Li, Y., Xu, H., Zhang, Y.-W., 2014. The  $\gamma$ -secretase complex: from structure to function. *Front Cell Neurosci* 8, 427. <https://doi.org/10.3389/fncel.2014.00427>
- Zhao, L., Zhao, J., Zhong, K., Tong, A., Jia, D., 2022. Targeted protein degradation: mechanisms, strategies and application. *Signal Transduct Target Ther* 7, 113. <https://doi.org/10.1038/s41392-022-00966-4>

- Zhou, B., Lin, W., Long, Y., Yang, Y., Zhang, H., Wu, K., Chu, Q., 2022a. Notch signaling pathway: architecture, disease, and therapeutics. *Signal Transduct Target Ther* 7, 95. <https://doi.org/10.1038/s41392-022-00934-y>
- Zhou, Y., Su, Y., Li, S., Kennedy, B.C., Zhang, D.Y., Bond, A.M., Sun, Y., Jacob, F., Lu, L., Hu, P., Viaene, A.N., Helbig, I., Kessler, S.K., Lucas, T., Salinas, R.D., Gu, X., Chen, H.I., Wu, H., Kleinman, J.E., Hyde, T.M., Nauen, D.W., Weinberger, D.R., Ming, G.-L., Song, H., 2022b. Molecular landscapes of human hippocampal immature neurons across lifespan. *Nature* 607, 527–533. <https://doi.org/10.1038/s41586-022-04912-w>
- Zhu, X., Zhang, J., Tollkuhn, J., Ohsawa, R., Bresnick, E.H., Guillemot, F., Kageyama, R., Rosenfeld, M.G., 2006. Sustained Notch signaling in progenitors is required for sequential emergence of distinct cell lineages during organogenesis. *Genes Dev* 20, 2739–2753. <https://doi.org/10.1101/gad.1444706>
- Zimmer, A.M., Pan, Y.K., Chandrapalan, T., Kwong, R.W.M., Perry, S.F., 2019. Loss-of-function approaches in comparative physiology: is there a future for knockdown experiments in the era of genome editing? *J Exp Biol* 222, jeb175737. <https://doi.org/10.1242/jeb.175737>
- Zupanc, G.K., 2001. Adult neurogenesis and neuronal regeneration in the central nervous system of teleost fish. *Brain Behav Evol* 58, 250–275. <https://doi.org/10.1159/000057569>
- Zupanc, G.K.H., Hinsch, K., Gage, F.H., 2005. Proliferation, migration, neuronal differentiation, and long-term survival of new cells in the adult zebrafish brain. *J Comp Neurol* 488, 290–319. <https://doi.org/10.1002/cne.20571>